Universitat Autònoma de Barcelona

Immunomodulation by mesenchymal stem cells for myocardial regeneration: cellular mechanisms and extracellular vesicles

Marta Monguió Tortajada

Immunomodulation by mesenchymal stem cells for myocardial regeneration: cellular mechanisms and extracellular vesicles

PhD thesis by

Marta Monguió Tortajada

2018

PhD program in Advanced Immunology
Department of Cellular Biology, Physiology and Immunology
Universitat Autònoma de Barcelona

Immunomodulation by mesenchymal stem cells for myocardial regeneration: cellular mechanisms and extracellular vesicles

Immunomodulació amb cèl·lules mare mesenquimals per la regeneració miocardíaca: mecanismes cel·lulars i vesícules extracel·lulars

Thesis presented by Marta Monguió Tortajada to qualify for the PhD degree in Advanced Immunology by the Universitat Autònoma de Barcelona.

The presented work has been performed in the Innovation in Vesicles and Cells for Application in Therapy Group (IVECAT), at the Germans Trias i Pujol Health Sciences Research Institute (IGTP) and directed by Dr Francesc E. Borràs.

Badalona, 26th October 2018

Marta Monguió Tortajada
(PhD candidate)

Dr Francesc E. Borràs
(Director)

Dra Dolores Jaraquemada
(Tutor)

TABLE OF CONTENTS

SUMMARY

Exacerbated immune responses hamper regeneration of injured tissues and organ transplantation, and lead to allergies and autoimmune disorders causing morbidity and mortality. One of these scenarios is the ischaemia-reperfusion injury (IRI) occurring upon myocardial infarction (MI). IRI triggers an intense inflammatory response that is initially necessary for dead cell clearance and the induction of cardiac repair, but its timely suppression is critical to minimize post-MI tissue damage, cardiac remodelling and ultimately, heart failure. In this context, mesenchymal stem cells (MSCs) are promising as a therapeutic strategy to counteract such unwanted immune responses, as MSC administration has a beneficial effect for the treatment of immune-related disorders and promote cardiac repair in preclinical models of MI, albeit their short lifespan after *in vivo* infusion. The aim of this thesis is to decipher the cellular and paracrine mechanisms that would help explain MSCs' long-lasting immunosuppressive and regenerative effects. The working hypothesis is that these could be mediated by the modulation of the host's immune cells for the generation of regulatory environments and enduring effect, in addition to the secretion of paracrine factors for a delocalized action that would also foster endogenous repair. With this in mind, we first studied MSC's influence on monocytes as part of the innate immune response. We confirmed MSCs' modulation of monocytes towards a wound-healing M2-like polarization, but with the added functionality of an active extracellular adenosinergic enzymatic activity. MSC-conditioned monocytes maintained CD39 and induced CD73 expression, which are responsible of the sequential hydrolysis of ATP/ADP to AMP and to Adenosine, respectively, to shift the pro-inflammatory milieu induced by extracellular ATP to the anti-inflammatory regulation by Adenosine. On the other side, MSCs also modulate the adaptive immune response, as we observed the immunosuppression of allogeneic lymphocyte polyclonal proliferation and inflammatory cytokine release. Regarding the paracrine activity of MSCs, we could identify extracellular vesicles (EVs) as one of the active components of MSC's immunosuppressive secreted factors. Specifically, we demonstrated the importance of accurate isolation of MSC-EVs to unravel their immunosuppressive functionality, which can be efficiently performed by size-exclusion chromatography (SEC). Finally, this knowledge made us design a novel construct composed of MSC-EVs embedded in a biocompatible three-dimensional engineered cardiac scaffold, envisioned for the local treatment of MI to foster cardiac repair. Its *in vitro* validation reinforced EV secretion as an important mechanism of MSCs to both modulate the immune system and foster endogenous repair, as they could actively recruit pro-regenerative cells. Our findings unravel new mechanisms for the engineering of innovative, targeted and off-the-shelf therapeutic products.

RESUM

Les respostes immunològiques descontrolades obstaculitzen la regeneració de teixits danyats i el transplantament d'òrgans, i provoquen al·lèrgies i trastorns autoimmunitaris, causant morbiditat i mortalitat. Un d'aquests casos és el dany causat per la isquèmia-reperfusió (IRI) que ocorre en un infart de miocardi (MI). El IRI provoca una intensa inflamació, que, tot i ser necessària per iniciar la neteja de les cèl·lules mortes i activar els mecanismes de reparació cardíaca, cal aturar a temps per minimitzar el dany tissular post-MI i el remodelat miocardíac, que pot esdevenir en insuficiència cardíaca. En aquest context, les cèl·lules mare mesenquimals (MSCs) es postulen com una estratègia terapèutica prometedora per contrarestar aquestes respostes immunitàries no desitjades. Tot i tenir una curta vida després de la seva administració *in vivo*, les MSCs han demostrat ser beneficioses tant per al tractament de patologies d'arrel immunitària com per la promoció de la regeneració cardíaca en models preclínics de MI. L'objectiu d'aquesta tesi és doncs desxifrar quins són els mecanismes cel·lulars i paracrins que capaciten les MSCs per tenir un efecte immunosupressor i regenerador a llarg termini. La hipòtesi de treball és que les MSCs aconsegueixen la generació d'ambients reguladors amb un efecte durador mitjançant la modulació de les cèl·lules immunes de l'hoste, mentre que la secreció de factors paracrins els permet tenir una acció deslocalitzada i promoure alhora la regeneració endògena. Amb aquesta idea, en primer lloc hem estudiat la influència de les MSCs en la biologia dels monòcits, com a part de la immunitat innata. Hem confirmat el paper de les MSCs en la modulació dels monòcits vers una polarització reparadora M2, descrivint la activitat enzimàtica adenosinèrgica extracel·lular com una funcionalitat afegida. Els monòcits condicionats amb MSCs mantenen l'expressió de CD39, mentre que s'indueix la de CD73, responsable de la hidròlisi seqüencial de ATP/ADP a AMP i adenosina, respectivament, per passar de l'ambient pro-inflamatori promogut per ATP extracel·lular a la regulació anti-inflamatòria de l'adenosina. Per altra banda, les MSCs també modulen la resposta immune adaptativa, ja que hem observat la supressió de la proliferació policlonal i resposta inflamatòria de limfòcits al·logènics. Pel que fa a la activitat paracrina de les MSCs, hem identificat les vesícules extracel·lulars (EVs) com un des components immunosupressors secretats per les MSCs. Concretament, hem demostrat la importància d'un aïllament acurat de les MSC-EVs per evidenciar el seu potencial immunosupressor, que es pot aconseguir eficientment mitjançant la cromatografia d'exclusió per mida (SEC). Finalment, aquest coneixement ens ha permès dissenyar un nou constructe format per una matriu biocompatible 3D de bioenginyeria cardíaca integrada amb MSC-EVs per al tractament local del MI i promoure regeneració cardíaca. La validació *in vitro* d'aquest constructe va reforçar la importància de la secreció de EVs com un mecanisme de les MSCs per modular el sistema immunitari i fomentar els processos de reparació endògena, donat que les MSC-EVs poden reclutar activament cèl·lules pro-regeneradores. Els nostres resultats aporten nous mecanismes a aprofitar per generar nous productes terapèutics dirigits, innovadors i fàcilment translacionals.

ABBREVIATIONS

5'AMP	adenosine 5'-monophosphate
7AAD	7-aminoactinomycin-D
Ab	antibody
Ado	adenosine
ADP	adenosine diphosphate
AF4	asymmetrical flow field-flow fractionation
ALIX	ALG-2 interacting protein X
ANOVA	analysis of variance
APCP	adenosine 5′(α,β-methylene)-diphosphate/ADP analogue/CD73 inhibitor
ARF6	ADP-ribosylation factor 6
ATP	adenosine triphosphate
BCB	bead coupling buffer
BMMSC	bone marrow mesenchymal stem cells
BMP-7	bone morphogenetic protein-7
Breg	regulatory B cell
BSA	bovine serum albumin
cADPR	cyclic adenosine diphosphate ribose
cATMSCs	cardiac adipose tissue-derived MSCs
CBA	cytometric bead array
CCL	C-C motif chemokine ligand
CCM/ECM	concentrated/eluted conditioned medium
CCR7	C-C motif chemokine receptor 7
CD	cluster of differentiation
CD203a/NPP	nucleotide pyrophosphatase/phosphodiesterase
CD23/FcεRII	low affinity receptor of IgE Fc portion
CD38/NADase	nicotinamide adenine dinucleotidase
CD39/NTPD-1	nucleoside triphosphate diphosphohydrolase
CD73/ecto-5'-NT	ecto-5′-nucleotidase
CEIC	comitè ètic d'investigació clínica
CFSE	carboxyfluorescein succinimidyl ester
CM	conditioned medium
Col III	type III collagen
COX2	cyclooxygenase-2
Cryo-EM	cryogenic electron microscopy
CsA	cyclosporine A
CTLA-4	cytotoxic T-lymphocyte-associated protein 4
cTnI	cardiac troponin I
CXCL	C-X-C motif chemokine ligand
Cy	cyanine
DALY	disability-adjusted life-years
DAMP	damage-associated molecular pattern
DAPI	4',6-diamidino-2-phenylindole dihydrochloride
DC	dendritic cell
DG	density gradient

DMEM	Dulbecco's modified Eagle's medium
DNA	deoxyribonucleic acid
dUC	differential ultracentrifugation
ECM	extracellular matrix
ELISA	enzyme-linked immunosorbent assay
ESCRT	endosomal sorting complex required for transport
EV	extracellular vesicle
FACS	fluorescence-assisted cell sorting
FBS	foetal bovine serum
FcγR	receptor of IgG Fc portion
FFF	field-flow fractionation
FFFF	flow field-flow fractionation
FITC	fluorescein isothiocyanate
FoxP3	forkhead box protein P3
FSC	forward-scattered light
FSP-1	fibroblast specific protein-1
GAPHD	glyceraldehyde 3 phosphate dehydrogenase
GBD	global burden of disease
GC	glucocorticoids
gp130	glycoprotein 130
HGF	hepatocyte growth factor
HLA	human leukocyte antigen
HLA-G	human leukocyte antigen-G
HMGB1	high mobility group protein B1
HO-1	heme oxygenase-1
HSP70	heat shock protein 70
IC	immunocomplexes
ICAM/CD54	intercellular adhesion molecule 1
IDO	indoleamine 2,3-dioxygenase
IFN	interferon
IFNAR	interferon receptor
IFTA	interstitial fibrosis and tubular atrophy
Ig	immunoglobulin
IHD	ischaemic heart disease
IL	interleukin
ILV	intraluminal vesicle
iNOS	inducible nitric oxygen synthase
Io	ionomycin
iPSC	induced pluripotent stem cell
IRF	interferon regulatory factor
IRI	ischemia-reperfusion injury
IU	international unit/unit of enzyme activity
IV	intravenous
LAMP1/CD107a	lysosomal-associated membrane protein 1
LFA-3	lymphocyte function-associated antigen 3

LPS	lipopolysaccharide
MAC	membrane attack complex
Mafb	V-maf musculoaponeurotic fibrosarcoma oncogene homolog B
MAPCs	multipotent adult progenitor cells
MCP-1	monocyte chemoattractant protein-1
M-CSF	macrophage colony stimulating factor
MDDC	monocyte-derived dendritic cell
MDSC	myeloid-derived suppressor cell
MERTK	tyrosine-protein kinase Mer
MFI	mean fluorescence intensity
MHC	major histocompatibility complex
MI	myocardial infarction
miRNA	micro RNA
MMF	mycophenolate mofetil
MMP	matrix metalloproteinase
mRNA	messenger RNA
MSC	mesenchymal stem cell
MVB	multivesicular body
MW	molecular weight
NAD	nicotinamide adenine dinucleotide
NADP	nicotinamide adenine dinucleotide phosphate
NET	neutrophil extracellular trap
NFκB	nuclear factor kappa-light-chain-enhancer of activated B cells
NIR dye	near infrared dye
NK	natural killer cell
NLR	NOD-like receptors
NO	nitric oxide
NTA	nanoparticle tracking analysis
OEC	outgrowth endothelial cell
PAMPs	pathogen-associated molecular patterns
PAX5	paired box protein 5
PBMC	peripheral blood mononuclear cell
PBS	phosphate-buffered saline
PD-1	programmed cell death-1
PD-L1/2	programmed death ligand 1 or 2
PE	phycoerythrin
PEG	polyethylene glycol
PG	prostaglandins
PGE2	prostaglandin E2
PHA	phytohemagglutinin
Pi	inorganic phosphate
PI3K/Akt	phosphatidylinositol-4,5-bisphosphate 3-kinase/protein kinase B
PKH dye	Paul Karl Horan dye
PMA	phorbol 12-myristate 13-acetate
POM1	DYRK-family kinase pom1/CD39 inhibitor
PPARγ	peroxisome proliferator activated receptor gamma

PROSPR	protein organic solvent precipitation
PRR	pattern recognition receptor
PS	phosphatidyl serine
qPCR	quantitative polymerase chain reaction
RAB	Ras-related proteins in brain
rATG	rabbit anti-thymocyte globulin
RhoA	Ras-homolog family member A GTPase
RLR	RIG-I-like receptors
RNA	ribonucleic acid
ROS	reactive oxygen species
RPMI	Roswell Park Memorial Institute medium
RT	room temperature
SDS	sodium dodecyl sulphate
SEC	size exclusion chromatography
SEM	scanning electron microscopy
SNARE	soluble N-ethylmaleimide-sensitive fusion attachment protein receptors
SOD3	superoxide dismutase
SSC	side-scattered light
STAT	signal transducer and activator of transcription
TCR	T cell receptor
TFF	tangential flow fractionation
TfR/CD71	transferrin receptor
TGFβ	transforming growth factor β
Th	helper T cell polarization
TLR	toll-like receptor
TNFα	tumour necrosis factor α
Treg	regulatory T cell
TSG101	tumour susceptibility gene 101
TSG6	tumour necrosis factor-inducible gene 6
Tw	transwell
UCMSC	umbilical cord mesenchymal stem cell
VEGF	vascular endothelial growth factor
VLA	very late antigen-4/integrin α4β1
VPS4	vacuolar protein sorting-associated protein 4
WHO	world health organization
α-MEM	minimum essential medium Eagle alpha modification

GENERAL INTRODUCTION

GENERAL INTRODUCTION

Myocardial Infarction

Heart failure is an extended, incapacitating and ultimately deadly disease (mainly due to sudden cardiac death, >50%) that not only represents a drastic reduction in quality of life of the patient, but is also related to enormous direct and indirect economic costs and loss of lives worldwide each year. Heart failure is a chronic and progressive condition defined by the reduced efficiency of the heart muscle in pumping blood to meet the body's needs (Jessup and Brozena 2003). Currently, there is no accepted standard for the etiological classification of heart failure and patients are classified in four different –although not excluding- functional categories according to their clinical symptoms and limitations while performing physical activity: the NYHA score (New York Heart Association). It is complemented with the American College of Cardiology (ACC) and American Heart Association (AHA) classification of chronic heart failure, which also stratifies patients clinically and considers concomitant diseases and risk factors for disease prognosis (Tanai and Frantz 2015).

The most common cause of non-congenital heart failure is ischaemic heart disease (IHD). Other causes of heart failure are congenital, idiopathic, drug-induced (doxorubicin, alcohol) cardiomyopathies, valve heart diseases or disorders in the rate/rhythm of the heart (Tanai and Frantz 2015). IHD is the leading cause of mortality and morbidity for both men and women in Europe (**FIGURE 1**, WHO 2016). It is also the first cause of death worldwide, and although it is differently distributed depending on the geographical area it always appears within the top 10 (calculated according to the WHO regions, **FIGURE 2**). It is in the African region, where data is actually scarce, and people have a much shorter life expectancy (56.4 years compared to 70 years worldwide in 2015), that IHD is not the main cause of death. Instead, there is a high burden of life-threatening communicable diseases such as lower respiratory tract infections, HIV/AIDS, diarrhoea, tuberculosis, malaria, coupled to unmet basic sanitation, like safe water supplies, and malnutrition. Nevertheless, there is an increasing rate of noncommunicable diseases such as hypertension, diabetes and IHD due to the increasing life expectancy and change in diet, which indicates the increasing burden of the disease (WHO Regional Office for Africa 2014).

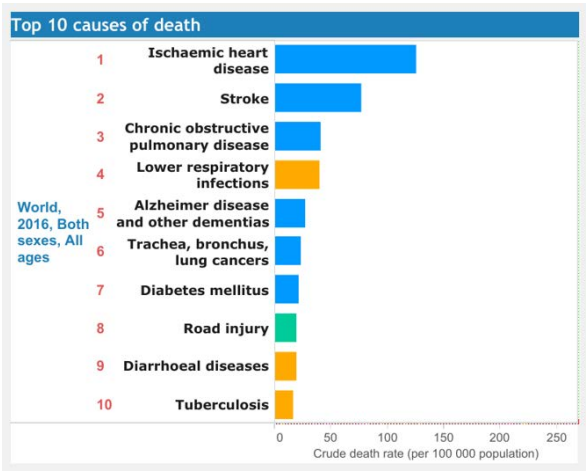

FIGURE 1 | Top 10 most common causes of death worldwide in 2016. Blue: noncommunicable, maternal, perinatal and nutritional conditions; Orange: communicable diseases; Green: injuries. Font: WHO webpage, July 2018.

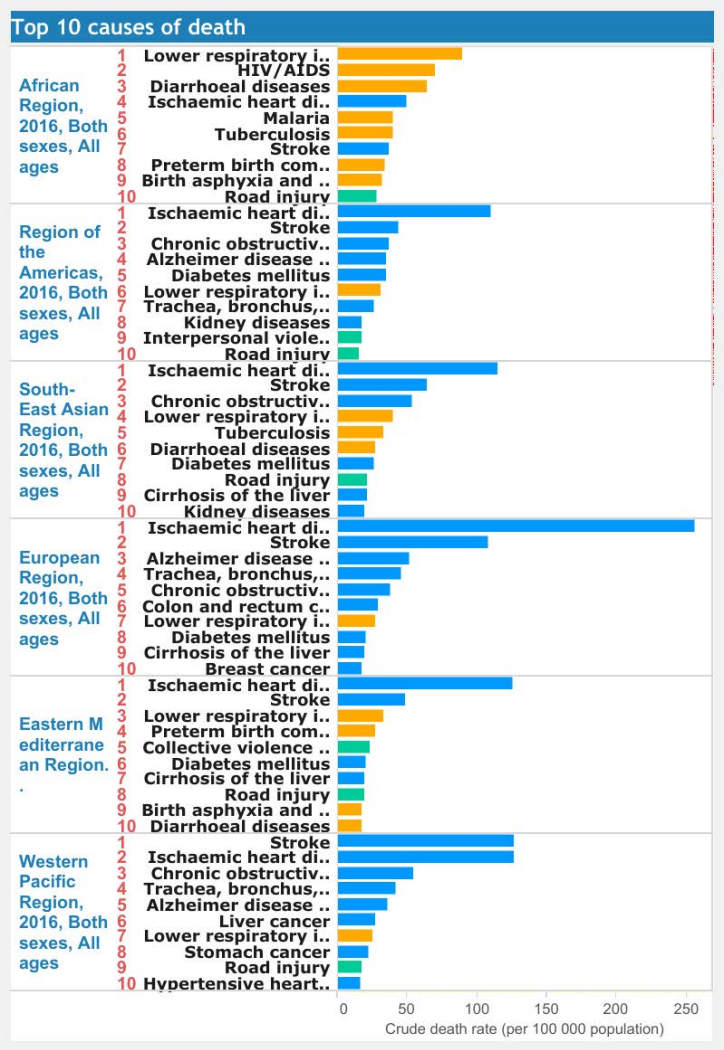

FIGURE 2 | Top 10 most common causes of death in each of the WHO regions in 2016. Blue: noncommunicable, maternal, perinatal and nutritional conditions; Orange: communicable diseases; Green: injuries. Font: WHO webpage, July 2018.

Specifically, in Spain, with a total population of 46.5 million, noncommunicable diseases are the main cause of death (92.8% of all deaths) with the leading five specific causes of death being IHD (14.6% of all deaths), Alzheimer disease and other dementias (13.6%), stroke (7.1%), chronic obstructive pulmonary disease (6.9%), and lung cancer (5.0%) according to the Global Burden of Disease (GBD) 2016. IHD appears also as the second cause of disability-adjusted life-years (DALYs), just after low back and neck pain (Soriano et al. 2018). Therefore, IHD accounts for a high prevalence and high incidence disease both country- and world-wise.

IHD occurs after hypoperfusion of the myocardium, mostly due to an acute or chronic myocardial ischemia. Myocardial ischemia, also known as myocardial infarction (MI) and popularly referred to as heart attack, is caused by a decreased blood flow and thus a lack of oxygen/nutrient supply to the heart after a thrombosis of the coronary arteries. This leads to cardiomyocyte death and produces a noncontractile collagen-rich fibrotic scar in the affected area of the myocardium. Heart failure following MI is linked to the development of adverse cardiac remodelling –changes in the structure and functioning- of both the infarcted and non-infarcted myocardium for the compensation of the sudden loss of contractile capacity and minimal regeneration of the

myocardium (Jessup and Brozena 2003). This maladaptive response after MI results in ventricular wall dilatation and narrowing, changes in ventricular shape towards increased sphericity and heart hypertrophy (Tanai and Frantz 2015). Therefore, this physiologic attempt at compensating the MI injury actually leads to an adverse progression that does not attain full restoration of cardiac function and can derivate in chronic or end-stage heart failure.

The MI pathology is initiated by the occlusion of the coronary arteries, which occurs after a blood clot is formed –generally an atheroma plaque- in the lumen of the artery, which stiffens, narrows and impedes normal blood circulation (Ibáñez et al. 2015). The main focus of public health programs in cardiology is thus to promote a healthy lifestyle to reduce atherosclerosis risk factors, educating for an equilibrated diet, regular exercise avoiding alcohol abuse and cessation of smoking. Nevertheless, when we are past prevention and the coronary obstruction is in place, time matters. If the obstruction of blood flow to the heart is prolonged, it leads to heart tissue necrosis and ultimately, cardiac arrest by mortal arrhythmias (ventricular fibrillation). Nowadays, treatments are therefore focused in the rapid reperfusion of the blocked artery (within the first 60 minutes following MI), which manages to save many lives. The main medical and interventional advances to minimize myocardial damage after MI, such as the importance of time managing, are the fibrinolytic/thrombolytic drug administration, the angioplasty-aided reperfusion (percutaneous coronary intervention) and the coronary artery bypass graft surgery (Jessup and Brozena 2003). However, when myocardial reperfusion is not fully achieved, new microthrombi from the release of fragments of the original thrombus can cause microvasculature damage, and also ischaemia-reperfusion injury (IRI) can occur, yielding cell apoptosis, ROS formation, calcium overload and cellular oedema (Ibáñez et al. 2015), all leading to chronic MI. To date, there are no definitive treatments available to fully restore cardiac function in chronic MI, in which the heart injury is well established, adverse remodelling has started, and current drugs only target on the symptoms of the progressing heart failure. Although greatly prolonging the patients' lifespan, they are merely palliative due to the absence of therapies to tackle the underlying cause of the disease. In this setting, the only therapeutic alternative is heart transplantation, which is highly limited by the shortage in compatible organ donors and needs complex organ rejection managing (Colvin et al. 2017). Therefore, improved knowledge on the pathophysiological processes occurring after MI is needed to unravel mechanisms that can be targeted by new treatments in order to prevent, rather than treat, heart failure. In this sense, the aim is to study mechanisms able to limit myocardial tissue injury and promote myocardial regeneration to restore heart function after MI.

Inflammatory response after Myocardial Infarction

Myocardial infarction triggers an intense inflammatory response that is essential for dead cell clearance post-IRI and the initiation of cardiac repair, but its timely suppression is critical to minimize post-MI remodelling and heart failure (N. G. Frangogiannis 2014b). Given the little regenerative power of the adult human heart, healing of the infarcted area leads to fibrogenesis, formation of a collagen scar that develops into cardiac remodelling. Therefore, mechanisms to modulate the immune system and inflammatory response after ischemic injury would limit the extent of tissue damage, promote intrinsic wound healing and prevent successive cardiac remodelling by diminishing the scar size. In fact, novel pharmacotherapeutic approaches target pro/anti-inflammatory cytokines, endotoxins, adhesion molecules and chemokines in an attempt to prevent the development of heart failure (Christia and Frangogiannis 2013).

In the past, therapies that looked promising in small and even large preclinical animal models unfortunately did not translate in clinical success, as maybe oversimplified targeting approaches were not successful in clinical trials. For instance, the modulation of the onset of inflammation by blockage of the pro-inflammatory TNFα looked promising in rat models of myocardial IRI. In these, TNFα inhibition (etanercept) immediately after MI had protective effects against IRI and preserved cardiac function by reducing apoptosis, extracellular matrix degradation and myocardial infarction area, by greatly decreasing oxidative stress and leukocyte infiltration (Berry et al. 2004; M. Yang et al. 2014). Nevertheless, it was only effective when administered right after arterial occlusion in the animal model, and did not translate into clinical benefit in patients with acute MI (Padfield et al. 2013).

The increasing knowledge in the dual role that inflammation plays in reaction to an injury has shown that has both detrimental and protective pathways, promoting either remodelling or repair of the infarcted heart. This actually accounts for the potential treatment of IRI of any other tissue/organ, such as other thrombo-embolic syndromes (peripheral vascular thrombosis, stroke) or organs for transplant (Kosieradzki and Rowiński 2008; Wanderer 2008), in which the modulation of the immune response has been proven to ameliorate the tissue/organ state after IRI.

The inflammatory response for cardiac repair occurs in a succession of events that overlap after IRI: it starts by i) the inflammatory phase triggered by tissue injury, necessary to clear up dead cells and extracellular matrix (ECM) debris during the first two weeks to prepare the tissue for ii) the proliferative phase, promoted by reparative macrophages that activate mesenchymal reparative cells (myofibroblasts and endothelial cells) to preserve the structure of the myocardium and angiogenesis to initiate cardiac healing, that is followed by the iii) the maturation phase, when a cross-linked collagen scar replaces the necrotic tissue of the infarcted area, completed by 4-8 weeks. As these phases overlap, repair and regeneration processes occur together with cellular apoptosis, autophagy, and necrosis thus the extent of tissue healing depends on whether cell death or regeneration prevails. While this immune response is necessary to clear up all dead cells and translate into tissue repair, the timely repression of the first inflammatory phase would protect the myocardium from excessive inflammatory injury, preventing enlargement of damaged tissue and advancing to the proliferative phase.

Innate immune response

The deprivation of nutrients and oxygen after occlusion of blood supply provokes mitochondrial disfunction, cellular oedema, acidosis, calcium overload and free radicals formation, which motivates rapid apoptotic and necrotic death of cardiomyocytes. The final stage of ischemic injury occurs during reperfusion, in which endothelial injury mainly develops. Tissue necrosis releases intracellular constituents and stress signals or "alarmins" to the extracellular space that constitute danger-associated molecular patterns (DAMPs), including reactive oxygen species (ROS), heat shock proteins, nuclear proteins (including HMGB1 (high mobility group protein B1) and histones), DNA and RNA, ATP and components of degraded ECM like hyaluronan (Wanderer 2008). DAMPs detection by neighbouring cells, immune cells and epithelial cells triggers their activation, secretion of pro-inflammatory mediators (IL1β, IL6 and TNFα) and recruitment of innate immune cells for the initiation of a sterile immune response (Wanderer 2008). Concomitantly, necrosis activates the Complement system, proteolytically activating potent anaphylatoxins (C3a, C4a, C5a) that amplify the inflammatory response.

The innate immune cells (neutrophils, natural killer cells, monocytes/macrophages, DCs, epithelial cells) are critical for the rapid recognition, containment and clearance of pathogens and damaged cells. For that end, they are equipped with an array of pattern recognition receptors (PRRs) that identify pathogen-associated molecular pattern (PAMPs) and DAMPs to detect pathogen invasion and tissue damage, respectively. DAMPs such as ROS activate oxidative stress signalling; HMGB1, extracellular DNA, RNA involve membrane-bound PRRs like toll-like receptor (TLR) and cytoplasmic PRRs like NOD-like receptors (NLR) and RIG-I-like receptors (RLR) signalling; and ATP is recognized through purinergic P2 (P2X and P2Y). PRR downstream signalling leads to innate cell activation, antigen capture and processing by antigen presenting cells (APCs) and cytokine/chemokine secretion, which initiates a proinflammatory response, innate cell recruitment and determines the prospective adaptive immune response.

Inflammatory signals recruit neutrophils to the infarct zone, and monocytes/macrophages shortly thereafter. Neutrophils accumulate in the first hours after onset of ischemia in response to the chemokines IL8/CXCL8 and CXCL1, that are markedly and consistently induced after 1h and persist beyond 24h after reperfusion of coronary artery occlusion in MI (N. Frangogiannis, Smith, and Entman 2002). Infiltration and cell adherence to the infracted myocardium occurs then thanks to the adhesion molecules L- and P-selectin and ICAM-1 expressed on activated epithelial cells and myocytes (M. Nahrendorf, Pittet, and Swirski 2010). Neutrophils would be generally in charge of rapid infection containment, and in this context of aseptic inflammation, they degrade ECM debris and clear up dead cells. To do so, neutrophils release proteolytic enzymes, generate ECM fragments and ROS, that generate a certain degree of bystander killing of surrounding live myocytes and amplification of inflammation (Christia and Frangogiannis 2013). This releases recruitment factors for monocytes/macrophages, peaking at 2-3 days (Carter-Monroe et al. 2010).

In an event of injury, circulating monocytes would respond to cell recruitment mainly through the chemokine receptors-ligands CCR1-CCL5, CCR2-CCL2/MCP-1, CCL7/MCP-3 and CCL12, CCR5-CCL5 and CX3CR1-CX3CL1 (Shi and Pamer 2011), then interact through adhesion molecules with the activated epithelium for extravasation (Selectins CD62E/P/L, Integrins CD11a/b, VLA-4 and ICAM-1/2, to name a few (Gerhardt and Ley 2015)) and infiltrate in the inflamed tissue, referred then as macrophages.

In the context of myocardial infarction, monocytes/macrophages enter the infarcted area in a recruitment depending on MCP-1/CCL2 secretion, recognized by CCR2 (Kaikita et al. 2004; Dewald 2005), and the binding the integrin VLA-4 of monocytes to the adhesion molecule VCAM-1, upregulated in the infarct (Matthias Nahrendorf et al. 2007). Monocytes are called out from circulation, but are also massive and rapidly deployed from spleen to participate in wound healing of the infarcted tissue (Swirski et al. 2009). Macrophages dominate the cellular infiltrate for the first two weeks after MI and participate in dead cell clearance as well as infarct wound healing to replace the necrotic area with scar tissue. In fact, macrophages have been found decisive in the timing of the response and switch from the initial inflammatory phase to its resolution and promotion of tissue repair mechanisms, and there are two non-exclusive observations that help explain this.

On one side, the initial acute inflammatory response has been shown to trigger a biphasic monocyte recruitment to the heart, with an early peak of circulating inflammatory $CD14^+CD16^-$ 'classical' monocytes followed by an increase of $CD14^+CD16^+$ 'non-classical' monocytes in patients (Tsujioka et al. 2009). Interestingly, the levels of $CD14^+CD16^-$ monocytes (representing the 90% of circulating monocytes (Mosser and Edwards 2008)) affected both the extent of myocardial salvage and the recovery of left ventricular function after MI. A similar temporal profile was observed in a mouse model of MI, with a first wave of inflammatory $Ly6C^{hi}$ and a second one of anti-inflammatory $Ly6C^{low}$ monocytes (Matthias Nahrendorf et al. 2007; Bönner et al. 2012). These studies advocate for an inflammatory-to-resolutive phase differentiation determined by the distinct subset of monocytes recruited at different stages of infarction (M. Nahrendorf, Pittet, and Swirski 2010).

On the other side, the switch from inflammation to tissue repair can rely on the high functional plasticity of monocytes/macrophages (**FIGURE 3**). They can promote inflammation as well as

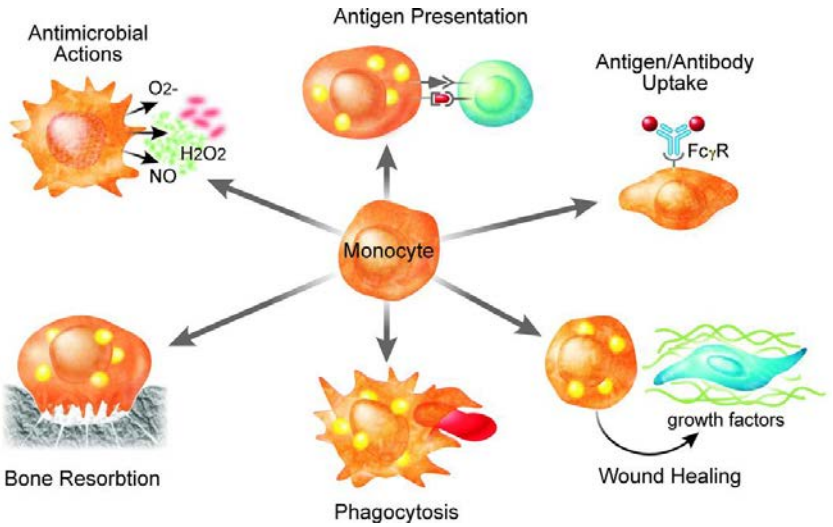

FIGURE 3 | Functional heterogeneity of macrophage activation. Monocytic cells give rise to resident and recruited macrophages in tissues, which display tremendous functional heterogeneity. Clockwise from top left. Macrophages provide a first line of defence against intracellular pathogens by generating an inflammatory and respiratory burst and initiating antigen presentation to activate adaptive immunity; by clearing immune complexes and downregulating inflammatory responses; and by promoting wound healing via elaboration of growth factors. A subset of tissue macrophages, such as splenic red pulp macrophages and osteoclasts, become highly specialized in their location and function. The splenic red pulp macrophages are adapted for clearance and recycling of senescent red blood cells, whereas osteoclasts are critical for remodelling of bone throughout adult life. Reprinted from Chawla et al. 2010 *Circ Res*.

resolution of inflammation and tissue healing depending on the temporal managing of their activation, effector function and metabolism, conventionally termed as classic or inflammatory M1 and alternative or anti-inflammatory M2 macrophage polarizations (Mosser and Edwards 2008). They are not definitive phenotypes, as switch from one to another can happen depending on the PRRs engaged, cytokine profile perceived and previous activation status of the macrophage, generating actually a continuous spectrum of different functional activation. Therefore, the classic dichotomy M1-M2 can be extended to different intermediate states of macrophage polarization, separated in as many groups as polarizing stimuli (Mantovani et al. 2004; Murray et al. 2014) or functional activities are defined (Mosser and Edwards 2008; Mantovani et al. 2013). While being aware of this complexity, in this thesis, macrophages are classified into inflammatory (M1) or wound healing (M2a) and regulatory (M2b/c) phenotypes (**TABLE 1**).

This way, an M1 polarization can be generated experimentally with IFNγ and LPS, inducing STAT1 signalling, IRF5 and NFκB activation. M1 macrophages are characterized by a high glycolytic metabolism, upregulation of class II MHC and co-stimulatory molecules, great production of pro-inflammatory cytokines (TNFα, IL1β, IL6, IL12 and IL23) and chemokines for

TABLE 1 | Summary of macrophage polarization. Depending on the stimuli perceived in the microenvironment, macrophages activate distinct transcription factors that lead to a more pro-inflammatory (M1) or resolutive, anti-inflammatory (M2) phenotypes with characteristic surface marker expression, cytokine/chemokine profiles and function. Data is referred to human macrophages.

	M1 **Inflammatory**	**M2a** **Wound healing**	**M2b/c** **Reparative**
Stimuli	IFNγ, LPS, TNFα	IL4, IL13	IL10, GC, IC, PG, efferocytosis, Ado
Signalling	STAT1 → IRF5	STAT6 → PPARγ	STAT3 → Mafb
Metabolism	Glycolytic	Oxidative	Oxidative
Surface markers	Class II MHC, CD40, CD80, CD86	CD206, CD23, CD204, TGM2	CD163, CD206, MERTK
Cytokine/ chemokine profile	TNFα, IL1β, IL6, IL12, IL23, CXCL9, CXCL10, CXCL5	IL10, TGFβ, IL1rα, VEGF, CCL17, CCL22, CCL24	IL10, TGFβ, CXCL13, CXCL16, CCL18
Th polarization	Th1/Th17	Th2	Treg
Function	Pro-inflammatory Low efferocytosis Pathogen and tumour cell cytotoxicity	Resolution of inflammation High efferocytosis Angiogenesis and tissue repair Fibrosis	Resolution of inflammation High efferocytosis Angiogenesis and tissue repair Fibrosis Tumour growth

Abbreviations meaning as they appear: IFN: interferon; LPS: lipopolysaccharide; IL: interleukin; GC: glucocorticoids; IC: immunocomplexes; PG: prostaglandins; efferocytosis: phagocytosis of apoptotic bodies; Ado: adenosine; STAT: signal transducer and activator of transcription; IRF: interferon regulatory factor; PPARγ: peroxisome proliferator activated receptor gamma; Mafb: V-maf musculoaponeurotic fibrosarcoma oncogene homolog B; MHC: major histocompatibility complex; CD: cluster of differentiation; MERTK: Tyrosine-protein kinase Mer; TNF: tumour necrosis factor; TGF: tumour growth factor; CXCL: C-X-C motif chemokine ligand; CCL: C-C motif chemokine ligand; Th: helper T cell polarization.

recruitment of effector cells, driving to a Th1/Th17 T cell polarization (Sica and Mantovani 2012) (see below for its relevance in the prospective Adaptive immune response). These inflammatory macrophages are critical for cytotoxic activity, pathogen killing and host defence against intracellular microorganisms, but their exacerbated activation can lead to host-tissue damage and immunopathologies such as autoimmune diseases (Mosser and Edwards 2008).

On the other side, M2 macrophages include wound-healing (M2a) as well as regulatory (M2b/c) phenotypes. M2a macrophages are induced by IL4 and IL13, resulting in STAT6 activation of PPARγ for alternatively activated macrophages, switched to oxidative metabolism (Varga et al. 2016). M2a markers include FcεRII, mannose and scavengers receptors (CD23, CD206, CD204) and TGM2, induced by IL4 in both mouse and human macrophages (F. O. Martinez et al. 2013). They produce pro-reparative cytokines IL10, TGFβ, IL1rα, VEGF and chemokines CCL17, CCL22, CCL24 that altogether results in Th2 polarization and tissue repair promotion (Murray et al. 2014).

Regarding M2c macrophages, there are many inducers described: IL10, glucocorticoids (GC), prostaglandins (PG), efferocytosis, adenosine. They can act alone or synergistically for STAT3 activation of Mafb and rendering M2c macrophages, with immunoregulatory functions. They are characterized by production of high levels of IL10, TGFβ and chemokines CXCL13, CXCL16, CCL18 to induce Tregs. Surface markers include high expression of endocytic receptors CD163, CD206, MERTK, indicative of their maintained high efferocytosis capacity. Unlike M2a macrophages, M2c macrophages mediate resolution of inflammation and tissue repair but do not contribute to production of ECM (Mosser and Edwards 2008). Nevertheless, when M2a/c macrophages action is unleashed, it can also cause allergies, fibrosis or tumour growth, respectively.

M2 macrophages can be further differentiated as M2b macrophages, specifically generated through FcγR ligation by immunocomplexes (IC) together with TLR stimulation (LPS). This renders alternatively activated macrophages that produce IL10 and low levels of IL12, inducing Th2-like immune responses (C. F. Anderson, Gerber, and Mosser 2002; Yue et al. 2017).

Back to myocardial infarction, the first macrophages to respond to pro-inflammatory IRI would be thus functionally defined as an M1 phenotype (**FIGURE 4**). They would be activated by the inflammatory milieu to deploy their effector functions: cytotoxicity and phagocytosis of injured and apoptotic cells (efferocytosis), production of reactive oxygen species (ROS), nitric oxide (NO), myeloperoxidase and pro-inflammatory mediators (Yan et al. 2013; M. Nahrendorf, Pittet, and Swirski 2010). M1 macrophages would dominate the first (1-3) days after IRI, whereas M2 macrophages would arise after that and predominate after 5 days (M. Nahrendorf, Pittet, and Swirski 2010). M2 macrophages would then promote resolution of inflammation for wound healing and tissue repair. There are different options that can occur for M1 to M2 switch. There is evidence showing that IL4 and IL13 are innate and rapidly produced in an event of aseptic tissue injury, even in absence of T cells (Loke et al. 2007). As aforementioned, these cytokines would promote M2a polarization. Also, efferocytosis has been widely associated to promote an M2 switch by the tolerogenic signals induced after clearance of phosphatidyl-serine (PS)-rich apoptotic bodies (Pujol-Autonell et al. 2013; Kumar, Calianese, and Birge 2017). Furthermore, in the context of tumour immune evasion, it has been shown that hypoxia and hyaluronan fragments (from degraded ECM) can induce regulatory macrophages (Knowles and Harris 2001; Kuang et al. 2007).

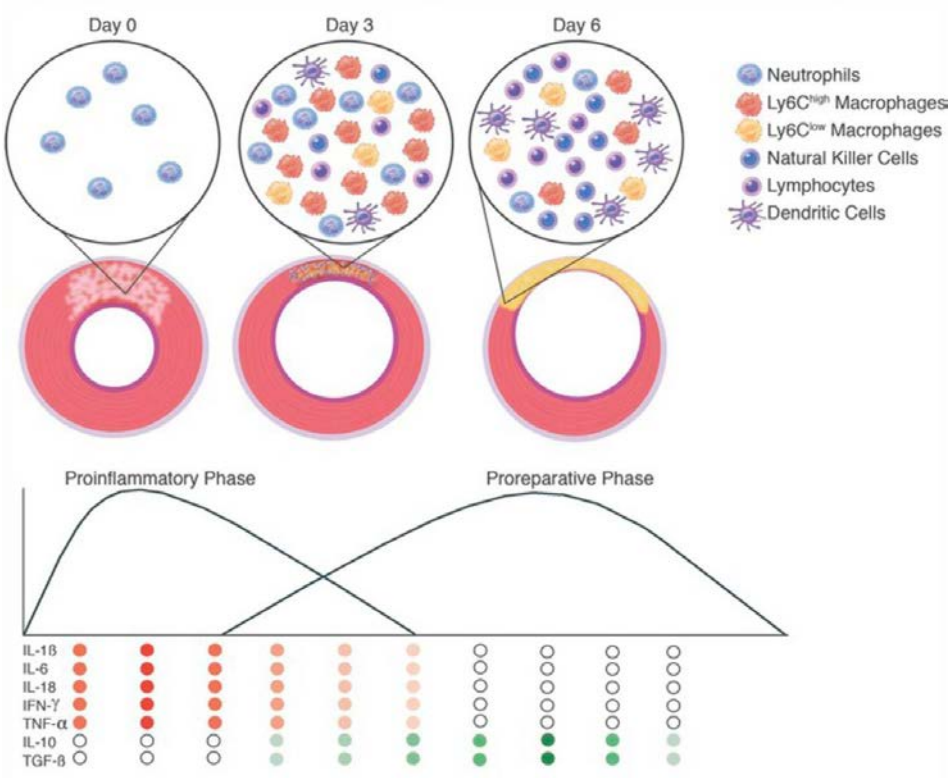

FIGURE 4 | Inflammation and remodelling after acute myocardial infarction: simplified depiction of cellular and cytokine responses. The immune cells infiltration (top) and cytokine response (bottom) reflect the evolution of the post-MI myocardium (illustration of a cross-section, middle), in which the initial pro-inflammatory phase triggered by post-IRI necrosis switches to a proliferative and then reparative phases, that ends up with scar formation. Neutrophils quickly infiltrate ischemic myocardium and release granule contents, which further exacerbate inflammatory signaling and establish chemotactic gradients to guide other leukocyte populations to the injury site. Proinflammatory cytokine levels, indicated by the changing intensity of the red circles, rapidly increase and cause further infiltration of immune or inflammatory cells into the infarct zone. Ly6C^{high} macrophages arrive and phagocytize cellular detritus, thereby removing necrotic cardiomyocytes from the injured area. Other leukocytes such as T lymphocytes, B lymphocytes, dendritic cells, and natural killer cells begin to arrive on approximately the third day after ischemic insult. Through mechanisms that are the subject of continuing study, these cells aid in the transition of the proinflammatory phase of healing to the pro-reparative phase of healing. This shift may be accomplished through modulation of macrophage phenotype from Ly6C^{high} to Ly6C^{low}, production of anti-inflammatory cytokines (including, but not limited to, those indicated by the changing intensity of the green circles), and inhibition of matrix metalloproteinases. IFN: interferon; IL: interleukin; TGF: transforming growth factor; TNF: tumor necrosis factor. Reprinted from Westman et al. 2016 *J Am Coll Cardiol* under CCC License.

All these point to a dynamic change of the infiltrated macrophage population, from an early M1 to a late M2 phenotype, which has been proposed to be mediated through negative feedback loops relying on SOCS proteins (Chawla 2010). The management of this timing, length and degree of activation might be helpful to modulate the extent of inflammatory injury and limit fibrosis (Westman et al. 2016). For instance, patients with prolonged pro-inflammatory mediators involved in macrophage recruitment have worse prognosis in cardiac remodelling (Pennock et al. 2013).

After the innate immune response has infiltrated the infarcted area and directly interact with wounded tissue, cells of the innate immunity can also act as antigen presenting cells (APCs) to initiate an adaptive immune response.

Adaptive immune response

The interaction of APCs with T cells relies in three signals: 1) cognate antigen recognition through processed peptide presentation in the context of an MHC molecule, 2) interaction with co-stimulatory or inhibitory molecules and 3) release of specific cytokine environment. Signal (1) allows the clonal activation of antigen-specific T cells according to their unique TCR, which needs to be accompanied by signal (2) for activation or rather inhibition of their response, as its absence leads to anergy or hyporesponsiveness. Then, activated but still functionally uncommitted T cells would integrate signal (3) to differentiate into a variety of T helper (Th) subsets. Th polarization leads to distinct effector mechanisms appropriate for eliminating the pathogen. For this, each Th subset is characterized by the production of a distinct set of cytokines and chemokines, programmed by transcription factors downstream of signal (3), that define a specific adaptive immune response (summarized in **TABLE 2** and reviewed in (Yan et al. 2013)). T cell activation can be mimicked *in vitro* by stimulation with anti-CD3 for signal (1) and anti-CD2/CD28 for signal (2), thus to study the influence of a given stimulus as signal (3). This way,

TABLE 2 | **Molecular signalling involved in the interaction of APCs with T cells.** The molecules expressed by APCs, their ligands and downstream effect on T cells are enumerated and classified according to their correspondence to the classically defined signals 1) peptide-MHC-TCR, 2) co-stimulatory molecule or 3) cytokine milieu.

Signal	APC molecule	Ligand on T cell	Effect on T cells
1	Peptide-MHC class I	TCR-CD3 + CD8	Stimulation of CD8 T cells
	Peptide-MHC class II	TCR-CD3 + CD4	Stimulation of CD4 T cells
2	B7-1/CD80 B7-2/CD86	CD28	Co-stimulation
		CTLA-4/CD152	Co-inhibition
	LFA-3/CD58	CD2	Adhesion, Co-stimulation
	CD40	CD40L/CD154	Co-stimulation
	PD-L1/B7-H1/CD274	PD-1	Co-inhibition
3	IL2	IL2R(α/CD25 + β/CD122 + γ/CD132)	Proliferation
	IFNα/β IL12	IFNAR(1 or 2) IL12R/CD212	Th1 polarization: IFNγ, TNFα Cytotoxic CD8 T cell: IFNγ, TNFα
	IL4	IL4R/CD124	Th2 polarization: IL4, IL5, IL13
	IL4 TGFβ	IL4R/CD124 TGFβR(I, II or III/β-glycan)	Th9 polarization: IL4, IL13, IL9
	IL6 TGFβ IL21 IL23	IL6R/CD126 + gp130/CD130 TGFβR(I, II or III/β-glycan) IL21R/CD360 IL23R + IL12Rβ1	Th17 polarization: IL8, IL17
	IL21 IL27	IL21R/CD360 IL27Rα + gp130/CD130	Tfh polarization: IL21, germinal center generation of B cells
	IL10 TGFβ	IL10R(α+β) TGFβR(I, II or III/β-glycan)	Treg polarization: IL10, TGFβ

Abbreviations meaning as they appear: APC: antigen presenting cell; MHC: major histocompatibility complex; TCR: T cell receptor; CD: cluster of differentiation; CTLA-4: cytotoxic T-lymphocyte-associated protein 4; LFA-3: lymphocyte function-associated antigen 3, PD-L1: programmed death ligand 1; IL: interleukin; IFN: interferon; IFNAR: interferon receptor; TGFβ: transforming growth factor β; gp130: glycoprotein 130.

there is higher control of T cell activation variability to compare stimuli than a mixed-lymphocyte reaction using *in vitro*-generated APCs. Other options are the ones that bypass T cell receptor signalling and act directly on intracellular mediators of activation, like PMA and ionomycin or PHA stimulation.

Physiologically, a Th1 polarization is generated to fight intracellular pathogens such as viruses and mycobacteria, Th2 responses are needed for antibody generation by B cells, Th2 and Th9 are meant for parasite infections, while tolerance and healing response induction would be mediated by regulatory T cells (Treg).

It is important to note that immunological diseases occur when these responses are exacerbated and not properly controlled. Persistent inflammation can lead to unresolved Th1 and Th17 cell activation, which causes sterile inflammation in autoimmune diseases or fibrosis, while uncontrolled Th2 and Th9 responses link to asthma and allergies. Also, untimely or misdirected activation of Tregs can cause fibrosis or even suppression of host tumour immune surveillance, allowing oncogenic cells immune evasion. Thus, host homeostasis relies on the fine tuning of immune balance, which depends on the temporal regulation of immune activation and suppression of both the innate and adaptive immune responses.

In the case of MI, the predominant $CD4^+$ T cell subsets that are initially present in the infarcted myocardium are mainly Th1 polarized (U. Hofmann and Frantz 2015). Moreover, experiments in RAG1 KO mice reconstituted with $CD4^+$ T cells from WT or IFNγ KO mice clearly demonstrate that Th1 $CD4^+$ T cells contribute to myocardial ischemia-reperfusion injury involving IFNγ expression (Z. Yang et al. 2006; Boag, Andreano, and Spyridopoulos 2016). On later stages, Tregs might appear, whereas Th2 and Th17 cells are usually minor populations (Tsujioka et al. 2009). The promotion of an earlier Treg polarization has been proposed to restrain post-MI inflammation to limit excessive ECM degradation and reduce cardiac remodelling (Dobaczewski et al. 2010; Boag, Andreano, and Spyridopoulos 2016).

Overall, exacerbated immune responses hamper regeneration of injured tissues, lead to allergies, autoimmune diseases and organ rejection. The innate immune cells act as initiators of this response, and APCs are responsible of linking the innate and adaptive phases of the immune response, providing signals to either trigger or down-modulate this response. Thus, in some clinical settings, such as regeneration after MI, modulation of monocyte polarization, DC maturation and/or T cell response are key points to prevent an unwanted immune response. There are many pharmacologically-based approaches that target common immune activation pathways for immune suppression (corticosteroids, mTOR inhibitors, calcineurin inhibitors or antiproliferative drugs to name a few (Monguió-Tortajada, Lauzurica, and Borràs 2014)). Nevertheless, these approaches lead to adverse side effects like opportunistic infections and tumorigenicity due to the systemic, unspecific immune suppression that they exert. Therefore, research on naturally occurring, physiological mechanisms for immune modulation may open the way for new targeted, fine-tuned biological therapies. In this context, mesenchymal stem cells appear in the spotlight for their immunosuppressive as well as regenerative capabilities.

Stem cells

A broad definition of stem cells includes a clonogenic population capable of self-renewal and differentiation to different cell lineages. Stem cells hold promising features, including regenerative properties, ability to give rise to cells of several lineages and immunomodulatory capacity, which opened the door to their study as cell therapeutic agents in various diseases. Stem cells can be roughly divided in two groups: embryonic stem cells and non-embryonic stem cells. Embryonic stem cells (ESCs), derived from the inner mass of the embryo in the blastocyst stage, are pluripotent with the capability to differentiate to any cell type of the postnatal organism. Given their origin, the use of ESC is restricted to preclinical studies by ethical issues. In contrast, non-embryonic stem cells or adult stem cells are derived from postnatal somatic tissue and are pluripotent, thus can give rise to multiple, but not all cell types. Also, differentiated somatic cells can be reprogramed to a stage similar to ESCs by over-expression of stem cell-related genes, obtaining induced pluripotent stem cells (iPS) (Takahashi and Yamanaka 2006). Within non-embryonic stem cells, mesenchymal stem or stromal cells (MSCs) and iPS have caught most of the scientific and medical attention for their therapeutic potential. Nevertheless, despite promising abilities for regeneration, iPS are rather used as a disease model due to their teratogenesis potential. Therefore, only MSC are prefferentially investigated and used in pre-clinical and clinical studies for their pro-regenerative and especially, immunomodulatory capacity.

Mesenchymal Stem/Stromal Cells

MSC are a heterogeneous population of non-hematopoietic multipotent progenitor stem cells with a fibroblast-like appearance that share three main characteristics as defined by the International Society for Cellular Therapy: plastic adherence, ability to differentiate into tissues of mesodermal lineages, such as adipocytes, chondrocytes and osteocytes and expression of several surface markers such as CD29, CD44, CD73, CD90 and CD105 among others (Dominici et al. 2006). Moreover, they are characterized by a low expression of class II MHC and lack of class I MHC unless stimulated, which endows them low immunogenicity. MSCs can be highly expanded *ex vivo*, maintaining their differentiation plasticity (Pittenger et al. 1999), and possess unique immunomodulatory and regenerative properties (Katarina Le Blanc and Mougiakakos 2012; Hoogduijn et al. 2010). All together makes MSCs a good candidate as a potential biological therapeutic for MI and other IRI-related diseases.

MSC were initially isolated by A. J. Friedenstein in the 1960's from bone marrow, but were soon found in almost any postnatal connective tissue. MSCs can be obtained from several compartments of the umbilical cord (umbilical cord blood, umbilical vein subendothelium and the Wharton's jelly (Troyer and Weiss 2008)), adipose tissue and solid organs (Watt et al. 2013). In the present thesis, the study is focused on MSCs from the subamnion connective tissue surrounding the umbilical vessels or Wharton's jelly (here namely UCMSC), which includes a primitive self-renewing cell population with the characteristics of MSCs, and cardiac adipose tissue-derived MSCs (cATMSCs), as they represent a mesenchymal-like cell population with intrinsic cardiomyogenic potential (Antoni Bayes-Genis et al. 2010),

While the immune capabilities of UCMSC have been poorly described yet, MSCs from bone marrow and adipose tissue have been widely demonstrated to possess immunosuppressive functions, which some argue to be boosted after encountering an inflammatory stimulus, such as *in vitro* priming by IFNγ (Menard et al. 2013; Krampera, Cosmi, et al. 2006; Polchert et al. 2008; Renner et al. 2009; Ryan et al. 2007; de Witte et al. 2015). Moreover, increasing evidence has shown that the restorative functions exerted by MSCs are not through self-replication and

differentiation of the injured tissue, but through the release of trophic factors to foster endogenous repair mechanisms and modulation of the host's immune response. In fact, MSCs get mainly trapped in lungs after intravenous administration, and very low numbers of administered MSCs are actually found in the injured tissue itself (Fischer et al. 2009; R. H. Lee et al. 2009; Eggenhofer et al. 2012). Nevertheless, they still manage to promote paracrine and systemic, long-lasting control of inflammation and enhanced tissue regeneration.

Immunomodulatory capacity of MSC

MSCs have been shown to be potent immune suppressors *in vitro* and *in vivo*. Increasing evidence has shown that the restorative and immunosuppressive functions exerted by MSCs are both cell-contact dependent and also mediated through the secretion of a broad range of soluble immunosuppressive molecules such as interleukin (IL)-6, transforming growth factor-β (TGF-β), prostaglandin E2 through COX2, hepatocyte growth factor (HGF), soluble human leukocyte antigen-G (HLA-G), tumour necrosis factor-inducible gene 6 (TSG6) and programmed death-1 ligands (PD-L1 and PD-L2) amongst others (Regateiro et al. 2011; Madrigal, Rao, and Riordan 2014; Meisel et al. 2004; K. Chen et al. 2010).

MSCs are also able to hydrolyse extracellular pro-inflammatory ATP towards anti-inflammatory adenosine through CD39/CD73 action. Murine MSCs exert potent immunosuppression by locally increasing nitric oxide (NO) through inducible nitric oxide synthase (iNOS), whereas human MSCs express indoleamine 2,3-dioxygenase (IDO), the rate-limiting enzyme involved in the catabolism of the essential amino acid tryptophan, required for cell proliferation, and resulting in the accumulation of N-formyl-kynurenine, which also suppresses T cell responses (Terness et al. 2002). Moreover, secreted chemokines and adhesion molecules can recruit and retain immune cells in the vicinity of MSC, where cell contact together with these paracrine mediators can down-modulate immune cell activation. A summary of the most representative immune mediators secreted by MSCs is listed in **TABLE 3**.

In terms of cellular target, MSCs can suppress the innate immune response by inhibiting neutrophil infiltration, oxidative burst and neutrophil extracellular trap (NET) release (Selmani et al. 2008; Németh et al. 2009; N. Wang et al. 2012; Sala et al. 2015; D. Jiang et al. 2016; Magaña-Guerrero et al. 2017), reducing NK cell activation, proliferation and cytotoxic activity (Aggarwal and Pittenger 2005; Sotiropoulou et al. 2006; Krampera, Pasini, et al. 2006; Spaggiari et al. 2008; Patel et al. 2010), and also controlling activation of the complement system by the production of the C3b-regulatory protein Factor H (Tu et al. 2010; Ma et al. 2018).

Several studies have shown as well the ability of MSCs to modulate effector cellular immune responses, as MSCs are able to inhibit mitogenic, antigenic and allogeneic T cell proliferation, reduce T cell migration and cytotoxic activity of $CD8^+$ T cells and promote apoptosis of activated T cells. They induce the shift from inflammatory Th1 and Th17 towards a Th2 polarization of T cell response, by reducing interferon gamma (IFN-γ) and IL-17 and promoting IL-4 secretion instead. MSCs are also capable of inducing the generation of regulatory T cells ($CD4^+$ $CD25^+$ $FoxP3^+$, IL-10 and TGF-β-producing Tregs), either through the direct action of IDO and TGF-β or helped by the generation of anti-inflammatory M2 monocytes, producers of anti-inflammatory TGF-β, IL-10 and CCL18.

Regarding antigen presenting cells, MSCs skew monocytes and macrophages towards an M2 anti-inflammatory phenotype (Nauta, Kruisselbrink, et al. 2006; Cutler et al. 2010; Melief, Schrama, et al. 2013), impair their differentiation towards dendritic cells and restrict their maturation

(Spaggiari et al. 2009). MSCs can directly modulate also the humoral effector immune response, as they inhibit B cell activation and proliferation, impair B cell maturation and differentiation to plasmablasts, thus reducing IgM and IgG production. In *in vitro* studies, it has been observed also the generation of IL-10-producing regulatory B cells by MSC co-culture. A summary of MSC effect on immune cell targets are enumerated in **TABLE 4**.

These properties make thus MSC an excellent candidate as a potential cell therapy for immune-related diseases such as the management of inflammation in autoimmune diseases, after tissue injury and necrosis and graft rejection after tissue/organ transplantation. Furthermore, extracellular vesicles secreted by MSCs have shown to mirror their immunosuppressive and reparative functions by packaging soluble and membrane-bound bioactive molecules, protected within and thus long-term functionally active (T. Li et al. 2013; Lener et al. 2015; Yáñez-Mó et al. 2015). On the other side, there are different strategies that can be used for efficient MSC delivery for cardiac repair.

TABLE 3 | **Immunosuppressive mechanisms of MSCs.** Soluble mediators secreted by MSCs and/or membrane-bound enzymes used by MSCs to modify soluble molecules related to immune modulation. The effect on target cells is indicated as well as its expression (constitutive/inducible when specifically known, and species).

Molecule	Target	Effect	Expression	Reference
CCL2/MCP-1	Monocytes	Recruitment	Constitutive (mouse and human)	(Rafei et al. 2008; H. J. Lee et al. 2015)
CD39, CD73	Monocytes, DC, B, T cells	Adenosine production for immune suppression	Constitutive (mouse and human)	(Amarnath et al. 2014; Kerkelä et al. 2016; Saldanha-Araujo et al. 2011; Huang et al. 2017)
CD59	MAC	Inhibition of MAC formation, final step of Complement system-mediated cell lysis	Human	(Moll et al. 2011)
COX2		Production of PGE2 – *see PGE2*	Constitutive and increased by IFNγ and TNFα(mouse)	(Karen English et al. 2007)
IL6	Monocytes	Impaired differentiation to dendritic cells	Mouse	(Djouad et al. 2007)
		Impaired differentiation to dendritic cells	Human	(Nauta, Kruisselbrink, et al. 2006; Y. Deng et al. 2016)
		M2 skewing		(Melief, Geutskens, et al. 2013a)
	T cells	Inhibition of mitogenic or allogeneic T cell proliferation	Mouse	(Djouad et al. 2007)
	Endothelial cells	Reduced leukocyte recruitment and transendothelial migration	Human	(Luu et al. 2013)
IL10	Neutrophils	Reduced neutrophil infiltrate by inducing IL10 expression to resident macrophages	Induced to resident macrophages (mouse)	(Németh et al. 2009)
			Not expressed by murine or human MSCs	(Krampera et al. 2003; Karen English et al. 2007; Németh et al. 2009; W. Deng et al. 2015)

HGF	Monocytes	M2 skewing	Mouse and human	(P.-M. Chen et al. 2014; Y. Deng et al. 2016)
	T cells	Inhibition of allogeneic proliferation	Constitutive (mouse)	(Karen English et al. 2007)
			Constitutive (human)	(Di Nicola et al. 2002)
HLA-G	NK cells	Reduced NK cytolytic activity	Human	(Selmani et al. 2008)
	T cells	Inhibition of allogeneic proliferation and induction of Treg		
IDO	NK cells	Inhibition of IL2-induced proliferation	human	(Spaggiari et al. 2008; Krampera, Cosmi, et al. 2006)
	Monocytes	M2 skewing: increased CD206, decreased CD80; increased IL10 and decreased TNFα production	Human	(François et al. 2012)
	T cells	Suppression of T cell proliferation by depletion of the essential aminoacid tryptophan and kynurenine accumulation	Inducible by IFNγ (mouse)	(Karen English et al. 2007; Wei Ge et al. 2010)
			Inducible by IFNγ (human)	(Meisel et al. 2004; Krampera, Cosmi, et al. 2006; Ryan et al. 2007; Menard et al. 2013; Huang et al. 2017)
Factor H	C3b	Inhibition of Complement activation: blockage of C3b activation, cofactor for C3b elimination, deployment of C3 convertase (C3bBb)	Constitutive and inducible by IFNγ (human)	(Tu et al. 2010; Ma et al. 2018)
M-CSF	monocytes	M2 skewing, impaired differentiation and maturation of dendritic cells	Constitutive (human)	(Melief, Schrama, et al. 2013; Nauta, Kruisselbrink, et al. 2006)
MMP	B cells	Reduced IgG/IgM production by MMP processing of CCL2 for reduced STAT3 and induced PAX5	Constitutive (mouse)	(Rafei et al. 2008)
iNOS	T cells	Nitric oxide production for T cell suppression through inhibition of Stat5 phosphorylation	Inducible by allogeneic T cell contact (mouse)	(Sato et al. 2007)

PD-L1/2	T cells	Inhibition of proliferation and cytokine production (IL2), T cell death	Constitutive (mouse)	(Augello et al. 2005)
			Inducible by IFNγ and TNFα (human)	(Karen English et al. 2007; Davies et al. 2017)
PGE2	NK	Inhibition of cytotoxic activity	Human	(Spaggiari et al. 2008)
	Monocytes	M2 skewing: increased IL10 and decreased TNFα and IL6 production	Mouse	(Németh et al. 2009)
		M2 skewing	Human	(Chiossone et al. 2016)
		Impaired differentiation to dendritic cells and maturation		(Spaggiari et al. 2009)
	T cells	Inhibition of allogeneic proliferation	Constitutive and increased by IFNγ and TNFα (mouse)	(Karen English et al. 2007)
			Constitutive and increased by IFNγ and TNFα (human)	(Aggarwal and Pittenger 2005)
TGFβ	T cells	Inhibition of allogeneic proliferation	Constitutive (mouse)	(Karen English et al. 2007)
			Constitutive (human)	(Di Nicola et al. 2002)
		Induction of Treg	Human	(Patel et al. 2010; Melief, Schrama, et al. 2013)
TSG6	Neutrophils	Reduced neutrophil infiltration and activation	Mouse	(Dyer et al. 2014; Sala et al. 2015)
			Rat *in vivo*	(N. Wang et al. 2012)
		Diminish ROS and NETs release	Human	(Magaña-Guerrero et al. 2017)
	Monocytes	M2 skewing, limit inflammation and fibrosis	Mouse *in vitro* and *in vivo*	(Qi et al. 2014)
		Decreased NF-κB-mediated inflammatory cytokines production through CD44 receptor signalling	Human	(Choi et al. 2011)
	T cells	Suppress alloreactive T cells, attenuate acute kidney rejection	Rat *in vivo*	(Kato et al. 2014)

CCL: C-C motif chemokine ligand; MCP-1: monocyte chemoattractant protein-1; CD: cluster of differentiation; DC: dendritic cell; MAC: membrane attack complex; COX2: cyclooxygenase 2; PGE2: prostaglandin 2; IFN: interferon; TNF: tumour necrosis factor; IL: interleukin; HGF: hepatocyte growth factor; HLA-G: human leukocyte antigen G; IDO:

indoleamine 2,3-dioxygenase; M-CSF: macrophage colony stimulating factor; MMP: matrix metalloproteinase; iNOS: inducible nitric oxide synthase; PD-L1/2: programmed death ligand 1/2; TGF: transforming growth factor; TSG6: tumour necrosis factor-inducible gene 6; ROS: reactive oxygen species; NETS: neutrophil extracellular traps; NFκB: nuclear factor kappa-light-chain-enhancer of activated B cells.

TABLE 4 | **Cellular targets of MSC immunosuppression.** The effects on immune cell targets of MSCs are listed, with the corresponding mechanism of action in the cases it was deciphered.

Target	Mechanism	Effect	Model	Reference
Neutrophils	IL10, TSG6 SOD3	Reduction of infiltration by inducing IL10 expression to resident macrophages, blockage of CXCL8 by TSG6 production. Prevention of neutrophil death, ROS, NETs and matrix degrading neutrophil elastase, gelatinase and myeloperoxidase release.	Mouse, *in vitro* and *in vivo*	(Németh et al. 2009; Dyer et al. 2014; Sala et al. 2015; D. Jiang et al. 2016)
	TSG6, SOD3, HLA-G	Reduction of infiltration	Rat *in vivo*	(N. Wang et al. 2012)
		Decreased oxidase-1, HO-1; reduced VEGF; reduced IL8, IFNγ and increased COX2 for a dampened oxidative; vascular; and inflammatory activity. Reduced neutrophil death, ROS and NETs release.	Human *in vitro*	(Khan et al. 2014; Magaña-Guerrero et al. 2017; D. Jiang et al. 2016; Selmani et al. 2008)
Natural Killer (NK) cells	Contact-dep; Contact-indep: IDO, PGE2, HLA-G, TGFβ1	Downregulation of NK activating receptors, inhibition of IL2-induced proliferation (through IDO), cytotoxic activity (through PGE2) and IFNγ production	Human *in vitro*	(Spaggiari et al. 2008; Patel et al. 2010; Krampera, Cosmi, et al. 2006; Aggarwal and Pittenger 2005; Sotiropoulou et al. 2006)

Monocytes/macrophages		Support survival in *in vitro* culture	Human *in vitro*	(Chiossone et al. 2016; Melief, Schrama, et al. 2013)
	Contact-dep; Contact-indep: HGF, PGE2, TSG6	M2 skewing: increased CD206, decreased CD80; increased IL10 and decreased TNFα production	Mouse *in vitro*	(P.-M. Chen et al. 2014; Németh et al. 2009; Qi et al. 2014)
	Contact-dep; Contact-indep: M-CSF, HGF, PGE2		Human *in vitro*	(Melief, Schrama, et al. 2013; Melief, Geutskens, et al. 2013a; Cutler et al. 2010; P.-M. Chen et al. 2014; Chiossone et al. 2016; François et al. 2012; J. Kim and Hematti 2009)
	IL6	Impaired differentiation to dendritic cells and maturation: reduced CD1a, HLA-II and costimulatory molecules expression and less T cell priming	Mouse *in vitro*	(Saeidi et al. 2013; Djouad et al. 2007)
	Contact-dep; Contact-indep: PGE2, IL6		Human *in vitro*	(X.-X. Jiang et al. 2005; W. Zhang et al. 2004; Spaggiari et al. 2009; Y. Deng et al. 2016)
	Partly by IL6 and M-CSF			(Nauta, Kruisselbrink, et al. 2006; Melief, Geutskens, et al. 2013a)
Dendritic cells		Reduced CCR7 expression to inhibit migration to lymph nodes	Mouse BMMSC *in vitro* and *in vivo*	(Chiesa et al. 2011; Karen English, Barry, and Mahon 2008; H. Li et al. 2008)
		Reduced cross-presentation to $CD8^+$ T cells	Mouse BMMSC *in vivo*	(Chiesa et al. 2011)
		Decreased MHC-II and costimulatory molecules expression, impaired cytokine production	Mouse BMMSC *in vitro* and *in vivo*	(Chiesa et al. 2011; W Ge et al. 2009; Aggarwal and Pittenger 2005; Karen English, Barry, and Mahon 2008)

T cells	NO, PGE2, IL6	Inhibition of mitogenic or allogeneic T cell proliferation	Mouse *in vitro*	(Sato et al. 2007; Krampera et al. 2003; Augello et al. 2005; Djouad et al. 2007)
	TSG6		Rat *in vitro*	(Kato et al. 2014)
			Baboon *in vitro*	(Bartholomew et al. 2002)
	Contact-dep: PD-L1; Contact-indep: PGE2, IDO, HGF, TGFβ, Adenosine, HLA-G		Human *in vitro*	(Di Nicola et al. 2002; Meisel et al. 2004; Grinnemo et al. 2004; Tse et al. 2003; Krampera, Cosmi, et al. 2006; K Le Blanc et al. 2003; Mancheño-Corvo et al. 2015; Kerkelä et al. 2016; Huang et al. 2017; Selmani et al. 2008)
		Impaired cytotoxic activity of $CD8^+$ T cells	Human *in vitro*	(Patel et al. 2010; Engela, Baan, et al. 2013)
		Impaired cytotoxic activity of γδ T cells	Mouse *in vitro*	(Xiaohuan Liu et al. 2015)
		Upregulation of CCR7 and CD62L for retention in secondary lymphoid organs	Mouse *in vitro*	(H. Li et al. 2008)
		Reduced CXCR3 (CXCL10-R) and adhesion molecules expression for reduced transendothelial migration	Human *in vitro*	(Benvenuto et al. 2015)
	M2/MDSC induction	Shift to Th2 from Th1 or Th17 polarization	Mouse *in vitro*	(Luz-Crawford et al. 2012; Xingxia Liu et al. 2015; Obermajer et al. 2014)
			Human *in vitro*	(Aggarwal and Pittenger 2005; Patel et al. 2010)
	IDO	Induction of Tregs (cont.)	Mouse *in vitro*	(W Ge et al. 2009; Luz-Crawford et al. 2013; Wei Ge et al. 2010)
	Contact-dep		Human *in vitro*	(Ghannam et al. 2010; K. English et al. 2009)

T cells (cont.)	Contact-indep: TGFβ, HLA-G, PGE2	Induction of Tregs (cont.)		(Patel et al. 2010; Engela, Hoogduijn, et al. 2013; Wei Ge et al. 2010; Selmani et al. 2008)
	Need M2 skewing (CCL18 production)			(Melief, Schrama, et al. 2013; Obermajer et al. 2014; Groh et al. 2005; Chiossone et al. 2016)
	IDO	Apoptosis of activated T cells	Mouse *in vitro*	(Akiyama et al. 2012; Lim et al. 2010; Fallarino et al. 2002)
			Human *in vitro*	(Plumas et al. 2005; Meisel et al. 2004; Augello et al. 2005)
		Promote survival and expansion of quiescent T cells	Mouse *in vitro*	(Nauta, Westerhuis, et al. 2006)
			Human *in vitro*	(Benvenuto et al. 2007; Crop et al. 2010)

B cells	Contact-dep: PD-1	Inhibition of mitogenic proliferation	Mouse *in vitro*	(Augello et al. 2005; Schena et al. 2010)
			Human *in vitro*	(M. Franquesa et al. 2015)
	IL1RA	Impaired B cell maturation and plasmablast differentiation	Mouse *in vitro*	(Luz-Crawford et al. 2016; Asari et al. 2009; Schena et al. 2010)
			Human *in vitro*	(M. Franquesa et al. 2015)
	MMP processing of CCL2 for reduced STAT3 activation and induced PAX5 transcription	Reduced production of IgG and IgM under strong stimulation	Mouse *in vitro*	(Rafei et al. 2008)
			Human *in vitro*	(Comoli et al. 2008; Rasmusson et al. 2007)
		Induction of Bregs	Mouse *in vitro*	(Guo et al. 2013)
	Contact-dep; Contact-indep: IDO		Human *in vitro*	(Luk et al. 2017; M. Franquesa et al. 2015; Peng et al. 2015)

Abbreviations meaning as they appear: SOD3: superoxide dismutase; IL: interleukin; CXCL: C-X-C motif chemokine ligand; TSG6: tumour necrosis factor-inducible gene 6; ROS: reactive oxygen species; NETS: neutrophil extracellular traps; HLA-G: human leukocyte antigen G; HO-1: heme oxygenase-1; VEGF: vascular endothelial growth factor; IFN: interferon; COX2: cyclooxygenase-2; IDO: indoleamine 2,3-dioxygenase; PGE2: prostaglandin E2; TGF: transforming growth factor; CD: cluster of differentiation; TNF: tumour growth factor; M-CSF: macrophage colony stimulating factor; HGF: hepatocyte growth factor; HLA: human leukocyte antigen; CCR7: C-C motif chemokine receptor 7; MHC: major histocompatibility complex; NO: nitric oxide; MDSC: myeloid-derived suppressor cell; Treg: regulatory T cell; PD-1: programmed death-1; STAT3: signal transducer and activator of transcription 3; PAX5: paired box protein 5; Breg: regulatory B cell.

Extracellular Vesicles

The term Extracellular Vesicles (EVs) refers to the broad range of membrane nanovesicles that cells can generate, containing cytosol and membrane molecules from the secreting cell. There have been multiple names used to refer to EVs, according to their origin, features or functions, and many still use the popular word "exosomes" to refer to all of them.

Exosomes were first described in the '80s by Dr Rose M Johnstone and Dr Phil Stahl groups, while studying the mechanisms by which the transferrin receptor (TfR; CD71) is recycled and shed during reticulocyte maturation. The two groups simultaneously described 30-100 nm vesicles originating in multivesicular bodies (MVB) and carrying TfR, that would be released upon MVB fusion with the plasma membrane, as beautifully shown by electron microscopy images (**FIGURE 5**) (Pan and Johnstone 1983; Harding, Heuser, and Stahl 1983; Pan et al. 1985). Back then, "exosomes" (termed by Johnstone et al. 1987) were thought to be mere garbage bags for reticulocytes to get rid of unwanted cell material in their process to differentiate into erythrocytes. Exosomes were kind of overlooked until late 1990's, when the works by Raposo et al. and Zitvogel et al. showed that exosomes have functional importance, as B cell-derived exosomes carry functional MHC-II molecules (Raposo et al. 1996) and dendritic cell (DC)-derived exosomes have, in addition, co-stimulatory molecules to generate specific T-cell responses (Zitvogel et al. 1998). Since then, exosomes gathered much more attention and research on the field has grown exponentially (**FIGURE 6**).

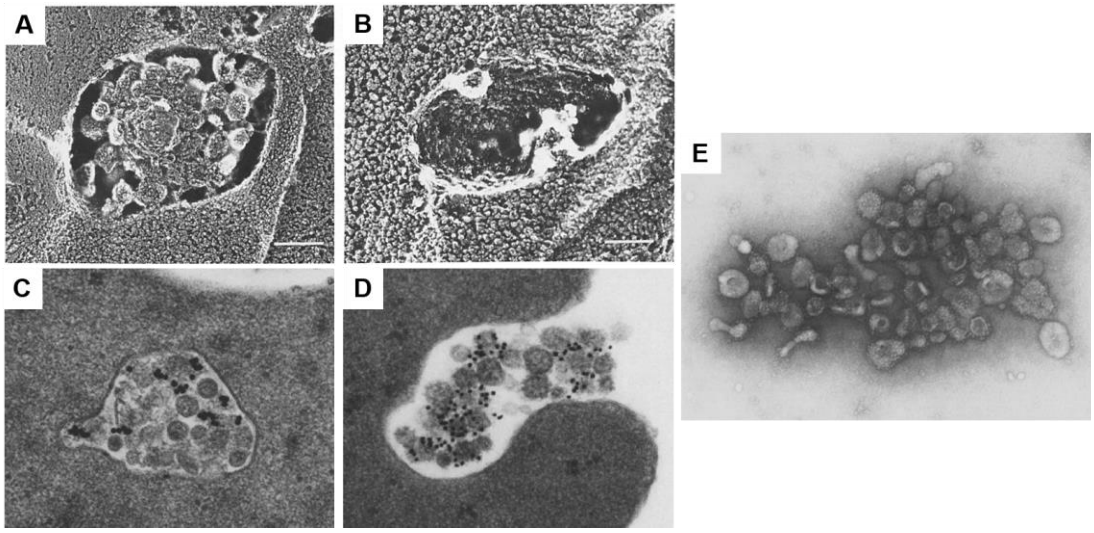

FIGURE 5 | **First descriptions of exosomes. (A-B)** Freeze-fracture, deep-etch TEM images of MVBs from rat reticulocytes. (A) MVB filled with numerous exosomes. Scale bar = 200 nm. **(B)** Bright white dots are 15-nm colloidal gold-conjugated anti-TfR antibodies, bound to the MVB walls and clustered in the exosome-to-be inclusions. Scale bar = 100 nm (Harding et al. 1983). **(C-D)** TEM images of sheep reticulocytes after internalization of 15-nm colloidal gold-conjugated IgG antibodies. **(C)** MVB containing exosomes together with internalized 15-nm colloidal gold-labelled IgG suggests the endocytic origin of exosomes (x85,000 magnification). **(D)** Fusion of MVB with the plasma membrane releases exosomes of ~50 nm together with the internalized gold-labelled IgG (x98,625 magnification) (Pan et al. 1985). **(E)** TEM images of negatively stained exosomes from sheep reticulocytes show cup-shaped vesicles bound to ^{125}I-labelled anti-TfR antibodies. Exosomes were isolated from a 12,000 x*g*-cleared supernatant, harvesting the void volume of a Sepharose 6B SEC and pelleted through a 100,000 x*g* ultracentrifugation for 1h (x123,000 magnification) (Pan et al. 1983). *Republication under CCC License.*

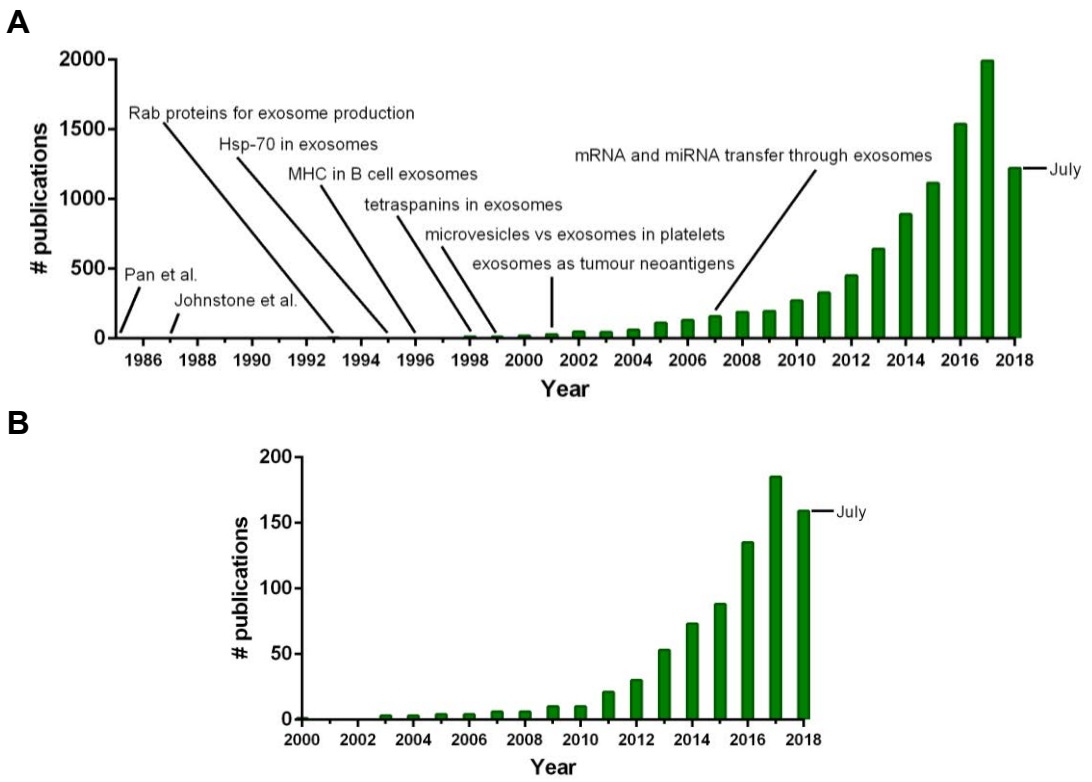

FIGURE 6 | **EV research has grown exponentially the last few years. (A)** The number of indexed publications that can be found after an unfiltered Pubmed search on "exosomes" is shown, as it still is the most common word used as reference for EV-related publications. The main breakthroughs in EV research are highlighted in their corresponding year of publication. **(B)** The number of publications on "exosomes" related to cardiovascular research represents around the 10% of the total EV literature.

Nowadays the knowledge on EV biology and biogenesis is much deeper, and is yet constantly expanding. The current consensus separates EVs in two different groups depending on their biogenesis: exosomes and microvesicles (MVs), although apoptotic bodies cannot be excluded from EV preparations. Exosomes, as mentioned before, are specifically those nanovesicles of intracellular origin, formed along the endocytic pathway through inward budding of the endosomal membrane, forming the intraluminal vesicles (ILVs) that constitute MVB (**FIGURE 7**). Exosome biogenesis in the endosomal compartments has been best-described to rely on the ESCRT (Endosomal Sorting Complex Required for Transport) machinery and its associated proteins. There are four ESCRT complexes with defined functions: ESCRT-0 clusters transmembrane proteins in the endosomal membrane in a ubiquitin-dependent manner, ESCRT-I and ESCRT-II induce bud formation, and ESCRT-III finally mediates vesicle scission. The process can restart again thanks to the accessory proteins, mainly ALIX (ALG-2 interacting protein X) and VPS4 (vacuolar protein sorting-associated protein 4), which dissociate and recycle the ESCRT complexes. Nevertheless, blockage studies of the ESCRT pathway have shown that there are also ESCRT-independent processes for inward budding of the MVB membrane. They involve lipid-mediated membrane curvature (cholesterol, phosphatidic acid, the sphingolipid ceramide), tetraspanins, flotillin or heat shock proteins (Trajkovic et al. 2008; van Niel et al. 2011; Perez-Hernandez et al. 2013).

Exosomes are then released when MVBs fuse with the plasma membrane instead of ending in the lysosomal route of degradation (**FIGURE 7**) (Van Niel, D'Angelo, and Raposo 2018). This process is orchestrated by members of the RAB family of GTPases and SNARE complexes (for

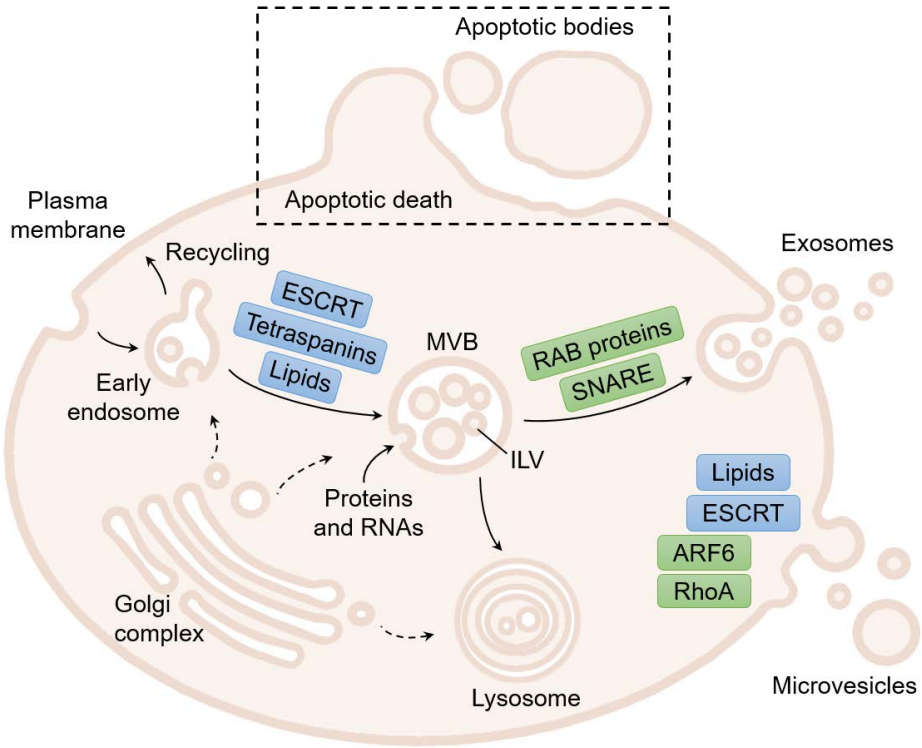

FIGURE 7 | Schematic representation of EV biogenesis and secretion. The proteins or family of proteins implicated in the formation (in blue) and release (in green) of EVs is shown. **Exosomes** originate within the endocytic pathway, by invagination of the endosomal membrane, forming intraluminal vesicles (ILVs) in a multivesicular body (MVB). ILV generation relies on the ESCRT machinery, tetraspanins and/or lipid-mediated membrane curvature, and are loaded with proteins and RNAs (miRNA, mRNA...) from the originating cell and/or the endocytic pathway. Then, the RAB proteins mediate the trafficking through microtubules, docking to sub-membrane actin and the SNARE proteins cause the fusion of MVBs with the plasma membrane, to release exosomes. Alternatively, early endosomes can recycle back to the plasma membrane, and MVBs can end up in the lysosome or autophagosome to degrade and recycle its cargo. **Microvesicles** are instead shedding directly from the plasma membrane. Although a clear mechanism is not fully defined, the loss of lipid asymmetry is important for the curvature of plasma membrane, while components of the ESCRT and SNARE machineries have been also related to the outward budding of the plasma membrane. Then, cytoskeletal remodelling through cleavage or depolymerization of cytoskeletal proteins (ARF6, RhoA) is needed for microvesicle release. The third type of EVs that can be found, **apoptotic bodies**, are generated upon apoptotic cell death. They are generally bigger than exosomes and microvesicles and carry "eat-me" and DAMP signals like damaged DNA. Abbreviations: ARF6: ADP-ribosylation factor 6; DAMP: damage-associated molecular pattern; ESCRT: endosomal sorting complex required for transport; ILV: intraluminal vesicle; MVB: multivesicular body; RAB: Ras-related proteins in brain (member of the superfamily of GTPases); SNARE: soluble N-ethylmaleimide-sensitive fusion attachment protein (SNAP) receptors; RhoA: Ras-homolog family member A GTPase. *Original graphical artwork.*

soluble N-ethylmaleimide-sensitive fusion attachment protein (SNAP) receptors). RAB proteins are membrane-bound regulators of general membrane trafficking, and are involved in the MVB interaction with cytoskeleton for intracellular vesicular trafficking and MVB docking to the plasma membrane). Then, SNARE proteins mediate fusion of MVBs with the plasma membrane (reviewed in Kowal, Tkach, and Théry 2014; Colombo, Raposo, and Théry 2014). Different members of the RAB and SNARE proteins have been involved in exosome release in distinct cell models (mainly cell lines), thus highlighting the varied subpopulations of exosomes that can be secreted from different MVB stages of endosomal maturation.

Therefore, thanks to the growing knowledge on exosome biogenesis there is more evidence on the heterogeneity of EV populations (Colombo et al. 2013), but at the same time, it provides exosome-enriched markers for their definition. To name a few, these can be hallmark molecules of early/late endosomes or MVBs like the tetraspanin CD63, lysosomal-associated membrane proteins LAMP1 and LAMP2; proteins associated to the ESCRT machinery such as TSG101 (ESCRT-I component), ALIX, syndecan, syntenin (ESCRT-III-associated); ESCRT-independent tetraspanins (CD9, CD63, CD81) or Flotillin; mechanisms for inclusion of soluble cytosolic proteins into exosomes like ubiquitinated proteins and chaperones (HSC70, HSP70); Rab proteins (RAB2B, RAB5A, RAB7, RAB9A, RAB11, RAB27A/B, RAB35) or SNARE proteins (VAMP7, YKT6).

Microvesicles (MVs), on the other hand, bud directly from the plasma membrane and have a wider size range than exosomes do, from 50nm to up to 1µm (**FIGURE 7**). MV release is quickly induced after stimuli such as calcium ionophores, but the exact mechanism for MV formation and shedding remains not fully deciphered. The major mechanisms described so far for MV release is relying on a rise in intracellular calcium that modulates lipid-metabolism enzymes for lipid raft formation: it stimulates floppase and scramblase activity while inhibiting flippase, which generates a local loss of membrane lipid asymmetry. The phosphatydilserine exposure, together with cholesterol and phosphatidic acid clustering induces membrane curvature for MV budding. Finally, cytoskeleton remodelling through cleavage or depolymerization of cytoskeletal proteins (ARF6, RhoA) releases MVs (Hugel et al. 2005). Some have described the use of the ESCRT and SNARE machineries (TSG101, VPS4 or RAB22A, but independently of ESCRT-0) for the outward budding of MVs (Booth et al. 2006; T. Wang et al. 2014). Others have proposed a membrane fission event similar to the abscission step occurring during cytokinesis (Muralidharan-Chari et al. 2010). Although some claim MVs-enriched markers are thus phosphatidylserine -enriched membranes and annexins, MVs are though indistinguishable from exosomes because they are enriched in classic exosome markers such as CD63, CD81, TSG101, and have similar size and density.

Finally, EVs can also include apoptotic bodies, which originate throughout the membrane blebbing process upon caspases-controlled cell death induction, apoptosis (**FIGURE 7**). Apoptotic bodies have a diameter of 1 to 5 µm, contain condensed DNA, are rich in phosphatydilserine in the outer leaflet of the membrane and have a density between 1.16-1.8 g/ml, which partly overlaps with that of exosomes and MVs (Edwin van der Pol et al. 2012). Therefore, apoptosis induction must be controlled specially in *in vitro* EV production to avoid artefacts coming from apoptotic bodies contamination instead of non-death-related EVs.

EVs are released by all cells and species studied so far (from bacteria and yeast to plants and mammals) as vesicular formation, trafficking and fusion mechanisms are evolutionary conserved across species. In multicellular organisms, EVs have been found in all types of biofluids (Yáñez-Mó et al. 2015). Due to their small size and nature, EVs from different cell sources can be found systemically with protected, intact cargo and functional properties from the originating cell: membrane-bound and soluble proteins, nucleic acids and lipids (**FIGURE 8**). Therefore, EVs are being envisioned as potential non-invasive sources of biomarkers and also as cell-free therapeutic platforms. Amongst their advantages to cells as therapeutic agents account the fact that they would be unchanged by the microenvironment once administered, no concern on embolism or differentiation, better biodistribution, easy to handle and store, and sterilisable by filtration.

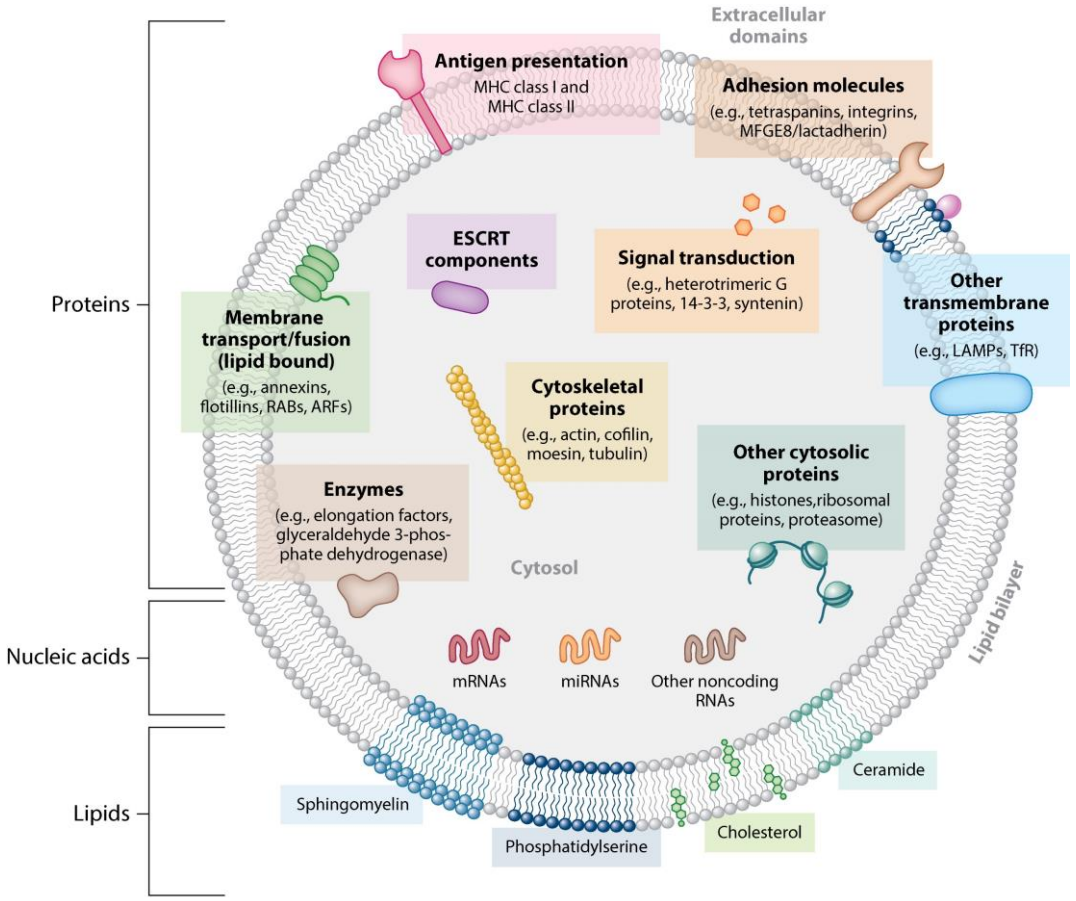

FIGURE 8 | **Representation of EV composition.** EVs contain cytosolic and membrane proteins, lipids and RNAs from the cell they originate from, thus with specific cargo of a given tissue, cell type and activation state. EV markers include hallmarks of the endocytic pathway and of the plasma membrane, indicative of their biogenesis. Reprinted from Colombo M, et al. 2014 *Annu Rev Cell Dev Biol* under CCC License.

Methods for EV isolation

The high heterogeneity of EV populations found in a biofluid in terms of sizes, cargo content and EV markers reflects the different cell and subcellular origins that they have (Colombo et al. 2013; Willms et al. 2016; H. Zhang, Zhang, and Lyden 2018). There are different EV isolation methods, relying either on the physical or molecular characteristics of EVs for their harvest (D. D. Taylor and Shah 2015; Willms et al. 2018), but due to their small size, the purification of EVs is a challenging enterprise. An agreement on a gold-standard method is still missing since every EV isolation protocol might have a certain bias toward subsets of EVs or contamination of non-vesicular particles. Next, the main characteristics of EV isolation methods are explained, and a succinct summary of the most widespread methods is depicted in **FIGURE 9**.

Differential ultracentrifugation (dUC), based on sedimentation of solutes including EVs at a high centrifuging force, was the first described technique for EV isolation, and thus most commonly found in the literature (Gardiner et al. 2016). However, this method is relatively time-consuming, operator-sensitive, requiring prior training and the availability of a specialised ultracentrifuge, which limits processivity and its scaling up to the clinical setting. There are plenty of protocols using different rotor types, washing steps, centrifugal g-forces, time and clearing factors (k-factor) that need to be adapted to the volume and viscosity of the sample (Momen-

Heravi et al. 2012) and thus can influence the yield and purity of vesicles with distinct sedimentation coefficients (Cvjetkovic, Lötvall, and Lässer 2014; Baranyai et al. 2015; D. D. Taylor and Shah 2015). The rough consensus consists on two first rounds of 400 x*g* and 2,000 x*g* to eliminate cells and debris, respectively, with an optional centrifugation at 10,000 x*g* to obtain microvesicles, and then a UC of 100,000 x*g* for 1-2h to obtain an EV pellet that can be further resuspended and washed in a final UC of 100,000 x*g* for 1-2h (Théry et al. 2006). Nevertheless, it has been shown that added rounds of UC yields extra amounts of EVs, indicating the inefficient, low recovery of the method (Baranyai et al. 2015; Welton et al. 2015). Given that the sedimentation efficiency parameters are not standardized, the down-stream analyses of these varying preparations can yield discordant results and misleading conclusions. Moreover, there are growing evidences in the field showing that centrifuging at such high speeds can negatively affect the intactness of EVs. dUC might lead to aggregation and co-precipitation with soluble proteins present in the biofluid, as albumin in plasma, or even cause vesicle rupture or fusion with contaminants and other proteins, affecting the physical properties of the exosomes and the downstream analysis of the preparation (Baranyai et al. 2015; Linares et al. 2015; Edwin van der Pol et al. 2012).

On the other side, there are the **precipitation-based protocols**, which are user-friendly, cheap and easy to implement in the clinics, firstly described to attain the highest recovery. The most used method is the polyethylene glycol (PEG)-based volume exclusion precipitation, while there have been also described the salting-out neutralization with sodium acetate (NaAc) and the protein precipitation with organic solvents (PROSPR). They all allege for a high recovery but not as much purity or EV integrity, as it basically precipitates all soluble particles, including EVs -and PEG as the precipitating agent-, to a pellet (Gámez-Valero et al. 2016). Variations of the PEG method can be found in isolation kits available from different companies: ExoQuick (patent number: US20130337440 A1) and Total Exosome Isolation (TEI; US20130273544 A1) reagents contain volume-excluding polymers (e.g.: dextrans, or polyvinyls), the Urine Exosome RNA Isolation kit from Norgen or the miRCURY Exosome Isolation kit from Exiqon. The precipitating agent is hardly removed from the final preparation, and as the pellet is obtained by centrifugation or filtration it is commonly contaminated with off-target protein aggregates. Nevertheless, these methods, with high translational potential given their manageable standardization and scalability, are being studied and compared with dUC to switch to an easier EV isolation method.

In terms of recovery and purity of the EV sample, dUC yields a lower recovery rate but higher purity compared to commercial kits based on polymeric precipitation, although contaminating proteins are still found in the EV pellet (Tang et al. 2017; Helwa et al. 2017). Depending on the principle and affinity of the isolation method, preparations vary enormously, including subpopulations with different protein contents, enriched in different EV protein markers (Royo et al. 2016). In addition, their combination with different RNA extraction methods changes RNA yield and purity, with discordant small RNA profiles and miRNA content (Tang et al. 2017), and RNA levels might not even correlate to sample size (Helwa et al. 2017). Therefore, although they are easy to implement, precipitation-based isolation might not be the right method of choice for descriptive nor functional analysis of EVs.

There are then more stringent methods, like floatation in a density barrier or in a density gradient after dUC, that allows improvement of EV purity and classification of EV subpopulations based on exosomes having densities between 1.1 and 1.19 g/ml while protein at 1.3 g/ml. The **floatation in a sucrose cushion** (discontinuous UC) allows the separation of EVs from protein aggregates,

based on their differential floatability on a 30% sucrose-D_2O solution (density, 1.210 g/cm^3). This way, non-EV material like protein or protein-RNA aggregates that would be co-purified in the dUC pellet is removed. For a more refined purification or fractionation of the different subpopulations of EVs, the **density gradient (DG) floatation** method can be employed. DG separates according to their physical characteristics (size, shape and density), in which EVs migrate to their equilibrium buoyant density in a continuous (optiprep – iodixanol, for higher resolution) or discontinuous gradient (20-60% sucrose layers), with EV finding equilibrium at the 35-40% sucrose layer as already described in the early definition of exosomes (Pan and Johnstone 1983). The sample loading can be performed for a bottom-up or a top-down migration, and the

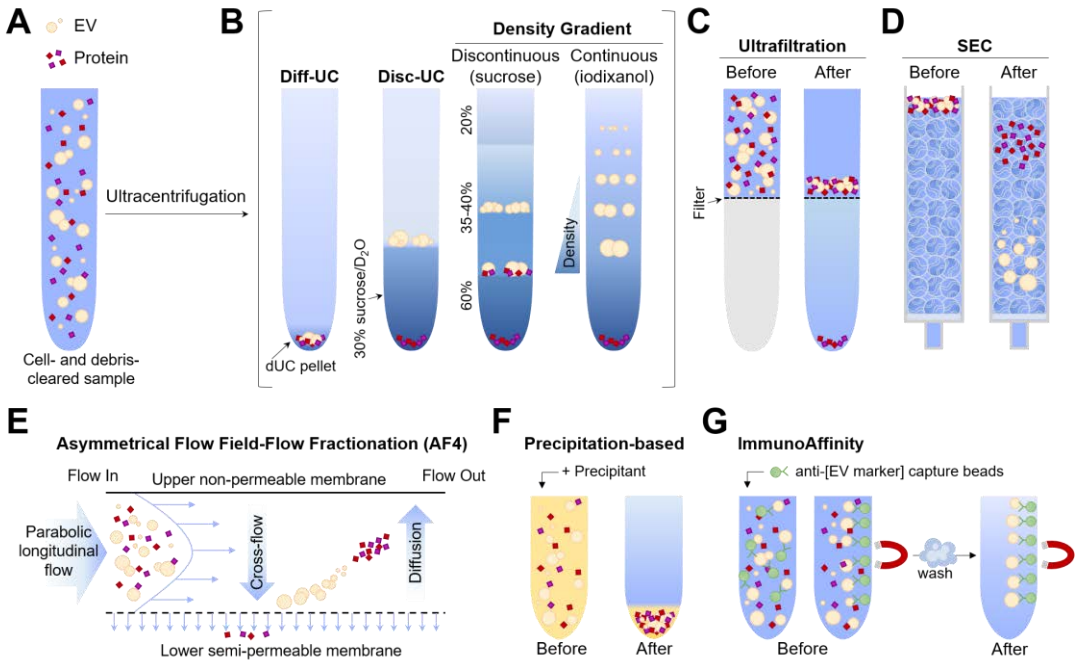

FIGURE 9 | Graphical summary of mainly used EV isolation methods. (A) The starting sample is a cell- and debris-cleared biofluid containing EVs and proteins in suspension. **(B)** Ultracentrifugation renders an EV pellet that also contains proteins (dUC pellet), that can be further purified by discontinuous ultracentrifugation (floatation) in a sucrose cushion or by density gradient (DG) ultracentrifugation: in a discontinuous gradient using different sucrose % solutions or in a continuous, self-making gradient using iodixanol (optiprep). This way, proteins and the different EV populations are separated by their density. **(C-E)** Ultrafiltration, Size-exclusion chromatography (SEC) and Asymmetrical Flow Filed-Flow Fractionation (AF4) separate molecules by their hydrodynamic radius (size). **(C)** Ultrafiltration is a dead-end filtration system that allows the separation of molecules according to the molecular weight cut-off (size) of the filter pore used. It renders a mixed sample of EVs and proteins, but allows great sample volume reduction. **(D)** In SEC, the first to elute are the molecules bigger than the matrix pores (EVs), while smaller particles within the fractionation range (proteins) get slowed down by entering the matrix bead pores, and so elute later on. **(E)** In AF4, a cross-flow (field) perpendicular to the longitudinal laminar flow forces particles towards the semi-permeable membrane. Particles smaller than the membrane pore are removed through the membrane. Retained ones migrate away due diffusion, and flow in the equilibrium position of the two forces (field and diffusion) according to their size. The velocity of the longitudinal flow increases parabolically, thus smaller particles, in the centre of the flow, are carried faster and elute before bigger ones. This way, proteins and differently sized EV populations are separated. **(F)** Precipitation-based isolation relies on the addition of water-excluding precipitants like PEG to concentrate all particles in one pellet. **(G)** Immunoaffinity isolation is based on EV capture using a specific antibody that recognizes an EV-specific marker, coupled to beads that can be separated by centrifugation or magnetically (like depicted). Given the lack of pan-EV markers, not all EV populations are isolated. *Original graphical artwork.*

gradient ranges adjusted for the distinction of EV subpopulations according to the viscous solution used to form the gradient, considering to always wash it off for EV functional analysis to reduce osmotic pressure, toxicity and potential methodological artefacts. These methods are mainly used in research studies addressing the basic science of EV heterogeneity and biology, as can differentiate exosomes from other EV types (Bobrie et al. 2012; Aalberts et al. 2012; Jeppesen et al. 2014; Willms et al. 2016). However, they are surely difficult to translate into the clinics given their more expensive and time-consuming costs, their low and operator-dependent yield, the need of an ultracentrifuge and lack of automatization.

Besides the methods that rely on the physical characteristics of EVs for their isolation, there are also techniques based on the analysis and/or separation of specific EVs according to their surface protein expression. The study of the EV subpopulations that DG allows and the research on EV biogenesis has contributed to the knowledge of markers enriched on EVs, which can be used in **immunoaffinity isolation** of EVs. Immunoaffinity isolation can be used in small volumes, in an analytics (ELISA-like) approach but also can be coupled to magnetic isolation, which renders an EV preparation that can be used for content or even functional downstream analysis (Koliha et al. 2016). Nevertheless, a pan-EV marker has not been found yet, so the EV preparations obtained in this case is always a biased EV subpopulation expressing the marker(s) used for isolation. There are different kits already available in the market using mainly antibodies against the tetraspanins CD9, CD63 and CD81 alone or in combination for "total" EV fishing from a biofluid (Wiklander et al. 2018). Other approaches use cell/tissue-specific markers to isolate or detect only the EVs coming from a target cell/tissue of interest, which is a quite attractive option on a pathological context, such as cardiovascular diseases or cancer. Although promising, this technique is still missing specific and fully deterministic EV markers, which biases EV biology study and biomarker screening and also, being still the most expensive method, deters its wide use in the clinics.

There are relentless efforts put in detection and isolation of EVs by **flow cytometry**, as it would allow high-throughput, multi-parametric analysis and separation of single EVs based on their surface composition. Nevertheless, their submicron size and low refraction index are major drawbacks in using this technique (Welsh et al. 2017). The first issue is that particles of <600nm (EVs) fall below the detection limit of the forward/side scattered (FSC/SSC) light detectors, with scattered light signals overlapping with the buffer's and electrical noise in the current sensitivity of flow cytometers. This can be solved by working with fluorescently-labelled EVs, which allows to use a fluorescence rather than the FSC or SSC trigger channel for EV detection. The second problem is to find proper size-standardization beads of adequate refractive index to better correlate scatter units to EV diameter and signals between instruments (E. van der Pol et al. 2018). The third problem of their small size is swarm detection in current fluidics systems. This means that more than one particle is analysed at once, something easily avoided in cell analysis with the doublet exclusion gating, but not possible in EV analysis due to the negligible differences between the FSC-A/HW nor SCC-A/H/W signals and interference of non-vesicular in the light scatter and fluorescence parameters. This can be improved by serially diluting the EV sample to work on the EV concentration that has a linear correlation with EV detection numbers (Libregts et al. 2018). There are also modified high resolution flow cytometers for the specialised analysis and sorting of EVs, with dedicated fluidics (i.e. varying nozzle size and sheath pressure), but still relying on stained EV preparations that thus need proper controls to minimize dye or antibody-related artefacts (Nolte-'t Hoen et al. 2012; Kormelink et al. 2016; Higginbotham et al. 2016). Therefore,

this powerful technique needs still optimization and standardization for its full work on the EV field.

Alternative methods have been established in recent years to replace traditional EV isolation techniques, looking for more user- and EV-friendly procedures. There are methods gaining interest that separate EVs according to their size relying on the correlation between elution volume or diffusion coefficient and the molecule's hydrodynamic radius, without the need of ultra-high centrifugations nor content-based selection of EV subpopulations. These are size-exclusion chromatography (SEC, also known as gel filtration) (Grubisic, Rempp, and Benoit 1967; Böing et al. 2014), ultrafiltration, flow field-flow fractionation (FFFF, also known as cross or tangential flow filtration, TFF) (Giddings and Myers 1976) and its lately evolved version, the asymmetrical flow FFF (AF4) (H. Zhang, Zhang, and Lyden 2018).

The isolation by **size-exclusion chromatography (SEC)** is based on the differential elution profiles of particles of different size running through a porous polymer, constituting the stationary phase (also known gel filtration matrix) of the SEC column. Small particles, such as proteins, are slowed down by entering the pores of the polymer, so they elute later on than EVs, that, bigger than the polymer's pores, travel quicker and so elute first (Grubisic, Rempp, and Benoit 1967). There are different stationary phases that can be used (**TABLE 5**). Sepharose CL-2B, was the first one to be employed for successful EV isolation with better purity and recovery than dUC (Böing et al. 2014; Muller et al. 2014). Although this is still the main matrix type employed, there are some studies arguing the use of other polymers such as sepharose 6B as initially described (Pan and Johnstone 1983), or sepharose CL-4B, Sephacryl S-400 for a more refined separation of particles from serum and plasma, to avoid co-elution with common contaminants such as lipoproteins or albumin (Baranyai et al. 2015). Also, SEC can be used in a downstream separation of EV subpopulations according to their sizes, than can resemble that obtained by DG (Willms et al. 2016; Willis et al. 2017).

SEC is scaling up to be more widely used for EV fractionation, as it offers a simpler, quicker, purer and more functional, untouched EV product than traditional methods. Moreover, SEC would be easily translated to the clinics as it does not require special equipment and is relatively cheap. Samples to be fractionated can be concentrated before loading to SEC, by means of dead-end ultrafiltration for small volumes (≤500ml) or TFF, which is scalable for larger volumes, using different pore sizes.

TABLE 5 | Classic stationary phase polymer types used for SEC isolation of EVs.

	Polymer type	Matrix bead size (μm)	Fractionation range (kDa)[1]	Exclusion limit (kDa)[1]
Sepharose CL-2B	2% cross-linked agarose	60-200	70-40,000	40,000
Sepharose CL-4B	4% cross-linked agarose	45-165	60-20,000	20,000
Sepharose CL-6B	6% cross-linked agarose	40-165	10-4,000	4,000
Sephacryl S-400	cross-linked allyl dextran and N,N'-methylene bisacrylamide	25-75	20-8,000	8,000 kDa

[1]according to MW of globular proteins

EV fractionation by **ultrafiltration (UF)** allows for separation using semipermeable membranes with defined pore size or molecular weight cut-offs (Xu et al. 2015; Xu, Simpson, and Greening

2017). Nevertheless, the deviation/range of particles going through a given pore size does not allow the fractionation of the different EV types nor assures protein separation. It is nonetheless a quick, easy and valid method to reduce sample volume with minimal EV interference, which has been proven to yield a better recovery than concentrating EVs by UC (Welton et al. 2015).

Another technique that separates EVs with minimal interaction is **field-flow fractionation (FFF)**. This technology relies on separation of particles in a channel with parabolic longitudinal flow combined with an external gradient or "field". The field can be generated through the application of thermal energy (thermal FFF), centrifugal force (sedimentation FFF), electrostatic force (electrical FFF) or cross/tangential flow applied through one (AF4) or two semipermeable membranes (FFFF/TFF). This way, depending on the interaction of the field with the particles, they separate in different layers. At the same time, a longitudinal flow (perpendicular to the generated field) carries particles through the channel, and given the parabolical velocities of the flow streamlines, particles running in the different field-induced layers are separated (Giddings and Myers 1976). This technology has been lately adopted for EV separation, fractionating EVs according to their distinct electrophoretic mobility by electrical FFF or hydrodynamic diameter (size/molecular weight) by FFFF/TFF/AF4 (**FIGURE 9**) (Kang et al. 2008; K. E. Petersen et al. 2014). For instance, AF4 manages a high resolution EV subpopulation separation, with 10 nm accuracy (H. Zhang, Zhang, and Lyden 2018). While its use is still at its infancy in the EV field, its lack of a static phase and label-free isolation permits the absence of interactions with the sample given, yielding untouched EV preparations with potential large-scale EV production.

Finally, **microfluidics and on-chip biosensors** are very promising technologies for high-throughput analysis using a minimal sample volume and reagent consumption in integrated miniaturized devices, separating EVs according to size, external markers, or innovative sorting mechanisms such as acoustic, electrophoretic or electromagnetic fields. Recently reviewed by Gholizadeh et al., these new methods are an ongoing research, not yet developed enough for standardized, broad use for EV isolation (Gholizadeh et al. 2017; Kanwar et al. 2014).

In view of the lack of a gold-standard EV isolation method, all these many different methodologies for EV isolation and the high heterogeneity of EV products and purity levels that they yield, there are controversial results in the literature. In an attempt to increase reproducibility and criteria for comparable studies, the EV-TRACK consortium was created to specially improve the reporting on EV isolation and characterization parameters (Van Deun et al. 2017).

In summary, each method has its own strengths and pitfalls, and thus depending on the type of initial sample to be processed and purpose/downstream use of the EVs, a specific method would be advised (**TABLE 6**). At the same time, little is known on the variation in functional activity of isolated EVs depending on the isolation method used. For instance, as we lately reported, precipitation-based isolation of EVs may affect cell viability of target cells (Gámez-Valero et al. 2016). Therefore, further characterization of EV products would help decipher specific EV-related effects, distinguish them from a method- or contaminant-related artefact, and also speed up their clinical translation.

TABLE 6 | Summary of the qualities of the different EV isolation techniques.

	diff-UC	disc-UC	DG	Precip	IA	FC	SEC	UF	FFF	MF
Purity[a]	1	3	3	1	3	2	3	1	3	3
Resolution[a]	1	2	3	1	3	2	2	1	3	2
Ease of use[a]	2	1	1	3	2	1	3	3	1	2
Time[a]	2	1	1	3	2	2	3	3	2	2
Recovery[a]	1	1	1	3	2	1	3	2	3	1
Scalability[a]	1	1	1	2	2	2	2	2	2	2
Automatization[a]	2	2	2	2	1	1	2	2	2	1
Functional studies[b]	2	1	1	3	1	1	3	3	2	2
Cost[a]	1	3	3	1	3	2	3	1	3	3

[a]Qualitatively, from 1(bad) to 3(good); [b]Yes(2)-No(1). UC: ultracentrifugation; diff-UC: differential UC; disc-UC: discontinuous (cushion) UC; DG: density gradient UC; Precip: precipitation-based isolation; IA: immunoaffinity isolation; FC: flow cytometry; SEC: size exclusion chromatography; UF: ultrafiltration; FFF: field-flow fractionation; MF: microfluidics technology.

Cardiac tissue engineering

There are several strategies that have been tested to deliver biological therapies to the injured heart. Amongst them, the most used routes of administration are the intra-aortic, intracoronary (IC), intravenous (IV) and transcoronary sinus delivery, and the transendocardial (via catheter) or epicardial (sternotomy) intramyocardial (IM) injection (**FIGURE 10**) (Strauer and Steinhoff 2011; Windecker et al. 2013). With the aim to optimize cell delivery, a few studies compared these different infusion options in terms of safety, feasibility, cell retention and functional outcome in ischemic murine and swine models and also patients with AMI (S.-H. Li et al. 2009; Hou et al. 2005; M. Hofmann 2005; de Witte et al. 2018). In general, myocardial cell engraftment was very poor, with the vast majority of cells being unspecifically distributed, mainly in lungs, liver, and kidneys. For instance, only a 1.3-2.6% of IC-delivered MSCs ended up in the myocardium of AMI patients (M. Hofmann 2005), compared to the 11% that was attained through IM delivery (Hou et al. 2005). Moreover, cell viability was very poor, with most cells dead 48h after administration (S.-H. Li et al. 2009; de Witte et al. 2018). In regard to the functional outcome, a meta-analysis of MSC performance in preclinical (58 acute and chronic MI studies; n=1,165 mouse, rat, swine) and clinical studies (6 clinical acute MI trials; n=334 patients) taking in account the different administration routes showed that transendocardial IM injection was the most prominent one because of its reduction in infarct size and improvement of LVEF (Kanelidis et al. 2017). Therefore, indicating that forthcoming endeavours should focus on more efficient cell administration methods to the infarcted area and border zone.

The modest results obtained with infused cell therapies might be then related to the massive cell loss after administration, low cellular survival or influence of the adverse post-infarction microenvironment (hypoxic conditions, loss of mechanical properties and inflammation). To overcome these limitations, novel approaches have been proposed, including tissue engineering (TE) (**FIGURE 10**).

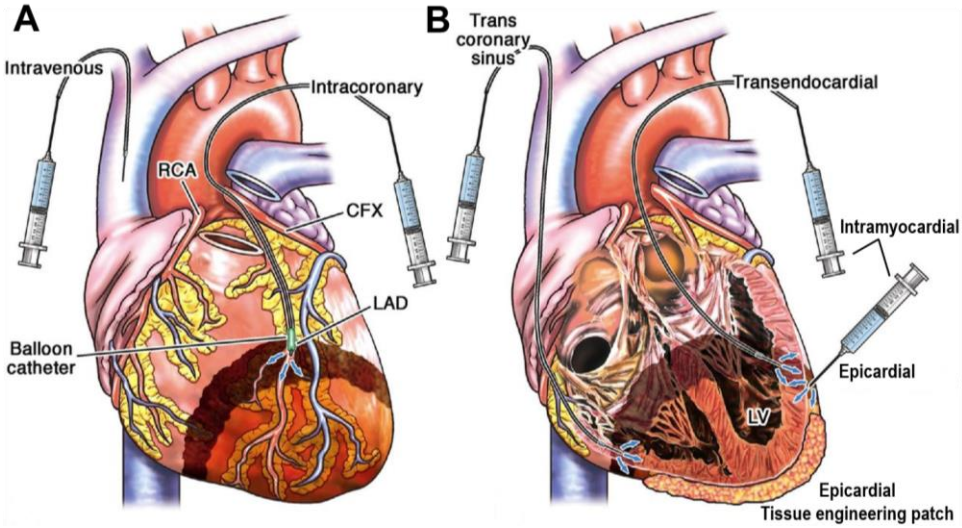

FIGURE 10 | Major routes of administration used for vascular and myocardial delivery in cardiac intervention and cardiac surgery. Cardiac patches and injectable biomaterials can be either used as acellular scaffolds, or delivery vehicles for cells and/or biological molecules. **(A)** Intravenous (IV) and intracoronary (IC) delivery; **(B)** transcoronary sinus delivery, transendocardial (via catheter) and epicardial (direct) intramyocardial (IM) injection and epicardial tissue engineering patches. CFX: circumflex artery; LAD: left anterior descending artery; LV: left ventricle; RCA: right coronary artery (adapted from Strauer & Steinhoff 2011 *JACC*). *Republication under CCC License.*

TE is defined as the combination of regenerative cells together with a three-dimensional (3D) supportive biomaterial (natural or synthetic) mimicking the target tissue's ECM, and optionally, complemented with growth factors, cytokines, proangiogenic or trophic factors that favour cell functional properties (Hirt, Hansen, and Eschenhagen 2014), and they can even be combined with devices for online monitoring of scar maturation (Prat-Vidal et al. 2014). In this context, the optimal biomaterial for cardiac repair would be one that (i) provides a suitable cellular microenvironment for cell survival and regeneration, (ii) is biocompatible and biodegradable to be replaced by endogenous ECM deposition, (iii) mimics the structure and biochemical characteristics of the native myocardium, (iv) vascularizes and innervates upon engraftment, and (v) allows mechanical and electrical coupling with host tissues (Perea Gil 2017). There are multiple approximations of engineered cardiac patches or grafts that seek to fulfil all, or most, of these requirements, divided in two main categories: cell sheets and cell-containing scaffolds.

- **Cell sheets**: this alternative is actually free of an exogenous scaffold, as cells are sustained over their own synthesized and secreted ECM. These cell-based structures are built up by the alignment and stacking of cell monolayers for a 3D structure. This layering of already differentiated cell types allows cardiomyocyte electronic coupling (Shimizu et al. 2002), but it is currently limited by the inability to generate patches with sizable thickness, as there is a finite number of cell sheets that enables sufficient oxygen diffusion and nutrient supply. Vascularization and perfusion can be increased by intercalating vascular-prone cells, but it also increases complexity in manufacture (Sakaguchi, Shimizu, and Okano 2015).

In an attempt to overcome these challenges, strategies using scaffolds for cell delivery appeared: they are more easily vascularized by the host's circulatory system, are more readily prepared for off-the-shelf approaches and consequently, are at present more suitable for clinical applications. The most used biomaterials in cardiac TE for scaffold generation are (1) biodegradable synthetic materials (approved by FDA for clinical purposes): polyethylene glycol (PEG), polylactic acid (PLA), poly(lactic-co-glycolic) acid (PLGA), polycaprolactone (PCL) and polypeptides; and (2) natural materials: collagen, fibrin, chitosan, alginate, hyaluronic acid, matrigel, gelatine and decellularized ECM (Sarig and Machluf 2011; Hirt, Hansen, and Eschenhagen 2014). They can be used to produce two main types of scaffold structures:

- **Hydrogels**: they constitute a group of cross-linked polymeric, semi-solid materials, the hydrophilic structure of which renders their 3D networks greatly water-swollen, providing them with flexibility similar to natural tissue (E. M. Ahmed 2015). Acellular hydrogels are already promising for cardiac repair as provide support and can be carriers of bioactive molecules such as growth factors, cytokines and DNA plasmids. Then, hydrogels can be used for direct injection of cells into the infarcted tissue, but the elevated pressure can greatly alter cell survival (Hasan et al. 2015). Thus, a modification of this strategy is the *ex vivo* patch preparation for epicardial placement.

  Election of the hydrogel biomaterial is based on its capacity to maintain cell survival, growth, differentiation and neovascularization, given by its porous, 3D structure, biodegradability and lack of toxicity. On one side, synthetic polymers have strong mechanical properties and easily malleable and controllable features. The most commonly used are polypeptides and poly(α-esters), including polylactides, polyglycolide, polyethylene and polycaprolactone (Dhandayuthapani et al. 2011). Amongst them, polypeptides are specially interesting given their ECM mimicry and controlled jellification by pH or salt concentration. On the other side,

natural protein (collagen, gelatine, fibrin…), polysaccharide (hyaluronic acid, chitosan, …) or mixed polymers (decellularized ECM or mix of the formers) are usually more supportive of cellular activities. Despite their low mechanical strength, possible immunoreactivity, variability and complexity, natural biomaterials continue to be greatly used given their enhanced biocompatibility, bioactivity and ECM mimicry (Hasan et al. 2015). Alternatively, different hydrogel types can be mixed resulting in those referred to as *composite hydrogels*.

- **Matrices**: they are porous, solid materials that simulate the native cardiac ECM structure and properties and provide the biological and mechanical support to deliver exogenous cells or for being repopulated by host cells. Also, matrices envisioned for cardiac repair need also electromechanical coupling, contractility capacity, promotion of vascularization and integration with the host tissue with newly synthesized ECM by ingrowing cells. There are several synthetic polymers that have been used to develop matrices (polyglycolic, polylactic acids, polyurethane, poly(lactide-co-ε-caprolactone) (Sarig and Machluf 2011). In addition, natural matrices can be made from collagen, fibrin, alginate, gelatine, chitosan and matrigel, or obtained from decellularized natural tissues like pericardium and myocardium (Perea-Gil, Prat-Vidal, and Bayes-Genis 2015). This last option is especially interesting, as the decellularization process eliminates all the cellular material from the tissue, but maintains the ECM substantially intact. Therefore, these are the matrices that most resemble the porosity and structure, stiffness and contractility capacity of the original tissue, and the preserved ECM composition can also enhance cell adhesion and interaction (Perea-Gil et al. 2018).

  A recent development for artificial scaffolds engineering is 3D bioprinting. This new technique is based on the artificial printing of "bioink", in other words, precisely multilayering a defined 3D structure with the biomaterial(s) of choice and even combined with the concomitant addition of cells (Duan 2017).

Therefore, TE approaches use scaffolds that can be one or a combination of the aforementioned structures, made up of synthetic or natural biomaterials. Biodegradable synthetic polymers might be easier to manufacture and control, but natural biomaterials might be preferable for achieving the scaffold purposes because they are more biocompatible and biodegradable and resemble better cardiac composition, mechanical properties and/or structure. Indeed, a good option can be hybrid scaffolds, the combination of natural and synthetic materials to integrate advantages of both approaches.

In the recent years, the ICREC research group has explored different approximations for MSC delivery to the post-infarcted myocardium, starting from direct intramyocardial delivery (Antoni Bayes-Genis et al. 2010), epicardial placement through a fibrin patch (Roura et al. 2012; Llucià-Valldeperas et al. 2017), to embedding MSCs in hydrogel within myocardial (Perea-Gil et al. 2016) and pericardial scaffolds (Cristina Prat-Vidal et al. 2014; Gálvez-Montón, Bragós, et al. 2017), as collectively revised in (Roura, Gálvez-Montón, Mirabel, et al. 2017). Decellularized scaffolds replenished with polypeptide hydrogel provide a niche that recreates the native cardiac environment for administered and endogenous stem or progenitor cells. These constructs have shown neovascularization and neoinnervation, effectively integrating themselves after implantation over the ischemic myocardium without identified detectable side effects. They manage to limit scar size and improve heart function following myocardial infarction (Perea-Gil et al. 2016; Cristina Prat-Vidal et al. 2014; Gálvez-Montón, Bragós, et al. 2017). At the same time, acellular constructs also manage effective graft integration (Gálvez-Montón et al. 2015),

and we hypothesize that they could be upgraded with bioactive components from the MSC's secretome like MSC-EVs to foster endogenous cardiac repair and work with an actual off-the-shelf product.

Hypothesis and objectives

HYPOTHESIS

Exacerbated immune responses hamper regeneration of injured tissues, and lead to allergies, autoimmune diseases and organ rejection. For instance, the inflammation that occurs after an IRI event such as MI must be timely repressed to prevent worsening of the post-infarction wound and promote instead tissue regeneration. In this context, MSCs are attractive candidates as a biological therapy thanks to their reported long-lasting immunosuppressive and regenerative properties, albeit their short lifespan after *in vivo* infusion. We hypothesize that these effects could be firstly mediated by the secretion of paracrine factors for delocalized/systemic effects that foster endogenous repair, and secondarily by the modulation of the host's immune cells for the generation of regulatory environments and enduring effect. Deciphering the mechanisms that mediate MSCs' action can boost the design of innovative and more efficient therapies in regenerative medicine.

AIM AND OUTLINE OF THE THESIS

The aim of this thesis was to unravel the cellular and paracrine mechanisms that mediate MSCs' immunosuppressive capabilities to design alternative biological therapeutic approaches. For that purpose, we divided the work in three chapters with specific objectives:

Chapter 1 – To study MSC's immunomodulation of monocytes as part of the host's link of the innate and adaptive immune responses.

- To study the monocyte polarization induced by MSCs
- To analyze the role of the adenosinergic pathway in MSC-conditioned monocytes *in vitro* and in the swine preclinical MI model

Chapter 2 – To assess the immunological properties of the different fractions found in MSC's conditioned medium, with a special attention to MSC-derived EVs.

- To efficiently isolate and characterize EVs from MSC's conditioned medium
- To compare the immunosuppressive effect of the EV, non-EV fractions and full conditioned medium towards allogeneic T cell proliferation and cytokine response and monocyte polarization

Chapter 3 – To develop a cell-free cardiac graft for the local delivery of multifunctional swine MSC-EV envisioned for immune modulation and cardiac repair after MI.

- To isolate and characterize porcine MSC-EV
- To assess the immune suppressive functions and recruitment of pro-regenerative cells of porcine MSC-EV
- To evaluate the retention of MSC-EVs in decellularized cardiac scaffolds

CHAPTER 1

Based on "Mesenchymal Stem Cells induce expression of CD73 in human monocytes *in vitro* and in a swine model of myocardial infarction *in vivo*"

Marta Monguió-Tortajada[1,2,*], Santiago Roura[3,4,5,*], Carolina Gálvez-Montón[3,5], Marcel·la Franquesa[1,6], Antoni Bayes-Genis[3,5,7,8,†], Francesc E. Borràs[1,2,6,†]

[1]REMAR-IVECAT Group, Health Science Research Institute Germans Trias i Pujol, Can Ruti Campus, Badalona, Spain, [2]Department of Cell Biology, Physiology and Immunology, Universitat Autònoma de Barcelona (UAB), [3]ICREC Research Program, Health Science Research Institute Germans Trias i Pujol, Can Ruti Campus, Badalona, Spain, [4]Center of Regenerative Medicine in Barcelona, Barcelona, Spain, [5]CIBERCV, Instituto de Salud Carlos III, Madrid, Spain, [6]Nephrology Service, Germans Trias i Pujol University Hospital, Badalona, Spain, [7]Cardiology Service, Germans Trias i Pujol University Hospital, Badalona, Spain, [8]Department of Medicine, Universitat Autònoma de Barcelona (UAB), Barcelona, Spain
* Both authors contributed equally to this work
† Corresponding author

Published in the Open Access Journal *Frontiers in Immunology*, 2017 Nov 20;8:1577.
doi: 10.3389/fimmu.2017.01577. PMID: 29209319

ABSTRACT

The ectoenzymes CD39 and CD73 regulate the purinergic signalling through the hydrolysis of ATP/ADP to AMP and to Adenosine, respectively. This shifts the pro-inflammatory milieu induced by extracellular ATP to the anti-inflammatory regulation by Adenosine. Mesenchymal stem cells (MSCs) have potent immunomodulatory capabilities, including monocyte modulation towards an anti-inflammatory phenotype aiding tissue repair. *In vitro*, we observed that human cardiac adipose tissue-derived MSCs (cATMSCs) and umbilical cord MSCs (UCMSCs) similarly polarize monocytes towards a regulatory M2 phenotype, which maintained the expression of CD39 and induced expression of CD73 in a cell contact dependent fashion, correlating with increased functional activity. In addition, the local treatment with porcine cATMSCs using an engineered bioactive graft promoted the *in vivo* CD73 expression on host monocytes in a swine model of myocardial infarction. Our results suggest the upregulation of ectonucleotidases on MSC-conditioned monocytes as an effective mechanism to amplify the long-lasting immunomodulatory and healing effects of MSCs delivery.

INTRODUCTION

MSCs have been widely associated to both immunomodulatory and regenerative capabilities (Katarina Le Blanc and Mougiakakos 2012; Roura et al. 2015; Monguió-Tortajada, Roura, Gálvez-Montón, Pujal, et al. 2017). For instance, cardiac adipose tissue-derived MSCs (cATMSCs), which represent a mesenchymal-like cell population with intrinsic cardiomyogenic potential (Antoni Bayes-Genis et al. 2010), abrogate allogeneic T cell proliferation upon stimulation with third party mature monocyte-derived DCs to the same extent as foetal-derived MSCs (Perea-Gil, Monguió-Tortajada, et al. 2015) and also promote tissue repair and immune suppression in an *in vivo* model of MI (Cristina Prat-Vidal et al. 2014; Gálvez-Montón, Bragós, et al. 2017).

Among a broad number of mechanisms of action, MSCs generally modulate monocyte polarization towards an anti-inflammatory M2 phenotype (Melief, Schrama, et al. 2013; Cutler et al. 2010; Ben-Mordechai et al. 2013) and restrain DC differentiation, resulting in the inhibition of the host immune response (Spaggiari et al. 2009; Nauta, Kruisselbrink, et al. 2006; X.-X. Jiang et al. 2005). At the same time, different *in vivo* models have demonstrated the need for monocytes/macrophages modulation to achieve healing and tissue repair by MSC treatment (Ben-Mordechai et al. 2013; Blázquez, Sánchez-Margallo, Crisóstomo, et al. 2016; Dayan et al. 2011).

The immune response can be specifically modulated by signals from the milieu, including cytokines, chemokines, and others such as purinergic mediators. Among them, adenosine triphosphate (ATP) promotes inflammation when it is found in high amounts during apoptosis and necrosis in damaged tissues, such as after MI (Mizumoto et al. 2002; Antonioli et al. 2013; Murphy et al. 2017); on the contrary, removal of extracellular ATP avoids exacerbated tissue inflammation. Extracellularly, ATP is sequentially hydrolyzed to ADP and 5'AMP by the ectoenzyme nucleoside triphosphate diphosphohydrolase (NTPD-1/CD39) and to adenosine (Ado) by the ecto-5′-nucleotidase (ecto-5′-NT/CD73) (Haskó and Cronstein 2013; Antonioli et al. 2013). The final product, Ado, is a powerful anti-inflammatory purine nucleoside, which has been described to immunosuppress macrophages, DCs, natural killer (NK), T and B cells to promote tolerance (A. Ohta and Sitkovsky 2014; Regateiro, Cobbold, and Waldmann 2013). Therefore, ATP hydrolysis is not only beneficial to reduce the pro-inflammatory ATP levels, but also to produce the anti-inflammatory Ado. CD73 expression has been linked to the regulatory phenotypes of T and NK cells (Chatterjee et al. 2014; Beavis et al. 2012; Regateiro, Cobbold, and Waldmann 2013), and it is also a cell marker for progenitor or mesenchymal stem cells (MSCs) (Dominici et al. 2006).

In this first chapter, we comparatively assess whether UCMSCs and cATMSCs (as distinct sources of MSCs) contribute to induce the functional expression of CD73 on monocytes, promoting the activation of their adenosinergic enzymatic activity. *In vivo*, we evaluate the presence of infiltrated host monocytes expressing CD73 once cATMSCs are infused into swine post-infarcted myocardium.

MATERIAL AND METHODS

Human cATMSC and UCMSC isolation and culture

The study protocols were approved by the Clinical Research Ethics Committee of our institution (Comitè Ètic d'Investigació Clínica, HuGTiP, Refs. CEIC: EO-10-13, EO-10-016 and EO-12-022), and conformed to the principles outlined in the Declaration of Helsinki. Written informed consent was obtained from donors (adipose tissue samples) or parents (umbilical cord samples).

Human cATMSCs were extracted from adipose tissue surrounding the base of the heart and around the aortic root from patients undergoing cardiothoracic surgery prior to coronary artery bypass graft initiation (n=6), as reported in (Antoni Bayes-Genis et al. 2010; Perea-Gil, Monguió-Tortajada, et al. 2015).

Additionally, fresh Umbilical Cords (UC, n = 6) were obtained after birth and maintained in phosphate-buffered saline buffer (PBS; Gibco Life Technologies/Invitrogen, Carlsbad, CA) supplemented with 5,000 U heparin (Sigma Aldrich, St. Louis, MO) and 1% penicillin/streptomycin (Gibco) before tissue processing to isolate UCMSCs. UCs (10 g) were sectioned into 3-6 mm^3 pieces and carefully washed in PBS to eliminate residual blood contained in arteries and vein. During mechanical disruption, elimination of UC vein and subendothelium was achieved. Further procedures include two enzymatic disaggregation at 37ºC with gentle agitation and a filtration step using Falcon Cell Strainers (BD Biosciences, San Diego, CA) in order to release uniform cell suspensions. First digestion was conducted using Collagenase type-I (880 U/mL; Gibco) plus Hyaluronidase II (3,960 U/mL; Sigma Aldrich) for 60 min, followed by a second digestion using Trypsin-EDTA (0,125%; Gibco) plus DNase I (0.2 mg/mL; Roche Diagnostics, Mannheim, Germany) for 30 min. The supernatants from both digestions were mixed together and centrifuged at 1,200 rpm for 10 min. Cell pellet was then resuspended in α-MEM (Sigma) supplemented with 10% heat-inactivated Foetal Bovine Serum (FBS; Life Technologies, Carlsbad, CA), 2 mM L-glutamine and 1% penicillin/streptomycin (Gibco) and 5 μg/mL plasmocin (Invivogen, San Diego, CA). Adherent cells were maintained under standard culture conditions until third-passage cells, when cells were used to analyse their surface marker expression profile and multipotency, as previously described (A Bayes-Genis et al. 2005; C Prat-Vidal et al. 2007; Ullah et al. 2013).

Monocyte isolation

Peripheral blood mononuclear cells (PBMCs) were obtained from leukocyte residues from healthy donors from the Blood and Tissue Bank (Barcelona, Spain) (n=22) by Ficoll Hypaque Pus™ density gradient centrifugation (GE Healthcare Biosciences) at 1800rpm for 30 minutes, and $CD3^+$ cells were depleted using the RosetteSep™ Human CD3 Depletion Cocktail (StemCell Technonogies). Monocytes were then isolated using the EasySep™ Human anti-CD14 Positive Selection Kit (StemCell Technologies) or the MagniSort Human CD14 Positive Selection kit (eBioscience) following manufacturers' instructions. Recovered cells were counted using PerfectCount Microspheres (Cytognos) and assessed for purity (>90% $CD14^+$) and viability (≥93% by FSC/SSC and $7AAD^-$ (BD) gating) in a Canto II flow cytometer (BD).

Monocyte differentiation to Dendritic Cells

Monocytes were cultured at $1x10^6$ cells/ml in complete medium composed of RMPI 1640 (Gibco) supplemented with 2 mM L-Glutamine (Sigma), 100U/ml Penicillin (Cepa), 100 µg/ml

Streptomycin (Normon Laboratories), 5% Human platelet lysate (Lonza) and dendritic cell differentiation cytokines: 300 IU/ml IL-4 and 450 IU/ml GM-CSF (Miltenyi Biotech). After six days, monocyte-derived dendritic cells (MDDCs) were harvested, counted and assessed for viability and differentiation by 7AAD and CD11c staining, respectively (both from BD).

Monocyte and MDDC conditioning

Monocytes or MDDCs were cultured at $1x10^6$ cells/ml in a 20:1 ratio over a layer of cATMSCs or UCMSCs, which were previously let adhere to the culture plates for 4 h. As a control, monocytes were cultured alone or in the presence of 500 ng/ml LPS (Sigma). Contact dependency was assessed using a 24-well transwell system with 0.4 μm-pore polycarbonate membrane (Costar). Monocytes ($4x10^5$) were seeded in each well and cATMSCs or UCMSCs ($2x10^4$; 20:1 ratio) were applied to the upper chamber. Alternatively, monocytes were cultured in the presence of UCMSC conditioned media (CM) as in *Chapter 2*.

After co-culture, monocytes or MDDCs were detached using accutase (Sigma) and washed with FACSFlow (BD) + 2% FBS. Monocytes were stained with CD14-FITC and CD90-PE/Cy7 (BD) and separated by FACS in an Aria II sorter (BD). MDDCs were separated by FACS according to CD11c-Bv421$^+$ (BD). Purity was always assured to be over 98%. Monocytes and MDDC were then pelleted and frozen at -80ºC for whole RNA extraction.

Cell phenotype was assessed by incubation with CD11c-Bv421, CD14-FITC, CD25-PerCP/Cy5.5, CD38-PE, CD39-Bv650, CD40-APC, CD73-PE, CD90-PE/Cy7, CD163-Bv711, CD206-PE-CF594 (BD) and/or CD80-PEVio770 (Miltenyi Biotech) or corresponding isotype control antibodies and acquisition in FACSCanto II and LSR Fortessa flow cytometers (BD). Analysis was performed using FlowJo X software.

RNA extraction and qPCR

Whole RNA content was isolated from cells using the RNeasy Mini kit (Qiagen). cDNA was synthesized using random hexamers (Qiagen) and the iScript^{TM} One-Step RT–PCR Kit (BioRad Laboratories) according to supplier's protocol. Analysis of the monocyte polarization markers expression was performed, by amplification of each cDNA in a LightCycler® 480 PCR system (Roche Life Science) using the KAPA SYBR Fast Master Mix (KAPA Biosystems) and the primer sequences indicated in **Supplementary Table 1**. Samples were incubated for an initial denaturation at 95°C for 5 min, and then 40 PCR cycles were performed at 95°C for 10 s, 60°C for 20 s and 72°C for 10 s. The values obtained by the "Fit point" method were correlated to a standard curve and normalized to the expression levels of the endogenous reference gene 18S. The gene expression levels of each stimulus were calculated as a fold change relative to non-activated monocytes.

Alternatively, 8 μl of cDNA was preamplified with the TaqManW PreAmp Master Mix Kit (Applied Biosystems) in a final volume of 50 μl. Subsequently, 15 μl of preamplified cDNA were amplified in a final volume of 50 μl containing 25 μl TaqMan 2X Universal PCR Master Mix and 2 μl of the following FAM-labelled primer/probes (Applied Biosystems): CD73 (Hs00169777_m1), CD90 (Hs00264235_s1) and 18S (Hs99999901_s1). Data from four independent experiments were collected and analysed on the LightCyclerW 480 Real-Time PCR System (Roche); each sample was analysed in duplicate. The difference in threshold cycle $2^{-\Delta\Delta Ct}$ method was used to quantify the relative expression for each gene using 18S as endogenous reference (Livak and Schmittgen 2001).

Cytokine determination

The human IL10 and TNFα levels were measured in supernatants of 72h-cultured monocytes using commercial ELISA kits (U-Cytech, The Netherlands) following manufacturer's instructions.

CD73 enzyme activity

Either MSCs or FACS-sorted conditioned monocytes were washed three times with MES buffer (0.025M MES (Sigma) in 0.9% NaCl (Braun) pH 6.0) and cultured at 50,000 cells/well in the presence or absence of 5'AMP (Sigma) and the CD39 inhibitor POM1 (Tocris) or CD73 inhibitor APCP (ADP analogue; Sigma) when indicated. After 2 h at 37ºC, cells were centrifuged and supernatants harvested to freshly quantify Pi concentration using the malachite green phosphate colorimetric assay kit (BioVision), following manufacturer's instructions. 5'AMP and APCP alone were confirmed to yield negative values, and Pi production was calculated as the subtraction [Pi]cells+5'AMP – [Pi]cells alone. Alternatively, the 2h-supernatant was snap frozen at -80ºC and analysed for Adenosine concentration using the Adenosine assay kit (BioVision), following manufacturer's instructions.

Animal experimentation and Immunostaining

Allogeneic porcine cATMSCs were isolated from cardiac adipose biopsy samples (average 0.4 – 5.9 g) from pigs undergoing cardiac surgery (n = 5), and processed as previously described (Cristina Prat-Vidal et al. 2014). Succinctly, tissue specimens were washed in phosphate-buffered saline (PBS) to remove contaminating debris and red blood cells, and digested in 0.015% collagenase (Type II-B, Sigma-Aldrich) for 30 min at 37°C in gentle agitation. The collagenase was inactivated by dilution with α−MEM containing 10% foetal bovine serum (FBS), 2 mM glutamine, 1% penicillin–streptomycin (Gibco Invitrogen Corp) (α−MEM-FCS). The cell suspension was centrifuged for 10 min at 1,200 × g, and the pellet was resuspended in α−MEM-FCS and filtered through a 100-µm mesh. Adhered cells were finally grown to subconfluence in α−MEM supplemented with 10% foetal bovine serum (FBS), and cultured under standard conditions.

Engineered bioactive graft generation and implantation, MI induction, and immunohistological analysis was performed as described in previous studies (Cristina Prat-Vidal et al. 2014; Gálvez-Montón, Bragós, et al. 2017). In brief, a decellularized human pericardium-derived scaffold embedded with GFP-labelled porcine cATMSCs (treated animals; n=7) or without cells (control animals; n=7) was implanted covering the ischemic area in Landrace X Large White pigs 30 minutes after MI induction. Additionally, a group submitted to the engineered bioactive graft enriched with cATMSCs but without MI induction was included (sham animals; n=3). Animals were sacrificed after 30 days of follow-up.

Immunostaining was performed on cells grown in µ-dishes with glass bottom (Ibidi) or 10-µm myocardial sections against GFP, cardiac troponin I (Abcam), CD73, and CD163 (Novus Biologicals) Abs (1:100). Subsequently, secondary Abs (1:500) conjugated to Alexa Fluor 488, Alexa Fluor 594, Alexa Fluor 647 (Molecular Probes), Cy2 and Cy3 (Jackson ImmunoResearch Laboratories) were applied. Samples were finally counterstained with Atto 488-conjugated phalloidin (1:40) and/or 4',6-diamidino-2-phenylindole dihydrochloride (DAPI) (1:10,000) (Sigma), and analysed under an Axio Observer Z1 confocal microscope (Zeiss). For $CD163^{+}$ and

$CD73^+$ cell quantification, at least four different optical fields from each section were measured under Image-Pro Plus software (6.2.1 version; Media Cybernetics, Inc., Bethesda, MD).

Statistical analysis

Values are expressed as mean + or ± standard deviation (SD). Kolmogorov-Smirnov analysis was used to check for normality of data and appropriate statistical tests are indicated for each dataset. Analyses were performed using the Graphpad Prism (6.0 version) and SPSS (21.0.0.0 version) software, and differences were considered significant when $p<0.05$.

RESULTS

Monocyte polarization by cATMSCs and UCMSCs

To investigate the effect of MSC conditioning, we first analysed the capacity of different human MSCs to skew monocyte polarization in vitro. Monocytes were co-cultured for 48h with either cATMSCs or UCMSCs, and LPS as a positive control of monocyte activation. After co-culture, monocytes ($CD14^{+}/CD90^{mid}$) were easily isolated from MSCs ($CD14^{dim}/CD90^{high}$) by FACS according to both their CD14 expression and lower expression of CD90 compared to MSCs (**FIGURE 11A**). Monocytes exhibited better viability with MSCs co-culture (**FIGURE 11B**).

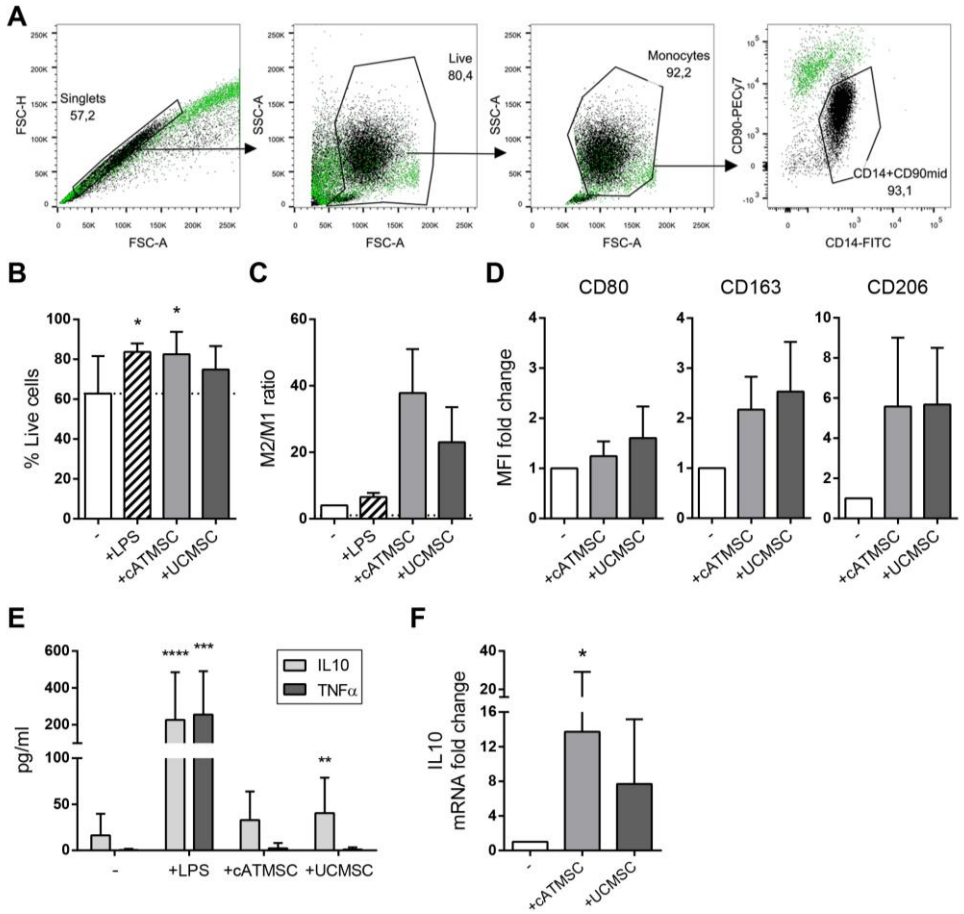

FIGURE 11 | **cATMSCs and UCMSCs skew monocytes towards an "M2" phenotype. (A)** Live monocytes ($CD14^{+}/CD90^{mid}$) were separated by FACS after co-culture with LPS, cATMSCs or UCMSCs ($CD14^{dim}/CD90^{high}$). A representative gating analysis of monocytes co-cultured with UCMSCs (black dots) compared to UCMSCs alone (green dots) is shown. **(B)** Viability of co-cultured monocytes. Data is mean + SD of eleven independent experiments. **(C)** FACS-sorted monocytes were checked for the expression of M1 and M2 markers by qPCR after 48h of co-culture. Data is expressed as mean + SD of the ratio between the M2 (ΣmRNA fold change of CD163, CD206, TGM2 and CCL18) and M1 marker (mRNA fold change of CD80) depicted in Supplementary Figure 1. Data accounts for three independent experiments. **(D)** Fold increase in CD80, CD163 and CD206 MFI of monocytes cultured for 72h with LPS, cATDPCs or UCMSCs, relative to monocytes alone (-). Data accounts for three independent experiments. **(E)** IL10 and TNFα cytokine levels in 72h-culture supernatants. Data is mean + SD of twelve independent experiments. **(F)** Fold increase in IL10 mRNA of monocytes cultured for 48h with cATDPCs or UCMSCs, relative to monocytes alone (-). Data accounts for four independent experiments. Statistical differences are indicated where *p<0.05 by One-way ANOVA and **p<0.01, ***p<0.001 by Two-way ANOVA with Tukey's post-hoc test compared to monocytes cultured alone (-).

Both cATMSC and UCMSCs managed to upregulate the M2 markers CD163, CD206, TGM2 and CCL18 in monocytes at the mRNA level (**Supplementary Figure 1**), while the M1 marker CD80 remained unchanged. On the contrary, LPS activation of monocytes led to the increased expression of CD80. The relative mRNA expression of all markers studied (**FIGURE 11C**), suggested that both MSCs were promoting an M2 phenotype in monocytes. This phenotype was further assessed by surface protein expression, and while CD80 was unchanged, CD163 and CD206 did increase when monocytes were co-cultured with MSCs (**FIGURE 11D**).

Furthermore, the cytokine profile showed that MSCs promoted the secretion of IL10 by monocytes, while no TNFα was detected (**FIGURE 11E**). The increased IL10 mRNA transcription of sorted monocytes after co-culture with MSCs (**FIGURE 11F**) together with the undetectable IL10 in MSC's supernatants (data not shown) could attribute IL10 production to monocytes, further confirming an anti-inflammatory profile induced by MSC co-culture.

Expression of adenosinergic ectoenzymes in monocytes

After confirming the M2 skewing capabilities of cATMSCs and UCMSCs towards monocytes, we next studied the expression of adenosinergic ectoenzymes on these cells. The canonical and major enzymatic pathway that would lead to Adenosine production in the inflammatory context of tissue injury, in which the ATP concentration increases and is readily available extracellularly, is the CD39/CD73 axis.

CD39, that starts the phosphohydrolysis of ATP/ADP to 5'AMP, was already present in fresh blood peripheral blood monocytes (data not shown) and remained highly expressed on monocytes cultured alone or in the presence of LPS, cATMSCs or UCMSCs (**FIGURE 12**).

In parallel with the canonical adenosinergic ectoenzymes, there is also a non-conventional machinery relying on the action of CD38/CD203a to convert $NAD^+/NADP^+$ into cADPR, ADP-ribose and NAADP and then converging to 5'AMP production. While CD203a is a known macrophage marker, expressed by both human and porcine monocytes upon *in vitro* culture (Singleton et al. 2016; Franzoni et al. 2017; Jacobsen et al. 2016), CD38 expression is ubiquitous in the hematopoietic lineage, and its expression can vary with activation status of cells. CD38 was expressed by human monocytes, and while cells maintained a positive expression (% of $CD38^+$

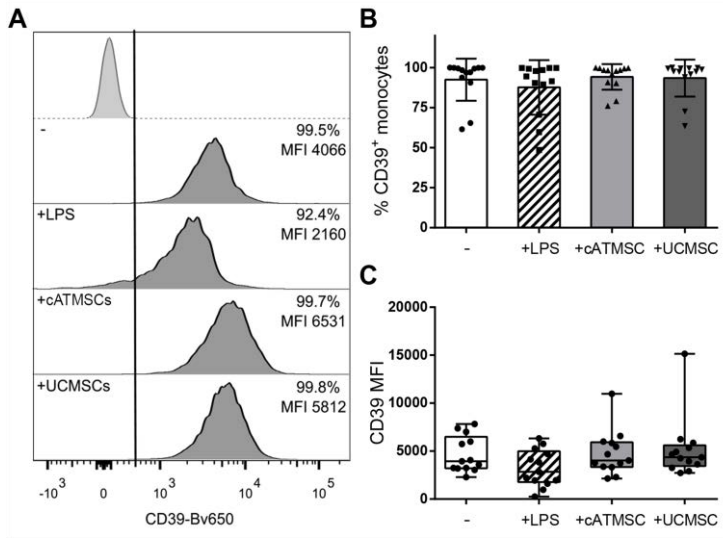

FIGURE 12 | CD39 expression is maintained in monocytes co-cultured with MSCs.
(A) Representative histograms depicting the CD39 expression of monocytes cultured for 72h alone (-) or with LPS, cATMSCs or UCMSCs. The isotype control is depicted in the top row; the % of positive cells and the MFI for the total monocyte population ($CD14^+/CD90^{mid}$) are indicated in each plot. **(B)** Percentage of $CD39^+$ and **(C)** CD39 MFI of monocytes cultured for 72h alone (-) or with LPS, cATMSCs or UCMSCs. Data accounts for twelve independent experiments.

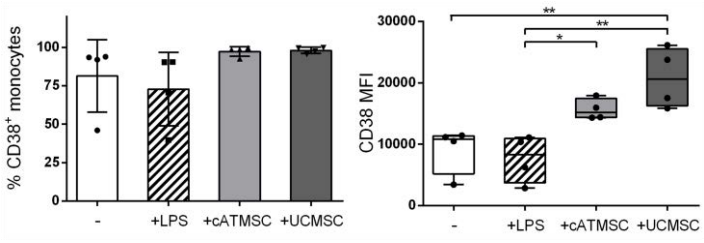

FIGURE 13 | Percentage of $CD38^+$ and CD38 MFI of monocytes cultured for 72h alone (-) or with LPS, cATMSCs or UCMSCs. Data accounts for four independent experiments. *p<0.05, **p<0.01 by One-way ANOVA with Tukey's post-hoc test compared to monocytes

positive cells), their expression level significantly increased after monocytes were co-cultured with either ATDPC or UCMSCs (**FIGURE 13**).

Induction of CD73 expression in monocytes

Interestingly, monocytes cultured on a layer of both types of MSCs expressed higher levels of CD73 protein at 24 and 48h of culture compared to control (**FIGURE 14A**). CD73 mRNA was incremented more than 500 times in monocytes after 48h of co-culture with either cATMSCs or UCMSCs in comparison to cultured alone (**FIGURE 14B**), pointing to the induction of protein expression. Of note, LPS-activation of monocytes also incremented CD73 expression. As a negative control, another classical MSC marker, CD90, was analysed in conditioned monocytes. CD90 was found to be unchanged both at a protein and RNA levels (**FIGURE 14C and D**), suggesting the apparent specificity to CD73 acquisition and absence of a trogocytosis-like phenomenon.

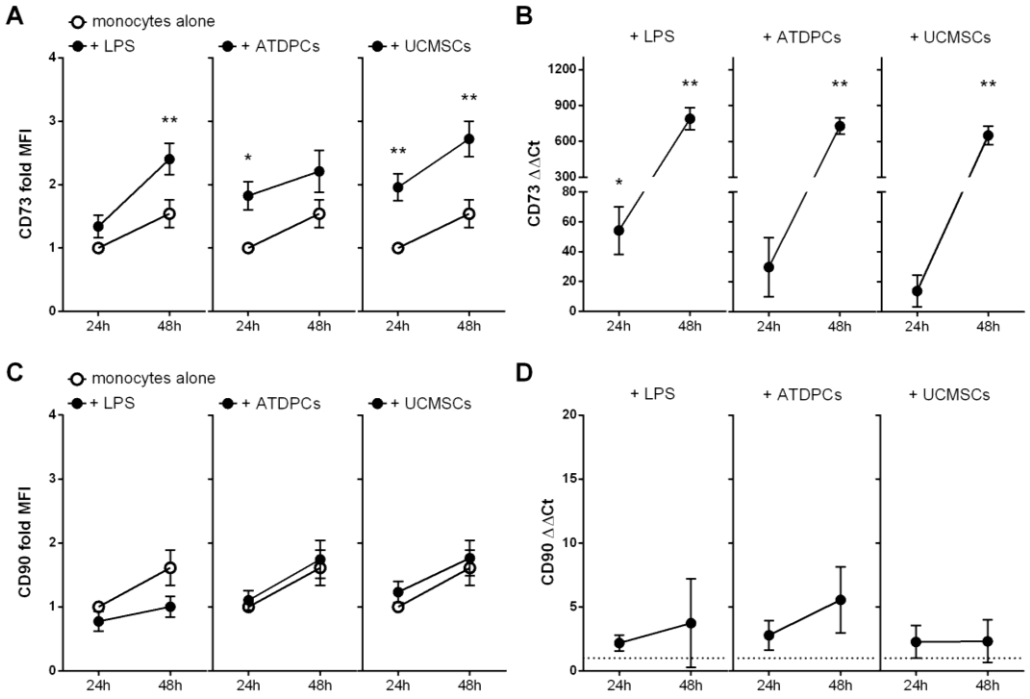

FIGURE 14 | **CD73 is induced while CD90 remains unchanged in monocytes co-cultured with cATMSCs and UCMSCs. (A, C)** Fold increase in CD73 and CD90 MFI of monocytes cultured for 24h or 48h with LPS, ATDPCs or UCMSCs (black dots), relative to 24h-cultured monocytes alone (white dots). Statistical differences are indicated where *p<0.05 and **p<0.01 by Two-way ANOVA compared to monocytes cultured alone. **(B, D)** Fold increase in CD73 and CD90 mRNA (ΔΔCt) of monocytes, relative to monocytes cultured alone. Statistical differences are indicated where *p<0.05; **p<0.01 and ***p<0.001 by One-sample T test. Data is expressed as mean ± SD and accounts for four independent experiments of different monocyte and MSC donors.

As high levels of CD73 mRNA were detected after 48h of conditioning, the CD73 protein expression and functional activity was further evaluated at 72h of co-culture. Monocytes co-cultured with both cATMSCs and UCMSCs expressed higher levels of CD73 on the surface in comparison to control monocytes and LPS-stimulated monocytes (**FIGURE 15A-C**).

We also investigated whether direct cell contact between MSCs and monocytes was necessary to induce CD73 expression. For that purpose, co-culture experiments were performed using transwell culture plates, in which monocytes did not increase CD73 expression to the same extent compared to direct co-culture with MSCs (**FIGURE 15B-C**). To corroborate such observations,

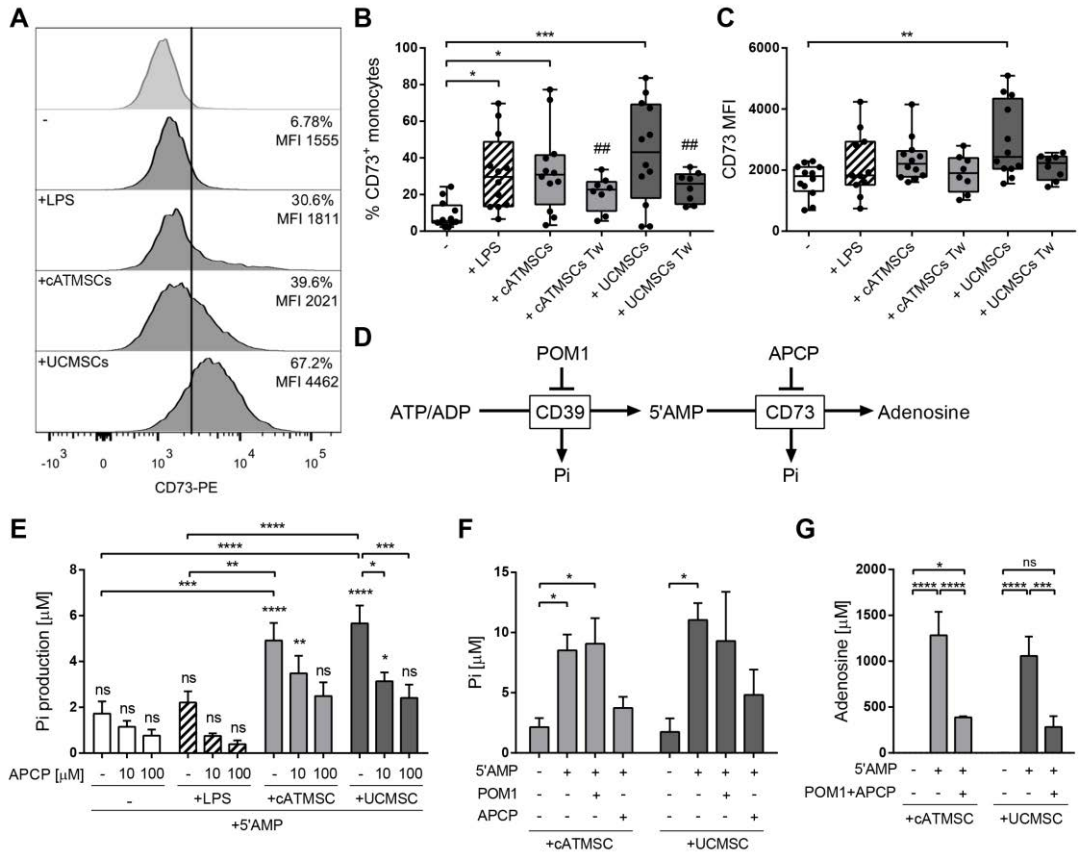

FIGURE 15 | Monocytes co-cultured with cATMSCs or UCMSCs upregulate the adenosinergic enzymatic activity. Monocytes cultured for 72h alone (-) or with LPS, cATMSCs or UCMSCs were checked for CD73 surface expression and activity. **(A)** Representative histograms of CD73 expression. The isotype control is depicted in the top row; the % of positive cells and the MFI for the total monocyte population ($CD14^{+}/CD90^{mid}$) are indicated in each plot. **(B)** Percentage of $CD73^{+}$ and C: CD73 MFI of monocytes as mean ± SD of twelve independent experiments. Tw: co-culture in transwell system. Statistical differences are indicated where *p<0.05, **p<0.01 and ***p<0.001 by One-way ANOVA with Tukey's post-hoc analysis. **(D)** Schematic representation of the enzymatic hydrolysis of ATP/ADP to 5'AMP by CD39 and to Adenosine by CD73, which can be inhibited by POM1 and APCP, respectively. Inorganic phosphate (Pi) is produced as a byproduct in each step. **(E)** Levels of inorganic phosphate (Pi) produced by FACS-sorted monocytes analyzed after the addition of the CD73 substrate (5'AMP; 1 mM) with or without the CD73 inhibitor (APCP). Data is presented in bars as the mean + SD concentration of Pi subtracted from the Pi present in monocytes without 5'AMP. Data account for nine to thirteen independent experiments. **(F, G)** Levels of inorganic phosphate (Pi) **(F)** and of Adenosine **(G)** produced by FACS-sorted monocytes analyzed after the addition of the CD73 substrate (5'AMP; 1 mM) with or without the CD39 inhibitor (POM1) or the CD73 inhibitor (APCP). Data is presented in bars as the mean + SD concentration of Pi. Data accounts for four independent experiments. Statistical differences in each bar are compared to cells without 5'AMP or to the indicated groups where *p<0.05, **p<0.01, ***p<0.001 and ****p<0.0001 by Two-way ANOVA with Tukey's post-hoc analysis.

monocytes were cultured in the presence of MSC's conditioned medium (**Supplementary Figure 2**), which neither induced CD73 expression in monocytes.

CD73 induced in conditioned monocytes is functional

The functionality of CD73 was then evaluated through the production of inorganic phosphate (Pi) and Adenosine yielded from the hydrolysis of the CD73 substrate 5'AMP (**FIGURE 15D**). Confirming the high upregulation of CD73, MSC-co-cultured monocytes induced a much greater amount of Pi production compared to control and also LPS-stimulated monocytes (**FIGURE 15E**). Pi production was only detected when 5'AMP was added to the cells, as an indication of CD73 action rather than from other ectoenzymes. Enzyme activity inhibition was also evaluated by using the ADP analogue APCP. These experiments showed a dose-dependent abrogation of Pi production by MSC-conditioned monocytes and a fully blocked Pi production in LPS-stimulated monocytes (**FIGURE 15E**).

In parallel experiments, CD73 enzyme functionality was also confirmed in cATMSCs and UCMSCs as a positive control. As expected by their higher CD73 expression, both cATMSCs and UCMSCs displayed a higher 5'AMP hydrolytic activity which was dose-dependently blocked with APCP (**Supplementary Figure 3**). Furthermore, CD73 activity was responsible in part of the abrogation of allogeneic T cell proliferation by MSCs (**Supplementary Figure 4**).

In order to further discard the production of Pi from other upstream hydrolysis, we checked the Pi concentration in the presence of the CD39 inhibitor POM1 (**FIGURE 15F**). Again, Pi was only produced in the presence of the CD73 substrate 5'AMP, and while POM1 did not affect Pi production by MSC co-cultured monocytes, it was inhibited when APCP was added (**FIGURE 15F**). We then confirmed the production of Adenosine by MSC co-cultured monocytes, which was found in the supernatant only when 5'AMP was added to the monocytes, and was abrogated by APCP addition (**FIGURE 15G**), indicating a CD73 functional enzymatic action.

MDDCs are not affected by MSC conditioning

In light of monocyte modulation by MSCs, we sought to explore the ability of MSCs to alter the maturation and CD73 expression of further differentiated cells such as monocyte-derived dendritic cells (MDDCs). Opposed to monocytes, the levels of CD73 and CD90 remained unchanged in MDDCs co-cultured with cATMSCs or UCMSCs (**FIGURE 16A-B**), which was

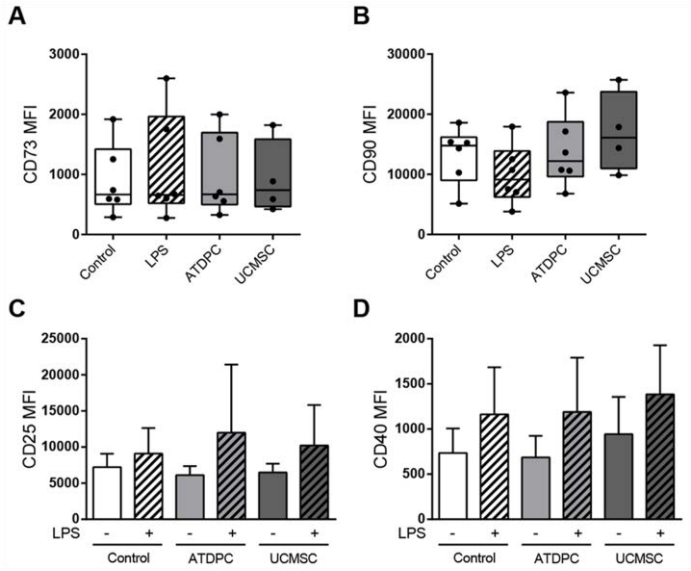

FIGURE 16 | CD73 and CD90 are not induced by MSC co-culture in MDDCs. (A, B) CD73 and CD90 MFI of MDDCs cultured for 48h alone or with LPS, ATDPCs or UCMSCs. **(C, D)** MFI values of the maturation markers CD25 and CD40 of MDDCs cultured for 48h with or without cATMSCs or UCMSCs, and further stimulated with LPS (dashed bars) or not. Data is expressed as min-max boxplot (A,B) or mean + SD (C,D), and account for six independent experiments.

confirmed as well by studying the mRNA levels of both CD markers (data not shown). On the other hand, MSCs failed to modulate MDDC maturation markers CD25 and CD40 (**FIGURE 16C-D**), which were upregulated to the same extent by LPS stimulation, regardless of MSC co-culture.

Host monocytes acquire CD73 in vivo in swine post-infarcted myocardium treated with porcine cATMSCs

To investigate whether this in vitro effect occurred in vivo, we analysed the presence of infiltrating monocytes and CD73 expression in a swine model of myocardial infarction (MI) locally treated with porcine cATMSCs, previously reported by our group to reduce the amount of infiltrating effector T cells in the infarcted tissue and to ameliorate the regeneration of the myocardium (Prat-Vidal et al. 2014; Gálvez-Montón et al. 2017). In these studies, treated animals versus controls experimented a significant reduction in infarct size (3.4±0.6% vs. 6.5±1%; p = 0.015) and fibrosis in the infarct scar (collagen I/III ratio; 0.49±0.06 vs. 1.66±0.5; p = 0.019), and improved in cardiac function (left ventricular ejection fraction; 7.5±4.9% vs. 1.4±3.7%; p = 0.038, and stroke volume; 11.5±5.9 ml vs. 3±4.5 ml; p = 0.019).

MSCs were delivered in the ischemic area by the implantation of an allogeneic engineered bioactive graft comprising GFP-labelled porcine cATMSCs, compared to the use of an "empty" graft in control animals. In the present study, one month after the implantation we detected how GFP+ cells (cATMSCs), expressing CD73 but not the monocyte marker CD163 (**FIGURE 17A and B**), actively migrated from the graft to the infarcted tissue and persisted within the damaged area in treated animals. Noticeably, treated, control and sham animals had infiltrating monocytes

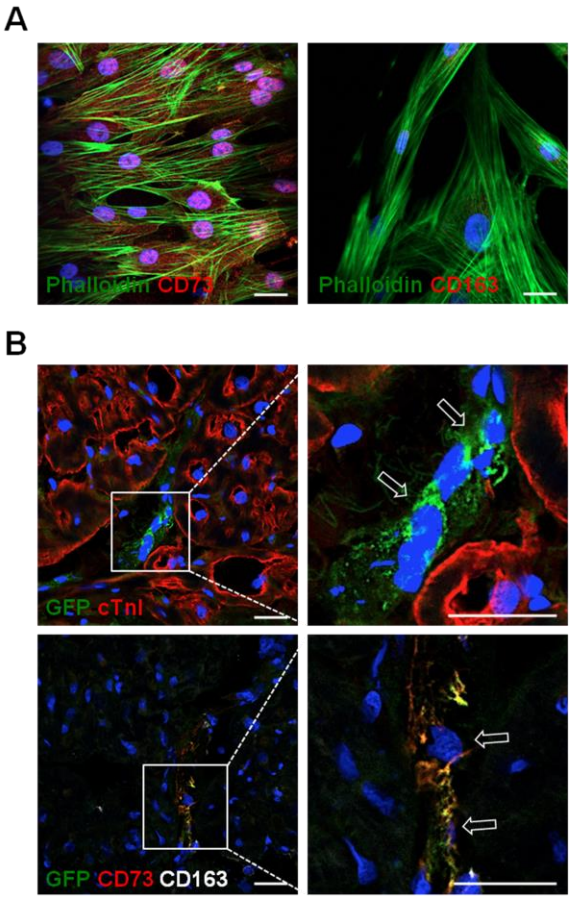

FIGURE 17 | Allogeneic cATMSCs migrated to the infarcted myocardium after graft implantation in swine. Representative confocal microscope images showing **(A)** porcine cATMSCs in *in vitro* culture or **(B)** sections within the infarcted myocardium. **(A)** Porcine cATMSCs are positive for CD73 (left, red) and negative for CD163 (right, red). **(B)** Presence of GFP^{+} porcine cATMSCs (empty arrows) in post-infarcted myocardium, also positive for CD73 but negative for CD163 (lower panels). Cell morphology, cardiac muscle and cell nuclei are also counterstained using Atto 488-phalloidin, anti-cTnI Ab and DAPI, respectively. Scale bars = 50 μm.

(CD163+) in the infarcted tissue (**FIGURE 18A, B, and C**), but only in treated animals receiving cATMSCs after MI the infiltrating host monocytes gained CD73 expression. After quantification, no differences were found in the amount of CD163+ infiltrating monocytes between groups (**FIGURE 18D**). However, we could corroborate the gain on CD73 expression on host monocytes in treated versus both control and sham animals in terms of absolute numbers (3.95±2.45 vs. 1.12±0.66 vs. 0.54±0.83 CD73 CD163 cells; p = 0.028 and p = 0.019, respectively) (FIGURE 18**E**), and also in the percentage of CD73+ out of CD163+ monocytes (35±11% vs. 8±6% vs. 9±12%; p = 0.001 and p = 0.0001, respectively) (**FIGURE 18F**).

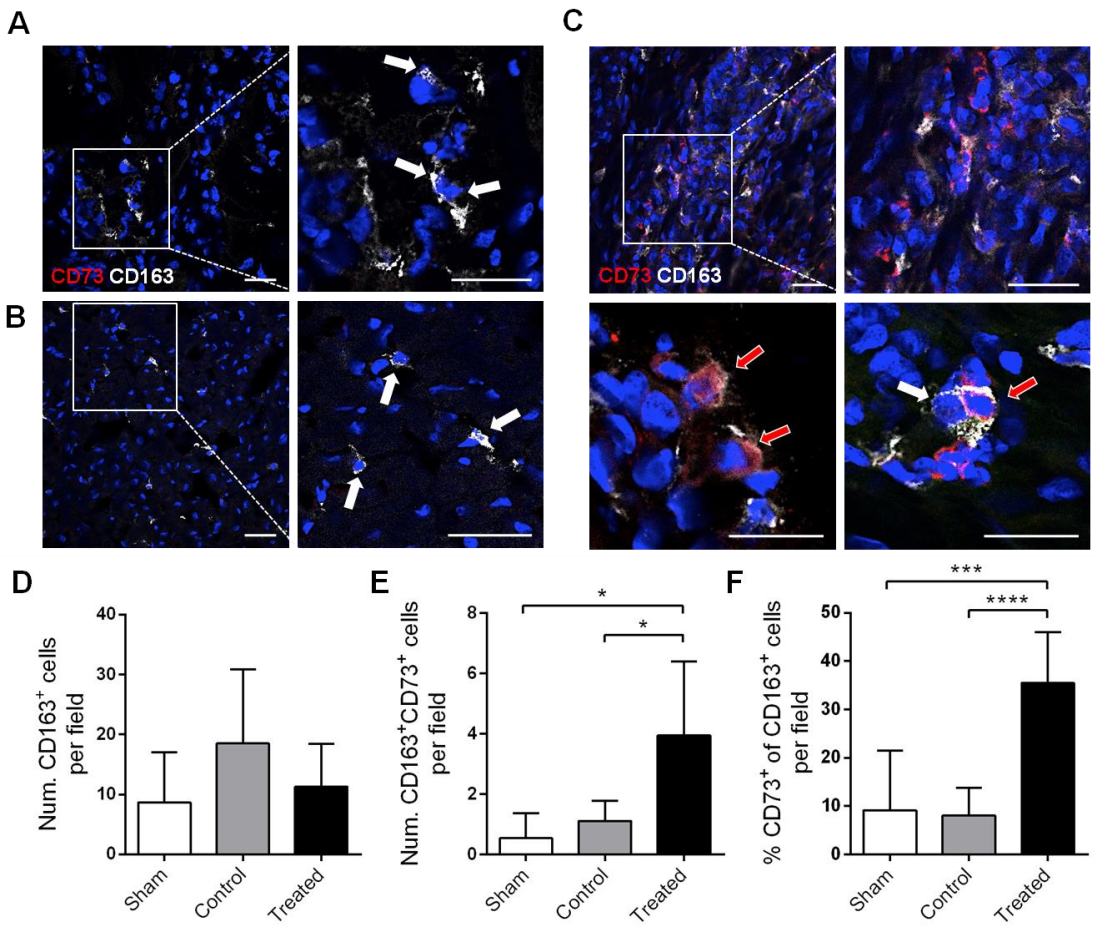

FIGURE 18 | CD73 is also induced *in vivo* in host monocytes in swine post-infarcted myocardium treated with porcine cATMSCs. (A-C) Infiltrating CD163$^+$ monocytes (white arrows), some of them expressing CD73 (red arrows) in a cATMSC-treated animal **(A)**, and CD163$^+$ monocytes (white arrows) in a control **(B)** and sham **(C)** animals, both negative for CD73. CD73 is shown in red and CD163 in white, and nuclei are counterstained with DAPI in blue. Scale bars = 50 μm. **(D, E)** Histograms showing the number of CD163$^+$ monocytes **(D)**, CD73$^+$ CD163$^+$ monocytes **(E)** per optical field in all studied groups. **(F)** Percentage of CD73$^+$ monocytes out of the CD163$^+$ monocytes. Differences in immunohistochemical quantifications were compared using one-way ANOVA for multiple comparisons, with Tukey's test for the *post hoc* analysis.

DISCUSSION

In this first chapter we demonstrate the molecular interplay between MSCs and monocytes, and highlight the induction of the adenosinergic pathway on monocytes as an additional mechanism of immunomodulation and tissue healing. Particularly, we show that both human UCMSCs and human cATMSCs induce specifically in monocytes the expression of the CD73 ectonucleotidase. By this function, together with the constitutive expression of CD39, monocytes would gain the ability to sequentially hydrolyse ATP to increase extracellular Ado concentration. Moreover, we corroborate this effect *in vivo*, as the local delivery of porcine cATMSCs into post-infarcted swine myocardium effectively resulted into the expression of CD73 on infiltrating host monocytes, fostering an anti-inflammatory milieu.

The degradation of exogenous pro-inflammatory ATP into anti-inflammatory Ado has been attributed a key role for the control of inflammation in the local environment, and also to have systemic effects (Regateiro, Cobbold, and Waldmann 2013; A. Ohta and Sitkovsky 2014; Schenk et al. 2011; Szabo and Pacher 2012). Ado reduces NK, macrophage, dendritic, B and T cells activation (Erdmann et al. 2005; Haskó and Cronstein 2013; Panther 2001; Csóka et al. 2012), neutrophil accumulation (H. K. Eltzschig et al. 2004), while promotes the generation of M2 macrophages and expansion of regulatory T cells ($CD39^+/CD73^+$), thus establishing an adenosinergic amplification loop (Mandapathil et al. 2010; Q. Zhou et al. 2009; Deaglio et al. 2007; Regateiro et al. 2011; A. Ohta and Sitkovsky 2014). It further proves to be a powerful systemic immunosuppressant as Ado production is used as an immune evasion strategy by pathogens (Nikolova et al. 2011; Thammavongsa et al. 2009; Smail et al. 1992) and cancer cells (Clayton et al. 2011; Stagg et al. 2010; Beavis et al. 2012), and its accumulation leads to a severe combined immunodeficiency in patients lacking ADA for Ado degradation (Gaspar et al. 2009; Giblett et al. 1972). Remarkably, Ado production also helps in wound healing and tissue repair (Haskó et al. 2008), as inhibits post-hypoxic vascular leakage (Thompson et al. 2004) and promotes angiogenesis via VEGF production by macrophages (Leibovich et al. 2002). These effects have been proven *in vivo*, where increased Ado levels reduced necrotic injury and oedema formation, and limited infarct size in mouse and swine models of MI (Kohler et al. 2007; Vilahur et al. 2016).

The presence of the purinergic ectoenzymes CD39/CD73 has been described for different organs and cell types. For instance, while MSCs and endothelial cells display a constitutive expression (Saldanha-Araujo et al. 2011; M. Ohta et al. 2013), CD39/CD73 are triggered upon cell activation in the generation of Tregs, whereas CD73 is reduced in activated B cells (Saze et al. 2013). MSCs have also been shown to induce CD73 expression in NK cells, although to a much lesser extent than we observed in monocytes (Chatterjee et al. 2014). In our experiments, we interestingly observed that LPS stimulation of TLR4 incremented CD73 expression in monocytes, probably as a balancing mechanism of cell activation, like it was observed in mouse before (Pinhal-Enfield et al. 2003; Leibovich et al. 2002). However, only MSC co-culture lead to sustained CD73 expression and to active 5'AMP hydrolysis by these cells, in a mechanism dependent of cell contact. Monocytes were polarized by both cATMSCs and UCMSCs towards an anti-inflammatory M2-like phenotype and to secrete immunomodulatory cytokines (IL10, CCL18) (Melief, Schrama, et al. 2013; W. Deng et al. 2015; J. Kim and Hematti 2009), but it is worth to mention that other M2 switches such as the classical "M2A" induction by IL4 does not promote CD73 upregulation (Eichin et al. 2015).

We focused our attention to the presence of the ectoenzymes mediating the canonical pathway of Adenosine production, given that ATP would be incremented and readily available in sites of injury and inflammation such as a post-MI tissue (Mizumoto et al. 2002). Nevertheless, we observed that the non-canonical enzymatic pathway leading to the extracellular availability of 5'AMP, as it is the conversion of NAD^+ to AMP by CD38/CD203a (Horenstein et al. 2013) may be also playing a part in MSC-conditioned monocytes, as CD38 expression was also increased by MSC co-culture. On the other hand, CD203a is a known marker of macrophages (C. B. Petersen et al. 2007; Singleton et al. 2016). Both pathways (CD38/CD203a and CD39) converge in the formation of 5'AMP, thus the upregulation of CD73 is relevant in both enzymatic scenarios.

These observations are important given the reported short lifespan of MSCs after infusion *in vivo*. Once injected *iv*, MSCs get trapped in the lung barrier because of their big size, and are removed by monocytes/macrophages within hours (Fischer et al. 2009; Eggenhofer et al. 2012; R. H. Lee et al. 2009; Xian-bao Liu et al. 2012), thus theoretically impeding the action of MSCs in the target tissue. Nevertheless, MSCs still promote a long-lasting systemic immunosuppressive effect for the resolution of inflammation and regeneration of wounded tissue. These effects could be firstly mediated temporarily by paracrine mediators, but secondarily by the modulation of the host's immune cells. In this sense, soluble molecules such as IL6, PGE2, TGFβ, IDO, HGF, HLA-G, TSG6 and EVs have been attributed to promote such paracrine effects (Soleymaninejadian, Pramanik, and Samadian 2012; Monguió-Tortajada, Roura, Gálvez-Montón, Pujal, et al. 2017; R. H. Lee et al. 2009). Moreover, given that MSCs express CD39 and CD73 constitutively, Ado production is also part of MSC's paracrine immunosuppressive activity. In fact, CD73 itself can also have systemic effects. It can be both shed from the membrane, acting in its soluble form (Yegutkin, Samburski, and Jalkanen 2003; Maksimow et al. 2014; Airas et al. 1997), and also be released within EVs, as proved by Amarnath et al. in an animal model of Th1 inflammation treated with infused MSCs, in which systemic Ado production by released CD73 mediated the resolution of inflammation (Amarnath et al. 2014).

Following these MSC paracrine primary immunomodulatory effects, MSCs may modulate the action of immune cells for the generation of regulatory environments. Monocytes, which are present in great numbers especially in the lungs, would interact with the infused MSCs and acquire an M2-like phenotype, including CD73 mRNA expression in less than 24 hours, as shown by our results. These $CD38^+/CD39^+/CD73^+$ monocytes are fit to easily go through the lung barrier and migrate to the inflamed tissue to promote *in situ* immunomodulation and healing. Although the level of CD73 activity was much higher in MSCs, monocytes would have the advantage of a more competent migration and thus delivering a targeted local effect.

At the same time, when MSCs are delivered directly to the injured tissue, they can regulate monocyte function locally, which are, together with granulocytes, the first cells to infiltrate into inflamed tissue (Bönner et al. 2012). Remarkably, we previously demonstrated the use of a scaffold of decellularized human pericardium for the local delivery of porcine cATMSCs to the post-MI injured tissue. MSC treatment attained *in vivo* attenuation of inflammation (i.e. fewer activated T cells) and promoted the regeneration of the damaged myocardial tissue in post-infarcted pigs (Gálvez-Montón, Bragós, et al. 2017). Here, we also show the acquisition of CD73 expression by infiltrated host monocytes in MSC-treated animals, thus establishing an adenosinergic positive loop. The gain in CD73 by host monocytes was dependant on the combination of monocyte activation in response to proinflammatory DAMPs released after MI

and the modulation by cATMSCs contained within the graft, given that both control and sham animals lacked presence of CD73 in monocytes.

This finding agrees with those reported by others confirming that collaboration with monocytes has been found to be essential for MSCs activity, from immunomodulation and Treg generation (Melief, Schrama, et al. 2013; Groh et al. 2005) to stopping infiltration and aiding in the regeneration of inflamed tissue (Lu et al. 2015; Blázquez, Sánchez-Margallo, Álvarez, et al. 2016; Ben-Mordechai et al. 2013; Dayan et al. 2011).

Noteworthy, since the *in vitro* co-culture setting and the *in vivo* local administration of MSCs hinders the distinction between monocyte- and MSC-derived soluble CD73, we did not check for presence of soluble CD73, which is a limitation of our study. This might be underestimating the upregulation in CD73 protein expression by monocytes and thus could explain in part the differences between the mRNA and protein fold increase found in monocytes.

Our functional experiments were focused to check the functionality of CD73 upregulation on MSC-conditioned monocytes. Therefore, we studied the last enzymatic step of extracellular Adenosine production mediated by the ectonucleotidase CD73. Pi and Adenosine levels did not increase in the absence of 5'AMP, and their production was only affected by APCP while not by POM1. Thus, Pi and Adenosine production could be attributed to CD73-mediated 5'AMP hydrolysis and discarded the action of other ectoenzymes such as CD39 or Pi release due to FACS-related sheer stress, as all cells underwent the same FACS separation.

Finally, studies on the modulation by MSC of further differentiated cells such as dendritic cells have been proven controversial. Most studies describe MSCs able to modulate dendritic cell biology specially when added early in the differentiation process. However, in line with our observations, some authors report no effect of MSCs on later steps of differentiation or maturation process (Spaggiari et al. 2009; Nauta, Kruisselbrink, et al. 2006). This seems to indicate that the MSC modulation would preferentially act on non-activated cells.

In sum, the upregulation of CD73 in MSC-conditioned monocytes emerges as an additional potential mechanism supporting the long-lasting immunomodulatory and healing effects of MSCs delivery. A better understanding of the signalling pathways triggered in monocytes by MSCs will help to better define new therapies for tissue injury and regenerative medicine.

SUPPLEMENTARY FIGURES

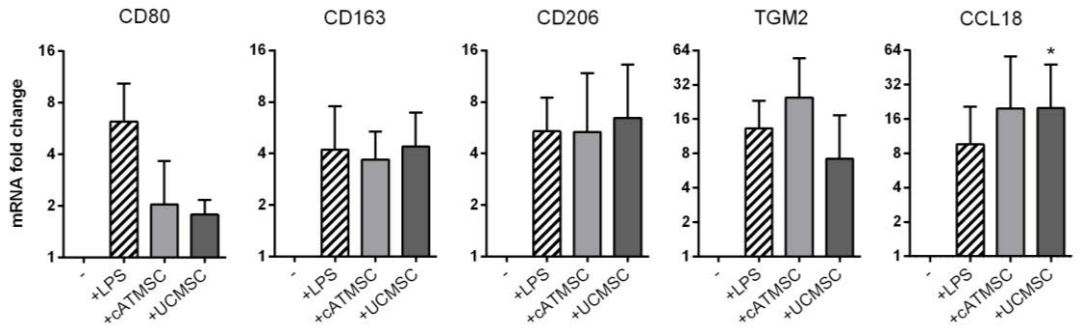

Supplementary Figure 1 | **Polarization markers.** mRNA fold change of the M1 marker CD80 and M2 markers CD163, CD206, TGM2 and CCL18 in monocytes stimulated with LPS or co-cultured with cATMSCs or UCMSCs compared to monocytes alone (-). Statistical differences are indicated where *p<0.05 to monocytes alone by One-way ANOVA with Tukey's post-hoc test.

Related to **FIGURE 11**.

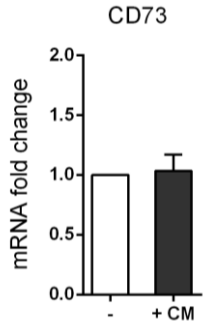

Supplementary Figure 2 | **CD73 mRNA expression in monocytes is unchanged by MSC's conditioned media.** mRNA fold change of CD73 ($2^{-\Delta\Delta Ct}$) of monocytes cultured in the presence of UCMSC's conditioned media (CM), relative to monocytes cultured alone. Data is expressed as mean + SD and accounts for four independent experiments of different monocyte and UCMSC donors.

Related to **FIGURE 15**.

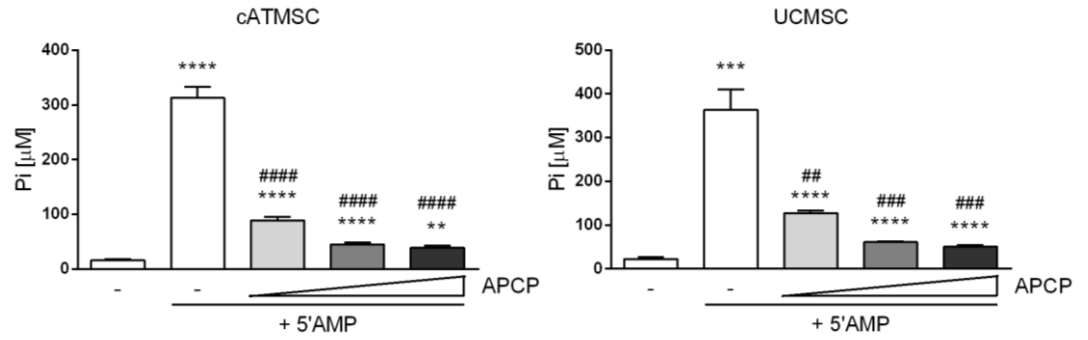

Supplementary Figure 3 | **CD73 activity of MSCs.** Levels of inorganic phosphate produced by cATMSCs and UCMSCs after 2h of the addition of the CD73 substrate 5'AMP (1 mM), with or without the CD73 inhibitor (APCP; 10, 50 or 100 µM). Data is represented as the mean + SD of six independent experiments. Statistical differences are indicated where **p<0.01, ***p<0.001, ****p<0.0001 compared to cells without 5'AMP by One-way ANOVA with Tukey's post-hoc test; and ##p<0.01, ###p<0.001, ####p<0.0001 compared to cells with 1mM 5'AMP and without APCP, by Student's T-test.

Related to **FIGURE 15**.

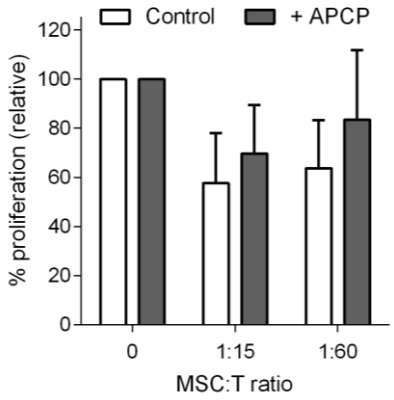

Supplementary Figure 4 | **CD73 activity is partly responsible of the abrogation of allogeneic T cell proliferation by MSCs.** CFSE-labelled T cells were stimulated with anti-CD2/3/28 beads and co-cultured with allogeneic UCMSCs in the presence (dark bars) or not (white bars) of APCP (10 μM; CD73 inhibitor). Polyclonal proliferation of T cells ($FSC^{high}/CFSE^{low}$) is expressed as relative to T cells alone. Data account for five independent experiments. *For detailed Material and Methods see Chapter 2*.

Related to **FIGURE 15**.

Supplementary Table 1 | Primers used for real time PCR.

Gene	Primer	Sequence (5'-3')	Tm[1] [ºC]	%GC	Amplicon size [bp]
18S	Forward	TCTTTCTCGATTCCGTGGGT	58.74	50	145
	Reverse	TCTAAGAAGTTGGGGGACGC	59.39	55	
CCL18	Forward	GCTGCCTCGTCTATACCTCC	59.4	60	113
	Reverse	CCGGCCTCTCTTGGTTAGGA	60.98	60	
CD80	Forward	CTGCCTGACCTACTGCTTTG	58	55	77
	Reverse	GGCGTACACTTTCCCTTCTC	58	55	
CD163	Forward	CACCAGTTCTCTTGGAGGAACA	59	50	82
	Reverse	TTTCACTTCCACTCTCCCGC	59	55	
CD206	Forward	ACACAAACTGGGGGAAAGGTT	59.99	47.62	174
	Reverse	TCAAGGAAGGGTCGGATCG	58.8	57.89	
IL10	Forward	CGAGATGCCTTCAGCAGAGT	59.82	55	189
	Reverse	CGCCTTGATGTCTGGGTCTT	60.04	55	
TGM2	Forward	CCTCGTGGAGCCAGTTATCAA	59	52	223
	Reverse	GTCTGGGATCTCCACCGTCTTC	62	59	

[1]Tm: primer melting Temperature

CHAPTER 2

Based on "Nanosized UCMSC-derived extracellular vesicles but not conditioned medium exclusively inhibit the inflammatory response of stimulated T cells: implications for nanomedicine"

Marta Monguió-Tortajada[1,*], Santiago Roura[2,3,*], Carolina Gálvez-Montón[2], Josep Maria Pujal[4], Gemma Aran[5], Lucía Sanjurjo[5], Marcel·la Franquesa[1,6], Maria-Rosa Sarrias[5], Antoni Bayes-Genis[2,7,8], Francesc E. Borràs[1,6,†]

[1]REMAR-IVECAT Group, Health Science Research Institute Germans Trias i Pujol, Can Ruti Campus, Badalona, Spain, [2]ICREC Research Program, Health Science Research Institute Germans Trias i Pujol, Can Ruti Campus, Badalona, Spain, [3]Center of Regenerative Medicine in Barcelona, Barcelona, Spain, [4]Cell Processing Laboratory, Parc Científic i Tecnològic Universitat de Girona, Girona, Spain, [5]Innate Immunity Group, Health Sciences Research Institute Germans Trias i Pujol, Badalona, Spain, [6]Nephrology Service, Germans Trias i Pujol University Hospital, Badalona, Spain, [7]Cardiology Service, Germans Trias i Pujol University Hospital, Badalona, Spain
[8]Department of Medicine, UAB, Barcelona, Spain
*Both authors contributed equally to this work
† Corresponding author

Published in the Open Access Journal *Theranostics,* 2017 Jan 1;7(2):270-284.

doi: 10.7150/thno.16154. PMID: 28042333

ABSTRACT

Undesired immune responses have drastically hampered outcomes after allogeneic organ transplantation and cell therapy, and also lead to inflammatory diseases and autoimmunity. Umbilical cord mesenchymal stem cells (UCMSCs) have powerful regenerative and immunomodulatory potential, and their secreted extracellular vesicles (EVs) are envisaged as a promising natural source of nanoparticles to increase outcomes in organ transplantation and control inflammatory diseases. However, poor EV preparations containing highly-abundant soluble proteins may mask genuine vesicular-associated functions and provide misleading data. Here, we used Size-Exclusion Chromatography (SEC) to successfully isolate EVs from UCMSCs-conditioned medium. These vesicles were defined as positive for CD9, CD63, CD73 and CD90, and their size and morphology characterized by NTA and cryo-EM. Their immunomodulatory potential was determined in polyclonal T cell proliferation assays, analysis of cytokine profiles and in the skewing of monocyte polarization. In sharp contrast to the non-EV containing fractions, to the complete conditioned medium and to ultracentrifuged pellet, SEC-purified EVs from UCMSCs inhibited T cell proliferation, resembling the effect of parental UCMSCs. Moreover, while SEC-EVs did not induce cytokine response, the non-EV fractions, conditioned medium and ultracentrifuged pellet promoted the secretion of pro-inflammatory cytokines by polyclonally stimulated T cells and supported Th17 polarization. In contrast, EVs did not induce monocyte polarization, but the non-EV fraction induced CD163 and CD206 expression and TNFα production in monocytes. These findings increase the growing evidence confirming that EVs are an active component of MSC's paracrine immunosuppressive function and affirm their potential for therapeutics in nanomedicine. In addition, our results highlight the importance of well-purified and defined preparations of MSC-derived EVs to achieve the immunosuppressive effect.

INTRODUCTION

MSCs represent a promising strategy for a variety of medical conditions, including treatment of damaged tissue, inflammatory diseases and transplantation(Roura et al. 2015; Katarina Le Blanc et al. 2004). Better knowledge on the cellular conditions to unleash their full potential would help design the most efficient biological product. While the immune capabilities of UCMSC (Wharton's jelly) have been poorly described yet, MSCs from bone marrow and adipose tissue have been suggested to acquire better immunosuppressive functions after encountering an inflammatory stimulus, such as *in vitro* priming by IFNγ (Menard et al. 2013; Krampera, Cosmi, et al. 2006; Polchert et al. 2008; Renner et al. 2009; Ryan et al. 2007; de Witte et al. 2015).

Moreover, increasing evidence has shown that the restorative and immunosuppressive functions exerted by MSCs are both cell-contact dependent and also mediated through a variety of secreted soluble factors in a paracrine fashion, including tryptophan depletion by IDO, production of immunosuppressive molecules and cytokines such as adenosine, NO, PGE_2, IL-10 and TGFβ (Regateiro et al. 2011; Madrigal, Rao, and Riordan 2014; Meisel et al. 2004; K. Chen et al. 2010) and also released extracellular vesicles (EVs) (T. Li et al. 2013; Lener et al. 2015).

EVs are membrane nanovesicles, which range approximately from 30 to 200 nm, carrying molecules that reflect the phenotype and functions of the cells of origin (Yáñez-Mó et al. 2015). To date, therapeutic applications of MSC-EVs include treatment of experimental acute and chronic kidney injury (Gatti et al. 2011), reduction of ischemia/reperfusion injury (Lai et al. 2010) and Graft-versus-Host Disease suppression (Kordelas et al. 2014). Taken together, these studies point to MSC-EVs as promising candidates for novel cell-free therapies (Lener et al. 2015; Katsuda et al. 2013). In the context of bionanotechnology, however, there are still open questions regarding the best method of EV preparation and concentration, characterization in terms of biological activity (Lötvall et al. 2014; Marcella Franquesa et al. 2014), and definition of the underlying mechanisms of action for the standardization of EV preparations that can be used in the clinical setting (Fais et al. 2016). These points, along with the reported non-beneficial effect of non-purified MSC conditioned medium (CM) itself (Conforti et al. 2014; Gouveia de Andrade et al. 2015), stress the need for refining more efficient MSC-EV preparations and characterize them in terms of immunomodulatory potential.

Thus, in the second chapter, we examine the suppressive potential of Size-Exclusion Chromatography (SEC)-enriched EVs derived from UCMSCs and compared the data with the non-EV containing fractions, non-purified CM and its ultracentrifuged pellet (UC pellet). The presented results demonstrate that nanosized EVs retain the immunosuppressive effect of MSCs mainly by inhibiting T cell proliferation and preventing the secretion of pro-inflammatory cytokines by polyclonally stimulated T cells.

MATERIALS AND METHODS

UC collection, MSC isolation, culture and characterization

The study protocols were approved by the Clinical Research Ethics Committee of our institution (Comitè Ètic d'Investigació Clínica, HuGTiP, Refs. CEIC: EO-10-016 and EO-12-022) and conformed to the principles outlined in the Declaration of Helsinki. With the consent of the parents, fresh umbilical cords (n= 10) were obtained after birth and UCMSCs were isolated and cultured as reported in *Chapter 1*.

Cells were labelled with 7AAD for viability and the antibodies anti-CD73-PE, -CD90-PE-Cy7, -HLA-DR-APC-H7 or the corresponding IgG isotype control (all from BD) for immunophenotyping. Labelling was performed at room temperature for 15 min, washed with FACSFlow 2% FBS and centrifuged at 400 *xg* for 5 min. Data was acquired in a Canto II flow cytometer (BD) and analysed by FlowJo v.X software (TreeStar, Ashland, OR).

Generation of EV-depleted culture medium

Complete culture medium was composed of α-MEM (Sigma Aldrich) or TexMACS (Miltenyi Biotech, Bergisch Gladbach, Germany) medium supplemented with 2 mM L-Glutamine (Sigma Aldrich), 100 U/ml Penicillin (Cepa S.L., Madrid, Spain), 100 µg/ml Streptomycin (Normon Laboratories S.A., Madrid, Spain) and 10% (v/v) Heat Inactivated-FBS or Human platelet lysate (Lonza, Basel, Switzerland) for MSC and T cell culture, respectively. Plasmocin (5 μg/mL; Invivogen) was added for MSC culture.

Culture medium was depleted of bovine/human EVs by ultracentrifugation of 2x complete medium in polypropylene ultracentrifugation tubes (Beckman coulter, Brea, CA) at 100,000 *xg* for 16 h (SW28 rotor, 28000 rpm, adjusted k-Factor= 253.96). The supernatant was collected and filtered through a 0.22 µm filter (Sarstedt, Germany) to sterilize the medium, which was finally diluted to 1x working concentration with αMEM/TexMACS medium alone for cell culture.

EV isolation

All relevant data regarding our experiments have been submitted to the EV-TRACK knowledgebase (EV-TRACK ID: EV170002) (Van Deun et al. 2017). EVs were isolated from UCMSCs following the scheme in **FIGURE 20A**. For MSCs-CM generation, $5x10^6$ UCMSCs were seeded in bovine EV-depleted culture medium with or without 200 ng/ml (120 IU/ml) IFNγ (Peprotech; cat#300-02, Rocky Hill, NJ) when indicated. Supernatant was collected after 48 h and sequentially centrifuged at 400 *xg* for 5 min and at 2,000 *xg* for 10 min to exclude cells and cell debris, respectively. This debris-cleared CM was then concentrated by 100 kDa ultrafiltration using Amicon Ultra (Millipore, Millerica MA) at 2,000 *xg* for 35 min, obtaining typically 250 µl concentrated CM (CCM). The eluted CM (ECM) was kept for additional experiments.

UCMSC-EVs were then isolated from the CCM by SEC using a modification of the previously published method (I. Lozano-Ramos et al. 2015). Briefly, 1 ml of Sepharose CL-2B (Sigma Aldrich) was extensively washed with PBS (Oxoid, Hampshire, UK) and packed in a 1-ml syringe (BD). A 100 µl sample of CCM was loaded into the column and 100-µl fractions (up to 20) were collected immediately after loading. Protein elution was checked by reading absorbance at 280 nm of each fraction using Nanodrop (Thermo Scientific, San Diego, CA).

In some experiments, CM was ultracentrifuged at 100,000 *xg* for 2 h (SW55Ti rotor, 32500 rpm, adjusted k-Factor= 138.67), and the UC pellet was used for comparative experiments. As a control, 15 ml of bovine EV-depleted culture medium alone was incubated and followed the same EV isolation procedure. All fractions were kept at 4ºC and used within 24h for in vitro experiments, or frozen (-1ºC/min) at -80ºC for NTA and cryo-EM analysis. In the indicated experiments, fractions were concentrated seven-fold by 90 min vacuum concentration at 30ºC using the miVac (GeneVac, Ipswich, UK).

EV characterization

Flow cytometry

The presence of EVs in the SEC fractions was determined according to their content in tetraspanins by bead-based flow cytometry. Briefly, EVs were coupled to 4 µm aldehyde/sulphate-latex microspheres (Invitrogen, Carlsbad, CA) for 15 min at RT and blocked in BCB buffer (PBS/0.1% BSA/0.01% NaN_3; both from Sigma Aldrich) on overnight rotation. EV-coated beads were spun down at 2000 *xg* for 10 min, washed with BCB buffer and re-suspended in PBS.

EV-coated beads were then labelled with the fluorochrome-conjugated antibodies anti-CD73-PE, -CD90-PE-Cy7, -HLA-ABC-FITC or -HLA-DR-APC-H7 (all from BD) or indirectly labelled with the primary antibodies anti-CD9 (Clone VJ1/20) and -CD63 (Clone TEA3/18) or the IgG isotype control (Abcam, Cambridge, UK) and secondary antibody FITC-conjugated Goat F(ab')2 Anti-Mouse IgG (Bionova, Halifax, NS, Canada). Labelling was performed at room temperature for 30 min under mild shaking, and EV-coupled beads were washed after each step with BCB buffer and centrifuged at 2,000 *xg* for 10 min. Data was acquired in a FACSVerse flow cytometer (BD) and analysed by FlowJo v.X software (TreeStar).

Nanoparticle Tracking Analysis

Size distribution of particles on SEC fractions was determined by NTA in a NanoSight LM10-12 instrument (Malvern Instruments Ltd, Malvern, UK), equipped with a 638 nm laser and CCD camera (model F-033). Data was analysed with the NTA software version 3.1. (build 3.1.46), with detection threshold set to 5, and blur, Min track Length and Max Jump Distance set to auto. Samples were diluted 10 or 20 times with PBS to reach optimal concentration for instrument linearity: 20-120 particles/frame as advised by the manufacturer. Readings were taken on triplicates of 60 s at 30 frames per second, at a camera level set to 16 and with manual monitoring of temperature.

Cryo-electron microscopy

SEC fractions were examined for EV size and morphology by cryo-electron microscopy (cryo-EM). Vitrified specimens were prepared by placing 3 µl of a sample on a Quantifoil® 1.2/1.3 TEM grid, blotted to a thin film and plunged into liquid ethane-N2(l) in the Leica EM CPC cryoworkstation (Leica, Wetzlar, Germany). The grids were transferred to a 626 Gatan cryoholder and maintained at -179ºC. Samples were analysed with a Jeol JEM 2011 transmission electron microscope (Jeol, Tokyo, Japan) operating at an accelerating voltage of 200 kV. Images were recorded on a Gatan Ultrascan 2000 cooled charge-coupled device (CCD) camera with the Digital Micrograph software package (Gatan, Pleasanton, CA).

Proliferation assay

Whole blood was obtained from healthy donors after informed consent approved by the local Ethics Committee (Germans Trias i Pujol Universitary Hospital). PBMCs were obtained by Ficoll Hypaque Plus™ (GE Healthcare, Uppsala, Sweden) density centrifugation and T cells were then isolated using the negative selection EasySep™ Human T cell Enrichment Kit (StemCell Technologies, Grenoble, France) following manufacturer's instructions. Enriched T cells were then washed and stained with Carboxyfluorescein succinimidyl ester (CFSE, Molecular Probes, Leiden, The Netherlands) to assess cell proliferation. Succinctly, enriched T cells were resuspended in PBS for staining with an equal volume of 0.8 μM CFSE for 10 min, after which unbound dye was quenched with RPMI + 10% FBS. Labelled cells were washed twice with RPMI + 10% FBS before resuspending in 1x human EV-depleted TexMACS complete medium. T cells were routinely >93% pure (CD3+) and >94% viable in all experiments performed.

CFSE-labelled T cells ($3x10^5$) were stimulated with anti-CD2/CD3/CD28 coated microbeads (Pan T Cell Activation Kit; Miltenyi Biotech) or uncoated microbeads as a negative control in a 1:10 bead:T cell ratio, in flat-bottomed well plates in which allogeneic UCMSCs had been previously seeded (20000, 5000, 1250, 625, 325 or 160 cells/well). In parallel experiments, CFSE-labelled T cells were plated at $5x10^4$ cells/well in round-bottomed well plates and stimulated in the same way with anti-CD2/CD3/CD28 coated microbeads. T cells were co-cultured in the presence of 1:1 or 1:2 (v/v) EV, proximal or distal non-EV fractions, CCM, ECM or CM, corresponding to $2.5x10^5$ or $1.25x10^5$ initial UCMSCs, respectively. Alternatively, 1:20 (v/v) vacuum concentrated samples were added to stimulated T cells, corresponding to $2.5x10^5$, $1.25x10^5$ (1/2 dilution) or $2.5x10^4$ (1/10 dilution) initial UCMSCs. T cell proliferation was measured after 3.5 days in a LSR Fortessa Analyzer (BD Biosciences) and expressed as the percentage of $FSC^{high}CFSE^{low}$ cells out of the living cells gated by FSC/SSC using the proliferation module of the FlowJo V9.8.2.

Monocyte polarization

PBMCs were obtained from leukocyte residues from healthy donors from the Blood and Tissue Bank (Barcelona, Spain) by Ficoll Hypaque Plus™ density gradient centrifugation (GE Healthcare Biosciences), and CD3+ cells were depleted using the RosetteSep™ Human CD3 Depletion Cocktail (StemCell Technonogies). Monocytes were then isolated using the MagniSort Human CD14 Positive Selection kit (eBioscience) according the instructions supplied by manufacturer. Recovered cells were counted using PerfectCount Microspheres (Cytognos, Salamanca, Spain) and assessed for purity (>93% $CD14^+$) and viability (≥97% by FSC/SSC and $7AAD^-$ (BD) gating) in a Canto II flow cytometer (BD).

Monocytes were plated at $1x10^6$ cells/ml in RPMI medium containing 5% FBS and the polarizing stimuli for M1(LPS+IFNγ), 50ng/mL IFNγ (Preprotech) plus 100ng/mL LPS from *E. coli* O111:B4 (Sigma-Aldrich); M2a(IL-4), 40 ng/ml IL4 (Preprotech); M2c(IL10), 50 ng/ml IL10 (Preprotech), or with the EV, proximal non-EV fractions or full CM, and PBS alone (non-activated control). After 48h, the supernatant was harvested for cytokine determination and whole RNA was extracted from cells using the RNeasy Mini Kit (Qiagen). cDNA was synthesized using random hexamers (Qiagen) and the iScript™ One-Step RT–PCR Kit (BioRad Laboratories) according to supplier's protocol. Each cDNA was then amplified in a LightCycler® 480 PCR system (Roche Life Science) using the KAPA SYBR Fast Master Mix (KAPA Biosystems) and the primer sequences indicated in **Supplementary Table 2**. Samples were incubated for an initial

denaturation at 95°C for 5 min, and then 40 PCR cycles were performed at 95°C for 10 s, 60°C for 20 s and 72°C for 10 s. The values obtained by the "Fit point" method were correlated to a standard curve and normalized to the expression levels of the endogenous reference gene 18S. The gene expression levels of each stimulus were calculated as a fold change relative to non-activated monocytes.

Measurement of cytokine production

Cytokines present in supernatants from alloproliferation assays collected at day 3.5 were measured using the CBA human Th1/Th2 or the Th1/Th2/Th17 Cytokine kit (both from BD Biosciences), the TGFβ1 ELISA (eBioscience, San Diego, CA) and IL-17 ELISA (U-CyTech, Utrecht, The Netherlands) following manufacturer's instructions. Cytokines present in supernatants of 48h-cultured monocytes were measured using the human IL10 and TNFα ELISA (U-CyTech). Concentrations given by CBA were assessed in an LSR Fortessa Analyzer (BD) and concentrations of ELISA determinations in a Varioskan LUX multimode microplate reader (Thermo Scientific). The minimum detectable concentration (pg/ml) of each protein was 2.6 for IL2 and IL4, 3.0 for IL6, 2.8 for IL10 and TNFα, 7.1 for IFNγ, 8 for TGFβ1, 2 for IL17 and 1 for IL10 and TNFα.

Statistical Analysis

Values are expressed as mean ± standard deviation (SD). Kolmogorov-Smirnov analysis was used to check for normality of data. ANOVA one-way with Tukey's post-hoc analysis was applied to determine significance among more than two groups of parametric data. Paired T test and Wilcoxon matched-pairs signed rank test were used to analyse differences between two paired parametric and non-parametric data groups, respectively. Kruskall-Wallis analysis was used to determine significance among groups and Mann-Whitney test to find differences between two groups of non-parametric data. One sample T test and Wilcoxon Signed Rank test were used to determine differences of normalized parametric and non-parametric data, respectively. Analyses were performed using the GraphPad Prism software (6.01 version) and the SPSS statistic software (19.0.1 version, SPSS Inc., Chicago, IL), and differences were considered significant when $p<0.05$.

RESULTS

UCMSCs characterization

Primary cultures of elongated fibroblast-like cells established from UC were recognized as bona fide MSCs when evaluated by flow cytometry and in differentiation assays. In particular, over 95% of cells expressed an MSC-like profile, being positive for CD105, CD44, CD166, CD10, CD73, CD90, CD49c, CD49d, CD49e, and HLA-ABC, and negative for CD117, CD106, CD34, CD45, CD29, CD14, CD133, CD31, VEGFR2 and HLA-DR. Moreover, commitment of cells to the adipogenic, osteogenic and chondrogenic pathways resulted in accumulation of intracellular lipid droplets, in high extracellular deposition of calcium and in active synthesis of proteoglycans, respectively (**Supplementary Figure 5**).

We subsequently explored the influence of IFNγ priming on the MSC's phenotype. As shown in **FIGURE 19A**, cultured cells had a typical spindle-shaped morphology regardless of IFNγ priming. In terms of MSC markers, 48h-IFNγ conditioning lead to unchanged CD73 and decreased CD90 levels, while MHC class II expression (HLA-DR) was significantly increased (**FIGURE 19B and C**).

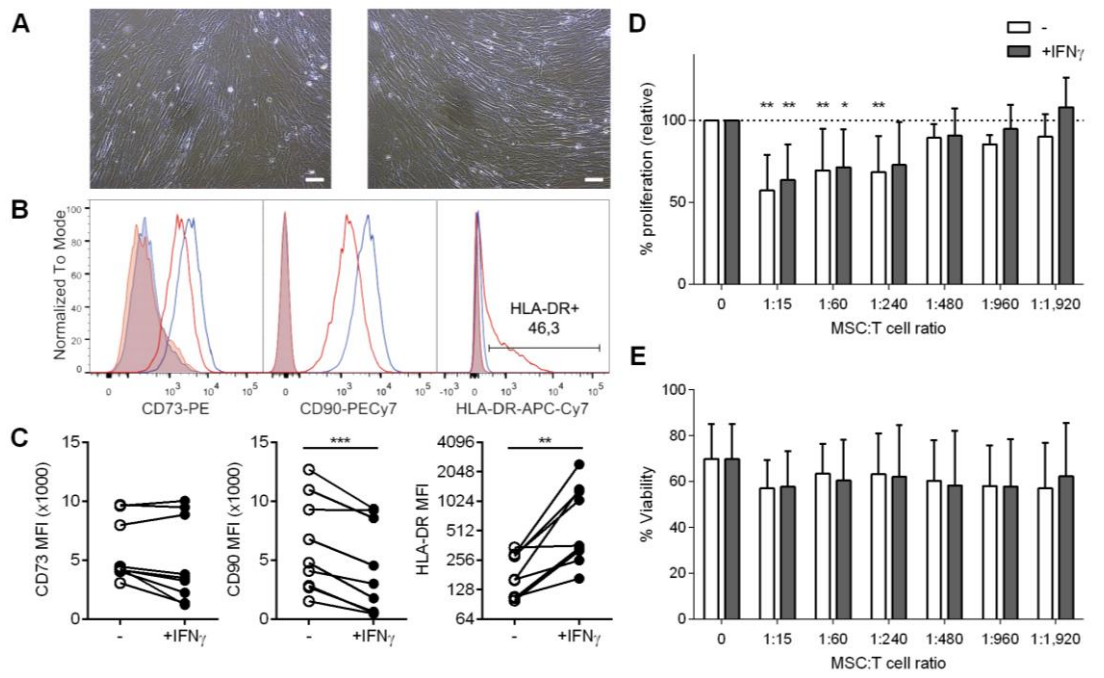

FIGURE 19 | **(A)** Bright-field images of UCMSC in culture media without (left) or with IFNγ (right). Scale bars = 100 μm. **(B-C)** UCMSCs primed with IFNγ expressed unchanged levels of CD73, lower levels of CD90 and higher levels of HLA-DR (class II MHC) on surface. **(B)** Representative histograms of unconditioned (blue line) and IFNγ-primed UCMSCs (red line) labelled for CD73, CD90 and HLA-DR. Isotype controls are depicted as shaded areas. **(C)** MFI values for CD73, CD90 and HLA-DR of UCMSCs after culture without (white circles) or with IFNγ (black circles). Data is shown for nine independent experiments. ***p<0.001 by Paired T test; **p<0.01 by Wilcoxon matched-pairs signed rank test. **(D-E)** Proliferation and viability of T cells stimulated with anti-CD2/CD3/CD28 coated microbeads in the absence or presence of unconditioned or IFNγ-primed UCMSCs at 1:15, 1:60, 1:240, 1:480, 1:960 or 1:1,920 cell ratios were analysed by CFSE loss and FSC/SSC gating, respectively. **(D)** Bars represent means ±SD of proliferation relative to their PBS control. **(E)** Bars represent means ± SD of the percentage of viable cells. Data accounts for seven independent experiments from different donor samples, performed in triplicates. Statistical differences are indicated for groups with *p<0.05 and **p<0.01 by One sample T test to the 100%.

UCMSCs suppress T cells proliferation

It has been widely shown that MSCs from different origins inhibit T cell proliferation. To determine whether human UCMSC possess this capability and to analyse the influence of IFNγ priming on these cells, T cells were stimulated in the presence of increasing numbers of unconditioned or IFNγ-conditioned UCMSCs. The results confirmed that UCMSCs were able to inhibit polyclonal T cell proliferation and only at extremely low UCMSC:T cell ratios this effect was lost (**FIGURE 19D**). Our experiments showed that IFNγ-conditioning did not change their immune regulatory capabilities, as the reduced T cell proliferation was similar to the unconditioned UCMSCs. In these experiments T cell viability was not affected (**FIGURE 19E**).

Isolation and characterization of EVs from UCMSCs

After confirming the immunosuppressive potential of UCMSCs, we aimed to investigate whether EVs could be a mediator of the paracrine immunosuppressive action. First, EVs produced by UCMSCs were enriched from concentrated 48h-Conditioned Medium (CCM) by SEC (**FIGURE 20A**). EVs were found in fractions 5 to 7 according to their positivity for the EV-associated tetraspanins CD9 and CD63 (**FIGURE 20B, C**). The MSC markers CD73 (70 kDa) and CD90 (25-37 kDa) co-eluted in the EV fractions (F5-7), suggesting their presence in EVs as recently published (H.-S. Kim et al. 2012). Bulk protein content of CCM was detected from fraction 9 onwards. Of note, CCM from both IFNγ-conditioned and unconditioned UCMSCs showed the same SEC elution pattern, in which EVs were successfully separated from the bulk of protein. In this scenario, three distinct pools of SEC fractions were collected for further studies: i) the EV fraction, a pool of the tetraspanin-peak fractions ("EV"; F5-7); ii) the early tetraspanin-negative fractions, pooled as the proximal non-EV fractions ("non-EV prox"; F10-11); and iii) the late tetraspanin-negative fractions, pooled as the distal non-EV fractions ("non-EV dist"; F13-14).

Subsequently, in order to confirm the presence of EVs, SEC fractions were processed for cryo-electron microscopy (cryo-EM) and analysed by nanoparticle tracking analysis (NTA). EV fractions were confirmed to contain round-shaped nanovesicles free of contaminating clumps or protein aggregates by cryo-EM (**FIGURE 20D, E** and **Supplementary Figure 6A**). NTA analysis of the tetraspanin-peak fractions showed the presence of particles with a mode diameter of 169.6 and 157.2 nm for unconditioned and IFNγ-primed UCMSC-EVs, respectively (**Supplementary Figure 6B**). On the other hand, NTA indicated the presence of particles with a modal size of 118.1 nm in the proximal and 155.1 nm in the distal non-EV fractions, but cryo-EM images confirmed the lack of EVs in those fractions (**Supplementary Figure 6B**). Overall, the concentration of particles calculated by NTA (regardless the presence or not of EVs) was very similar among all the experiments, ranging 2-6x10^{10} particles/ml (**Supplementary Figure 6A**).

Analyses of the effect of IFNγ priming on EV production showed similar protein content, CD9 and CD63 presence and particle concentration in EV-containing SEC fractions (**FIGURE 20F** and **Supplementary Figure 6A**). MFI values were then normalized to the expression of CD9 and, unlike the results observed in cells, HLA molecules remained absent in the majority of EV batches after IFNγ priming. Regarding MSC markers, CD73 was unchanged and CD90 decreased, resembling parental cells' behaviour (**FIGURE 20G**).

Due to the apparent insubstantial benefits of IFNγ priming on the immunomodulatory capacities of UCMSCs, these would not recommend using IFNγ-priming on UCMSCs, especially in the

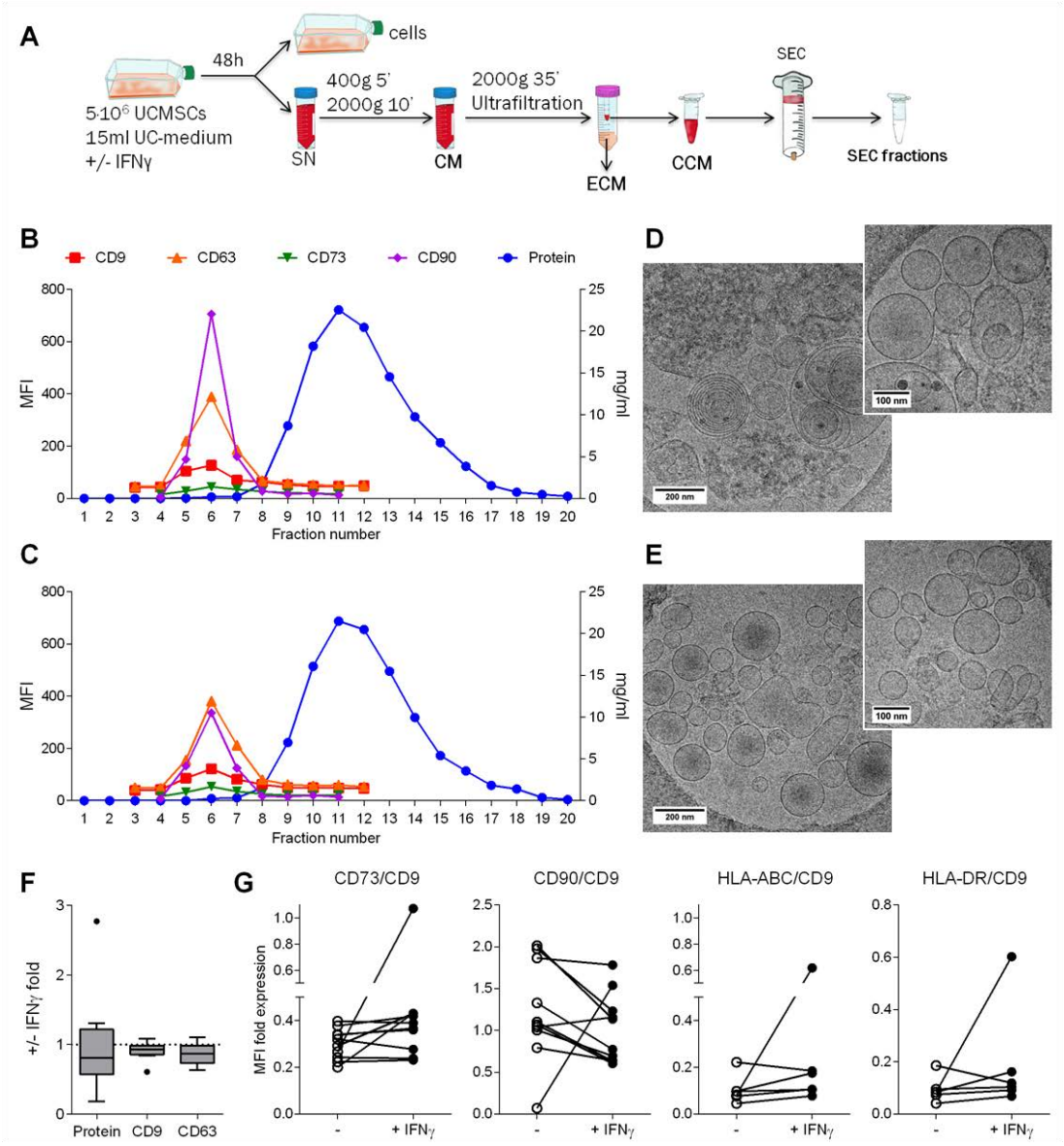

FIGURE 20 | EVs were successfully isolated by SEC. (A) Scheme of the methodological procedure followed for the generation of the different study fractions obtained from UCMSC 48h-culture: supernatant was cleared of debris by centrifugation to obtain conditioned media (CM); concentrated CM (CCM) and eluted CM (ECM) were collected after ultrafiltration; CCM was loaded to the SEC column and fractions collected. **(B-C)** UCMSC-EVs were found on fractions 5-7 while protein eluted after fraction 8 on both samples coming from unconditioned **(B)** and IFNγ-conditioned UCMSCs **(C)**. SEC eluted fractions were checked for EV markers (CD9 and CD63), MSC markers (CD73 and CD90) by bead-based flow cytometry (left axis). Protein elution was monitored by absorption at 280nm (right axis). **(D-E)** Cryo-EM images confirmed UCMSC-EVs presence in pooled EV fractions (F5-7) of unconditioned **(D)** and IFNγ-conditioned SEC preparations **(E)**. Images of 20,000x and 30,000x magnifications are shown, with 200nm and 100nm scale bars, respectively. **(F)** Box plot of the fold increase in protein content, CD9 and CD63 MFI of pooled EV fractions obtained from IFNγ-primed UCMSCs relative to unconditioned UCMSCs. Medians of ten independent experiments are depicted as horizontal bars, outliers as points. **(G)** CD73, CD90, HLA-ABC (MHC-I) and HLA-DR (MHC-II) expression on EVs from unconditioned (white dots) and corresponding IFNγ-primed MSCs (black dots) are shown normalized to their CD9 MFI. Each dot corresponds to an independent experiment (n=10 and 6).

allogeneic delivery setting given the HLA-DR overexpression in UCMSCs, also observed in few MSC-EV batches.

UCMSC-EVs reduce T cell proliferation and inflammatory cytokine production

Next, we aimed to delineate whether the EVs hold the immunosuppressive potential described for MSCs paracrine secretion. Thus, the three distinct pools of SEC fractions were compared by their ability to modify the T cell response. Additional controls included CM and its concentrated (CCM) and eluted (ECM) products after ultrafiltration (**FIGURE 21A**). Also, the UC pellet from CM was compared to SEC-EVs.

Only the SEC fractions containing EVs inhibited proliferation of stimulated T cells when added to the culture (34% reduction) (**FIGURE 21B**). This reduction of T cell proliferation showed a dose-dependent profile (**Supplementary Figure 7A, B**). Importantly, when either proximal or distal non-EV fractions were added to the culture, T cell proliferation remained unaltered (**FIGURE 21B**), similar to the addition of CCM, ECM and CM. Moreover, the UC pellet did not impair T cell proliferation (**FIGURE 21C**). Noticeably, neither did EVs obtained from IFNγ-primed UCMSCs (**Supplementary Figure 7A**). Viability of T cells was not altered in any of the conditions, thus discarding a principal apoptosis-mediated effect on T cell inhibited proliferation (**FIGURE 21D, E**). Then, in order to check the functional relevance of CD73 on EVs as it did have in MSC-mediated suppression of T cell proliferation (*Chapter 1*, **Supplementary Figure 4**), the same experiment was performed but in presence of the CD73 inhibitor APCP. In this case,

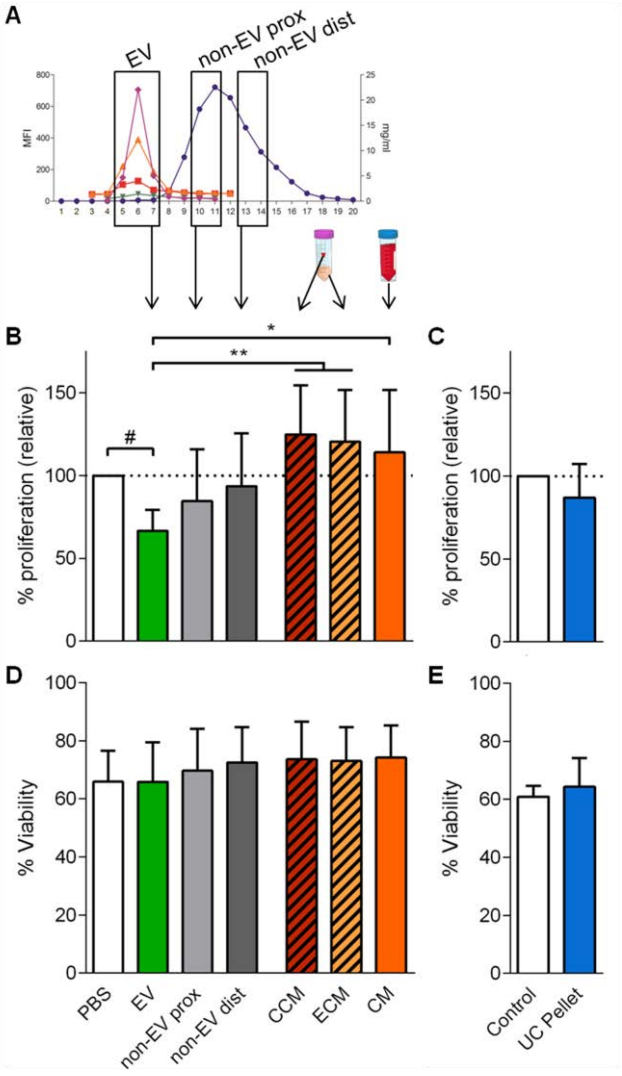

FIGURE 21 | Only the pooled EV fraction reduced T cell polyclonal proliferation. (A) The three different pooled SEC fractions: EV, proximal non-EV ("non-EV prox") and distal non-EV fractions ("non-EV dist") were analysed for T cell proliferation suppression capacity compared to the CCM, ECM, full CM, and ultracentrifuged pellet (UC Pellet). **(B, C)** Proliferation of T cells stimulated with anti-CD2/CD3/CD28 beads (10:1 ratio) was analysed by CFSE loss in the presence of pooled UCMSC-EVs, proximal and distal non-EV fractions, CCM, ECM and CM **(B)** or the UC Pellet **(C)**. Quantities were adjusted to $2.5x10^5$ initial UCMSC. Bars represent proliferation relative to their PBS control. **(D, E)** Viability of stimulated T cells assessed by FSC-A/SSC-A. Data represent means + SD for seven **(B, D)** and four **(C, E)** independent experiments. Statistical differences are indicated for groups with $p<0.05$ by Kruskall-Wallis; #$p<0.05$ by Wilcoxon Signed Rank test (to the 100%); *$p<0.05$ and **$p<0.01$ by Mann-Whitney test.

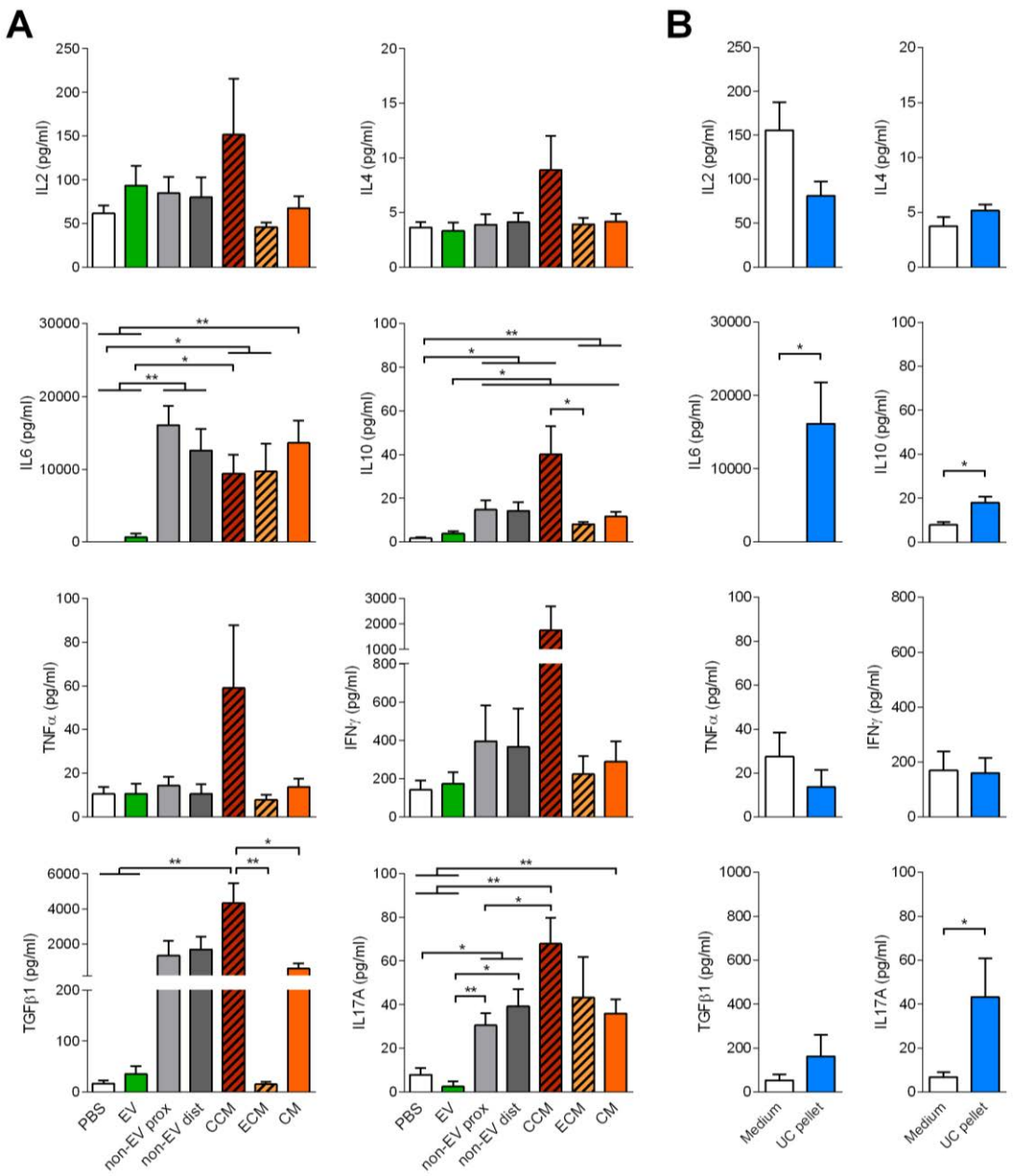

FIGURE 22 | Cytokines found in the supernatants of T cell proliferation assays corresponding to FIGURE 21 were analysed by CBA (IL2, IL4, IL6, IL10, TNFα, IFNγ, and IL17A) and TGFβ1 ELISA. Bars represent means + SD of seven (A) and four (B) independent experiments. Statistical differences are indicated for groups with *p<0.05 by Kruskall-Wallis; *p<0.05 and **p<0.01 by Mann-Whitney test.

inhibition of CD73 activity did not alter T cell abrogation of proliferation by EVs (**Supplementary Figure 8**). Finally, as an additional control to ratify the action by UCMSC-EV, complete medium alone was processed following the same SEC workflow, and the derived fractions did not suppress T cell proliferation (data not shown).

To further study the immunomodulatory effect of EVs, the cytokine profile of stimulated T cells was determined. Consistent with the reduced proliferation, no production of the pro-inflammatory cytokines IL6, TNFα or IFNγ nor IL2, was observed in T cell cultures to which EVs were added. In sharp contrast, IL6, TGFβ1, IL17A and, to a lesser extent IFNγ, were highly produced in the presence of both proximal and distal non-EV fractions and CM (**FIGURE 22A**).

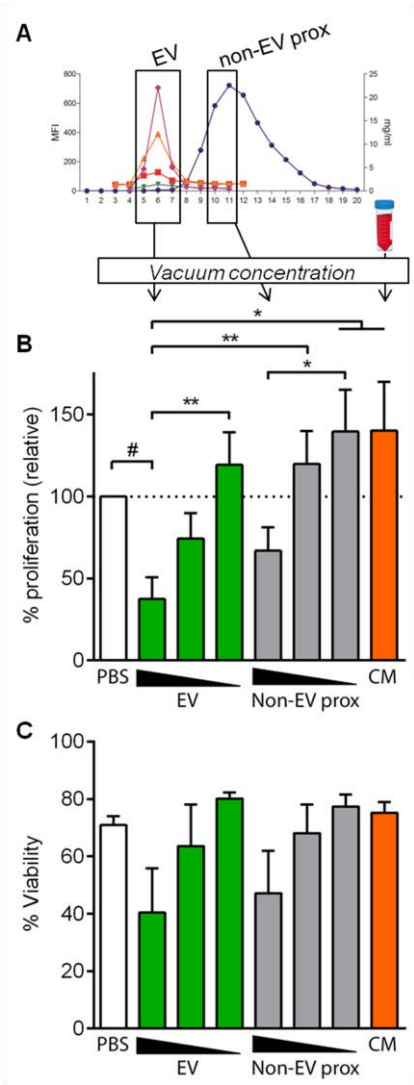

FIGURE 23 | Concentrated EV and non-EV fractions but not CM inhibit T cell polyclonal proliferation. (A) EV, proximal non-EV fractions and CM were vacuum-concentrated and checked for T cell proliferation suppression capacity. **(B)** Proliferation of T cells stimulated with anti-CD2/CD3/CD28 beads (10:1 ratio) was analysed by CFSE loss in the presence of vacuum-concentrated UCMSC-EVs, proximal non-EV fractions or CM. Quantities were adjusted to $2.5x10^5$ initial UCMSC, and dosage dependency was studied diluting samples 1/2 and 1/10 in PBS. Bars represent means + SD of proliferation relative to their PBS control, for three independent experiments. **(C)** Viability of stimulated T cells assessed by FSC-A/SSC-A. Data represent means + SD for five independent experiments. Statistical differences are indicated for groups with $p<0.05$ by Kruskall-Wallis; #$p<0.01$ by Wilcoxon Signed Rank test (to the 100%); *$p<0.05$ and **$p<0.01$ by Mann-Whitney test.

To our surprise, addition of full CCM to T cells promoted a cytokine rush, fostering the secretion of all the cytokines studied (IL2, IL4, IL6, IL10, TNFα, IFNγ, TGFβ1 and IL17A). On the other hand, addition of the UC pellet to T cells also fostered the production of IL6 and IL17A, resembling, rather than to SEC-EVs, the cytokine profile of T cells stimulated with CM (**FIGURE 22B**). These pro-inflammatory cytokines were also found in supernatants from MSC:T cell cultures at high cell ratios (**Supplementary Figure 9**). Of note, all cytokines were also determined in CCM, ECM and CM, showing values always below the cytokines found in T cell proliferation supernatants (**Supplementary Figure 10**), thus indicating that cytokine production in stimulated T cell cultures can be attributed genuinely to T cells.

Concentrated UCMSC-EVs further reduce T cell proliferation

In order to discard the possibility of a "dilution effect" of culture medium (volume added from SEC fractions) as an important factor influencing T cell proliferation, similar experiments were set up using vacuum concentration of the pooled fractions to minimize culture medium dilution (1.05-fold instead of 2-fold) (**FIGURE 23A**).

In these experimental conditions, concentrated EVs reduced polyclonal T cell proliferation more than a 60% (37.47% proliferation relative to control, **FIGURE 23B**), compared to the 34% reduction in non-concentrated conditions (**FIGURE 21B**). Intriguingly, in some experiments T

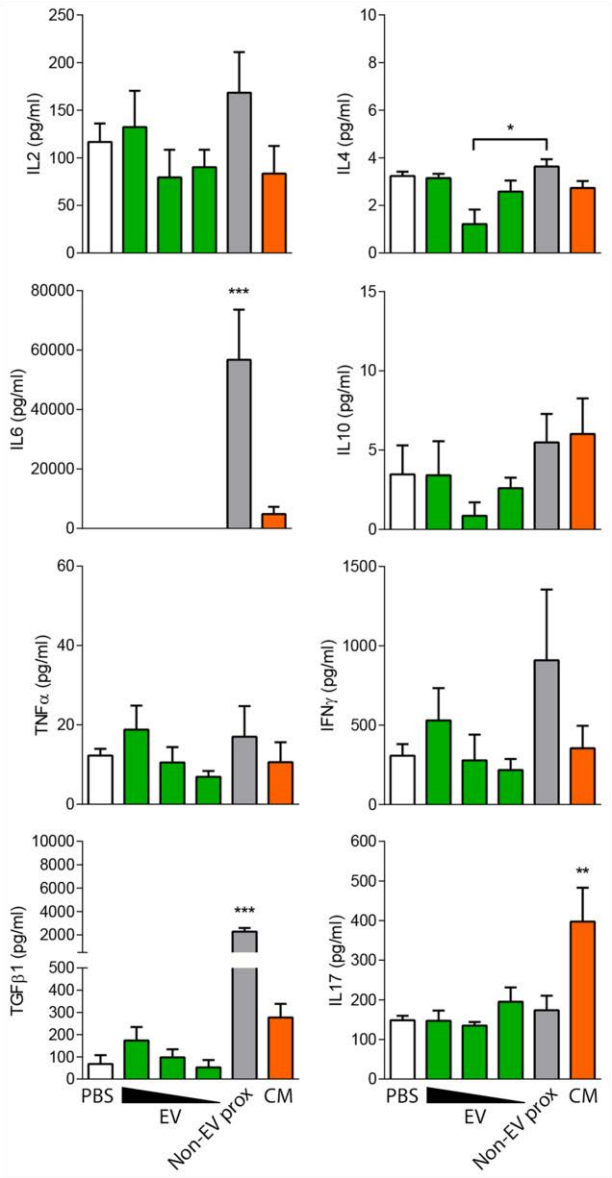

FIGURE 24 | Non-EV fractions and CM induce an inflammatory response on stimulated T cells. Cytokines found in the supernatants of T cell proliferation assays corresponding to FIGURE 23 were analysed by CBA (IL2, IL4, IL6, IL10, TNFα and IFNγ) and TGFβ1 and IL17 ELISA. Bars represent means + SD of three independent experiments for IL2, IL4, IL6, IL10, TNFα and IFNγ and five independent experiments for TGFβ1 and IL17. Statistical differences are indicated for groups with *p<0.05, **p<0.01 and ***p<0.001 by One-way ANOVA with Tukey's post hoc analysis.

cell viability was affected when concentrated EVs were added to the culture, although this effect was not statistically significant (**FIGURE 23C**). All these effects were lost upon EV dilution, confirming the EV-mediated T cell inhibition (**FIGURE 23B and Supplementary Figure 7C**).

An unexpected result was to observe that the concentrated proximal non-EV fraction turned out to mildly reduce T cell proliferation in a dose-dependent manner (**FIGURE 23B**), a feature that was not seen before in non-concentrated samples. Nevertheless, when the cytokine profile of stimulated T cells was analysed, an enormous production of IFNγ, IL6 and TGFβ1 was uniquely detected in supernatants from T cells stimulated in the presence of the proximal non-EV fraction (**FIGURE 24**), alerting of a pro-inflammatory stimulation of T cells, a feature that was completely absent in T cells incubated with EVs. Moreover, in accordance to non-concentrated experiments, CM was unable to suppress T cell polyclonal activation (**FIGURE 23B**).

To summarize, these results indicate that only the isolated SEC-EV fraction managed to greatly immunosuppress polyclonal T cell activation, while non-EV fractions, CM and UC pellet surprisingly promoted an inflammatory milieu and Th17 polarization of T cells.

Effect of UCMSC-EVs on monocyte polarization

We also explored the effect of the pooled SEC fractions and full CM in the skewing of monocyte polarization. In this setting, we used three different well-determined monocyte polarizing stimuli as positive controls (Murray et al. 2014; Fernando O Martinez and Gordon 2014): LPS plus IFNγ as an inflammatory "M1" phenotype inducer, and IL4 or IL10 to generate anti-inflammatory "M2a" or "M2c" phenotypes, respectively. As expected, M1 (LPS+IFNγ) macrophages highly increased CD80 mRNA, showed mild changes in CD163, and downregulated the expression of CD206 (**FIGURE 25A**). These cells also produced high levels of TNFα and IL10 (**FIGURE 25B**). In sharp contrast, M2a (IL4) and M2c (IL10) monocytes did not undergo changes in CD80 while upregulated CD206. Only M2c (IL10) also incremented CD163 expression, and had IL10 in supernatants (probably as carryover effect from the activation stimulus used). None of the M2-skewing stimuli induced the secretion of TNF- (**FIGURE 25B**).

We then analysed the capacity of UCMSCs media to skew monocyte polarization. Culture with UCMSC-EVs maintained monocytes in a non-activated state, as cells did not substantially modify the expression of CD80, CD163, CD206 or IL10 compared to the control ($p>0.05$ to non-activated monocytes). Moreover, no TNFα was detected in supernatants, indicating that samples did not contain pro-inflammatory mediators.

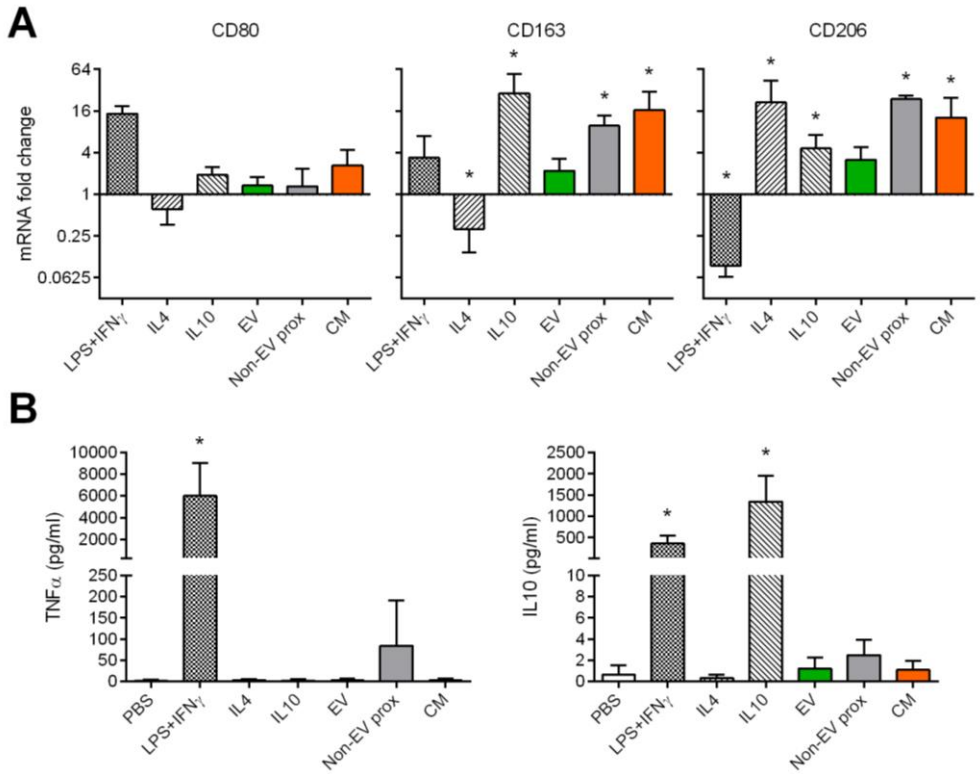

FIGURE 25 | UCMSC-EVs do not affect CD80, CD163 and CD206 polarization marker expression in monocytes, while the non-EV fraction and CM induce increased expression of CD163 and CD206. Monocytes were cultured for 48h with polarizing cytokines to induce an inflammatory M1 (LPS+IFNγ) or anti-inflammatory M2a (IL4) and M2c (IL10) phenotypes, or with the EV, proximal non-EV fractions or full CM. **(A)** mRNA fold change of the M1 marker CD80 and M2 markers CD163 and CD206, as analysed by real time PCR. Values are relative to 18S and expressed as a fold change to the PBS-treated monocytes in a log2 scale. **(B)** Levels of TNFα and IL10 in the supernatants of monocytes as measured by ELISA. Data are expressed as mean + SD and account for two different UCMSC and four monocyte donors. Statistical differences are indicated for groups with *$p<0.05$ by Kruskall-Wallis; *$p<0.05$ by Mann-Whitney test.

Conversely, the proximal non-EV fraction and CM induced the expression of CD163 and CD206, while not altering that of CD80, thus resembling an M2c(IL10) polarization (**FIGURE 25A**), although not relevant amounts of IL10 were detected (**FIGURE 25B**). Of note, some TNF-α could be found when the proximal non-EV fraction was added.

DISCUSSION

In this chapter, we demonstrate that EVs isolated from UCMSCs by SEC strongly immunomodulate activated T cells *in vitro*. In particular, our results indicate that the SEC-purified EV fraction greatly abrogates polyclonal T cell proliferation and cytokine production in comparison with non-EV fraction, CM and UC pellet, which conversely result in an inflammatory T cell response and foster the Th17 polarization of T cells. Additionally, EVs do not induce monocyte polarization or cytokine secretion, but the non-EV fraction induces the expression of CD163 and CD206 and some production of TNFα by monocytes. These findings not only increase the growing evidence confirming that EVs are an active component of MSC's paracrine immunosuppressive function, but also highlight the importance of working with well purified EV preparations to specifically achieve this effect.

MSCs have been described to suppress the immune response affecting T cell proliferation and polarization, to induce regulatory T cells, and to module Antigen Presenting Cells (APCs) (Kilpinen et al. 2013; Patel et al. 2010; de Witte et al. 2015; Katarina Le Blanc and Mougiakakos 2012; Regateiro, Cobbold, and Waldmann 2013). In our settings, UCMSCs were confirmed to have potent suppressive capabilities on T cell proliferation, but whereas IFNγ conditioning enhances immunosuppressive functions of both bone marrow- and adipose tissue-derived MSCs (Renner et al. 2009; Krampera, Cosmi, et al. 2006; Mancheño-Corvo et al. 2015), no differences were found comparing IFNγ-primed to non-primed UCMSCs. This observation could be explained by the intrinsic capacity of UCMSCs to suppress T cell proliferation at low ratios compared to other studies (1:240 MSC to T cells), which may indicate that these cells own already a potent modulatory capacity of the T cell response. Another explanation might be the lack of APCs in our experimental setting, which have been described to partially mediate T suppression induced by MSCs (Groh et al. 2005). In line, MSCs have been described to modulate the immune response by polarizing monocytes towards a M2 phenotype, which would in turn further modulate inflammation (Melief, Schrama, et al. 2013). In any case, our results confirmed that non-primed UCMSCs showed a high immunomodulatory capacity at low MSC:T cell ratios.

Also in line with previous studies, IFNγ increased the expression of HLA-II molecules in UCMSCs (Tipnis, Viswanathan, and Majumdar 2010; Chan et al. 2006; C. Zhou et al. 2011), which may have detrimental effects in the allogeneic scenario. Expression of HLA-II molecules in MSCs would trigger the activation of the host's innate immune system which in turn would impede their potential immunomodulatory effect. In fact, it has been suggested that the increased HLA expression in EVs from umbilical cord blood-derived MSCs after treatment with IFNγ may be responsible of the loss of their protective effect against ischemic acute kidney injury (Kilpinen et al. 2013). Given that our results suggest that non-primed UCMSCs are as potent as primed MSCs in regulating T cell responses, we would consider using non-primed cells in therapeutic approaches.

In the context of cell therapy, transplantation of MSCs to induce immune suppression and tissue regeneration has still some limitations. Such drawbacks include the right homing and implantation –which is impaired by the entrapment of cells in the lung barrier upon systemic administration (Fischer et al. 2009; R. H. Lee et al. 2009)-, the possible change in phenotype of the infused cells -influenced by the initial inflammatory phase occurring after *in vivo* infusion of MSCs (Hoogduijn et al. 2013)-, the requirement of cell viability after transplantation and ease of storage and availability. The majority of these caveats could be overcome by using EVs, resulting in a number

of reports describing their benefits (Katsuda et al. 2013; Lai, Chen, and Lim 2011). As MSCs exert their function through both cell contact and soluble mechanisms, it is expected that higher concentrations of EVs would be needed to reach the same level of inhibition obtained using MSCs, as we observed in our results. However, in the context of cell-free therapeutic approaches it is of relevance that one of the paracrine mechanisms of T cell inhibition by MSCs is based on well-defined and effectively enriched MSC-derived EVs.

Recent studies have shown that MSC-EV products can efficiently modulate inflammatory disorders *in vivo*, including rat and mouse models and also human clinical trials (Kordelas et al. 2014; Zhao et al. 2015; J. Yang et al. 2015; Yu, Zhang, and Li 2014; Lener et al. 2015). Yet, several controversial studies noticed reduced immunosuppressive functions of CM and EVs compared to their parental cells (Conforti et al. 2014; Gouveia de Andrade et al. 2015). Nevertheless, most of the studies performed so far on MSC-EV effect *in vitro* and *in vivo* used ultracentrifugation or precipitation methods (Yu, Zhang, and Li 2014). These methods lead to EV preparations containing high quantities of non-EV proteins (Baranyai et al. 2015; Marcella Franquesa et al. 2014; Gámez-Valero et al. 2016), result in cytotoxicity (Gámez-Valero et al. 2016) and might explain the incongruous results on EV effects. Importantly, our results highlight the need of using well characterized and efficiently purified EVs to obtain an optimal cell-free immunosuppressive product.

Isolation of EVs from MSC-CM by SEC yielded highly purified EVs that could be easily detected not only by tetraspanin markers, but also the MSC markers CD73 and CD90, confirming previous observations (H.-S. Kim et al. 2012; Y. Yang et al. 2015; Amarnath et al. 2014). The contribution of CD73 expressed by MSCs to suppress T cell proliferation was observed before (*Chapter 1*, Supplementary Figure 4). Nevertheless, CD73 presence in EVs was quite low and it might explain the lack of CD73 functional significance in inhibiting EV-mediated abrogation of T cell proliferation, at least in our experimental conditions.

SEC ensured the separation of EVs from the bulk of protein and impurities found in CM, as confirmed by cryo-EM, as it has been widely demonstrated before using other complex fluids such as plasma or urine (Böing et al. 2014; de Menezes-Neto et al. 2015; I. Lozano-Ramos et al. 2015; Welton et al. 2015; Gámez-Valero et al. 2016). Stressing the importance of using a well-defined cell-free product, it was extremely relevant to observe that SEC-purified EVs significantly differ from the non-EV fractions, full CM, and UC pellet in their functional capabilities. While isolated EVs successfully suppressed T cell proliferation and concomitantly inhibited the induction of cytokine production in a dose dependent manner, the non-EV fraction, full CM, and UC pellet displayed completely divergent properties. Further concentration of purified EVs using vacuum concentration resulted in an enhanced reduction of T cell proliferation compared to the control situation. This effect may be partially explained by a reduced T cell viability, which has been described before as a possible mechanism used by MSCs to constrain T cell activation (Plumas et al. 2005; Akiyama et al. 2012). Nevertheless, in our hands, reduced T cell viability was highly dependent on the EV batch, and was not observed when EVs were further diluted.

In sharp contrast, the non-EV fractions only reduced T cell proliferation when they were vacuum concentrated, but at the same time induced the production of high amounts of inflammatory IL6 combined with TGFβ1. These two cytokines –along with IL1β and IL23-, are involved in the generation of Th17 responses (Volpe et al. 2008; Benwell and Lee 2010), and in fact we could find the induction of Th17 cells in all conditions except SEC-EVs. Th17 polarization is known to

be the cause of exacerbated inflammatory disorders and especially detrimental for autoimmune diseases such as multiple sclerosis, rheumatoid arthritis or to mediate GvHD and allergies (Annunziato et al. 2008; Volpe et al. 2008). In line with these results, recent studies delineate how EV products obtained by ultracentrifugation could lead to immune cell activation via NFκB (J. D. Anderson et al. 2016). Moreover, high levels of IL6 are the cause of inflammatory diseases and also have been linked with the exacerbated activation of the immune response causing the cytokine-release syndrome, an unexpected dangerous side effect found in some cell therapy clinical trials (Rossi et al. 2015; D. W. Lee et al. 2014; Maude et al. 2014).

Antigen Presenting Cells (APCs) may also be potential targets of the MSC regulatory effect. In this sense, monocytes have been claimed as necessary for Treg generation by MSCs and MSC-derived CM, through their skewing to an M2 phenotype (Cutler et al. 2010; Melief, Schrama, et al. 2013) and secretion of IL10 (Melief, Geutskens, et al. 2013b), a functional trait of M2 monocytes (Fernando O. Martinez et al. 2006; Murray et al. 2014). In line with these results, both CM and the non-EV fractions induced the expression of the M2 markers CD163 and CD206 on monocytes, with marginal amounts of IL10 detected in supernatants. However, monocytes cultured with the non-EV fraction produced some levels of TNFα, which may be indicative of unwanted cell activation. In sharp contrast, monocytes cultured in the presence of EVs did not show polarization or cytokine secretion, thus proving to be clean of polarizing stimuli or inflammatory mediators.

All these results strongly suggest the need to use well-defined, cell-free, highly purified EV products in therapeutic approaches, and put into further value the immunomodulatory role of SEC-derived EVs on T cells. Given the complexity of the immune response, in which many actors play fundamental roles, defining the specific effects of EVs and non-EV fractions on single cell populations is a fundamental step for the deciphering of the underlying mechanisms of EVs in the modulation of key players, such as T cells and monocytes.

In summary, the present study thoroughly characterizes the different fractions found in UCMSCs-CM in terms of immune modulation potential. We have proven the feasibility of a strategy based on SEC to effectively isolate nanosized EVs responsible at least in part of the genuine MSC immunomodulatory capacities. Most importantly, our results highlight the importance of purity and fine characterization of the EV product envisioned as a cell-free therapeutic approach to avoid unwanted inflammatory responses. In this sense, since EVs are apparently well-tolerated, their use paves the way for innovative and more efficient therapies based in nanomedicine avoiding the putative side effects associated to stem cell transplantation. Together with other potential uses such as targeting cell membranes, delivering bioactive molecules and being analysed for biomarkers (i.e., theranostics), this natural source of nanoparticles may be crucial in future developments on nanomedicine.

SUPPLEMENTARY FIGURES

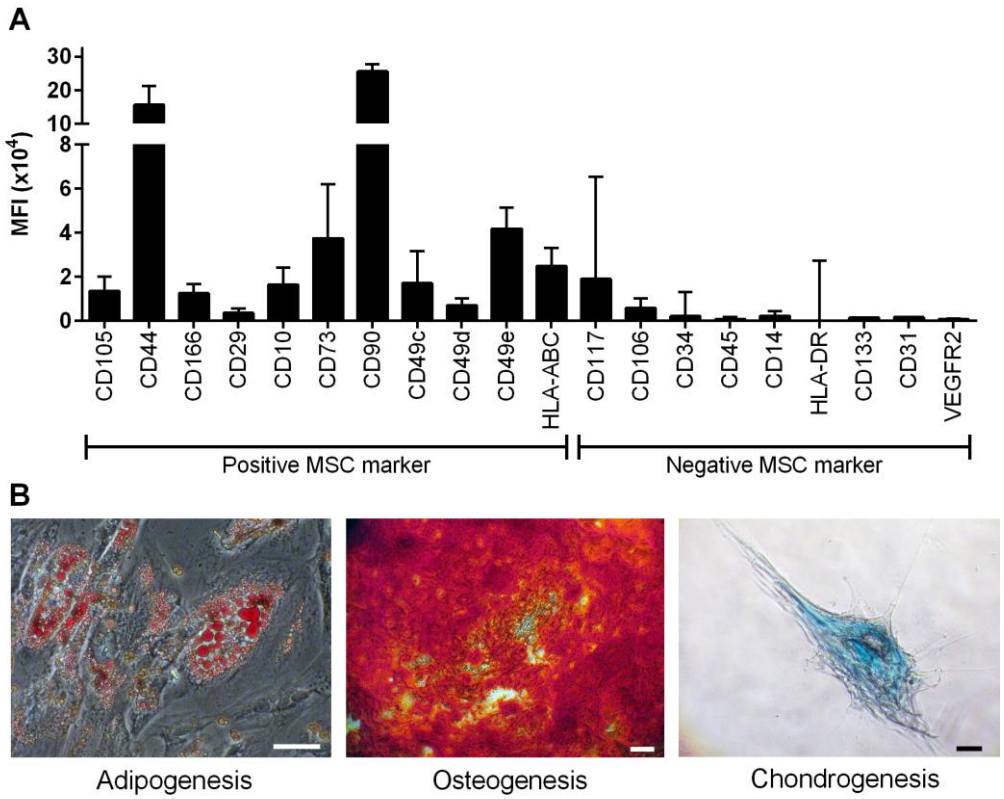

Supplementary Figure 5 | Characterization of UCMSCs by flow cytometry and differentiation assays. (A) UCMSCs were consistently positive for the common MSC markers CD105, CD44, CD166, CD10, CD73, CD90, CD49c, CD49d, CD49e and negative for CD117, CD106, CD34, CD45, CD14, CD29, CD133, CD31 and VEGFR2. Bars represent the mean + SD of the total cell population's MFI minus the isotype-matched MFI, of seven different UCMSC donors. **(B)** UCMSCs were successfully differentiated towards an adipogenic, osteogenic and chondrogenic lineages. Images show cell cultures after staining, from left to right, lipid droplets with Oil red O, calcium with Alizarin red S, and proteoglycans with Alcian blue. Scale bars = 100 μm.

A

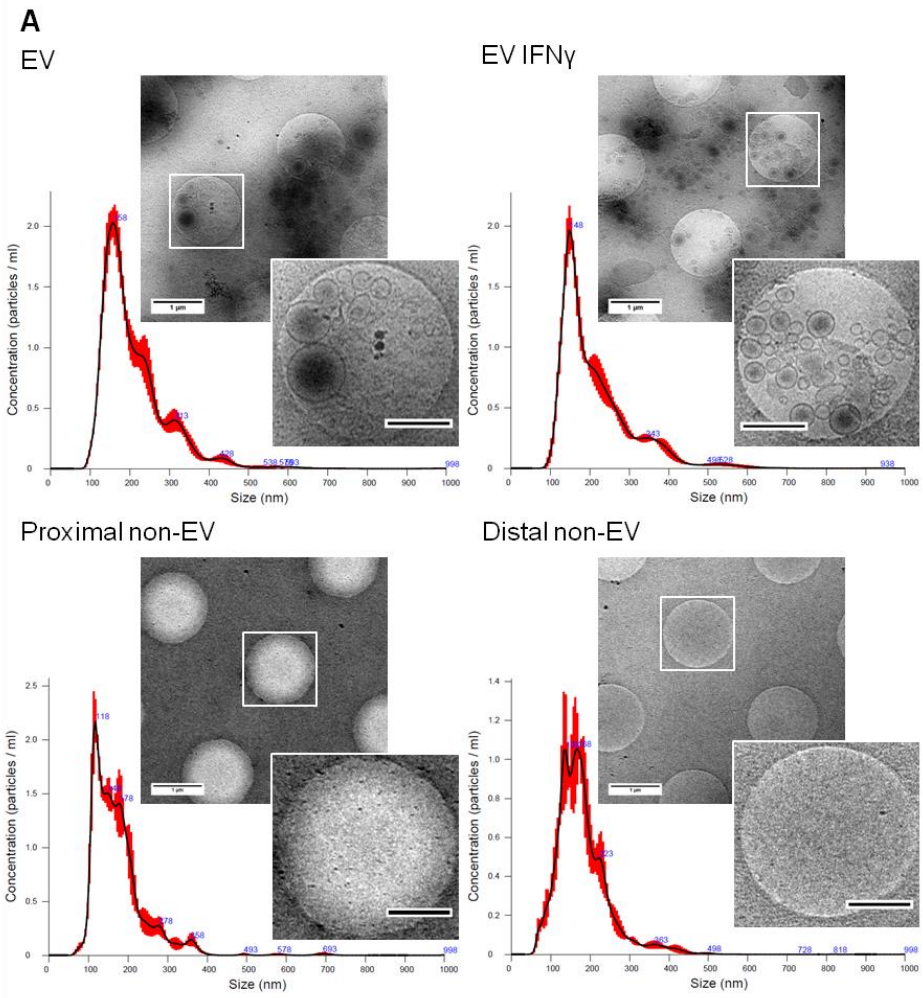

B

Sample	Diameter (nm)		Concentration
	Mean ± SD	Mode ± SD	particles/ml ± SD
EV	228.2 ± 25.6	169.6 ± 19.6	$5.51 \cdot 10^{10} \pm 1.14 \cdot 10^{10}$
EV IFNγ	238.7 ± 21.2	157.2 ± 12.5	$3.46 \cdot 10^{10} \pm 7.04 \cdot 10^{9}$
Proximal non-EV	168.4 ± 20.7	124.3 ± 24.3	$3.60 \cdot 10^{10} \pm 2.50 \cdot 10^{10}$
Distal non-EV	179.8 ± 20.6	155.1 ± 10.5	$2.54 \cdot 10^{10} \pm 3.82 \cdot 10^{8}$

Supplementary Figure 6 | UCMSC-EVs presence was confirmed by NTA and Cryo-EM in the EV fraction and absence in proximal and distal non-EV fractions obtained in SEC. (A) NTA profiles (size [nm] versus concentration [particles/ml]) and their corresponding Cryo-EM images of the pooled SEC fractions. Numerous EVs were observed in the EV-fractions from both untreated and IFNγ-primed UCMSCs (left and right, upper images), while proximal and distal non-EV fractions were found completely free of particles (left and right, bottom images). The grid's holes, measuring 1.5 µm in diameter, can be clearly distinguished as brighter circles, and are shown in close-up images of the indicated areas. Scale bars = 1 µm and 500 nm in open field and inserts, respectively. **(B)** Modal, mean size and mean quantification of particles found in pooled SEC fractions according to NTA analysis. Data of three independent experiments.

Related to **FIGURE 20**.

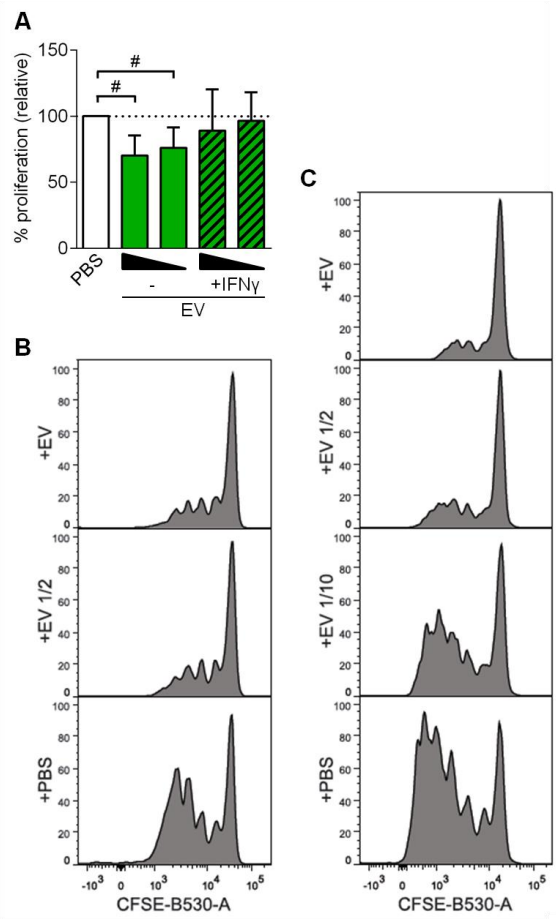

Supplementary Figure 7 | **Inhibition of T cell proliferation by EVs is dose-dependent.** T cells were stimulated with anti-CD2CD3/CD28 coated microbeads (10:1 ratio) and cultured in the presence of UCMSC-EVs corresponding to $2.5x10^5$, $1.25x10^5$ (1/2 dilution in PBS) or $2.5x10^4$ (1/10 dilution in PBS) initial UCMSCs, without **(A-B)** or after vacuum concentration **(C)**. **(A)** Data represents mean + SD of proliferation relative to the PBS control of seven and three independent experiments of unconditioned and IFNγ-conditioned UCMSC-EVs, respectively. Statistical differences are #$p<0.05$ by Wilcoxon Signed Rank test. **(B, C)** Representative histograms of proliferation analysis by CFSE loss. Generations can be clearly distinguished as CFSE-intensity peaks.

Related to **FIGURE 21** and **FIGURE 23**.

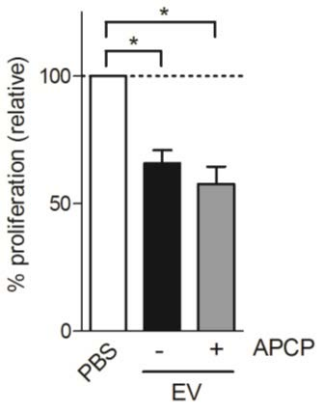

Supplementary Figure 8 | **CD73 inhibition does not affect EV-mediated immunosuppression of T cells.** Proliferation of T cells stimulated with anti-CD2/CD3/CD28 beads (10:1 ratio) was analysed by CFSE loss in the presence or not of pooled UCMSC-EVs corresponding to $2.5x10^5$ initial UCMSCs and APCP (CD73 inhibitor; 10 µM). Bars represent proliferation relative to their PBS control as mean + SD for three independent experiments. Statistical differences are indicated for *p<0.05 by Wilcoxon Signed Rank test (to the 100%).

Related to **FIGURE 21** and **Supplementary Figure 4**.

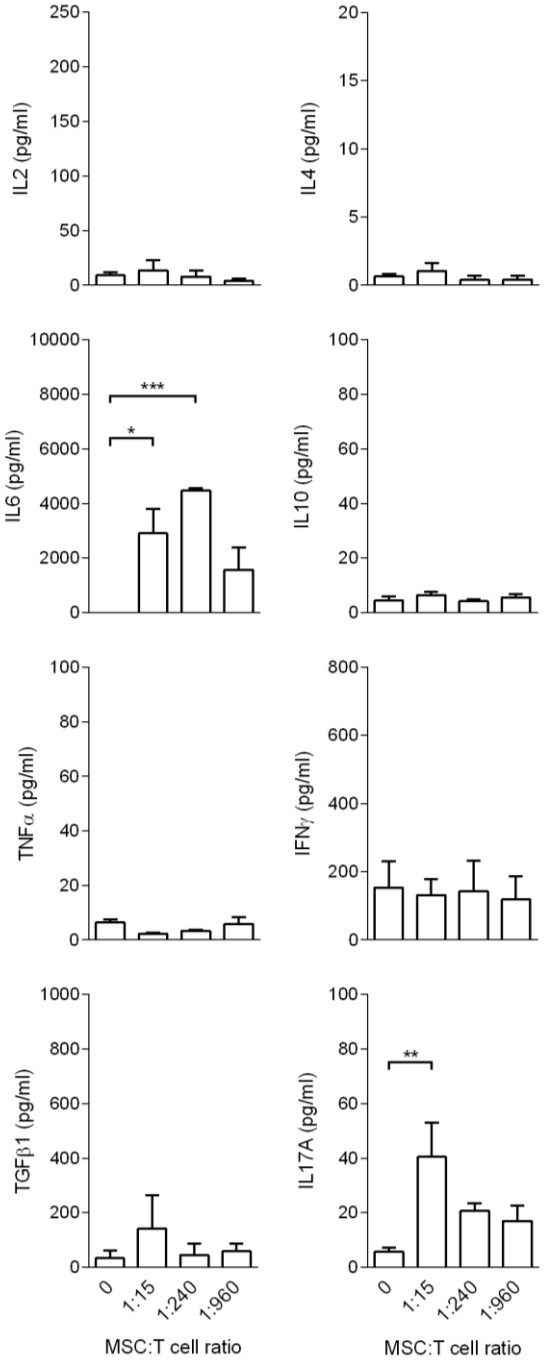

Supplementary Figure 9 | **Cytokines found in the supernatants of T cell proliferation assays corresponding to FIGURE 19D** were analysed by CBA (IL-2, IL-4, IL-6, IL-10, TNF-α, IFNγ and IL-17A) and TGF-β1 ELISA. Bars represent means ± SD of cytokines produced by 50,000 cells, from three independent experiments. Statistical differences are indicated for groups with *p<0.05, **p<0.01 and ***p<0.001 by One-way ANOVA with Tukey's post hoc analysis.

Related to **FIGURE 19** and **FIGURE 21**.

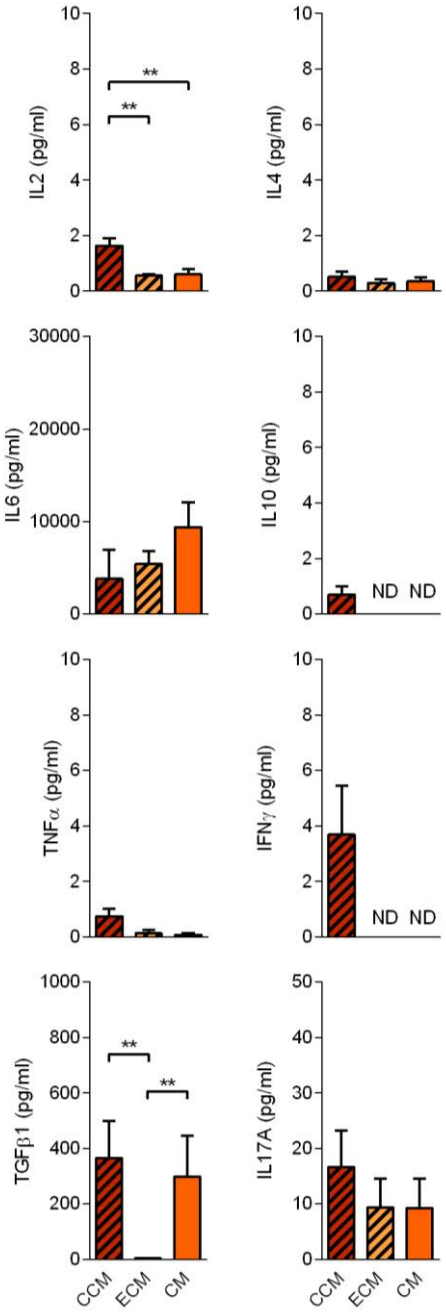

Supplementary Figure 10 | **Cytokines found in the CCM, ECM and CM** were analysed by CBA (IL-2, IL-4, IL-6, IL-10, TNF-α, IFNγ and IL-17A) and TGF-β1 ELISA. Bars represent means ± SD of five independent experiments. Statistical differences are indicated for groups with $p<0.05$ by Kruskall-Wallis; *$p<0.05$ and **$p<0.01$ by Mann-Whitney test. ND= not detected.

Related to **FIGURE 22**.

Supplementary Table 2 | Primers used for real time PCR.

Gene	Primer	Sequence (5'-3')	Tm[1] [ºC]	%GC	Amplicon size [bp]
18S	Forward	TCTTTCTCGATTCCGTGGGT	58.74	50	145
	Reverse	TCTAAGAAGTTGGGGGACGC	59.39	55	
CD80	Forward	CTGCCTGACCTACTGCTTTG	58	55	77
	Reverse	GGCGTACACTTTCCCTTCTC	58	55	
CD163	Forward	CACCAGTTCTCTTGGAGGAACA	59	50	82
	Reverse	TTTCACTTCCACTCTCCCGC	59	55	
CD206	Forward	ACACAAACTGGGGGAAAGGTT	59.99	47.62	174
	Reverse	TCAAGGAAGGGTCGGATCG	58.8	57.89	

[1]Tm: Primer melting Temperature.

CHAPTER 3

Based on "Development of engineered three-dimensional extracellular vesicle-rich bioactive cardiac grafts"

Marta Monguió-Tortajada[1,2,3], Cristina Prat-Vidal[1,4,5], Marta Clos-Sansalvador[1], Alexandra Calle[6], Anna Morancho[7], Carolina Gálvez-Montón[1,4], Miguel Ángel Ramírez[6], Anna Rosell[7], Antoni Bayes-Genis[1,4,8,9], Santiago Roura[1,4,*], Francesc E. Borràs[2,3,10,*]

[1]ICREC Research Program, Health Science Research Institute Germans Trias i Pujol, Can Ruti Campus, Badalona, Spain, [2]REMAR-IVECAT Group, Health Science Research Institute Germans Trias i Pujol, Can Ruti Campus, Badalona, Spain, [3]Department of Cell Biology, Physiology and Immunology, Universitat Autònoma de Barcelona, Bellaterra, Spain, [4]CIBERCV, Instituto de Salud Carlos III, Madrid, Spain, [5]Center of Regenerative Medicine in Barcelona (CMRB), Hospital Duran i Reynals, 3rd Floor, Av. Gran Via 199-203, 08098 Hospitalet de Llobregat, Barcelona, Spain, [6]Departamento de Reproducción Animal, Instituto Nacional de Investigación y Tecnología Agraria y Alimentaria (INIA), Madrid, Spain, [7]Neurovascular Research Laboratory, Vall d'Hebron Research Institute, UAB, Barcelona, Spain, [8]Cardiology Service, Germans Trias i Pujol University Hospital, Badalona, Spain, [9]Department of Medicine, UAB, Barcelona, Spain, [10]Nephrology Service, Germans Trias i Pujol University Hospital, Badalona, Spain

* Co-corresponding authors

This manuscript has been submitted for its publication in an indexed Journal.

ABSTRACT

The administration of mesenchymal stem cell (MSC)-derived extracellular vesicles (EVs) is a promising approach to cardiac repair after myocardial infarction (MI). EVs display biological properties of the originating cells, such that MSC-EVs exhibit immunomodulatory, regenerative, and pro-angiogenic capabilities both autologously and allogeneically. However, the optimal delivery strategy for EV therapy remains undetermined. Here we tested the use of biocompatible three-dimensional (3D) engineered scaffolds as an efficient support for local delivery of bioactive multifunctional EVs. EVs from porcine cardiac adipose tissue-derived MSCs (cATMSCs) were purified by size-exclusion chromatography (SEC) and morphologically and phenotypically characterized. These cATMSC-EVs reduced allogeneic polyclonal proliferation and abrogated production of the pro-inflammatory cytokines IFNγ, TNFα, and IL12p40, while maintaining IL6 and IL8 secretion. Moreover, the cATMSC-EVs recruited pro-regenerative cells, including peripheral blood-derived outgrowth endothelial cells (OECs) and allogeneic MSCs. We further generated two decellularized cardiac scaffolds with preserved structures from pericardial and myocardial tissues, and embedded these scaffolds with fluorescently-labelled cATMSC-EVs for tracking and retention assessment. Whole-scaffold fluorometric scanning, and confocal and scanning electron microscopy (SEM) imaging revealed that both engineered cardiac scaffolds retained cATMSC-EVs even after thorough washing and a week-long culture. Overall, our data indicated that both engineered cardiac scaffolds may be suitable for effective EV myocardial delivery. Confining the multifunctional cATMSC-EVs administration to a scaffold may increase the local EV dosage, generating a bioactive niche for cell migration and regeneration, and could be useful as a cell-free off-the-shelf product for post-infarction myocardial repair.

INTRODUCTION

The growing worldwide epidemic of cardiac-related diseases generates a great need for organs, which is presently unmet. For example, myocardial infarction (MI) causes myocardial necrosis with subsequent formation of a non-contractile scar, which can lead to adverse cardiac remodelling, heart enlargement and, ultimately, overt heart failure (Olivetti et al. 1991). Efforts to preserve cardiac function after injury include the investigation of cell-based therapies and cardiac tissue engineering approaches to mitigate inflammation and long-term myocardial damage (Curtis and Russell 2009). Recent studies have explored the administration of mesenchymal stem cells (MSCs) with immunomodulatory and regenerative capabilities in attempts to promote regeneration of infarcted tissue (Antoni Bayes-Genis et al. 2010; Cristina Prat-Vidal et al. 2014; Roura et al. 2015). Natural three-dimensional (3D) scaffolds, such as decellularized human pericardium and porcine myocardium, have also emerged as a promising tissue engineering option for restoring cardiac function after MI (Prat-Vidal et al. 2014; Gálvez-Montón et al. 2017a; Gálvez-Montón et al. 2017b; Perea-Gil et al. 2018). Animal studies with these engineered cardiac grafts demonstrate significant improvements of ventricular function, reporting appropriate scaffold integration with the underlying myocardium and induction of neovascularization and nerve sprouting, with only a modest number of cells ultimately nesting within the host myocardium.

At this time, the efficacy and value of cell therapy for cardiac repair and regeneration are debatable, and our present lack of mechanistic understanding limits the potential for advances, optimization, and implementation (Broughton et al. 2018). Current evidence suggests that MSCs may contribute to MI recovery due to their secretion of various soluble factors that can act on host tissue and promote endogenous repair in a paracrine fashion (Malliaras et al. 2013; Caplan and Arnold 2017). Amongst them, we confirmed in *Chapter 2* that EVs are an active component of the paracrine immunosuppressive function of MSCs, with potential use in nanomedicine. However, the optimal administration route to enable EVs to be locally active at a sufficient dose remains unknown.

In this third chapter, we describe the development and validation of two novel bioengineered 3D cardiac grafts for local delivery of bioactive multifunctional MSC-EVs. First, we functionally characterized MSC-EVs of porcine origin to validate their immunosuppressive and endogenous recruitment potential. Then, we investigated cell-free reparative strategies embedding MSC-secreted EVs into decellularized cardiac scaffolds.

MATERIALS AND METHODS

Porcine cardiac adipose tissue-derived MSC isolation and culture

Primary porcine cardiac adipose tissue-derived MSC (cATMSC) cultures were established from cardiac adipose biopsy samples (1.3 ± 0.4 g) obtained from pigs (Large White × Landrace) undergoing cardiac surgery (n = 25), as previously described (Prat-Vidal et al. 2014). Briefly, tissue specimens were washed in phosphate-buffered saline (PBS; Oxoid, Hampshire, UK) to remove contaminating debris and red blood cells, and then digested in 0.05% collagenase (Type II; Gibco Invitrogen Corp., Carlsbad, CA, USA) at 37°C with gentle agitation. After 30 min, the collagenase was inactivated by dilution with α-MEM (Sigma Aldrich, St. Louis, MO, USA) containing 10% heat-inactivated foetal bovine serum (FBS), 2 mM L-glutamine, 1% penicillin-streptomycin (P/S) (all from Gibco Invitrogen Corp.) and 5 µg/ml Plasmocin™ (Invivogen, San Diego, CA, USA) (α-MEM-FBS). The cell suspension was centrifuged for 10 min at 1,200 × g, and then the pellet was resuspended in α-MEM-FBS. Finally, the adhered cells were grown to subconfluence in α-MEM-FBS under standard culture conditions, with medium replacement every 3 days.

Extracellular vesicle production and isolation

EVs were produced and isolated as previously described (*Chapter 2*) (Monguió-Tortajada et al. 2017a). All relevant data regarding our experiments have been submitted to the EV-TRACK knowledgebase (EV-TRACK ID: EV180031) (Van Deun et al. 2017).

For depletion of bovine EVs, 2× complete medium was ultracentrifuged in polyallomer ultracentrifugation tubes (Thermo Fisher Scientific, San Diego, CA) at 100,000 *xg* for >16 h (TH641 rotor, adjusted k-Factor = 240.82) in a Sorvall WX Ultra 100 Series ultracentrifuge (Thermo Fisher Scientific). The supernatant was sterilized using a 0.22-µm filter (Sarstedt, Nümbrecht, Germany), and then diluted with α-MEM medium to a 1× working solution for cell culture.

For EV production, two T-175 flasks of porcine cATMSCs were grown to confluence, and then the culture media of each was changed to 15 mL EV-depleted culture medium. After 48 h, the conditioned medium (CM) was collected and centrifuged at 400 *xg* for 5 min to exclude cells, and then at 2,000 *xg* for 10 min to exclude cell debris. Trypan blue staining revealed cell viability to be >95%. To obtain concentrated CM (CCM), the cleared CM was subjected to 100-kDa ultrafiltration using an Amicon Ultra centrifugal filter (Millipore, Billerica, MA, USA) at 2,000 *xg* for 35 min.

From the CCM, we isolated EVs by size-exclusion chromatography (SEC) using a previously published method (Gámez-Valero et al. 2016; Monguió-Tortajada et al. 2017a; Lozano-Ramos et al. 2015). Briefly, 12 mL Sepharose CL-2B (Sigma Aldrich) was autoclaved, thoroughly washed with PBS, and packed into an autoclaved Puriflash dry load empty 12G flash column (Interchim-Cromlab, Barcelona, Spain). Then this SEC column was loaded with 500 µL CCM, sterile 10% sucrose (w/v) (Sigma Aldrich) was applied as an elution buffer, and 500-µL fractions were collected. In up to 35 collected fractions, protein elution was checked by reading the absorbance at 280 nm using a Nanodrop spectrophotometer (Thermo Fisher Scientific). Bead-based flow

cytometry was performed to assess CD44 and CD63 positivity, and the EV-containing (i.e., CD44+ CD63+) fractions were pooled together for use in further experiments.

Bead-based flow cytometry

To identify porcine cATMSC-EVs, we used bead-based flow cytometry to screen for EV and MSC markers. EVs were coupled to 4-µm aldehyde/sulphate-latex microspheres (Invitrogen-ThermoFisher Scientific) for 15 min at room temperature (RT), and then blocked by rotation for 2 h in BCB buffer comprising PBS, 0.1% bovine serum albumin (BSA), and 0.01% sodium azide (NaN_3) (both from Sigma Aldrich). These EV-coated beads were then spun down at 2000 × g for 10 min, washed with BCB buffer, and re-suspended in BCB buffer. Next, antibody labelling was completed at RT for 30 min under mild shaking, and the EV-coupled beads were washed with BCB buffer after each step, and centrifuged at 2,000 *xg* for 10 min. Labelling was performed using the fluorochrome-conjugated antibodies anti-CD73-PE and anti-CD90-PE-Cy7 (1:50; both from BD, Franklin Lakes, NJ, USA); or indirect labelling with the primary antibodies anti-CD9 (Clone VJ1/20; 1:10), anti-CD63 (Clone TEA3/18; 1:10), anti-CD81 (Clone 5A6; 1:10), and IgG isotype control (1:10; Abcam, Cambridge, UK); followed by incubation with the secondary antibody FITC-conjugated Goat F(ab')2 anti-Mouse IgG (1:10; Bionova, Halifax, NS, Canada). Labelling was also performed using the antibodies anti-CD29 (1:10; BD) and anti-CD44 (1:10; AbD Serotec, Oxford, UK), and the secondary antibody A488-conjugated Rabbit anti-Rat IgG (1:100; AbD Serotec). Data were acquired using a FACSVerse flow cytometer (BD), and analysed using FlowJo® v10 software (FlowJo, LLC, Ashland, OR, USA).

Cryo-electron microscopy

EV pools were vitrified, and then EV size and morphology were examined by cryo-electron microscopy (cryo-EM) using a Jeol JEM 2011 transmission electron microscope (Jeol, Tokyo, Japan) as previously described (*Chapter 2*) (Monguió-Tortajada et al. 2017a).

EV staining

For tracking purposes, we produced fluorescently-labelled EVs by staining producer cells with the lipophilic dyes NIR815 (excitation/emission 786/815 nm; Thermo Fisher Scientific) and PKH26 (excitation/emission 551/567 nm; Sigma Aldrich) following the manufacturers' protocols.

Porcine PBMC isolation and functional assays

We used 10-mL Vacutainer EDTA tubes (BD) to obtain whole blood from pigs (Landrace × Large White; average weight of 30 kg; indistinct sex). The whole blood samples were diluted and subjected to density gradient centrifugation over Ficoll (BD) to extract peripheral blood mononuclear cells (PBMCs). PBMCs were collected, washed twice with PBS + 1% FBS (Lonza, Basel, Switzerland), counted, and frozen. Upon thawing, PBMCs were labelled with Violet CellTrace dye (Thermo Fisher Scientific) according to the manufacturer's instructions. To avoid the presence of serum-derived EVs, the PBMCs were cultured in serum-free XVIVO medium (Lonza) supplemented with 2 mM L-glutamine and 1% P/S.

PBMCs were stimulated with phorbol 12-myristate 13-acetate (PMA; 0.6 ng/mL; Sigma Aldrich) and ionomycin (Io; 200 ng/mL; Sigma Aldrich), with or without cATMSC-EVs at the indicated ratios according to EV-producing cell equivalent. After 5 days of culture, supernatants were collected and stored. The percentage of proliferating cells was determined by flow cytometry with an LSRFortessa (BD), using FlowJo v.X software to gate the $FSC^{high}Violet^{low}$ cells.

Alternatively, PBMCs were cultured with or without stimulation by PMA + Io. Then, $10x10^5$ of these cells were transferred to 96-well plates with cardiac scaffolds (7.1 mm^2) containing either hydrogel alone or hydrogel with cATMSC-EVs. After 5 days of culture, the supernatants were collected for cytokine response analysis.

Cytokine response

To measure the levels of IL1β, IL4, IL6, IL8, IL10, IL12p40, IFNα, IFNγ, and TNFα in the supernatants of stimulated PBMCs, we used the Cytokine & Chemokine 9-Plex Porcine ProcartaPlex™ Panel 1 immunoassay (Invitrogen-ThermoFisher Scientific) in accordance with the manufacturer's instructions.

Porcine outgrowing endothelial progenitor cell cultures and characterization

Within 2 h after collection, 20-mL samples of venous blood from pigs (Landrace × Large White; 30–35 kg) were processed for the isolation of outgrowing colonies from endothelial progenitor cell cultures by Ficoll gradient (GE Healthcare, NJ, USA) as previously described (Navarro-Sobrino et al. 2010). PBMCs were treated with red cell lysis buffer (155 mM NH_4Cl, 10 mM $NaHCO_3$, and 0.115 mM EDTA), centrifuged for 5 min at 1500 rpm, and washed with endothelial growth medium-2 (EGM-2; Clonetics®, CA, USA), which comprises endothelial cell basal medium-2 (EBM-2) plus 10% FBS, human endothelial growth factor (hEGF), vascular endothelial growth factor (VEGF), human basic fibroblast growth factor (hFGF-B), insulin-like growth factor 1 (R3-IGF-1), GA-1000 (gentamicin and amphotericin-B), heparin, hydrocortisone, and ascorbic acid. Cells were seeded at $2x10^7$ cells/mL in fibronectin-coated plates (10 μg/mL; Sigma-Aldrich), and the media was changed every 2–3 days. Late outgrowth endothelial cell (OEC) colonies with clonogenic capacity appeared after 2 weeks in culture, further expanded in flasks in growing media and frozen in liquid nitrogen until use for OEC characterization and migration assays.

The cells were fixed with 4% paraformaldehyde (Sigma Aldrich) for 15 min, and then subjected to immunocytochemical analysis for the expression of endothelial-specific markers. The fixed cells were washed with 0.1% Tween-PBS (T-PBS), incubated for 1 h with blocking buffer (1% BSA in T-PBS), and then incubated overnight at 4ºC with the primary antibodies anti-VEGFR2 (1:50; Santa Cruz Biotechnology, Dallas, TX), anti-CD31 (1:50; Abcam), and anti-vWF (1:100; Sigma). After several washes with T-PBS, the cells were incubated for 1 h at RT with the secondary antibodies AlexaFluor 488 and AlexaFluor 568 (1:1000; Invitrogen). Finally, the cells were counterstained with DAPI mounting media (Vectashield) prior to visualization using an Olympus BX61 microscope (Olympus, Tokyo, Japan).

Flow cytometry was performed to corroborate the OECs' progenitor/hematopoietic origin. OECs were blocked for 15 min at RT with 25% AB human serum (Sigma-Aldrich) in PBA buffer (1% BSA and 0.1% NaN_3 in PBS). Then, the cells were labelled with anti-CD34-PE (BD) for 30 min at RT, washed with PBA buffer, and passed through a 30-μm filter (Partec, Münster, Germany). Finally, the cells were analysed using a FACSAria™ (BD).

An in vitro Matrigel assay was performed to evaluate the OECs for formation of vessel-like structures. First, we plated 200 μL of ice-cold Matrigel™ (growth factor-reduced; BD) and

incubated the plates at 37ºC for 30 min. Then, the plates were seeded with $4x10^4$ OECs and EBM-2, and incubated for 24 h. Finally, images were taken using the Olympus IX71 microscope.

Migration assay

We measured cell migration in agarose spots using an adaptation of a previously described protocol (Ahmed et al. 2017; Calle et al. 2018). First, the wells of a 6-well plate dedicated to OECs were coated with 10 µg/mL fibronectin (Biochrom, Berlin, Germany). After the fibronectin dried, quadrants were drawn in each well. In each quadrant, we applied to the surface three 5-µL droplets of 0.5% low-melting-point agarose (40ºC, Ecogen, Barcelona, Spain) mixed 1:1 (v/v) with either 10% sucrose (used as buffer), VEGF (50 ng/mL final concentration; Sigma Aldrich), or pooled EVs. The plates were incubated at 4ºC for 15 min to ensure gel solidification and adherence. Next, MSCs or OECs in α-MEM or EBM-2 complete medium (10% FBS), respectively, were poured into the corresponding wells, followed by incubation for 3 h at 37ºC to allow adherence. To avoid cell replication and promote chemoattractant detection by cells, the complete medium was then replaced with poor medium (0.2% FBS).

An Axioskop Z1 microscope (Zeiss, Oberkochen, Germany) was used to view random localizations centred in the border of agarose spots, and pictures (3 × 3 mosaic at 20× objective) were taken every hour for 21 h, with controlled temperature and CO_2 level. Videos were compiled, and we quantified the distance, velocity, and directionality of cell movement using the Manual tracking plug-in of Fiji software (Image J 1.54w, National Institutes of Health, Bethesda, MD, USA) and the Chemotaxis and Migration tool software version 2.0 (Ibidi Inc., Martinsried, Germany).

Generation of cardiac scaffolds

Decellularized cardiac scaffolds were generated from both pericardial and myocardial tissues. We obtained 19 pericardial scaffolds from healthy pericardia of patients (n = 12; 10 males, 2 females; mean age, 67 ± 12 years; range, 48–85 years) who were undergoing cardiac interventions at our institution, and who have their signed consent. Additionally, 21 myocardial scaffolds were obtained from porcine hearts from a slaughterhouse (Landrace × Large White; n = 4). This study was revised and approved by the Germans Trias i Pujol University Hospital ethics committee, and all the protocols conformed to the principles outlined in the Declaration of Helsinki.

We performed detergent-based decellularization (SDS and Triton X-100) followed by DNase I treatment, lyophilization, and sterilization procedures as previously described (Prat-Vidal et al. 2014; Perea-Gil et al. 2015b). Scaffold size was standardized to 50.3 mm^2 and 7.1 mm^2 using disposable 8-mm and 3-mm biopsy punches, respectively. Scaffolds were placed in 6-well or 96-well plates prior to EV loading.

EV delivery into decellularized scaffolds

The EV pool was concentrated using a sterile 2-mL 100-kDa ultrafiltration unit (Merck Millipore, Darmstadt, Germany), and then the volume was adjusted using 0.22-µm-filtered 10% sucrose buffer. We mixed the EV pool with 50 µL 0.3% PuraMatrix® peptide hydrogel (Corning, Corning, NY, USA) in 10% sucrose (1:1, v/v), and this mixture was added on top of the scaffolds (8-mm diameter; surface area, 50.27 mm2) in 6-well plates. Following a 30-min incubation at RT, α-MEM-FBS was added over the scaffold to promote hydrogel jellification. After 2 h, the scaffolds with NIR815-labelled EVs were analysed for EV detection, and maintained for 1 week under standard culture conditions. Scaffolds with PKH26-labelled EVs were washed 3 times with

PBS, fixed with 10% formalin (Sigma Aldrich) for 1 h at RT, rinsed 3 times with PBS, embedded in Tissue-Tek® O.C.T.™ compound (Sakura Finetek USA Inc., Torrance, CA, USA), and then cryopreserved.

Alternatively, scaffolds with a 3-mm diameter and surface area 7.1 of mm^2 were placed in 96-well plates. We added 4.2 µL of EV mixed with hydrogel on top of these scaffolds, and incubated them at RT for 30 min. Then 100 µL of complete medium was added for hydrogel jellification. One hour later, $1x10^5$ third party porcine PBMCs were added to each well. The cells were cultured for 5 days, the supernatant was stored, and the scaffolds were washed, fixed, and cryopreserved.

Near-infrared scaffold scanning

Six-well plates containing scaffolds embedded with hydrogel alone or mixed with NIR815-labelled EVs were scanned using an Odyssey CLx scanner (LI-COR Biosciences, Inc., Lincoln, NE) with the focus set at 2.5 mm, and resolution at 169 µm. Scaffold autofluorescence and the near-infrared fluorescent dye NIR815 were detected and quantified in the 700-nm and 800-nm channels, respectively.

Immunohistochemical analysis

To examine PKH26-EV retention within scaffolds, we performed immunostaining on 10-µm-thick native and decellularized tissue cryosections. Briefly, samples were blocked for 1 h at RT with TBS/10% horse serum/1% BSA/0.2% Triton-X-100 (all from Sigma Aldrich), and then incubated with primary antibody against cardiac troponin I (cTnI; 1:100; Abcam), sarcomeric α-actinin (1:100; Sigma), and type-III collagen (col-III; 1:100; Abcam). To visualize antibodies, the sections were incubated with Cy2-, Cy3-, and Cy5-conjugated secondary antibodies (1:500; Jackson ImmunoResearch Laboratories, West Grove, PA, USA) and nuclei counterstained with 4′,6-diamidino-2-phenylindole (DAPI; 0.1 µg/mL; Sigma-Aldrich). Immunofluorescence images were captured using an Axio-Observer Z1 confocal microscope (Zeiss).

Scanning electron microscopy

Scaffolds were fixed with 10% formalin, washed with sterile distilled water, dehydrated in ethanol solutions of increasing concentrations, and then dried using a CO_2 critical point dryer (EmiTech K850; Quorum Technologies, Lewes, UK). Finally, the scaffolds were sputter-coated with gold using an ion sputter (JFC 1100, Jeol), and then examined using a JSM-6510 scanning electron microscope (Jeol) at 15 kV.

Statistical analysis

Data are shown as mean ± SD unless otherwise stated. The appropriate statistical tests were performed in all datasets after checking for normality of data. Statistical differences are shown only when they are considered significant ($p < 0.05$). Analyses were performed using Graphpad Prism (6.0 version) software.

RESULTS

Porcine cATMSC-EV purification

EVs were isolated from porcine cATMSCs by SEC, and were screened for EV markers (CD9, CD63, and CD81) and MSC markers (CD24, CD44, CD73, and CD90). CD63 was the most relevant marker and CD44 the most consistently expressed; therefore, these two markers were used to track EVs in the elution fractions from SEC columns (**FIGURE 26A**). This process ensured EV purification from cell- and debris-cleared cATMSC-conditioned media, as previously published (Monguió-Tortajada et al. 2017a). The elution fractions positive for porcine cATMSC-EVs were pooled, and cryo-electron microscopy was used to confirm that cATMSC-EVs had a double membrane, round shape, and nanovesicle size (**FIGURE 26B**).

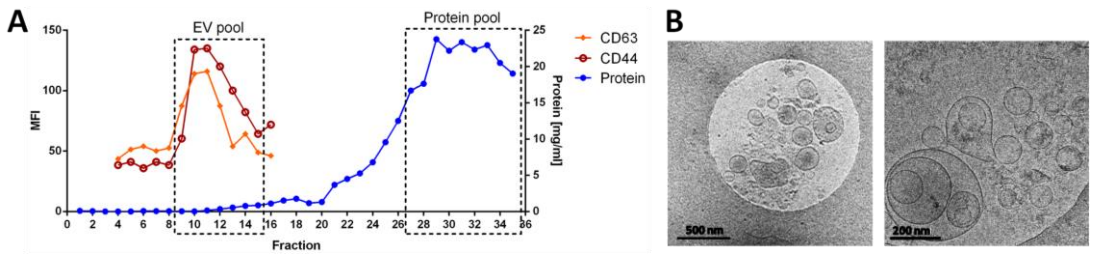

FIGURE 26 | EVs were isolated from porcine cATMSCs by size-exclusion chromatography (SEC), and phenotypically characterized. (A) SEC elution profile of porcine cATMSC-EVs by bead-based flow cytometry, positive for the EV and MSC markers CD63 and CD44. The protein was eluted later, measured by absorbance at 280 nm. A representative image of 35 independent EV isolations is shown. MFI: mean fluorescence intensity. **(B)** Cryo-transmission electron microscopy confirmed that cATMSC-EVs were double membrane nanovesicles of 50–300 nm. Scale bars are 500 nm and 200 nm, respectively.

cATMSC-EVs have immune suppressive properties

To test their immunomodulatory properties, we used cATMSC-EVs in potency assays with allogeneic porcine PBMCs. PBMCs were activated with PMA + Io to simulate the pro-inflammatory milieu found in the ischemic myocardium post-MI. Then we analysed their proliferative and cytokine profiles in the presence or absence of cATMSC-EVs. Pooled cATMSC-EVs dose-dependently abrogated the proliferation of allogeneic PBMCs (**FIGURE 27**). These experiments were performed using two different EV pools from 3 independent donors

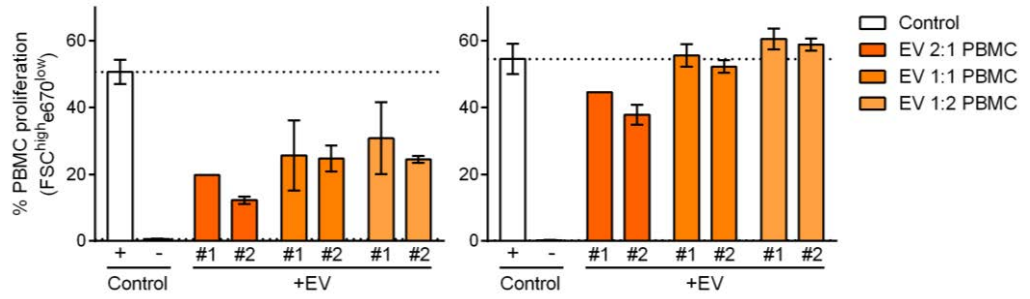

FIGURE 27 | Porcine cATMSC-EVs abrogate polyclonal proliferation of allogeneic PBMCs. Two EV pools (#1 and #2, each from three different EV pig donors) were tested in potency assays (with a starting dose corresponding to $2x10^5$ EV-producing cells) against two different fully allogeneic PBMC responders ($1x10^5$ cells) with polyclonal stimulation (PMA + Io). Proliferation was assessed as the percentage of $FSC^{high}e670^{low}$ cells. Data are shown as mean ± SD.

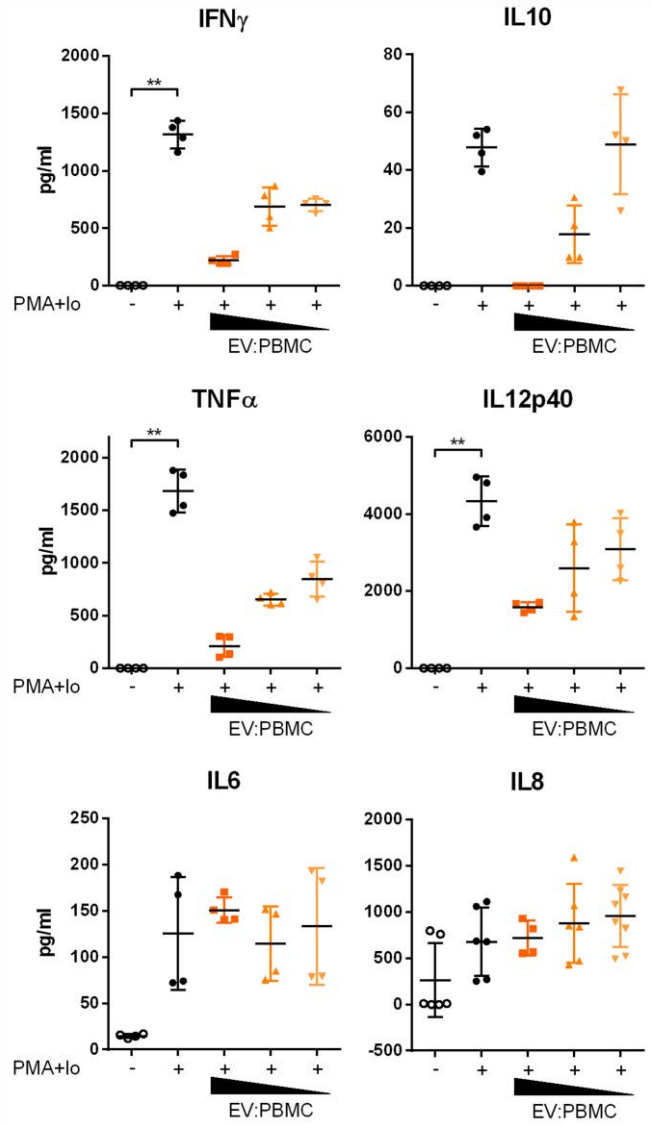

FIGURE 28 | Porcine cATMSC-EVs modulate the cytokine response of allogeneic PBMCs after polyclonal stimulation. We assessed the cytokine levels in supernatants of PBMCs in the presence or absence of cATMSC-EV pools (10:1, 2:1, and 1:1 cATMSC-EV:PBMC ratios) at 5 days after PMA + Io stimulation. Horizontal bars indicate mean ± SD. $^{**}p < 0.01$ by one-way ANOVA with Dunn's multiple comparison test.

each, and the capacity of cATMSC-EVs to suppress proliferation was not dependent on the specific EV pool, but rather on the utilized PBMCs.

Presence of cATMSC-EVs also abrogated the stimulated PBMCs' secretion of the pro-inflammatory cytokines IFNγ, TNFα, and IL12p40 (**FIGURE 28**). IL10 was also reduced by cATMSC-EVs. However, the lowest EV dose reduced the levels of pro-inflammatory cytokines levels while maintaining IL10 production, thus increasing the IFNγ:IL10 ratio. IL6 and IL8 secretion was not modified by cATMSC-EVs. Other cytokines, including IL1β, IL4, and IFNα, were present at very low levels and were also unchanged by cATMSC-EVs (data not shown). Notably, cATMSC-EVs did not induce a cytokine response from allogeneic PBMCs, suggesting an absence of alloreactivity, and the TNFα reduction indicated that the EV products were endotoxin-free.

Porcine cATMSC-EVs recruit allogeneic pro-regenerative cells

The success of EV administration confined within a scaffold for cardiac repair relies on the hypothesis that EVs will recruit endogenous cells. To test this hypothesis in vitro, we quantitatively analysed the chemotactic responses of allogeneic OECs and MSCs towards

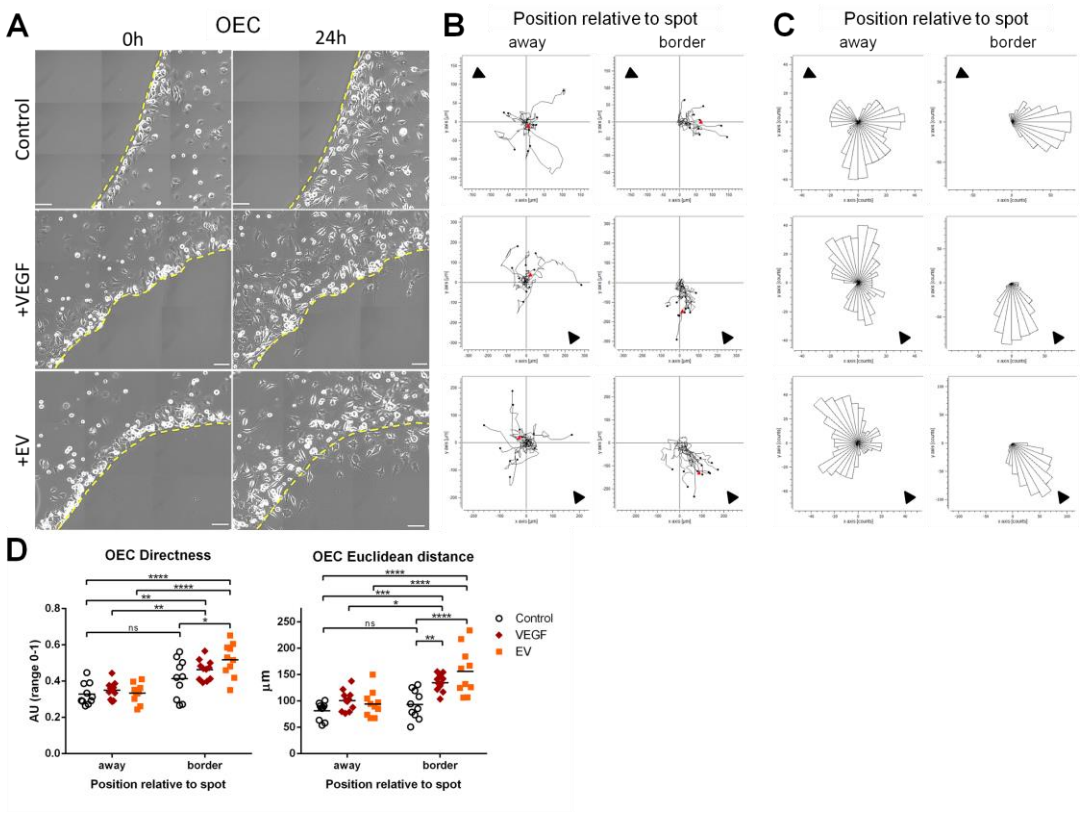

FIGURE 29 | Porcine cATMSC-EVs recruit allogeneic swine peripheral blood outgrowth endothelial cells (OECs). OECs were added to plates with agarose spots containing VEGF (positive control for OEC migration) or cATMSC-EVs (corresponding to $8x10^4$ cells), and cell migration was assessed over 24 h. **(A)** Representative images of agarose spot borders (dotted line) at 0 and 24 h. Migrating cells are observed only inside spots containing VEGF or EVs. Scale bars = 100 µm. **(B, C)** The corresponding tracking **(B)** and rose **(C)** plots of cell movement during the 24 h time-lapse. Arrow cap indicates the direction to the spot. **(D)** Directness and Euclidean distance (Δxy) of cell movement. Pictures were taken hourly, tracking ten cells in each position. Data account for three independent experiments with a minimum of three spot positions tracked for each condition. *$p < 0.05$, **$p < 0.01$, ***$p < 0.001$, and ****$p < 0.0001$ by two-way ANOVA with Tukey's post-hoc analysis.

cATMSC-EVs in agarose spots, using an adaptation of a previously described protocol (Ahmed et al. 2017; Calle et al. 2018).

From porcine peripheral whole blood samples, we isolated OECs, since it would be crucial that OECs migrate towards the infarcted tissue and promote revascularization of the necrotic myocardium. It was previously confirmed that OECs were true hematopoietic vascular precursors that expressed specific endothelial-lineage markers, such as VEGFR2, vWF, and CD31 (immunocytofluorescence; **Supplementary Figure 11A–C**), and CD34 (flow cytometry; **Supplementary Figure 11D**), and developed vascular-like networks when seeded in Matrigel (**Supplementary Figure 11E**).

Analysing the active migration of OECs and MSCs towards agarose spots revealed that no cells entered the spots containing buffer alone, while OECs invaded the spots containing cATMSC-EVs or VEGF (positive control for OEC migration) (**FIGURE 29** and **Supplementary videos 1–3**). Allogeneic MSCs also actively migrated inside the spots containing cATMSC-EVs, in a dose-dependent manner (**FIGURE 30** and **Supplementary videos 4–6**). OEC and MSC tracking over 24 h indicated cell movement directionality towards the EV-containing spots, demonstrated by an

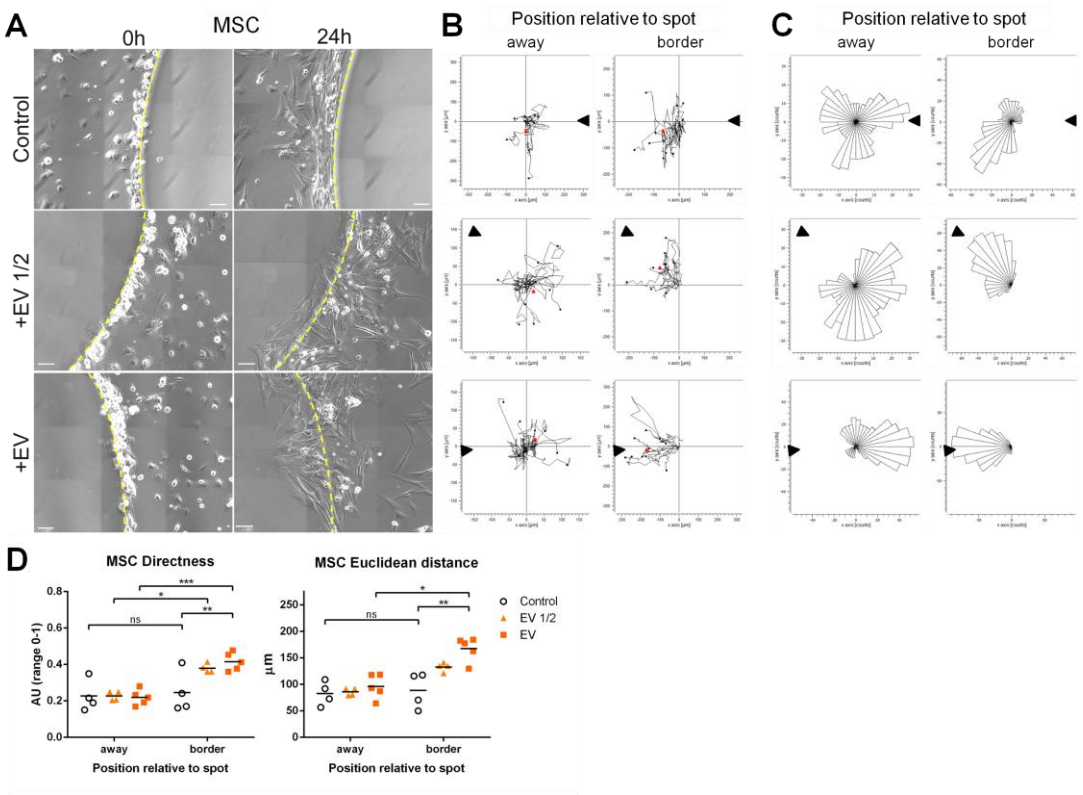

FIGURE 30 | **Porcine cATMSC-EVs recruit allogeneic swine cATMSCs.** Allogeneic cATMSCs were added to plates with agarose spots containing increasing doses of cATMSC-EVs (corresponding to $4x10^4$ and $8x10^4$ cells), and cell migration was assessed over 24 h. **(A)** Representative images of agarose spot borders (dotted line) at 0 and 24 h. Migrating cells are observed only inside spots containing EVs. Scale bars = 100 µm. **(B, C)** The corresponding tracking **(B)** and rose **(C)** plots of cell movement during the 24-h time-lapse. Arrow cap indicates direction to the spot. **(D)** Directness and Euclidean distance (Δxy) of cell movement. Pictures were taken hourly, tracking ten cells in each position. Data account for two independent experiments with a minimum of two spot positions tracked for each condition. *$p < 0.05$, **$p < 0.01$, and ***$p < 0.001$ by two-way ANOVA with Tukey's post-hoc analysis.

increased Directness of movement and Euclidean distance (Δxy) of cells, only when OECs or MSCs were initially in contact with the agarose spot (border versus away positioned cells; **FIGURE 29B–D, FIGURE 30B–D**). VEGF and cATMSC-EV presence increased the overall distance travelled and velocity of OECs in contact with the agarose spot, but no statistical differences were found (**Supplementary Figure 12**). We found no changes in the Accumulated distance (ΣΔxy) or Velocity of MSCs (**Supplementary Figure 13**).

Biocompatible 3D-engineered scaffolds maintain the internal ultrastructure and are devoid of cells after decellularization

We generated two decellularized cardiac scaffolds from human pericardial and porcine myocardial tissues, preserving the intrinsic structure and spatial 3D organization of the native matrix fibrils (**FIGURE 31A–D**). Complete pericardium and myocardium decellularization was confirmed by the absence of cell nuclei in both acellular scaffolds (**FIGURE 31F, H**). Additionally, proper marking of the representative matrix protein type-III collagen (**FIGURE 31E–H**) confirmed preservation of matrix protein components following decellularization, as previously described (Perea-Gil et al. 2018). Proteomic characterization revealed enrichment of matrisome/ECM-related proteins in the decellularized pericardial and myocardial scaffolds, as

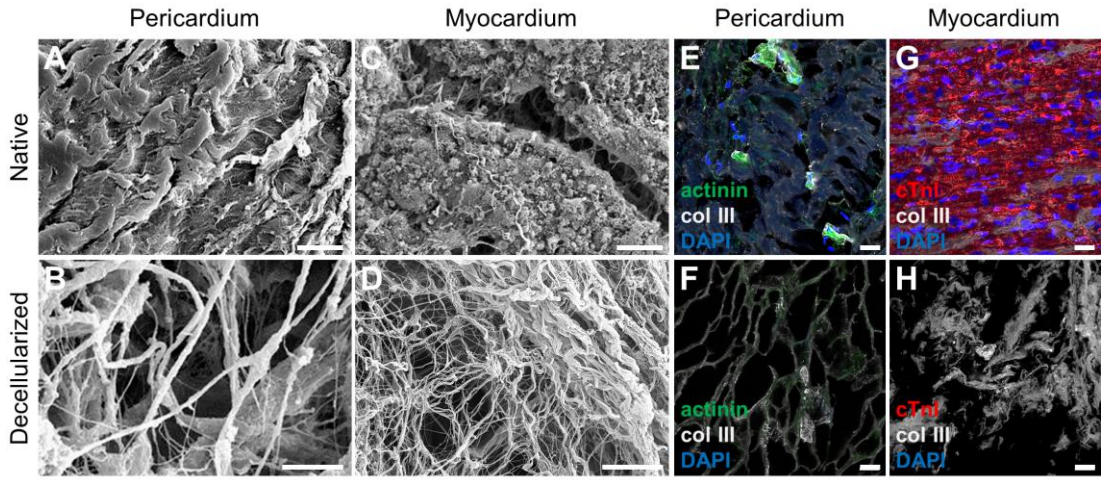

FIGURE 31 | Three-dimensional engineered scaffolds maintain their internal ultrastructure and are devoid of cells after decellularization. Ultrastructure determined by scanning electron microscopy (SEM) of the **(A)** native pericardium and **(B)** decellularized pericardial scaffolds; or **(C)** native myocardium and **(D)** decellularized myocardial scaffolds. Scale bars = 10 μm. **(E, F)** Representative images of the native pericardium and decellularized pericardial scaffolds, respectively; and **(G, H)** native myocardium and decellularized myocardial scaffolds showing immunostaining for actinin (green), cardiac troponin I (cTnI, red), and collagen III (col III, grey). Decellularization is indicated by the absence of actinin, cTnI, and cell nuclei (DAPI, blue). Scale bars = 20 μm.

well as the expression of major cardiac extracellular matrix (ECM) components, including collagens, ECM glycoproteins, ECM regulators, and proteoglycans (Perea-Gil et al. 2018).

Porcine cATMSC-EVs are successfully retained within 3D-engineered cardiac scaffolds

To assess the feasibility of using 3D-engineered cardiac scaffolds as an EV delivery platform, we evaluated the EV retention within the decellularized scaffolds. EV-producing cATMSCs were labelled with fluorescent lipophilic dyes, enabling the tracking of fluorescently-labelled EVs. This process avoided troublesome EV washing due to carry-over of lipophilic dye aggregates in EV preparations. A dot blot confirmed NIR815 labelling in SEC fractions containing the porcine cATMSC-EVs (**FIGURE 32A**). Next, the pooled EVs with ratified NIR815 fluorescence (**FIGURE 32A**, right) were mixed with the hydrogel, and used to fill both lyophilized pericardial and myocardial scaffolds. Hydrogel jellification was promoted by addition of complete medium. Scaffolds were then thoroughly washed and analysed by fluorometric scanning, which revealed cATMSC-EV retention in both 3D-engineered cardiac scaffolds (**FIGURE 32B**). As visible in the scanning images and confirmed by quantification of fluorescence intensity, the pericardial scaffolds held higher amounts of EVs, since the myocardial scaffolds reached saturation earlier (**FIGURE 32C**).

To confirm cATMSC-EV retention within the scaffolds, we also loaded PKH26-labelled cATMSC-EVs into the pericardial and myocardial scaffolds, following the above-described procedure. Indeed, confocal microscope imaging revealed cATMSC-EVs inside the scaffolds (**FIGURE 32D**). Moreover, SEM confirmed that porcine cATMSC-EVs were retained within the scaffolds after washing and a week-long culture, which appeared as 100- to 120-nm protuberances attached to the scaffolds within the hydrogel (**FIGURE 32E**).

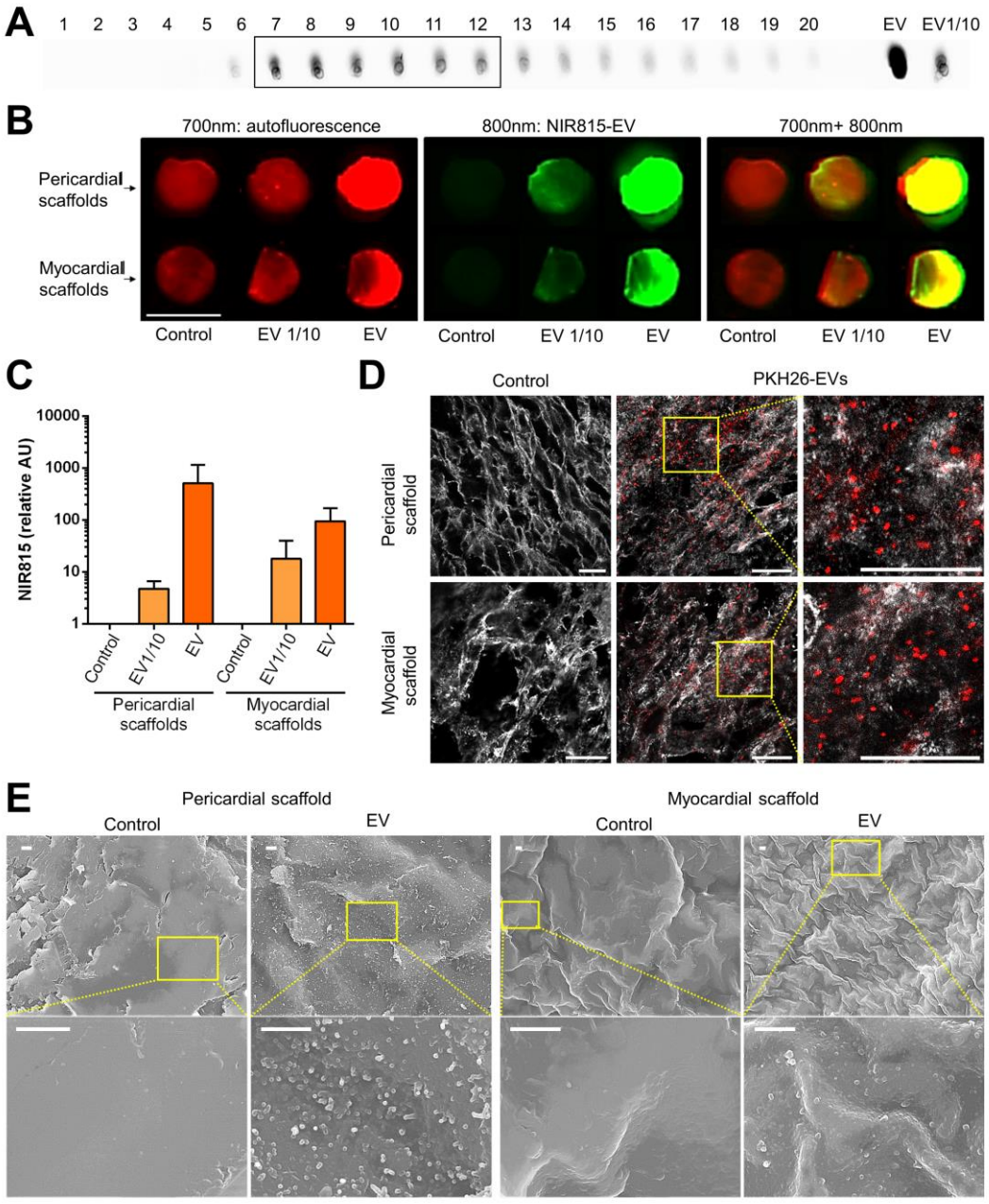

FIGURE 32 | Both 3-dimensional engineered cardiac scaffolds retained cardiac adipose tissue-derived mesenchymal stem cell extracellular vesicles (cATMSC-EVs), as shown by whole-scaffold fluorometric scanning (A–C) and confocal (D) and SEM imaging (E). (A) A dot blot confirmed NIR815 labeling in SEC fractions containing porcine cATMSC-EVs, with squared fractions pooled as EV batches. **(B–C)** NIR815-cATMSC-EVs in peptide hydrogel were added to pericardial and myocardial scaffolds, and were detected even after thorough washing by reading NIR815 fluorescence at 800 nm (green), and the scaffold's autofluorescence at 700 nm (red). Scale bar = 1 cm. **(C)** NIR815 fluorescence quantification expressed relative to the hydrogel-alone scaffold (background). **(D)** Immunostaining for collagen III (grey) revealed PKH26-cATMSC-EVs (red) inside the scaffolds. Scale bar = 20 µm. **(E)** SEM imaging confirms retention of porcine cATMSC-EVs within scaffolds after washing and week-long culture, which appear as 100- to 120-nm protuberances embedded in the hydrogel attached to the scaffolds. Controls are scaffolds filled with hydrogel alone. Scale bar = 1 µm.

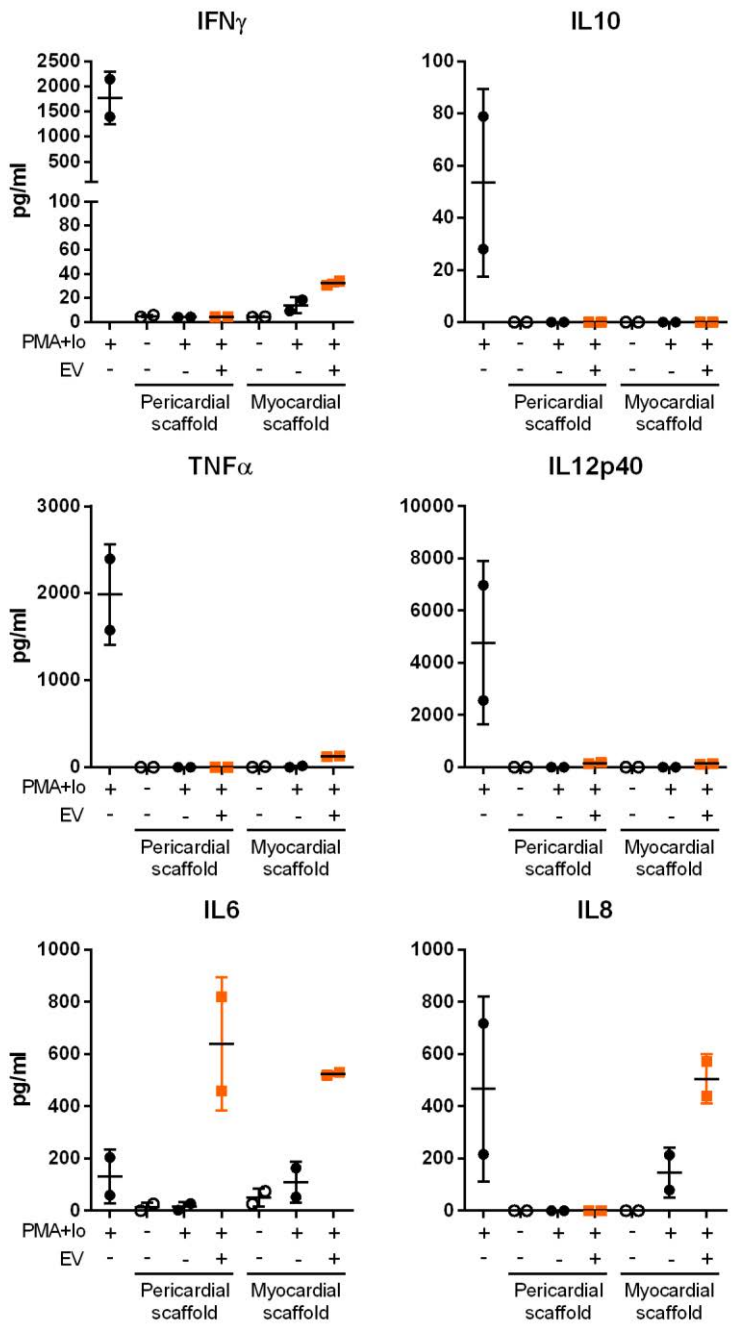

FIGURE 33 | Porcine cardiac adipose tissue-derived mesenchymal stem cell extracellular vesicles (cATMSC-EVs) embedded in cardiac scaffolds modulate cytokine responses of third-party PBMCs after polyclonal stimulation. Five days after PMA + Io stimulation, we assessed the cytokine levels in supernatants of PBMCs in the presence or absence of pericardial or myocardial scaffolds filled with cATMSC-EV pools in peptide hydrogel. Controls are scaffolds filled with hydrogel alone, with or without PMA + Io stimulation. Data points represent the average of 3 technical replicates. Horizontal bars indicate the mean ± SD.

EV-embedded cardiac scaffolds abrogate the cytokine response of allogeneic PBMCs

Finally, we evaluated the combined effect of cATMSC-EVs and cardiac scaffolds based on the cytokine response of stimulated third-party PBMCs. PBMCs, with or without stimulation with PMA + Io, were cultured in the presence of cardiac scaffolds replenished with hydrogel alone or

mixed with cATMSC-EVs. Scaffolds with hydrogel alone abrogated the secretion of pro-inflammatory cytokines (**FIGURE 33**). In the presence of myocardial scaffolds (alone or containing cATMSC-EVs), activated PBMCs secreted IL6 and IL8, and very low levels of IFNγ and TNFα. Notably, IL6 secretion was also increased in the presence of pericardial scaffolds embedded with cATMSC-EVs.

DISCUSSION

In this chapter, we developed a new generation of cell-free cardiac grafts comprising MSC-derived SEC-EVs embedded in decellularized scaffolds for local myocardial delivery.

For the past 15 years, our laboratory has been developing and testing innovative biotherapies using *in vitro* small and large animal models, and has even pioneered some first-in-human studies (Roura, Gálvez-Montón, Lupón, et al. 2017). Cardiac tissue engineering, which combines the use of cells and biomaterials, has been proposed as an alternative therapy for MI, with the potential to repair damaged myocardium, recover heart function, and prevent ventricular remodelling in end-stage heart failure. In this context, decellularized ECM is a biological scaffold derived from whole tissues with the cellular components removed, but with conserved micro- and macro-scale structural components and functional ECM proteins (Crapo, Gilbert, and Badylak 2011; Taylor et al. 2018).

Although no protocol has been identified as optimal due to variability in tissue composition, we have established decellularization methods for generating biocompatible acellular cardiac constructs with conserved native ECM structure and composition, and the ability to be repopulated with cATMSCs (Prat-Vidal et al. 2014; Perea-Gil et al. 2015b). In a preclinical swine MI model, the engineered grafts comprising cardiac scaffolds with cATMSCs integrate with the underlying myocardium, and show signs of neoinnervation and neovascularization, and improved cardiac function post-MI (Gálvez-Montón et al. 2015; Perea-Gil et al. 2016; Gálvez-Montón et al. 2017a; Perea-Gil et al. 2018). However, it remained unclear how the delivered cells contribute to MI recovery, since very few cells are retained in the tissue. Many others also report that, despite yielding promising results, the implanted therapeutic cells show low survival, engraftment, proliferation, and differentiation. This suggests that rather than replacing the injured tissue, these cells foster endogenous regeneration by reducing inflammation through modulation of the host's immune system. Specifically, they appear to reduce the amount of activated $CD4^+CD25^+$ T cells and induce M2-like monocyte polarization with CD73 expression (Gálvez-Montón et al. 2017a; Monguió-Tortajada et al. 2017b), as well as recruit peripheral progenitor cells through trophic factors (Lee et al. 2009; Eggenhofer et al. 2012; Le Blanc and Mougiakakos 2012; Ben-Mordechai et al. 2013; Malliaras et al. 2013). Moreover, increasing evidence suggests that EVs play important roles in these paracrine effects (Timmers et al. 2008; Yáñez-Mó et al. 2015; Monguió-Tortajada et al. 2017a).

Based on these previous findings—together with the fact that cell replacement approaches have disadvantages, including restricted cell engraftment and differentiation potential, immunologic incompatibility, and teratoma formation—we decided to work towards a new generation of cell-free therapy, and explore the immunosuppressive potential of cATMSCs-EVs embedded into our cardiac grafts. To this end, we worked with MSC-EVs isolated by SEC methodology, which is a fraction of the MSC secretome already reported to be immunomodulatory (Monguió-Tortajada et al. 2017a). Theoretically, EVs have advantages over cells in terms of their unchanged phenotype, lack of tumorogenicity, and better biodistribution and storage. In particular, our cATMSC-EVs showed immune suppressive properties and could recruit allogeneic pro-regenerative cells, including allogeneic MSCs and peripheral blood-derived OECs, suggesting that their administration would trigger on-site endogenous cardiac repair. Moreover, confinement of EV delivery within the scaffolds would increase the local dosage of administered EVs, thus reducing the required EV quantity. A previous study showed that EV recruitment towards an artificial 3D scaffold successfully modulated the dissemination pattern of metastatic cells *in vivo*, and encapsulated metastatic cancer cells enabling their localized surgical removal (de la Fuente et al.

2015). Our present experiments demonstrated that only the cells in contact with agarose spots containing cATMSC-EVs were attracted inside, indicating a lack of diffusion of chemoattractant away from the jellified agarose, and that cells were indeed sensing chemotactic molecules. More in-depth studies are needed to decipher the exact chemokines playing a role in this specific case. For instance, EVs can bear functional chemokines anchored in their surface, such as transmembrane CX3CL1 (Brown et al. 2018), or attached to surface glycans, like CCL18 (Berenguer et al. 2018), enabling recognition by cells. Moreover, recent studies provide direct evidence that EVs can act as an independent machinery, to continuously provide, amplify and sustain a chemotactic signal to promote effective directional sensing. Specifically, they showed that EVs can bear the full enzymatic machinery to autogenerate chemotactic molecules, such as the lipid leukotriene B4 (LTB4) by EVs from stimulated neutrophils (Majumdar et al. 2016), or cAMP by EVs from *Dictyostelium discoideum* (Kriebel et al. 2018).

In the context of MI, cardiomyocyte death and ECM degradation release danger-associated signals that activate the innate immune system and trigger inflammatory reactions, including production of cytokines (IL1β, IL6, IFNγ, and TNFα) and release of chemokines for immune cell recruitment. While this initial activation is important for dead cell clearance and tissue repair, it must be repressed in time to prevent excessive inflammation and extension of the ischemic injury (Frantz, Bauersachs, and Kelly 2005; Frangogiannis 2014b). Our present results confirmed that porcine cATMSC-EVs have the capacity to reduce polyclonal activation of allogeneic immune cells, comparable to post-MI circumstances. Importantly, they both reduced allogeneic PBMC proliferation and abrogated the production of pro-inflammatory cytokines. For instance, cATMSC-EVs completely inhibited the secretion of TNFα, which is extensively related to cardiac damage and worsening of heart failure symptoms (Frantz, Bauersachs, and Kelly 2005).

Previous *in vivo* data reveal that the $CD4^+$ T cells conventionally present in the infarcted myocardium are mainly Th1 polarized (Hofmann and Frantz 2015). Moreover, experiments in RAG1 KO mice reconstituted with $CD4^+$ T cells from WT or IFNγ KO mice clearly demonstrate that Th1 $CD4^+$ T cells contribute to myocardial ischemia-reperfusion injury involving IFNγ expression (Yang et al. 2006; Boag, Andreano, and Spyridopoulos 2016). Thus, it is encouraging that cATMSC-EVs were able to abrogate secretion of not only IFNγ but also of the Th1-inducing cytokine IL12. On the other hand, cATMSC-EVs did not alter IL6 and IL8 secretion. While IL6 production is related to initiation of reparative processes, IL8 is responsible for neutrophil recruitment. After MI, neutrophils are recruited, as they are needed for the clearance of dead cells and degraded ECM, and they contribute to the initial inflammatory phase. However, their absence does not correlate to a change in infarct size (Frangogiannis 2014a). Finally, the observed concomitant reduction in IL10 in our study might be attributed to its interferon- or IL12-dependent production (Rutz and Ouyang 2011; Stewart et al. 2013).

When PBMCs were combined with scaffolds, the presence of the scaffold alone abrogated cytokine production, likely due to minimized cell interaction in the presence of scaffolds. Under these experimental conditions, when cATMSC-EVs were added to either type of scaffold, IL6 production spiked. Only cATMSC-EV addition to myocardial scaffolds led to increases of IFNγ, TNFα, and IL8. Moreover, pericardial scaffolds seemed to retain EVs better than myocardial scaffolds. These findings support further *in vivo* experiments combining cATMSC-EVs with pericardial scaffolds.

In summary, here we confirmed that SEC is a valuable method for extracting highly purified EVs with unchanged functional properties, resembling their parental cells (Perea-Gil et al. 2015a; Monguió-Tortajada et al. 2017a). Moreover, our data indicated that biocompatible cardiac

scaffolds generated by decellularization of myocardium or pericardium maintained their structure and ECM composition, and may be useful for effective local administration of MSC-EVs. Further research is needed to confirm that the addition of multifunctional MSC-EVs within the scaffolds promotes cardiac repair by generating a highly bioactive niche that stimulates host pro-regenerative cell engraftment, and could thus be used as a cell-free off-the-shelf regenerative product for post-infarction myocardial repair.

SUPPLEMENTARY FIGURES

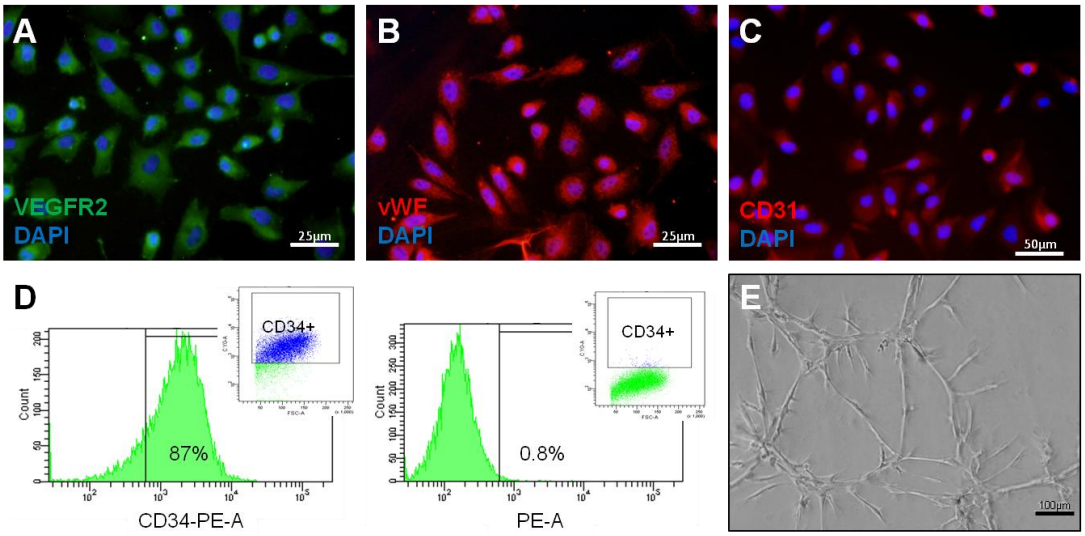

Supplementary Figure 11 | **Porcine outgrowth endothelial cell (OEC) characterization. (A–D)** Endothelial cell markers and hematopoietic origin were analysed by immunocytochemistry **(A–C)** and flow cytometry **(D)**. **(A–C)** Representative images of OECs immunostained for VEGFR2 (green), vWF (red), or CD31 (red) and nuclei stained with DAPI (blue). **(D)** Representative flow cytometry plots of CD34-labeled OECs or negative control (right panel). Most cells (up to 87%) were positive for the progenitor/hematopoietic marker CD34. **(E)** Matrigel assay showing that OECs formed vessel-like structures after 24 h.

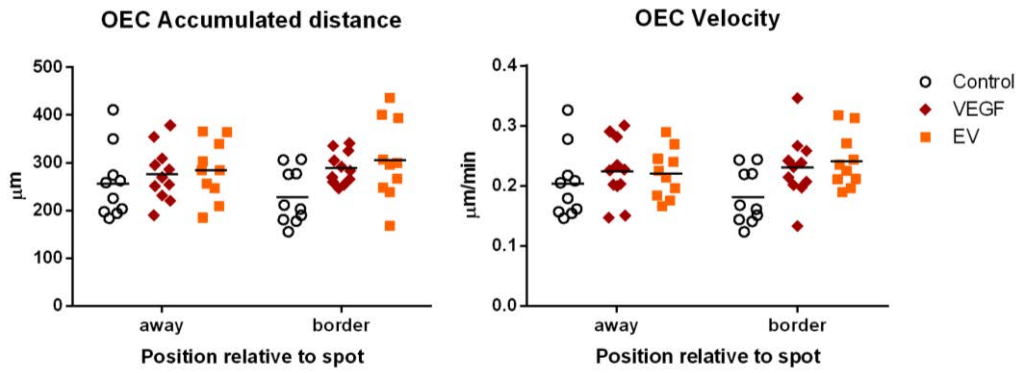

Supplementary Figure 12 | **Accumulated distance (ΣΔxy) and Velocity of OECs.** OECs were added to plates with agarose spots containing VEGF (positive control for OEC migration) or cATMSC-EVs (corresponding to $8x10^4$ cells), and cell migration was assessed over 24 h. Pictures were taken hourly, tracking ten cells in each position. Data account for three independent experiments with a minimum of three spot positions tracked for each condition. VEGF and cATMSC-EV presence increased the overall distance travelled and velocity of OECs in contact with the agarose spot, but no statistical differences were found by two-way ANOVA with Tukey's post-hoc analysis.

Related to **FIGURE 29**.

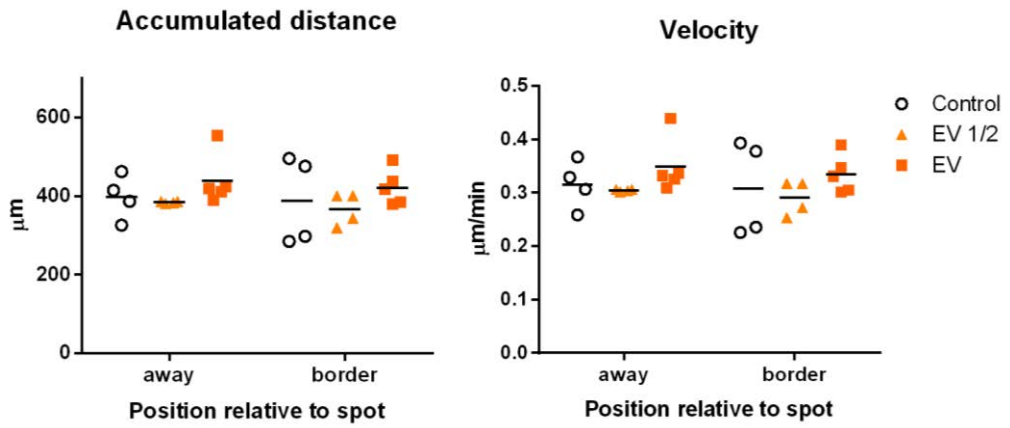

Supplementary Figure 13 | Accumulated distance (ΣΔxy) and Velocity of allogeneic swine cATMSC. Allogeneic cATMSCs were added to plates with agarose spots containing increasing doses of cATMSC-EVs (corresponding to $4x10^4$ and $8x10^4$ cells), and cell migration was assessed over 24 h. Pictures were taken hourly, tracking ten cells in each position. Data account for three independent experiments with a minimum of three spot positions tracked for each condition. No statistical differences were found by two-way ANOVA with Tukey's post-hoc analysis.

Related to **FIGURE 30**.

SUPPLEMENTARY VIDEO 1 | 20-h lapse video of **s**wine peripheral blood outgrowth endothelial cells (OECs) in contact with a control (10% sucrose buffer) agarose spot. OECs do not enter the spot, and delocalize away from the spot border to find available surface for attachment.

SUPPLEMENTARY VIDEO 2 | 20-h lapse video of **s**wine peripheral blood outgrowth endothelial cells (OECs) in contact with a VEGF-containing agarose spot. Some OECs can be seen entering the spot and actively migrating towards its centre.

SUPPLEMENTARY VIDEO 3 | 20-h lapse video of **s**wine peripheral blood outgrowth endothelial cells (OECs) in contact with an agarose spot containing porcine cardiac adipose tissue-derived mesenchymal stem cell extracellular vesicles (cATMSC-EVs). cATMSC-EVs recruit OECs, as they can be seen entering the spot and actively migrating towards its centre.

SUPPLEMENTARY VIDEO 4 | 20-h lapse video of allogeneic swine cATMSCs in contact with a control (10% sucrose buffer) agarose spot. cATMSC do not enter the spot, and delocalize away from the spot border to find available surface for attachment.

SUPPLEMENTARY VIDEO 5 | 20-h lapse video of allogeneic swine cATMSCs in contact with an agarose spot containing porcine cardiac adipose tissue-derived mesenchymal stem cell extracellular vesicles (cATMSC-EVs). cATMSC-EVs recruit Some OECs can be seen entering the spot and actively migrating towards its centre.

SUPPLEMENTARY VIDEO 6 | 20-h lapse video of allogeneic swine cATMSCs in contact with an agarose spot containing porcine cardiac adipose tissue-derived mesenchymal stem cell extracellular vesicles (cATMSC-EVs). A higher cATMSC-EVs concentration yields an increased allogeneic cATMSC recruitment towards the centre of the EV-containing agarose spot.

FINAL DISCUSSION AND CONCLUSIONS

FINAL DISCUSSION

The aim of this thesis was to unravel the cellular and paracrine mechanisms that would help explain MSCs' long-lasting immunosuppressive and regenerative effects, albeit their short lifespan after *in vivo* infusion. The starting hypothesis was that these could be mediated by the modulation of the host's immune cells for the generation of regulatory environments and enduring effect, in addition to the secretion of paracrine factors for a delocalized action that would also foster endogenous repair.

With this in mind, we first studied MSC's influence on monocytes as part of the innate immune response. We confirmed MSCs' modulation of monocytes towards a wound-healing M2-like polarization, but with the added functionality of an active extracellular adenosinergic enzymatic activity, which was actually a sustained effect, observable *in vivo* in infiltrating monocytes after a month since MSC local treatment to post-MI myocardium (***Chapter 1***). Also, MSCs were able to have an impact on the adaptive immune response, as they immunosuppressed allogeneic lymphocyte polyclonal proliferation and inflammatory cytokine release (***Chapter 2*** *– human MSC* and ***Chapter 3*** *– porcine MSC*). Regarding the paracrine activity of MSCs, we could identify EVs as one of the active components of MSC's immunosuppressive secreted factors. Specifically, we demonstrated the importance of accurate isolation of MSC-EVs to unravel their immunosuppressive functionality, and propose SEC as an appropriate method (***Chapter 2***). Finally, this knowledge made us design and test *in vitro* a novel construct composed of MSC-EVs embedded in a cardiac scaffold envisioned for myocardial repair in a porcine MI model. Its *in vitro* validation reinforced the idea of EV secretion as an important mechanism of MSCs to both modulate the immune system and foster endogenous repair (***Chapter 3***). A succinct graphical summary of the results presented can be found in **FIGURE 34**.

All these observations make us believe that EVs are an important mechanism for MSCs to promote immunosuppression and wound healing. Nevertheless, the fact that they were apparently not able to directly affect monocytes is a key point to address further. As explained in ***Chapter 1***, the collaboration of MSCs with monocytes has been found to be of essential importance to foster immune modulation and tissue repair (Groh et al. 2005; Melief, Schrama, et al. 2013; Blázquez, Sánchez-Margallo, Álvarez, et al. 2016), and specially demonstrated in monocyte-specific targeting or knock-down models (Ben-Mordechai et al. 2013; Dayan et al. 2011; Lu et al. 2015). Moreover, our results dispute other studies that do show modulation of monocyte polarization by MSC-EVs (Hyvärinen et al. 2018; Lo Sicco et al. 2017). One of the possible explanations for this disagreement is the divergent EV isolation of choice, considering the fact that the EV preparations tested in the other works are not attained by SEC isolation but rather by dUC, combining the EV effect with soluble proteins'. Another important detail is the fact that the aforementioned works described an EV-mediated M2 switch in macrophages differentiated from human monocytes (6-day culture with M-CSF) or mouse BM precursors (GM-CSF), respectively, instead of human primary monocytes, like us. This can be an important point, as monocytes are widely characterized to bear high functional heterogeneity and plasticity, thus monocytes and *in vitro*-derived macrophages can timely respond in many distinct ways to the cues from the local milieu. In this sense, monocytes can adapt their functionality according to the different nature, synergistic or sequential inputs that they may receive, even arguing for monocyte memory (Monguió-Tortajada et al. 2018). For instance, in our hands, MSCs alone (sham animals) did not trigger upregulation of CD73 on infiltrating monocytes *in vivo*, as it was dependent on its combination

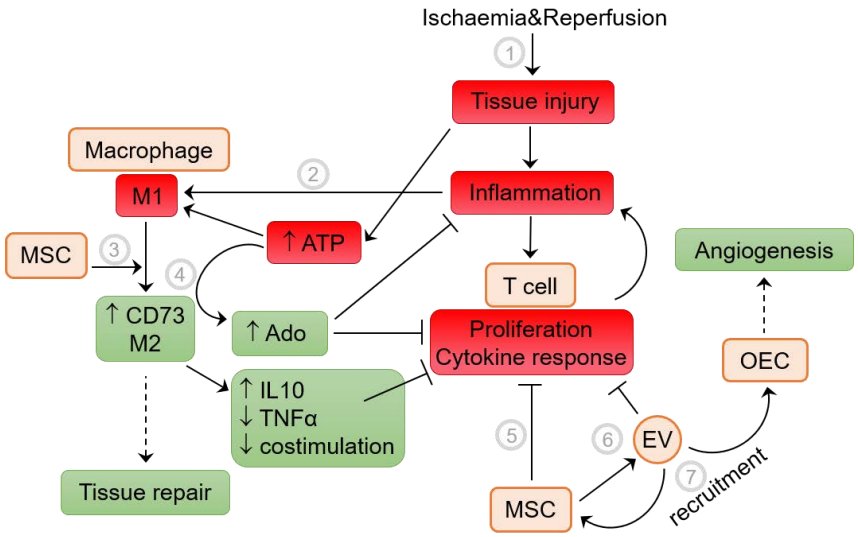

FIGURE 34 | Graphical summary of results. (1) Ischaemia and reperfusion induce tissue injury that leads to release of reactive species and DAMPs, which triggers inflammation. (2) Tissue inflammation recruits innate immune cells such as monocytes/macrophages and polarizes them towards an M1 pro-inflammatory phenotype. Also, inflammation causes T cells to activate, proliferate and secrete pro-inflammatory cytokines. (3) MSCs are able to switch macrophages from an M1 to an M2 polarization. This tissue repair-prone phenotype is characterized by the production of anti-inflammatory IL10, reduction of pro-inflammatory cytokines like TNFα and costimulatory molecules expression. This leads to reduced T cell activation. (4) MSCs also induce the adenosinergic pathway activation on M2 macrophages by triggering CD73 expression. This enables them to hydrolyse the pro-inflammatory extracellular ATP released by tissue necrosis to anti-inflammatory adenosine. (5) MSCs are also able to directly interact with stimulated T cells to reduce their proliferation and cytokine response. (6) MSCs secrete EVs that mediate T cell proliferation and cytokine response abrogation, while apparently not affecting macrophages polarization. (7) MSC-EVs promote recruitment of allogeneic MSCs that would be a positive feedback loop for immunomodulation and regeneration. EVs also recruit OECs that would potentially promote angiogenesis for enhanced tissue healing. Ado: adenosine; ATP: adenosine triphosphate; EV: extracellular vesicle; IL10: interleukin-10; MSC: mesenchymal stem cells; M1: macrophage polarization to M1 inflammatory phenotype; M2: macrophage polarization to M2 wound healing phenotype; OEC: outgrowth endothelial cell; TNFα: tumour necrosis factor α.

with the inflammatory sensing of DAMPs released after MI. Therefore, additional experiments are needed to decipher whether SEC-MSC-EVs are actually innocuous or not to monocytes, as phenotype modification by EVs might require a pre-stimulation, synergistic or secondary stimulation with an inflammatory signal. Also, it is also possible that SEC-MSC-EVs are not able themselves, alone, to alter monocyte/macrophage phenotype. In this case, there is still room for triggering endogenous MSC-mediated modulation of monocytes/macrophages after infused MSC-EV recruit them on-site (***Chapter 3***). Further experiments should be performed to validate these new hypotheses, with special attention to SEC-MSC-EV functionality *in vivo*.

By deciphering the mechanisms that mediate MSCs' action we can design innovative and more efficient therapies in regenerative medicine, like the use of MSC-EVs instead of MSC, which offers several advantages. First, given its non-viable condition, concerns related to cell-based therapy like uncontrolled cell division, unwanted differentiation, transformation or phenotype modification by the environment are off the board (Adamiak et al. 2018). EVs allow batch characterization and sterilization before application, are relatively stable, thus can be easily stored

and managed, and maintain the hypo-immunogenicity of resting MSCs, as they would be unchanged, not increasing class II MHC expression after administration in an inflammatory milieu as MSCs do. Moreover, the small size of EVs allows a better biodistribution, avoiding lung entrapment after systemic administration that cells encounter.

In the specific context of MI, the proposed local administration approach (***Chapter 3***) ensures that MSC-EVs are delivered were regeneration effort is more needed. The use of a natural 3D scaffold with hydrogel reduces EV leakage, creating a local high dose of bioactive EVs that allows reduction of total dose needed for treatment compared to a fluid formula for systemic/intravenous administration. Moreover, the human pericardial scaffold has been assessed already in the porcine preclinical model able to integrate in post-infarcted myocardium, promote nerve sprouting and neovascularization without triggering an adverse immune response (Gálvez-Montón et al. 2015). Therefore, the MSC-EV-embedded scaffold would integrate into the injured myocardium and provide a local niche for regeneration, with the structural traits of native tissue, for the EV-recruited endogenous pro-regenerative cells.

Although being still quite far away from clinical translation, one important point to consider while developing a new biological therapeutical product based on EVs embedded in a cardiac scaffold is its prospective standardization for the European Medicines Agency (EMA) approval. For that, classification within one of EMA's drug definitions is necessary to know the regulations that may apply. Following the flowchart and indications of EMA's committee for advanced therapies (CAT) (Committee for Advanced Therapies 2015), the presented construct (MSC-EVs combined with a cardiac decellularized scaffold and hydrogel) would be classified as a combined Advanced therapy medicinal product (ATMP) within the Tissue-engineered product (TEP) type: it consists on the combination of non-viable cells or tissues, but with active/immunological action; the cells are substantially manipulated (*ex vivo* culture and expansion, EV isolation) but are not genetically modified; it is intended for regeneration and repair, and has an active implantable medical device as an integral part (hydrogel). Therefore, the evaluation of the Quality, Safety, Efficacy, Pharmacovigilance and Environmental Risk Assessment (ERA) for combined ATMPs would apply. The main point that can be addressed at the current status of the experimental pipeline is the Quality aspects of the product (as summarized in **TABLE 7** on Appendices), which is mainly covered with non-clinical data, and for which the presented data may help.

Some of these Quality aspects are the structure, biological and physicochemical properties, specification of active substance(s) and impurities, stability and batch reproducibility of the product. The EV isolation method of choice may have a direct impact on all of these, as the high heterogeneity and physicochemical characteristics of EVs makes their purification complex. With this in mind, one of the main topics that were addressed in this thesis was the isolation of MSC-EVs and its impact on their functionality.

It was back in 2014 when Böing et al. resumed the use of SEC to isolate EVs from a biofluid. This methodology was actually already employed in the beginning of the EV field to demonstrate the existence of EV-enclosed proteins aside from the rest of soluble molecules (Pan and Johnstone 1983). Since then, our group has used and modified the published protocol (Böing et al. 2014) for optimized EV isolation from different biofluids: serum, urine, peritoneal effluent and cell culture conditioned medium (I. Lozano-Ramos et al. 2015; de Menezes-Neto et al. 2015; Carreras-Planella et al. 2017; Monguió-Tortajada, Roura, Gálvez-Montón, Pujal, et al. 2017). We were able to use this method to distinguish EV-associated proteins from rather soluble proteins (Roura,

Gálvez-Montón, de Gonzalo-Calvo, et al. 2017), that can misleadingly be associated to the EV preparation using other less stringent methods such as precipitation-based or ultracentrifugation methods. Also, the fact that SEC enables a more accurate EV purification allows novel biomarker screening that is not hindered by masking with the highly abundant soluble proteins (Roura et al. 2018; S. I. Lozano-Ramos et al. 2018; Carreras-Planella et al. 2017). This also applies when trying to unravel EV's genuinely functional capacities. As we presented in ***Chapter 2***, SEC allowed the purification of EVs that mimicked MSC's immunosuppressive functionality, while dUC did not. Furthermore, we also compared SEC to precipitating-based methods, demonstrating that it minimally alters the EV preparation (Gámez-Valero et al. 2016).

In terms of worldwide practice, the EV field is experiencing a subtle transition on the EV isolation method of choice. Besides ours, there are other works arguing also on the deficiencies of dUC: some have described its suboptimal performance in EV recovery and purity compared to SEC (Baranyai et al. 2015; D. D. Taylor and Shah 2015), others demonstrated the influence of dUC deficient standardization on efficiency (Momen-Heravi et al. 2012), and there is also evidence on dUC altering the intactness of EVs (Wiklander et al. 2018). Thus, although dUC is still the most commonly used (Gardiner et al. 2016), SEC is increasingly adopted and more widespread (**FIGURE 35** on Appendices). It is mainly employed as a combination method, like we described, with initial differential centrifugation steps to remove cells, debris and large vesicles, and ultrafiltration to manage sample volume.

In regard to the above-mentioned Quality aspects of EVs, we were able to determine their biological properties in both human and porcine samples, setting up analytical procedures that could be implemented as QC analysis of biological activity in the future. These have revealed the reasonable stability and reproducibility of SEC-EVs, given that they were able to promote similar immune suppressive effects both when human, fresh, single-MSC donor EV samples were used (***Chapter 2***) compared to porcine, frozen, pooled EV samples (***Chapter 3***). Also, we were able to demonstrate a great reduction on impurities of EVs when using SEC as isolation method, as it avoids the co-purification with soluble proteins. Therefore, it would ease active substance(s) recognition. Studies on the transcriptomic and proteomic profile of MSC-EVs would help unravel possible modes of action. There are a few candidate molecules that could mediate these beneficial effects, as EVs are enriched in specific membrane-bound and luminal protein cargo and protected bioactive mRNA/miRNA species compared to parental MSCs (Eirin et al. 2014, 2016). There are different examples of works denoting a clear prominent role of miRNAs mediating EV activity (Yáñez-Mó et al. 2015). Nevertheless, the majority of studies that have addressed this generally used EV products that were generated mainly by dUC and PEG-based precipitation, which, in light of our observations, makes extrapolation difficult. Therefore, this actually is an aspect that still remains unanswered, as we did not on look yet into the specific molecular mechanism of action of our MSC-EV preparation.

Besides this point, MSC-EVs and its administration within an engineered cardiac 3D scaffold has been validated *in vitro*, and indeed results indicated that it possesses very promising features for immune modulation and regeneration. Thus, its potential must be checked in a preclinical porcine model of MI to truly reveal whether EVs, as a cell-free product, are potent enough to mediate injury healing and alleviate cardiac remodelling to prospectively avoid heart failure. This study has already been designed and is currently on the experimental pipeline.

The findings presented in this thesis unravel new mechanisms used by MSCs for immune modulation and wound healing, a knowledge that can be used for the engineering of innovative, targeted and off-the-shelf therapeutic products.

CONCLUSIONS

A better understanding of the mechanisms for immunomodulation deployed by MSCs will help better define new biological therapies for tissue injury and regenerative medicine.

Chapter 1 – The upregulation of the adenosinergic pathway in human MSC-conditioned peripheral blood monocytes emerges as an additional potential mechanism supporting the long-lasting immunomodulatory and healing effects of MSCs delivery.

1.1. Both human UCMSC and cATMSC polarize allogeneic monocytes towards an anti-inflammatory M2-like phenotype and cytokine secretion profile.

1.2. CD39 is constitutively expressed in monocytes and maintained throughout short-term *in vitro* culture.

1.3. Both human UCMSC and cATMSC promote the upregulation of CD38 in co-cultured monocytes.

1.4. Both human UCMSC and cATMSC induce functionally active CD73 expression to monocytes in a contact-dependent manner. They do not when differentiated to MDDCs.

1.5. LPS stimulation of monocytes leads to increased CD73 expression, but only MSC co-culture leads to sustained expression and active 5'AMP hydrolysis/Adenosine production.

1.6. The local delivery of porcine cATMSC into post-infarcted swine myocardium synergistically results in the *in vivo* expression of CD73 by infiltrating monocytes. It does not occur in the absence of either cATMSCs or MI.

Chapter 2 – EV isolation based on SEC effectively purifies nanosized EVs responsible at least in part of the genuine MSC immunomodulatory capacities, highlighting the importance of purity and fine characterization of the EV product envisioned as a cell-free therapeutic approach to avoid unwanted inflammatory responses.

2.1. Human UCMSC are potent suppressors of allogeneic T cell proliferations and cytokine response already at low ratios (starting from 1:240 UCMSC:T cells).

2.2. IFNγ-priming induces class II MHC expression on UCMSC and does not increase their immune suppressive functions.

2.3. SEC-based procedure allows the separation of EVs from the bulk of protein found in UCMSC's CM. UCMSC-EVs bear the EV markers CD9, CD63 and the MSC markers CD73 and CD90 on their surface.

2.4. IFNγ-priming does not change EV production of UCMSCs but increments class I or II MHC presence in some UCMSC-EV batches.

2.5. NTA cannot distinguish EV-particles from protein-particles.

2.6. The SEC-purified EV fraction greatly abrogates polyclonal T cell proliferation and concomitantly inhibits the induction of cytokine production.

2.7. The non-EV fraction, CM and UC pellet do not inhibit T cell proliferation and result in inflammatory T cell response: IL6, TGFβ1 and IL17 production to foster Th17 polarization.

2.8. The SEC-EV fraction does not induce monocyte polarization nor cytokine response.

2.9. The non-EV SEC fraction induces the expression of CD163, CD206 and some production of TNFα by monocytes.

Chapter 3 – Biocompatible, cell-free cardiac grafts comprising MSC-derived EVs embedded in decellularized cardiac scaffolds may be useful for effective local administration of multifunctional MSC-EVs.

3.1. Porcine cATMSC-EVs isolated by SEC are nanovesicles that express CD63 and CD44.

3.2. Porcine cATMSC-EVs isolated by SEC reduce polyclonal proliferation of porcine allogeneic PBMCs and abrogate the production of pro-inflammatory cytokines (IFNγ, TNFα and IL12p40). They do not alter IL6 and IL8 production by stimulated PBMCs.

3.3. Porcine cATMSC-EVs isolated by SEC actively recruit allogeneic peripheral-blood derived OECs and cATMSCs in a dose-dependent manner.

3.4. Cardiac scaffolds generated by decellularization of myocardium or pericardium maintained their structure and ECM composition.

3.5. Presence of the cardiac scaffolds alone abrogates cytokine production of polyclonally-stimulated porcine PBMCs.

3.6. Pericardial scaffolds retain better porcine cATMSC-EVs than myocardial scaffolds.

3.7. Addition of cATMSC-EVs to any of the cardiac scaffolds induces IL6 production by polyclonally-stimulated porcine allogeneic PBMCs, while myocardial scaffolds leads to the additional increase in IL8, IFNγ and TNFα.

REFERENCES

REFERENCES

Aalberts, Marian, Federica M F van Dissel-Emiliani, Nick P H van Adrichem, Merel van Wijnen, Marca H M Wauben, Tom A E Stout, and Willem Stoorvogel. 2012. “Identification of Distinct Populations of Prostasomes That Differentially Express Prostate Stem Cell Antigen, Annexin A1, and GLIPR2 in Humans.” *Biology of Reproduction* 86 (3): 82. https://doi.org/10.1095/biolreprod.111.095760.

Adamiak, Marta, Guangming Cheng, Sylwia Bobis-Wozowicz, Lin Zhao, Sylwia Kedracka-Krok, Anweshan Samanta, Elzbieta Karnas, et al. 2018. “Induced Pluripotent Stem Cell (iPSC)–Derived Extracellular Vesicles Are Safer and More Effective for Cardiac Repair Than iPSCs Novelty and Significance.” *Circulation Research* 122 (2): 296–309. https://doi.org/10.1161/CIRCRESAHA.117.311769.

Aggarwal, Sudeepta, and Mark F Pittenger. 2005. “Human Mesenchymal Stem Cells Modulate Allogeneic Immune Cell Responses.” *Blood* 105 (4): 1815–22. https://doi.org/10.1182/blood-2004-04-1559.

Ahmed, Enas M. 2015. “Hydrogel: Preparation, Characterization, and Applications: A Review.” *Journal of Advanced Research* 6 (2): 105–21. https://doi.org/10.1016/J.JARE.2013.07.006.

Ahmed, Mohaned, Haneen A. Basheer, Jose M. Ayuso, Djevdet Ahmet, Marco Mazzini, Roshan Patel, Steven D. Shnyder, Victoria Vinader, and Kamyar Afarinkia. 2017. “Agarose Spot as a Comparative Method for in Situ Analysis of Simultaneous Chemotactic Responses to Multiple Chemokines.” *Scientific Reports* 7 (1): 1–11. https://doi.org/10.1038/s41598-017-00949-4.

Airas, L, J Niemelä, M Salmi, T Puurunen, D J Smith, and S Jalkanen. 1997. “Differential Regulation and Function of CD73, a Glycosyl-Phosphatidylinositol-Linked 70-kD Adhesion Molecule, on Lymphocytes and Endothelial Cells.” *The Journal of Cell Biology* 136 (2): 421–31. http://www.ncbi.nlm.nih.gov/pubmed/9015312.

Akiyama, Kentaro, Chider Chen, DanDan Wang, Xingtian Xu, Cunye Qu, Takayoshi Yamaza, Tao Cai, WanJun Chen, Lingyun Sun, and Songtao Shi. 2012. “Mesenchymal-Stem-Cell-Induced Immunoregulation Involves FAS-Ligand-/FAS-Mediated T Cell Apoptosis.” *Cell Stem Cell* 10 (5): 544–55. https://doi.org/10.1016/j.stem.2012.03.007.

Amarnath, Shoba, Jason E Foley, Don E Farthing, Ronald E Gress, Arian Laurence, Michael A Eckhaus, Jean-Yves Métais, et al. 2014. “Bone Marrow Derived Mesenchymal Stromal Cells Harness Purinergenic Signaling to Tolerize Human Th1 Cells In Vivo.” *Stem Cells (Dayton, Ohio)* 33 (4): 1–18. https://doi.org/10.1002/stem.1934.

Anderson, Charles F., Jeffrey S. Gerber, and David M. Mosser. 2002. “Modulating Macrophage Function with IgG Immune Complexes.” *Journal of Endotoxin Research* 8 (6): 477–81. https://doi.org/10.1177/09680519020080060501.

Anderson, Johnathon D, Henrik J Johansson, Calvin S Graham, Mattias Vesterlund, Missy T Pham, Charles S Bramlett, Elizabeth N Montgomery, et al. 2016. “Comprehensive Proteomic Analysis of Mesenchymal Stem Cell Exosomes Reveals Modulation of Angiogenesis via NFkB Signaling.” *Stem Cells (Dayton, Ohio)* 34 (3): 601–13. https://doi.org/10.1002/stem.2298.

Annunziato, Francesco, Lorenzo Cosmi, Francesco Liotta, Enrico Maggi, and Sergio Romagnani. 2008. “The Phenotype of Human Th17 Cells and Their Precursors, the Cytokines That Mediate Their Differentiation and the Role of Th17 Cells in Inflammation.” *International Immunology* 20 (11): 1361–68. https://doi.org/10.1093/intimm/dxn106.

Antonioli, Luca, Pál Pacher, E. Sylvester Vizi, and György Haskó. 2013. “CD39 and CD73 in

Immunity and Inflammation." *Trends in Molecular Medicine* 19 (6): 355–67. https://doi.org/10.1016/j.molmed.2013.03.005.

Asari, Sadaki, Shin Itakura, Kevin Ferreri, Chih-Pin Liu, Yoshikazu Kuroda, Fouad Kandeel, and Yoko Mullen. 2009. "Mesenchymal Stem Cells Suppress B-Cell Terminal Differentiation." *Experimental Hematology* 37 (5): 604–15. https://doi.org/10.1016/j.exphem.2009.01.005.

Augello, Andrea, Roberta Tasso, Simone Maria Negrini, Andrea Amateis, Francesco Indiveri, Ranieri Cancedda, and Giuseppina Pennesi. 2005. "Bone Marrow Mesenchymal Progenitor Cells Inhibit Lymphocyte Proliferation by Activation of the Programmed Death 1 Pathway." *European Journal of Immunology* 35 (5): 1482–90. https://doi.org/10.1002/eji.200425405.

Baranyai, Tamás, Kata Herczeg, Zsófia Onódi, István Voszka, Károly Módos, Nikolett Marton, György Nagy, et al. 2015. "Isolation of Exosomes from Blood Plasma: Qualitative and Quantitative Comparison of Ultracentrifugation and Size Exclusion Chromatography Methods." *PloS One* 10 (12): e0145686. https://doi.org/10.1371/journal.pone.0145686.

Bartholomew, Amelia, Cord Sturgeon, Mandy Siatskas, Karen Ferrer, Kevin McIntosh, Sheila Patil, Wayne Hardy, et al. 2002. "Mesenchymal Stem Cells Suppress Lymphocyte Proliferation in Vitro and Prolong Skin Graft Survival in Vivo." *Experimental Hematology* 30 (1): 42–48. http://www.ncbi.nlm.nih.gov/pubmed/11823036.

Bayes-Genis, A, S Roura, C Soler-Botija, J Farré, L Hove-Madsen, A Llach, and J Cinca. 2005. "Identification of Cardiomyogenic Lineage Markers in Untreated Human Bone Marrow-Derived Mesenchymal Stem Cells." *Transplantation Proceedings* 37 (9): 4077–79. https://doi.org/10.1016/j.transproceed.2005.09.103.

Bayes-Genis, Antoni, Carolina Soler-Botija, Jordi Farré, Pilar Sepúlveda, Angel Raya, Santiago Roura, Cristina Prat-Vidal, et al. 2010. "Human Progenitor Cells Derived from Cardiac Adipose Tissue Ameliorate Myocardial Infarction in Rodents." *Journal of Molecular and Cellular Cardiology* 49 (5). https://doi.org/10.1016/j.yjmcc.2010.08.010.

Beavis, Paul A, John Stagg, Phillip K Darcy, and Mark J Smyth. 2012. "CD73: A Potent Suppressor of Antitumor Immune Responses." *Trends in Immunology* 33 (5): 231–37. https://doi.org/10.1016/j.it.2012.02.009.

Ben-Mordechai, Tamar, Radka Holbova, Natalie Landa-Rouben, Tamar Harel-Adar, Micha S Feinberg, Ihab Abd Elrahman, Galia Blum, et al. 2013. "Macrophage Subpopulations Are Essential for Infarct Repair with and without Stem Cell Therapy." *Journal of the American College of Cardiology* 62 (20): 1890–1901. https://doi.org/10.1016/j.jacc.2013.07.057.

Benvenuto, Federica, Stefania Ferrari, Ezio Gerdoni, Francesca Gualandi, Francesco Frassoni, Vito Pistoia, Gianluigi Mancardi, and Antonio Uccelli. 2007. "Human Mesenchymal Stem Cells Promote Survival of T Cells in a Quiescent State." *Stem Cells (Dayton, Ohio)* 25 (7): 1753–60. https://doi.org/10.1634/stemcells.2007-0068.

Benvenuto, Federica, Adriana Voci, Enrico Carminati, Francesca Gualandi, Gianluigi Mancardi, Antonio Uccelli, and Laura Vergani. 2015. "Human Mesenchymal Stem Cells Target Adhesion Molecules and Receptors Involved in T Cell Extravasation." *Stem Cell Research & Therapy* 6 (December): 245. https://doi.org/10.1186/s13287-015-0222-y.

Benwell, Risa K, and David R Lee. 2010. "Essential and Synergistic Roles of IL1 and IL6 in Human Th17 Differentiation Directed by TLR Ligand-Activated Dendritic Cells." *Clinical Immunology (Orlando, Fla.)* 134 (2): 178–87. https://doi.org/10.1016/j.clim.2009.09.013.

Berenguer, Jordi, Tonny Lagerweij, Xi Wen Zhao, Sophie Dusoswa, Petra van der Stoop, Bart Westerman, Mark C. de Gooijer, et al. 2018. "Glycosylated Extracellular Vesicles Released by Glioblastoma Cells Are Decorated by CCL18 Allowing for Cellular Uptake via Chemokine

Receptor CCR8." *Journal of Extracellular Vesicles* 7 (1): 1446660. https://doi.org/10.1080/20013078.2018.1446660.

Berry, Mark F., Y. Joseph Woo, Timothy J. Pirolli, Lawrence T. Bish, Mireille A. Moise, Jeffrey W. Burdick, Kevin J. Morine, Vasant Jayasankar, Timothy J. Gardner, and H. Lee Sweeney. 2004. "Administration of a Tumor Necrosis Factor Inhibitor at the Time of Myocardial Infarction Attenuates Subsequent Ventricular Remodeling." *The Journal of Heart and Lung Transplantation* 23 (9): 1061–68. https://doi.org/10.1016/J.HEALUN.2004.06.021.

Blanc, K Le, L Tammik, B Sundberg, S E Haynesworth, and O Ringdén. 2003. "Mesenchymal Stem Cells Inhibit and Stimulate Mixed Lymphocyte Cultures and Mitogenic Responses Independently of the Major Histocompatibility Complex." *Scandinavian Journal of Immunology* 57 (1): 11–20. http://www.ncbi.nlm.nih.gov/pubmed/12542793.

Blanc, Katarina Le, and Dimitrios Mougiakakos. 2012. "Multipotent Mesenchymal Stromal Cells and the Innate Immune System." *Nature Reviews Immunology* 12 (5): 383–96. https://doi.org/10.1038/nri3209.

Blanc, Katarina Le, Ida Rasmusson, Berit Sundberg, Cecilia Götherström, Moustapha Hassan, Mehmet Uzunel, and Olle Ringdén. 2004. "Treatment of Severe Acute Graft-versus-Host Disease with Third Party Haploidentical Mesenchymal Stem Cells." *Lancet* 363 (9419): 1439–41. https://doi.org/10.1016/S0140-6736(04)16104-7.

Blázquez, Rebeca, Francisco Miguel Sánchez-Margallo, Verónica Álvarez, Alejandra Usón, and Javier G. Casado. 2016. "Surgical Meshes Coated with Mesenchymal Stem Cells Provide an Anti-Inflammatory Environment by a M2 Macrophage Polarization." *Acta Biomaterialia* 31 (February): 221–30. https://doi.org/10.1016/j.actbio.2015.11.057.

Blázquez, Rebeca, Francisco Miguel Sánchez-Margallo, Verónica Crisóstomo, Claudia Báez, Juan Maestre, Verónica Álvarez, and Javier G. Casado. 2016. "Intrapericardial Delivery of Cardiosphere-Derived Cells: An Immunological Study in a Clinically Relevant Large Animal Model." Edited by Maria Cristina Vinci. *PLOS ONE* 11 (2): e0149001. https://doi.org/10.1371/journal.pone.0149001.

Boag, Stephen E., Emanuele Andreano, and Ioakim Spyridopoulos. 2016. "Lymphocyte Communication in Myocardial Ischemia/Reperfusion Injury." *Antioxidants & Redox Signaling* 26 (12): ars.2016.6940. https://doi.org/10.1089/ars.2016.6940.

Bobrie, Angélique, Marina Colombo, Sophie Krumeich, Graça Raposo, and Clotilde Théry. 2012. "Diverse Subpopulations of Vesicles Secreted by Different Intracellular Mechanisms Are Present in Exosome Preparations Obtained by Differential Ultracentrifugation." *Journal of Extracellular Vesicles* 1 (1): 18397. https://doi.org/10.3402/jev.v1i0.18397.

Böing, Anita N, Edwin van der Pol, Anita E Grootemaat, Frank A W Coumans, Auguste Sturk, and Rienk Nieuwland. 2014. "Single-Step Isolation of Extracellular Vesicles by Size-Exclusion Chromatography." *Journal of Extracellular Vesicles* 3 (January). https://doi.org/10.3402/jev.v3.23430.

Bönner, Florian, Nadine Borg, Sandra Burghoff, and Jürgen Schrader. 2012. "Resident Cardiac Immune Cells and Expression of the Ectonucleotidase Enzymes CD39 and CD73 after Ischemic Injury." Edited by Holger K. Eltzschig. *PLoS ONE* 7 (4): e34730. https://doi.org/10.1371/journal.pone.0034730.

Booth, Amy M., Yi Fang, Jonathan K. Fallon, Jr-Ming Yang, James E.K. Hildreth, and Stephen J. Gould. 2006. "Exosomes and HIV Gag Bud from Endosome-like Domains of the T Cell Plasma Membrane." *The Journal of Cell Biology* 172 (6): 923–35. https://doi.org/10.1083/jcb.200508014.

Broughton, Kathleen M, Bingyan J Wang, Fareheh Firouzi, Farid Khalafalla, Stefanie Dimmeler, Francisco Fernandez-Aviles, and Mark A Sussman. 2018. “Mechanisms of Cardiac Repair and Regeneration.” *Circulation Research* 122 (8): 1151–63. https://doi.org/10.1161/CIRCRESAHA.117.312586.

Brown, Markus, Louise A Johnson, Dario A Leone, Peter Majek, Kari Vaahtomeri, Daniel Senfter, Nora Bukosza, et al. 2018. “Lymphatic Exosomes Promote Dendritic Cell Migration along Guidance Cues.” *The Journal of Cell Biology* 217 (6): 2205–21. https://doi.org/10.1083/jcb.201612051.

Calle, Alexandra, Clara Barrajón-Masa, Ernesto Gómez-Fidalgo, Mercedes Martín-Lluch, Paloma Cruz-Vigo, Raúl Sánchez-Sánchez, and Miguel Ángel Ramírez. 2018. “Iberian Pig Mesenchymal Stem/stromal Cells from Dermal Skin, Abdominal and Subcutaneous Adipose Tissues, and Peripheral Blood: In Vitro Characterization and Migratory Properties in Inflammation.” *Stem Cell Research & Therapy* 9 (1): 178. https://doi.org/10.1186/s13287-018-0933-y.

Caplan, Arnold I. 2017. “Mesenchymal Stem Cells: Time to Change the Name!” *Stem Cells Translational Medicine* 6 (6): 1445–51. https://doi.org/10.1002/sctm.17-0051.

Carreras-Planella, Laura, Jordi Soler-Majoral, Cristina Rubio-Esteve, Sara Inés Lozano-Ramos, Marcella Franquesa, Josep Bonet, Maria Isabel Troya-Saborido, and Francesc Enric Borràs. 2017. “Characterization and Proteomic Profile of Extracellular Vesicles from Peritoneal Dialysis Efflux.” Edited by Tatsuo Shimosawa. *PLOS ONE* 12 (5): e0176987. https://doi.org/10.1371/journal.pone.0176987.

Carter-Monroe, Naima, Elena Ladich, Renu Virmani, and Frank D. Kolodgie. 2010. “Histopathologic Assessment of Myocardial Regeneration.” In *Methods in Molecular Biology (Clifton, N.J.)*, 660:125–48. https://doi.org/10.1007/978-1-60761-705-1_9.

Chan, Jennifer L, Katherine C Tang, Anoop P Patel, Larissa M Bonilla, Nicola Pierobon, Nicholas M Ponzio, and Pranela Rameshwar. 2006. “Antigen-Presenting Property of Mesenchymal Stem Cells Occurs during a Narrow Window at Low Levels of Interferon-Gamma.” *Blood* 107 (12): 4817–24. https://doi.org/10.1182/blood-2006-01-0057.

Chatterjee, D., D. M. Tufa, H. Baehre, R. Hass, R. E. Schmidt, and R. Jacobs. 2014. “Natural Killer Cells Acquire CD73 Expression upon Exposure to Mesenchymal Stem Cells.” *Blood* 123 (4): 594–95. https://doi.org/10.1182/blood-2013-09-524827.

Chawla, Ajay. 2010. “Control of Macrophage Activation and Function by PPARs.” *Circulation Research* 106 (10): 1559–69. https://doi.org/10.1161/CIRCRESAHA.110.216523.

Chen, Ke, Ding Wang, Wei Ting Du, Zhi-Bo Han, He Ren, Ying Chi, Shao Guang Yang, Delin Zhu, Francis Bayard, and Zhong Chao Han. 2010. “Human Umbilical Cord Mesenchymal Stem Cells hUC-MSCs Exert Immunosuppressive Activities through a PGE2-Dependent Mechanism.” *Clinical Immunology (Orlando, Fla.)* 135 (3): 448–58. https://doi.org/10.1016/j.clim.2010.01.015.

Chen, P.-M., K.-J. Liu, P.-J. Hsu, C.-F. Wei, C.-H. Bai, L.-J. Ho, H.-K. Sytwu, and B. L. Yen. 2014. “Induction of Immunomodulatory Monocytes by Human Mesenchymal Stem Cell-Derived Hepatocyte Growth Factor through ERK1/2.” *Journal of Leukocyte Biology* 96 (2): 295–303. https://doi.org/10.1189/jlb.3A0513-242R.

Chiesa, S, S Morbelli, S Morando, M Massollo, C Marini, A Bertoni, F Frassoni, et al. 2011. “Mesenchymal Stem Cells Impair in Vivo T-Cell Priming by Dendritic Cells.” *Proceedings of the National Academy of Sciences* 108 (42): 17384–89. https://doi.org/10.1073/pnas.1103650108.

Chiossone, Laura, Romana Conte, Grazia Maria Spaggiari, Martina Serra, Cristina Romei, Francesca Bellora, Flavio Becchetti, Antonio Andaloro, Lorenzo Moretta, and Cristina Bottino. 2016. "Mesenchymal Stromal Cells Induce Peculiar Alternatively Activated Macrophages Capable of Dampening Both Innate and Adaptive Immune Responses." *STEM CELLS* 34 (7): 1909–21. https://doi.org/10.1002/stem.2369.

Choi, H., R. H. Lee, N. Bazhanov, J. Y. Oh, and D. J. Prockop. 2011. "Anti-Inflammatory Protein TSG-6 Secreted by Activated MSCs Attenuates Zymosan-Induced Mouse Peritonitis by Decreasing TLR2/NF- B Signaling in Resident Macrophages." *Blood* 118 (2): 330–38. https://doi.org/10.1182/blood-2010-12-327353.

Christia, Panagiota, and Nikolaos G. Frangogiannis. 2013. "Targeting Inflammatory Pathways in Myocardial Infarction." *European Journal of Clinical Investigation* 43 (9): 986–95. https://doi.org/10.1080/10810730902873927.Testing.

Clayton, Aled, Saly Al-Taei, Jason Webber, Malcolm D Mason, and Zsuzsanna Tabi. 2011. "Cancer Exosomes Express CD39 and CD73, Which Suppress T Cells through Adenosine Production." *The Journal of Immunology* 187 (2): 676–83. https://doi.org/10.4049/jimmunol.1003884.

Colombo, Marina, Catarina Moita, Guillaume van Niel, Joanna Kowal, James Vigneron, Philippe Benaroch, Nicolas Manel, Luis F Moita, Clotilde Théry, and Graça Raposo. 2013. "Analysis of ESCRT Functions in Exosome Biogenesis, Composition and Secretion Highlights the Heterogeneity of Extracellular Vesicles." *Journal of Cell Science* 126: 5553–65. https://doi.org/10.1242/jcs.128868.

Colombo, Marina, Graça Raposo, and Clotilde Théry. 2014. "Biogenesis, Secretion, and Intercellular Interactions of Exosomes and Other Extracellular Vesicles." *Annual Review of Cell and Developmental Biology* 30: 255–89. https://doi.org/10.1146/annurev-cellbio-101512-122326.

Colvin, M., J. M. Smith, M. A. Skeans, L. B. Edwards, K. Uccellini, J. J. Snyder, A. K. Israni, and B. L. Kasiske. 2017. "OPTN/SRTR 2015 Annual Data Report: Heart." *American Journal of Transplantation* 17 (January): 286–356. https://doi.org/10.1111/ajt.14128.

Committee for Advanced Therapies. 2015. "Reflection Paper on Classification of Advanced Therapy Medicinal Products." London, UK: European Medicines Agency (EMA). http://www.ema.europa.eu/docs/en_GB/document_library/Scientific_guideline/2015/06/WC500187744.pdf.

Comoli, Patrizia, Fabrizio Ginevri, Rita Maccario, Maria Antonietta Avanzini, Massimo Marconi, Antonella Groff, Angela Cometa, et al. 2008. "Human Mesenchymal Stem Cells Inhibit Antibody Production Induced in Vitro by Allostimulation." *Nephrology, Dialysis, Transplantation: Official Publication of the European Dialysis and Transplant Association - European Renal Association* 23 (4): 1196–1202. https://doi.org/10.1093/ndt/gfm740.

Conforti, Antonella, Marco Scarsella, Nadia Starc, Ezio Giorda, Simone Biagini, Alessandra Proia, Rita Carsetti, Franco Locatelli, and Maria Ester Bernardo. 2014. "Microvescicles Derived from Mesenchymal Stromal Cells Are Not as Effective as Their Cellular Counterpart in the Ability to Modulate Immune Responses In Vitro." *Stem Cells and Development*. https://doi.org/10.1089/scd.2014.0091.

Crapo, Peter M., Thomas W. Gilbert, and Stephen F. Badylak. 2011. "An Overview of Tissue and Whole Organ Decellularization Processes." *Biomaterials* 32 (12): 3233–43. https://doi.org/10.1016/j.biomaterials.2011.01.057.

Crop, Meindert J, Carla C Baan, Sander S Korevaar, Jan N M Ijzermans, Willem Weimar, and Martin J Hoogduijn. 2010. "Human Adipose Tissue-Derived Mesenchymal Stem Cells Induce Explosive T-Cell Proliferation." *Stem Cells and Development* 19 (12): 1843–53.

https://doi.org/10.1089/scd.2009.0368.

Csóka, Balázs, Zsolt Selmeczy, Balázs Koscsó, Zoltán H Németh, Pál Pacher, Peter J Murray, Diane Kepka-Lenhart, et al. 2012. "Adenosine Promotes Alternative Macrophage Activation via A2A and A2B Receptors." *FASEB Journal : Official Publication of the Federation of American Societies for Experimental Biology* 26 (1): 376–86. https://doi.org/10.1096/fj.11-190934.

Curtis, Matthew W, and Brenda Russell. 2009. "Cardiac Tissue Engineering." *The Journal of Cardiovascular Nursing* 24 (2): 87–92. https://doi.org/10.1097/01.JCN.0000343562.06614.49.

Cutler, Antony J, Vasanti Limbani, John Girdlestone, and Cristina V Navarrete. 2010. "Umbilical Cord-Derived Mesenchymal Stromal Cells Modulate Monocyte Function to Suppress T Cell Proliferation." *The Journal of Immunology* 185 (11): 6617–23. https://doi.org/10.4049/jimmunol.1002239.

Cvjetkovic, Aleksander, Jan Lötvall, and Cecilia Lässer. 2014. "The Influence of Rotor Type and Centrifugation Time on the Yield and Purity of Extracellular Vesicles." *Journal of Extracellular Vesicles* 3 (1): 23111. https://doi.org/10.3402/jev.v3.23111.

Davies, Lindsay C., Nina Heldring, Nadir Kadri, and Katarina Le Blanc. 2017. "Mesenchymal Stromal Cell Secretion of Programmed Death-1 Ligands Regulates T Cell Mediated Immunosuppression." *STEM CELLS* 35 (3): 766–76. https://doi.org/10.1002/stem.2509.

Dayan, Victor, Gustavo Yannarelli, Filio Billia, Paola Filomeno, Xing-Hua Wang, John E. Davies, and Armand Keating. 2011. "Mesenchymal Stromal Cells Mediate a Switch to Alternatively Activated Monocytes/macrophages after Acute Myocardial Infarction." *Basic Research in Cardiology* 106 (6): 1299–1310. https://doi.org/10.1007/s00395-011-0221-9.

Deaglio, Silvia, Karen M Dwyer, Wenda Gao, David Friedman, Anny Usheva, Anna Erat, Jiang-Fan Chen, et al. 2007. "Adenosine Generation Catalyzed by CD39 and CD73 Expressed on Regulatory T Cells Mediates Immune Suppression." *The Journal of Experimental Medicine* 204 (6): 1257–65. https://doi.org/10.1084/jem.20062512.

Deng, Wei, Weiwei Chen, Zhuoya Zhang, Saisai Huang, Wei Kong, Yue Sun, Xiaojun Tang, et al. 2015. "Mesenchymal Stem Cells Promote CD206 Expression and Phagocytic Activity of Macrophages through IL-6 in Systemic Lupus Erythematosus." *Clinical Immunology (Orlando, Fla.)* 161 (2): 209–16. https://doi.org/10.1016/j.clim.2015.07.011.

Deng, Yinan, Yingcai Zhang, Linsen Ye, Tong Zhang, Jintao Cheng, Guihua Chen, Qi Zhang, and Yang Yang. 2016. "Umbilical Cord-Derived Mesenchymal Stem Cells Instruct Monocytes Towards an IL10-Producing Phenotype by Secreting IL6 and HGF." *Scientific Reports* 6 (1): 37566. https://doi.org/10.1038/srep37566.

Deun, Jan Van, Pieter Mestdagh, Patrizia Agostinis, Özden Akay, Sushma Anand, Jasper Anckaert, Zoraida Andreu Martinez, et al. 2017. "EV-TRACK: Transparent Reporting and Centralizing Knowledge in Extracellular Vesicle Research." *Nature Methods* 14 (3): 228–32. https://doi.org/10.1038/nmeth.4185.

Dewald, O. 2005. "CCL2/Monocyte Chemoattractant Protein-1 Regulates Inflammatory Responses Critical to Healing Myocardial Infarcts." *Circulation Research* 96 (8): 881–89. https://doi.org/10.1161/01.RES.0000163017.13772.3a.

Dhandayuthapani, Brahatheeswaran, Yasuhiko Yoshida, Toru Maekawa, and D. Sakthi Kumar. 2011. "Polymeric Scaffolds in Tissue Engineering Application: A Review." *International Journal of Polymer Science* 2011 (September): 1–19. https://doi.org/10.1155/2011/290602.

Djouad, Farida, Louis-Marie Charbonnier, Carine Bouffi, Pascale Louis-Plence, Claire Bony,

Florence Apparailly, Céline Cantos, Christian Jorgensen, and Danièle Noël. 2007. "Mesenchymal Stem Cells Inhibit the Differentiation of Dendritic Cells Through an Interleukin-6-Dependent Mechanism." *Stem Cells* 25 (8): 2025–32. https://doi.org/10.1634/stemcells.2006-0548.

Dobaczewski, Marcin, Ying Xia, Marcin Bujak, Carlos Gonzalez-Quesada, and Nikolaos G. Frangogiannis. 2010. "CCR5 Signaling Suppresses Inflammation and Reduces Adverse Remodeling of the Infarcted Heart, Mediating Recruitment of Regulatory T Cells." *The American Journal of Pathology* 176 (5): 2177–87. https://doi.org/10.2353/ajpath.2010.090759.

Dominici, M, K Le Blanc, I Mueller, I Slaper-Cortenbach, Fc Marini, Ds Krause, Rj Deans, A Keating, Dj Prockop, and Em Horwitz. 2006. "Minimal Criteria for Defining Multipotent Mesenchymal Stromal Cells. The International Society for Cellular Therapy Position Statement." *Cytotherapy* 8 (4): 315–17. https://doi.org/10.1080/14653240600855905.

Duan, Bin. 2017. "State-of-the-Art Review of 3D Bioprinting for Cardiovascular Tissue Engineering." *Annals of Biomedical Engineering* 45 (1): 195–209. https://doi.org/10.1007/s10439-016-1607-5.

Dyer, D. P., J. M. Thomson, A. Hermant, T. A. Jowitt, T. M. Handel, A. E. I. Proudfoot, A. J. Day, and C. M. Milner. 2014. "TSG-6 Inhibits Neutrophil Migration via Direct Interaction with the Chemokine CXCL8." *The Journal of Immunology* 192 (5): 2177–85. https://doi.org/10.4049/jimmunol.1300194.

Eggenhofer, Elke, V Benseler, A Kroemer, F C Popp, E K Geissler, H J Schlitt, C C Baan, M H Dahlke, and M J Hoogduijn. 2012. "Mesenchymal Stem Cells Are Short-Lived and Do Not Migrate beyond the Lungs after Intravenous Infusion." *Frontiers in Immunology* 3 (January): 297. https://doi.org/10.3389/fimmu.2012.00297.

Eichin, Dominik, Juha P Laurila, Sirpa Jalkanen, and Marko Salmi. 2015. "CD73 Activity Is Dispensable for the Polarization of M2 Macrophages." *PloS One* 10 (8): e0134721. https://doi.org/10.1371/journal.pone.0134721.

Eirin, Alfonso, Scott M. Riester, Xiang-Yang Zhu, Hui Tang, Jared M. Evans, Daniel O'Brien, Andre J. van Wijnen, and Lilach O. Lerman. 2014. "MicroRNA and mRNA Cargo of Extracellular Vesicles from Porcine Adipose Tissue-Derived Mesenchymal Stem Cells." *Gene* 551 (1): 55–64. https://doi.org/10.1016/j.gene.2014.08.041.

Eirin, Alfonso, Xiang-Yang Zhu, Amrutesh S. Puranik, John R. Woollard, Hui Tang, Surendra Dasari, Amir Lerman, Andre J. van Wijnen, and Lilach O. Lerman. 2016. "Comparative Proteomic Analysis of Extracellular Vesicles Isolated from Porcine Adipose Tissue-Derived Mesenchymal Stem/stromal Cells." *Scientific Reports* 6 (1): 36120. https://doi.org/10.1038/srep36120.

Eltzschig, H. K., Linda F Thompson, Jorn Karhausen, Richard J Cotta, Juan C Ibla, Simon C Robson, and Sean P Colgan. 2004. "Endogenous Adenosine Produced during Hypoxia Attenuates Neutrophil Accumulation: Coordination by Extracellular Nucleotide Metabolism." *Blood* 104 (13): 3986–92. https://doi.org/10.1182/blood-2004-06-2066.

Engela, A U, C C Baan, N H R Litjens, M Franquesa, M G H Betjes, W Weimar, and M J Hoogduijn. 2013. "Mesenchymal Stem Cells Control Alloreactive CD8(+) CD28(-) T Cells." *Clinical and Experimental Immunology* 174 (3): 449–58. https://doi.org/10.1111/cei.12199.

Engela, A U, M J Hoogduijn, K Boer, N H R Litjens, M G H Betjes, W Weimar, and C C Baan. 2013. "Human Adipose-Tissue Derived Mesenchymal Stem Cells Induce Functional de-Novo Regulatory T Cells with Methylated FOXP3 Gene DNA." *Clinical and Experimental Immunology* 173 (2): 343–54. https://doi.org/10.1111/cei.12120.

English, K., J. M. Ryan, L. Tobin, M. J. Murphy, F. P. Barry, and B. P. Mahon. 2009. “Cell Contact, Prostaglandin E $_2$ and Transforming Growth Factor Beta 1 Play Non-Redundant Roles in Human Mesenchymal Stem Cell Induction of CD4 $^+$ CD25 ^{High} Forkhead Box P3 $^+$ Regulatory T Cells.” *Clinical & Experimental Immunology* 156 (1): 149–60. https://doi.org/10.1111/j.1365-2249.2009.03874.x.

English, Karen, Frank P. Barry, Ciara P. Field-Corbett, and Bernard P. Mahon. 2007. “IFN-γ and TNF-α Differentially Regulate Immunomodulation by Murine Mesenchymal Stem Cells.” *Immunology Letters* 110 (2): 91–100. https://doi.org/10.1016/j.imlet.2007.04.001.

English, Karen, Frank P. Barry, and Bernard P. Mahon. 2008. “Murine Mesenchymal Stem Cells Suppress Dendritic Cell Migration, Maturation and Antigen Presentation.” *Immunology Letters* 115 (1): 50–58. https://doi.org/10.1016/j.imlet.2007.10.002.

Erdmann, Andreas A, Zhan-Guo Gao, Unsu Jung, Jason Foley, Todd Borenstein, Kenneth A Jacobson, and Daniel H Fowler. 2005. “Activation of Th1 and Tc1 Cell Adenosine A2A Receptors Directly Inhibits IL-2 Secretion in Vitro and IL-2-Driven Expansion in Vivo.” *Blood* 105 (12): 4707–14. https://doi.org/10.1182/blood-2004-04-1407.

Fais, Stefano, Lorraine O’Driscoll, Francesc E Borras, Edit Buzas, Giovanni Camussi, Francesco Cappello, Joana Carvalho, et al. 2016. “Evidence-Based Clinical Use of Nanoscale Extracellular Vesicles in Nanomedicine.” *ACS Nano*, March. https://doi.org/10.1021/acsnano.5b08015.

Fallarino, F, U Grohmann, C Vacca, R Bianchi, C Orabona, A Spreca, M C Fioretti, and P Puccetti. 2002. “T Cell Apoptosis by Tryptophan Catabolism.” *Cell Death and Differentiation* 9 (10): 1069–77. https://doi.org/10.1038/sj.cdd.4401073.

Fischer, Uwe M, Matthew T Harting, Fernando Jimenez, Werner O Monzon-Posadas, Hasen Xue, Sean I Savitz, Glen A Laine, and Charles S Cox. 2009. “Pulmonary Passage Is a Major Obstacle for Intravenous Stem Cell Delivery: The Pulmonary First-Pass Effect.” *Stem Cells and Development* 18 (5): 683–92. https://doi.org/10.1089/scd.2008.0253.

François, Moïra, Raphaëlle Romieu-Mourez, Mengyang Li, and Jacques Galipeau. 2012. “Human MSC Suppression Correlates with Cytokine Induction of Indoleamine 2,3-Dioxygenase and Bystander M2 Macrophage Differentiation.” *Molecular Therapy: The Journal of the American Society of Gene Therapy* 20 (1): 187–95. https://doi.org/10.1038/mt.2011.189.

Frangogiannis, Nikolaos G., C.Wayne Smith, and Mark L Entman. 2002. “The Inflammatory Response in Myocardial Infarction.” *Cardiovascular Research* 53 (1): 31–47. https://doi.org/10.1016/S0008-6363(01)00434-5.

Frangogiannis, Nikolaos G. 2014a. “The Immune System and the Remodeling Infarcted Heart: Cell Biological Insights and Therapeutic Opportunities.” *Journal of Cardiovascular Pharmacology* 63 (3): 185–95. https://doi.org/10.1097/FJC.0000000000000003.The.

Frangogiannis, Nikolaos G. 2014b. “The Inflammatory Response in Myocardial Injury, Repair and Remodelling.” *Nature Reviews Cardiology* 11 (5): 255–65. https://doi.org/10.1038/nrcardio.2014.28.

Franquesa, M., F. K. Mensah, R. Huizinga, T. Strini, L. Boon, E. Lombardo, O. DelaRosa, et al. 2015. “Human Adipose Tissue-Derived Mesenchymal Stem Cells Abrogate Plasmablast Formation and Induce Regulatory B Cells Independently of T Helper Cells.” *STEM CELLS* 33 (3): 880–91. https://doi.org/10.1002/stem.1881.

Franquesa, Marcella, Martin J Hoogduijn, Elia Ripoll, Franka Luk, Mahdi Salih, Michiel G H Betjes, Juan Torras, Carla C Baan, Josep M Grinyó, and Ana Maria Merino. 2014. “Update on Controls for Isolation and Quantification Methodology of Extracellular Vesicles Derived

from Adipose Tissue Mesenchymal Stem Cells." *Frontiers in Immunology* 5. https://doi.org/10.3389/fimmu.2014.00525.

Frantz, Stefan, Johann Bauersachs, and Ralph A Kelly. 2005. "Innate Immunity and the Heart." *Current Pharmaceutical Design* 11 (10): 1279–90. http://www.ncbi.nlm.nih.gov/pubmed/15853684.

Franzoni, Giulia, Piero Bonelli, Simon Paul Graham, Antonio Giovanni Anfossi, Silvia Dei Giudici, Giovannantonio Pilo, Marco Pittau, Paola Nicolussi, and Annalisa Oggiano. 2017. "Comparative Phenotypic and Functional Analyses of the Effects of Autologous Plasma and Recombinant Human Macrophage-Colony Stimulating Factor (M-CSF) on Porcine Monocyte to Macrophage Differentiation." *Veterinary Immunology and Immunopathology* 187 (April): 80–88. https://doi.org/10.1016/j.vetimm.2017.04.006.

Gálvez-Montón, Carolina, Ramon Bragós, Carolina Soler-Botija, Idoia Díaz-Güemes, Cristina Prat-Vidal, Verónica Crisóstomo, Francisco M. Sánchez-Margallo, et al. 2017. "Noninvasive Assessment of an Engineered Bioactive Graft in Myocardial Infarction: Impact on Cardiac Function and Scar Healing." *STEM CELLS Translational Medicine* 6 (2): 647–55. https://doi.org/10.5966/sctm.2016-0063.

Gálvez-Montón, Carolina, M. Teresa Fernandez-Figueras, Mercè Martí, Carolina Soler-Botija, Santiago Roura, Isaac Perea-Gil, Cristina Prat-Vidal, Aida Llucià-Valldeperas, Ángel Raya, and Antoni Bayes-Genis. 2015. "Neoinnervation and Neovascularization of Acellular Pericardial-Derived Scaffolds in Myocardial Infarcts." *Stem Cell Research & Therapy* 6 (1): 108. https://doi.org/10.1186/s13287-015-0101-6.

Gálvez-Montón, Carolina, Carolina Soler-Botija, Oriol Iborra-Egea, Idoia Díaz-Güemes, Mercè Martí, Olalla Iglesias-García, Cristina Prat-Vidal, et al. 2017. "Preclinical Safety Evaluation of Allogeneic Induced Pluripotent Stem Cell-Based Therapy in a Swine Model of Myocardial Infarction." *Tissue Engineering. Part C, Methods* 23 (11): 736–44. https://doi.org/10.1089/ten.TEC.2017.0156.

Gámez-Valero, Ana, Marta Monguió-Tortajada, Laura Carreras-Planella, Marcella Franquesa, Katrin Beyer, and Francesc E Borràs. 2016. "Size-Exclusion Chromatography-Based Isolation Minimally Alters Extracellular Vesicles' Characteristics Compared to Precipitating Agents." *Scientific Reports* 6: 33641. https://doi.org/10.1038/srep33641.

Gardiner, Chris, Dolores Di Vizio, Susmita Sahoo, Clotilde Théry, Kenneth W Witwer, Marca Wauben, and Andrew F Hill. 2016. "Techniques Used for the Isolation and Characterization of Extracellular Vesicles: Results of a Worldwide Survey." *Journal of Extracellular Vesicles* 5: 32945. http://www.ncbi.nlm.nih.gov/pubmed/27802845.

Gaspar, H. Bobby, Alessandro Aiuti, Fulvio Porta, Fabio Candotti, Michael S. Hershfield, and Luigi D. Notarangelo. 2009. "How I Treat ADA Deficiency." *Blood* 114 (17).

Gatti, Stefano, Stefania Bruno, Maria Chiara Deregibus, Andrea Sordi, Vincenzo Cantaluppi, Ciro Tetta, and Giovanni Camussi. 2011. "Microvesicles Derived from Human Adult Mesenchymal Stem Cells Protect against Ischaemia-Reperfusion-Induced Acute and Chronic Kidney Injury." *Nephrology, Dialysis, Transplantation: Official Publication of the European Dialysis and Transplant Association - European Renal Association* 26 (5): 1474–83. https://doi.org/10.1093/ndt/gfr015.

Ge, W, J Jiang, M L Baroja, J Arp, R Zassoko, W Liu, A Bartholomew, B Garcia, and H Wang. 2009. "Infusion of Mesenchymal Stem Cells and Rapamycin Synergize to Attenuate Alloimmune Responses and Promote Cardiac Allograft Tolerance." *American Journal of Transplantation* 9 (8): 1760–72. https://doi.org/10.1111/j.1600-6143.2009.02721.x.

Ge, Wei, Jifu Jiang, Jacqueline Arp, Weihua Liu, Bertha Garcia, and Hao Wang. 2010. "Regulatory

T-Cell Generation and Kidney Allograft Tolerance Induced by Mesenchymal Stem Cells Associated with Indoleamine 2,3-Dioxygenase Expression." *Transplantation* 90 (12): 1312–20. https://doi.org/10.1097/TP.0b013e3181fed001.

Gerhardt, Teresa, and Klaus Ley. 2015. "Monocyte Trafficking across the Vessel Wall." *Cardiovascular Research* 107 (3): 321–30. https://doi.org/10.1093/cvr/cvv147.

Ghannam, Soufiane, Jérôme Pène, Gabriel Moquet-Torcy, Gabriel Torcy-Moquet, Christian Jorgensen, and Hans Yssel. 2010. "Mesenchymal Stem Cells Inhibit Human Th17 Cell Differentiation and Function and Induce a T Regulatory Cell Phenotype." *Journal of Immunology (Baltimore, Md. : 1950)* 185 (1): 302–12. https://doi.org/10.4049/jimmunol.0902007.

Gholizadeh, Shima, Mohamed Shehata Draz, Maryam Zarghooni, Amir Sanati-Nezhad, Saeid Ghavami, Hadi Shafiee, and Mohsen Akbari. 2017. "Microfluidic Approaches for Isolation, Detection, and Characterization of Extracellular Vesicles: Current Status and Future Directions." *Biosensors and Bioelectronics* 91 (May): 588–605. https://doi.org/10.1016/J.BIOS.2016.12.062.

Giblett, E R, J E Anderson, F Cohen, B Pollara, and H J Meuwissen. 1972. "Adenosine-Deaminase Deficiency in Two Patients with Severely Impaired Cellular Immunity." *Lancet (London, England)* 2 (7786): 1067–69. http://www.ncbi.nlm.nih.gov/pubmed/4117384.

Giddings, J C, and M N Myers. 1976. "Flow-Field-Flow Fractionation: A Versatile New Separation Method." *Science* 193 (4259): 1244–45. https://doi.org/10.1126/science.959835.

Gouveia de Andrade, Ana Valéria, Giuliana Bertolino, Julia Riewaldt, Karen Bieback, Jana Karbanová, Marcus Odendahl, Martin Bornhäuser, Marc Schmitz, Denis Corbeil, and Torsten Tonn. 2015. "Extracellular Vesicles Secreted by Bone Marrow- and Adipose Tissue-Derived Mesenchymal Stromal Cells Fail to Suppress Lymphocyte Proliferation." *Stem Cells and Development* 24 (11): 1374–76. https://doi.org/10.1089/scd.2014.0563.

Grinnemo, K H, A Månsson, G Dellgren, D Klingberg, E Wardell, V Drvota, C Tammik, et al. 2004. "Xenoreactivity and Engraftment of Human Mesenchymal Stem Cells Transplanted into Infarcted Rat Myocardium." *The Journal of Thoracic and Cardiovascular Surgery* 127 (5): 1293–1300. https://doi.org/10.1016/j.jtcvs.2003.07.037.

Groh, Margaret E, Basabi Maitra, Emese Szekely, and Omer N Koç. 2005. "Human Mesenchymal Stem Cells Require Monocyte-Mediated Activation to Suppress Alloreactive T Cells." *Experimental Hematology* 33 (8): 928–34. https://doi.org/10.1016/j.exphem.2005.05.002.

Grubisic, Z., P. Rempp, and H. Benoit. 1967. "A Universal Calibration for Gel Permeation Chromatography." *Journal of Polymer Science Part B: Polymer Letters* 5 (9): 753–59. https://doi.org/10.1002/pol.1967.110050903.

Guo, Yawei, Koon-Ho Chan, Wing-Hon Lai, Chung-Wah Siu, Shing-Cheong Kwan, Hung-Fat Tse, Philip Wing-Lok Ho, and Jessica Wing-Man Ho. 2013. "Human Mesenchymal Stem Cells Upregulate CD1d ^{high} CD5 $^{+}$ Regulatory B Cells in Experimental Autoimmune Encephalomyelitis." *Neuroimmunomodulation* 20 (5): 294–303. https://doi.org/10.1159/000351450.

Harding, C, J Heuser, and P Stahl. 1983. "Receptor-Mediated Endocytosis of Transferrin and Recycling of the Transferrin Receptor in Rat Reticulocytes." *The Journal of Cell Biology* 97 (2): 329–39. http://www.ncbi.nlm.nih.gov/pubmed/6309857.

Hasan, Anwarul, Ahmad Khattab, Mohammad Ariful Islam, Khaled Abou Hweij, Joya Zeitouny, Renae Waters, Malek Sayegh, Md Monowar Hossain, and Arghya Paul. 2015. "Injectable Hydrogels for Cardiac Tissue Repair after Myocardial Infarction." *Advanced Science* 2 (11):

1500122. https://doi.org/10.1002/advs.201500122.

Haskó, György, and Bruce Cronstein. 2013. "Regulation of Inflammation by Adenosine." *Frontiers in Immunology* 4 (January): 85. https://doi.org/10.3389/fimmu.2013.00085.

Haskó, György, Joel Linden, Bruce Cronstein, and Pál Pacher. 2008. "Adenosine Receptors: Therapeutic Aspects for Inflammatory and Immune Diseases." *Nature Reviews Drug Discovery* 7 (9): 759–70. https://doi.org/10.1038/nrd2638.

Helwa, Inas, Jingwen Cai, Michelle D. Drewry, Arthur Zimmerman, Michael B. Dinkins, Mariam Lotfy Khaled, Mutsa Seremwe, et al. 2017. "A Comparative Study of Serum Exosome Isolation Using Differential Ultracentrifugation and Three Commercial Reagents." Edited by Giovanni Camussi. *PLOS ONE* 12 (1): e0170628. https://doi.org/10.1371/journal.pone.0170628.

Higginbotham, James N, Qin Zhang, Dennis K Jeppesen, Andrew M Scott, H Charles Manning, Josiah Ochieng, Jeffrey L Franklin, and Robert J Coffey. 2016. "Identification and Characterization of EGF Receptor in Individual Exosomes by Fluorescence-Activated Vesicle Sorting." *Journal of Extracellular Vesicles* 5: 29254. http://www.ncbi.nlm.nih.gov/pubmed/27345057.

Hirt, M. N., A. Hansen, and T. Eschenhagen. 2014. "Cardiac Tissue Engineering: State of the Art." *Circulation Research* 114 (2): 354–67. https://doi.org/10.1161/CIRCRESAHA.114.300522.

Hofmann, M. 2005. "Monitoring of Bone Marrow Cell Homing Into the Infarcted Human Myocardium." *Circulation* 111 (17): 2198–2202. https://doi.org/10.1161/01.CIR.0000163546.27639.AA.

Hofmann, U., and S. Frantz. 2015. "Role of Lymphocytes in Myocardial Injury, Healing, and Remodeling After Myocardial Infarction." *Circulation Research* 116 (2): 354–67. https://doi.org/10.1161/CIRCRESAHA.116.304072.

Hoogduijn, Martin J, Felix Popp, Richard Verbeek, Mojgan Masoodi, Anna Nicolaou, Carla Baan, and Marc-H. Dahlke. 2010. "The Immunomodulatory Properties of Mesenchymal Stem Cells and Their Use for Immunotherapy." *International Immunopharmacology* 10: 1496–1500. https://doi.org/http://dx.doi.org/10.1016/j.intimp.2010.06.019.

Hoogduijn, Martin J, Marieke Roemeling-van Rhijn, Anja U Engela, Sander S Korevaar, Fane K F Mensah, Marcella Franquesa, Ron W F de Bruin, Michiel G H Betjes, Willem Weimar, and Carla C Baan. 2013. "Mesenchymal Stem Cells Induce an Inflammatory Response after Intravenous Infusion." *Stem Cells and Development* 22 (21): 2825–35. https://doi.org/10.1089/scd.2013.0193.

Horenstein, Alberto L, Antonella Chillemi, Gianluca Zaccarello, Santina Bruzzone, Valeria Quarona, Andrea Zito, Sara Serra, and Fabio Malavasi. 2013. "A CD38/CD203a/CD73 Ectoenzymatic Pathway Independent of CD39 Drives a Novel Adenosinergic Loop in Human T Lymphocytes." *Oncoimmunology* 2 (9): e26246. https://doi.org/10.4161/onci.26246.

Hou, Dongming, Eyas Al-Shaykh Youssef, Todd J Brinton, Ping Zhang, Pamela Rogers, Erik T Price, Alan C Yeung, Brian H Johnstone, Paul G Yock, and Keith L March. 2005. "Radiolabeled Cell Distribution after Intramyocardial, Intracoronary, and Interstitial Retrograde Coronary Venous Delivery: Implications for Current Clinical Trials." *Circulation* 112 (9 Suppl): I150-6. https://doi.org/10.1161/CIRCULATIONAHA.104.526749.

Huang, Feng, Maogen Chen, Weiqian Chen, Jian Gu, Jia Yuan, Yaoqiu Xue, Junlong Dang, et al. 2017. "Human Gingiva-Derived Mesenchymal Stem Cells Inhibit Xeno-Graft-versus-Host Disease via CD39–CD73–Adenosine and IDO Signals." *Frontiers in Immunology* 8 (February): 68. https://doi.org/10.3389/fimmu.2017.00068.

Hugel, Bénédicte, M. Carmen Martínez, Corinne Kunzelmann, and Jean-Marie Freyssinet. 2005. "Membrane Microparticles: Two Sides of the Coin." *Physiology* 20 (1): 22–27. https://doi.org/10.1152/physiol.00029.2004.

Hyvärinen, Kati, Minna Holopainen, Vita Skirdenko, Hanna Ruhanen, Petri Lehenkari, Matti Korhonen, Reijo Käkelä, Saara Laitinen, and Erja Kerkelä. 2018. "Mesenchymal Stromal Cells and Their Extracellular Vesicles Enhance the Anti-Inflammatory Phenotype of Regulatory Macrophages by Downregulating the Production of Interleukin (IL)-23 and IL-22." *Frontiers in Immunology* 9 (April): 1–13. https://doi.org/10.3389/fimmu.2018.00771.

Ibáñez, Borja, Gerd Heusch, Michel Ovize, and Frans Van de Werf. 2015. "Evolving Therapies for Myocardial Ischemia/Reperfusion Injury." *Journal of the American College of Cardiology* 65 (14): 1454–71. https://doi.org/10.1016/j.jacc.2015.02.032.

Jacobsen, Mette J., Caroline M.Junker Mentzel, Ann Sofie Olesen, Thierry Huby, Claus B. Jørgensen, Romain Barrès, Merete Fredholm, and David Simar. 2016. "Altered Methylation Profile of Lymphocytes Is Concordant with Perturbation of Lipids Metabolism and Inflammatory Response in Obesity." *Journal of Diabetes Research* 2016. https://doi.org/10.1155/2016/8539057.

Jeppesen, Dennis K, Michael L Hvam, Bjarke Primdahl-Bengtson, Anders T Boysen, Bradley Whitehead, Lars Dyrskjøt, Torben F Orntoft, Kenneth A Howard, and Marie S Ostenfeld. 2014. "Comparative Analysis of Discrete Exosome Fractions Obtained by Differential Centrifugation." *Journal of Extracellular Vesicles* 3: 25011. http://www.ncbi.nlm.nih.gov/pubmed/25396408.

Jessup, Mariell, and Susan Brozena. 2003. "Heart Failure." *New England Journal of Medicine* 348 (20): 2007–18. https://doi.org/10.1056/NEJMra021498.

Jiang, Dongsheng, Jana Muschhammer, Yu Qi, Andrea Kügler, Juliane C. de Vries, Mona Saffarzadeh, Anca Sindrilaru, et al. 2016. "Suppression of Neutrophil-Mediated Tissue Damage-A Novel Skill of Mesenchymal Stem Cells." *STEM CELLS* 34 (9): 2393–2406. https://doi.org/10.1002/stem.2417.

Jiang, Xiao-Xia, Yi Zhang, Bing Liu, Shuang-Xi Zhang, Ying Wu, Xiao-Dan Yu, and Ning Mao. 2005. "Human Mesenchymal Stem Cells Inhibit Differentiation and Function of Monocyte-Derived Dendritic Cells." *Blood* 105 (10): 4120–26. https://doi.org/10.1182/blood-2004-02-0586.

Johnstone, R M, M Adam, J R Hammond, L Orr, and C Turbide. 1987. "Vesicle Formation during Reticulocyte Maturation. Association of Plasma Membrane Activities with Released Vesicles (Exosomes)." *The Journal of Biological Chemistry* 262 (19): 9412–20. http://www.ncbi.nlm.nih.gov/pubmed/3597417.

Kaikita, Koichi, Takanori Hayasaki, Toshiyuki Okuma, William A. Kuziel, Hisao Ogawa, and Motohiro Takeya. 2004. "Targeted Deletion of CC Chemokine Receptor 2 Attenuates Left Ventricular Remodeling after Experimental Myocardial Infarction." *The American Journal of Pathology* 165 (2): 439–47. https://doi.org/10.1016/S0002-9440(10)63309-3.

Kanelidis, Anthony J., Courtney Premer, Juan Lopez, Wayne Balkan, and Joshua M. Hare. 2017. "Route of Delivery Modulates the Efficacy of Mesenchymal Stem Cell Therapy for Myocardial InfarctionNovelty and Significance." *Circulation Research* 120 (7): 1139–50. https://doi.org/10.1161/CIRCRESAHA.116.309819.

Kang, Dukjin, Sunok Oh, Sung-Min Ahn, Bong-Hee Lee, and Myeong Hee Moon. 2008. "Proteomic Analysis of Exosomes from Human Neural Stem Cells by Flow Field-Flow Fractionation and Nanoflow Liquid Chromatography−Tandem Mass Spectrometry." *Journal of Proteome Research* 7 (8): 3475–80. https://doi.org/10.1021/pr800225z.

Kanwar, Shailender Singh, Christopher James Dunlay, Diane M Simeone, and Sunitha Nagrath. 2014. "Microfluidic Device (ExoChip) for on-Chip Isolation, Quantification and Characterization of Circulating Exosomes." *Lab on a Chip* 14 (11): 1891–1900. https://doi.org/10.1039/C4LC00136B.

Kato, Taigo, Masayoshi Okumi, Masahiro Tanemura, Koji Yazawa, Yoichi Kakuta, Kazuaki Yamanaka, Koichi Tsutahara, et al. 2014. "Adipose Tissue-Derived Stem Cells Suppress Acute Cellular Rejection by TSG-6 and CD44 Interaction in Rat Kidney Transplantation." *Transplantation* 98 (3): 277–84. https://doi.org/10.1097/TP.0000000000000230.

Katsuda, Takeshi, Nobuyoshi Kosaka, Fumitaka Takeshita, and Takahiro Ochiya. 2013. "The Therapeutic Potential of Mesenchymal Stem Cell-Derived Extracellular Vesicles." *PROTEOMICS* 13: 1637–53. https://doi.org/10.1002/pmic.201200373.

Kerkelä, Erja, Anita Laitinen, Jarkko Räbinä, Sami Valkonen, Maarit Takatalo, Antti Larjo, Johanna Veijola, et al. 2016. "Adenosinergic Immunosuppression by Human Mesenchymal Stromal Cells Requires Co-Operation with T Cells." *Stem Cells* 34 (3): 781–90. https://doi.org/10.1002/stem.2280.

Khan, Imteyaz, LiYing Zhang, Moiz Mohammed, Faith Archer, Jehan Abukharmah, Zengrong Yuan, S. Saif Rizvi, et al. 2014. "Effects of Wharton's Jelly-Derived Mesenchymal Stem Cells on Neonatal Neutrophils." *Journal of Inflammation Research* 8 (December): 1. https://doi.org/10.2147/JIR.S71987.

Kilpinen, Lotta, Ulla Impola, Lotta Sankkila, Ilja Ritamo, Maria Aatonen, Sami Kilpinen, Jarno Tuimala, et al. 2013. "Extracellular Membrane Vesicles from Umbilical Cord Blood-Derived MSC Protect against Ischemic Acute Kidney Injury, a Feature That Is Lost after Inflammatory Conditioning." *Journal of Extracellular Vesicles*. http://www.journalofextracellularvesicles.net/index.php/jev/article/view/21927/31340.

Kim, Han-Soo, Do-Young Choi, So Jeong Yun, Seong-Mi Choi, Jeong Won Kang, Jin Woo Jung, Daehee Hwang, Kwang Pyo Kim, and Dong-Wook Kim. 2012. "Proteomic Analysis of Microvesicles Derived from Human Mesenchymal Stem Cells." *Journal of Proteome Research* 11 (2): 839–49. https://doi.org/10.1021/pr200682z.

Kim, Jaehyup, and Peiman Hematti. 2009. "Mesenchymal Stem Cell–educated Macrophages: A Novel Type of Alternatively Activated Macrophages." *Experimental Hematology* 37 (12): 1445–53. https://doi.org/10.1016/j.exphem.2009.09.004.

Knowles, H J, and A L Harris. 2001. "Hypoxia and Oxidative Stress in Breast Cancer. Hypoxia and Tumourigenesis." *Breast Cancer Research : BCR* 3 (5): 318–22. http://www.ncbi.nlm.nih.gov/pubmed/11597321.

Kohler, D., T. Eckle, M. Faigle, A. Grenz, M. Mittelbronn, S. Laucher, M. L. Hart, S. C. Robson, C. E. Muller, and H. K. Eltzschig. 2007. "CD39/Ectonucleoside Triphosphate Diphosphohydrolase 1 Provides Myocardial Protection During Cardiac Ischemia/Reperfusion Injury." *Circulation* 116 (16): 1784–94. https://doi.org/10.1161/CIRCULATIONAHA.107.690180.

Koliha, Nina, Yvonne Wiencek, Ute Heider, Christian Jüngst, Nikolay Kladt, Susanne Krauthäuser, Ian C D Johnston, Andreas Bosio, Astrid Schauss, and Stefan Wild. 2016. "A Novel Multiplex Bead-Based Platform Highlights the Diversity of Extracellular Vesicles." *Journal of Extracellular Vesicles* 5: 29975. http://www.ncbi.nlm.nih.gov/pubmed/26901056.

Kordelas, L, V Rebmann, A K Ludwig, S Radtke, J Ruesing, T R Doeppner, M Epple, P A Horn, D W Beelen, and B Giebel. 2014. "MSC-Derived Exosomes: A Novel Tool to Treat Therapy-Refractory Graft-versus-Host Disease." *Leukemia* 28 (4): 970–73. http://dx.doi.org/10.1038/leu.2014.41.

Kormelink, Tom Groot, Ger J. A. Arkesteijn, Frans A. Nauwelaers, Ger van den Engh, Esther N. M. Nolte-'t Hoen, and Marca H. M. Wauben. 2016. "Prerequisites for the Analysis and Sorting of Extracellular Vesicle Subpopulations by High-Resolution Flow Cytometry." *Cytometry Part A* 89 (2): 135–47. https://doi.org/10.1002/cyto.a.22644.

Kosieradzki, M., and W. Rowiński. 2008. "Ischemia/Reperfusion Injury in Kidney Transplantation: Mechanisms and Prevention." *Transplantation Proceedings* 40 (10): 3279–88. https://doi.org/10.1016/j.transproceed.2008.10.004.

Kowal, Joanna, Mercedes Tkach, and Clotilde Théry. 2014. "Biogenesis and Secretion of Exosomes." *Current Opinion in Cell Biology* 29 (1): 116–25. https://doi.org/10.1016/j.ceb.2014.05.004.

Krampera, Mauro, Lorenzo Cosmi, Roberta Angeli, Annalisa Pasini, Francesco Liotta, Angelo Andreini, Veronica Santarlasci, et al. 2006. "Role for Interferon-Gamma in the Immunomodulatory Activity of Human Bone Marrow Mesenchymal Stem Cells." *Stem Cells (Dayton, Ohio)* 24 (2): 386–98. https://doi.org/10.1634/stemcells.2005-0008.

Krampera, Mauro, Sarah Glennie, Julian Dyson, Diane Scott, Ruthline Laylor, Elizabeth Simpson, and Francesco Dazzi. 2003. "Bone Marrow Mesenchymal Stem Cells Inhibit the Response of Naive and Memory Antigen-Specific T Cells to Their Cognate Peptide." *Blood* 101 (9): 3722–29. https://doi.org/10.1182/blood-2002-07-2104.

Krampera, Mauro, Annalisa Pasini, Giovanni Pizzolo, Lorenzo Cosmi, Sergio Romagnani, and Francesco Annunziato. 2006. "Regenerative and Immunomodulatory Potential of Mesenchymal Stem Cells." *Current Opinion in Pharmacology* 6 (4): 435–41. https://doi.org/10.1016/j.coph.2006.02.008.

Kriebel, Paul W, Ritankar Majumdar, Lisa M Jenkins, Hiroshi Senoo, Weiye Wang, Sonia Ammu, Song Chen, Kedar Narayan, Miho Iijima, and Carole A Parent. 2018. "Extracellular Vesicles Direct Migration by Synthesizing and Releasing Chemotactic Signals." *The Journal of Cell Biology* 217 (8): 2891–2910. https://doi.org/10.1083/jcb.201710170.

Kuang, D.-M., Y. Wu, N. Chen, J. Cheng, S.-M. Zhuang, and L. Zheng. 2007. "Tumor-Derived Hyaluronan Induces Formation of Immunosuppressive Macrophages through Transient Early Activation of Monocytes." *Blood* 110 (2): 587–95. https://doi.org/10.1182/blood-2007-01-068031.

Kumar, Sushil, David Calianese, and Raymond B. Birge. 2017. "Efferocytosis of Dying Cells Differentially Modulate Immunological Outcomes in Tumor Microenvironment." *Immunological Reviews* 280 (1): 149–64. https://doi.org/10.1111/imr.12587.

la Fuente, Alexandre de, Lorena Alonso-Alconada, Clotilde Costa, Juan Cueva, Tomas Garcia-Caballero, Rafael Lopez-Lopez, and Miguel Abal. 2015. "M-Trap: Exosome-Based Capture of Tumor Cells as a New Technology in Peritoneal Metastasis." *Journal of the National Cancer Institute* 107 (9): djv184. https://doi.org/10.1093/jnci/djv184.

Lai, Ruenn Chai, Fatih Arslan, May May Lee, Newman Siu Kwan Sze, Andre Choo, Tian Sheng Chen, Manuel Salto-Tellez, et al. 2010. "Exosome Secreted by MSC Reduces Myocardial Ischemia/reperfusion Injury." *Stem Cell Research* 4 (3): 214–22. https://doi.org/10.1016/j.scr.2009.12.003.

Lai, Ruenn Chai, Tian Sheng Chen, and Sai Kiang Lim. 2011. "Mesenchymal Stem Cell Exosome: A Novel Stem Cell-Based Therapy for Cardiovascular Disease." *Regenerative Medicine* 6 (4): 481–92. https://doi.org/10.2217/rme.11.35.

Lee, Daniel W, Rebecca Gardner, David L Porter, Chrystal U Louis, Nabil Ahmed, Michael Jensen, Stephan A Grupp, and Crystal L Mackall. 2014. "Current Concepts in the Diagnosis and

Management of Cytokine Release Syndrome." *Blood* 124 (2): 188–95. https://doi.org/10.1182/blood-2014-05-552729.

Lee, Hyun Ju, Jung Hwa Ko, Hyun Jeong Jeong, Ah Young Ko, Mee Kum Kim, Won Ryang Wee, Sun-Ok Yoon, and Joo Youn Oh. 2015. "Mesenchymal Stem/stromal Cells Protect against Autoimmunity via CCL2-Dependent Recruitment of Myeloid-Derived Suppressor Cells." *Journal of Immunology (Baltimore, Md. : 1950)* 194 (8): 3634–45. https://doi.org/10.4049/jimmunol.1402139.

Lee, Ryang Hwa, Andrey A. Pulin, Min Jeong Seo, Daniel J. Kota, Joni Ylostalo, Benjamin L. Larson, Laura Semprun-Prieto, Patrice Delafontaine, and Darwin J. Prockop. 2009. "Intravenous hMSCs Improve Myocardial Infarction in Mice Because Cells Embolized in Lung Are Activated to Secrete the Anti-Inflammatory Protein TSG-6." *Cell Stem Cell* 5 (1): 54–63. https://doi.org/10.1016/j.stem.2009.05.003.

Leibovich, Samuel Joseph, Jiang-Fan Chen, Grace Pinhal-Enfield, Paula C. Belem, Genie Elson, Anthony Rosania, Madhuri Ramanathan, et al. 2002. "Synergistic Up-Regulation of Vascular Endothelial Growth Factor Expression in Murine Macrophages by Adenosine A2A Receptor Agonists and Endotoxin." *The American Journal of Pathology* 160 (6): 2231–44. https://doi.org/10.1016/S0002-9440(10)61170-4.

Lener, Thomas, Mario Gimona, Ludwig Aigner, Verena Börger, Edit Buzas, Giovanni Camussi, Nathalie Chaput, et al. 2015. "Applying Extracellular Vesicles Based Therapeutics in Clinical Trials - an ISEV Position Paper." *Journal of Extracellular Vesicles* 4 (January): 30087. http://www.ncbi.nlm.nih.gov/pubmed/26725829.

Li, Hong, ZiKuan Guo, XiaoXia Jiang, Heng Zhu, XiuSen Li, and Ning Mao. 2008. "Mesenchymal Stem Cells Alter Migratory Property of T and Dendritic Cells to Delay the Development of Murine Lethal Acute Graft-Versus-Host Disease." *STEM CELLS* 26 (10): 2531–41. https://doi.org/10.1634/stemcells.2008-0146.

Li, Shu-Hong, Teresa Y.Y. Lai, Zhuo Sun, Mihan Han, Eduardo Moriyama, Brian Wilson, Shafie Fazel, et al. 2009. "Tracking Cardiac Engraftment and Distribution of Implanted Bone Marrow Cells: Comparing Intra-Aortic, Intravenous, and Intramyocardial Delivery." *The Journal of Thoracic and Cardiovascular Surgery* 137 (5): 1225–1233.e1. https://doi.org/10.1016/j.jtcvs.2008.11.001.

Li, Tingfen, Yongmin Yan, Bingying Wang, Hui Qian, Xu Zhang, Li Shen, Mei Wang, et al. 2013. "Exosomes Derived from Human Umbilical Cord Mesenchymal Stem Cells Alleviate Liver Fibrosis." *Stem Cells and Development* 22 (6): 845–54. https://doi.org/10.1089/scd.2012.0395.

Libregts, S. F. W. M., G. J. A. Arkesteijn, A. Németh, E. N. M. Nolte-'t Hoen, and M. H. M. Wauben. 2018. "Flow Cytometric Analysis of Extracellular Vesicle Subsets in Plasma: Impact of Swarm by Particles of Non-Interest." *Journal of Thrombosis and Haemostasis*, June. https://doi.org/10.1111/jth.14154.

Lim, Jong-Hyung, Jung-Sik Kim, Il-Hee Yoon, Jun-Seop Shin, Hye-Young Nam, Seung-Ha Yang, Sang-Joon Kim, and Chung-Gyu Park. 2010. "Immunomodulation of Delayed-Type Hypersensitivity Responses by Mesenchymal Stem Cells Is Associated with Bystander T Cell Apoptosis in the Draining Lymph Node." *Journal of Immunology (Baltimore, Md. : 1950)* 185 (7): 4022–29. https://doi.org/10.4049/jimmunol.0902723.

Linares, Romain, Sisareuth Tan, Céline Gounou, Nicolas Arraud, and Alain R. Brisson. 2015. *High-Speed Centrifugation Induces Aggregation of Extracellular Vesicles*. *Journal of Extracellular Vesicles*. Vol. 4. Taylor & Francis. https://doi.org/10.3402/jev.v4.29509.

Liu, Xian-bao, Han Chen, Hui-qiang Chen, Mei-fei Zhu, Xin-yang Hu, Ya-ping Wang, Zhi Jiang, Yin-

chuan Xu, Mei-xiang Xiang, and Jian-an Wang. 2012. “Angiopoietin-1 Preconditioning Enhances Survival and Functional Recovery of Mesenchymal Stem Cell Transplantation.” *Journal of Zhejiang University. Science. B* 13 (8): 616–23. https://doi.org/10.1631/jzus.B1201004.

Liu, Xiaohuan, Ting Feng, Tianxiang Gong, Chongyang Shen, Tingting Zhu, Qihong Wu, Qiang Li, and Hong Li. 2015. “Human Umbilical Cord Mesenchymal Stem Cells Inhibit the Function of Allogeneic Activated Vγ9Vδ2 T Lymphocytes In Vitro.” *BioMed Research International* 2015 (January): 317801. https://doi.org/10.1155/2015/317801.

Liu, Xingxia, Shaoda Ren, Xuebin Qu, Chaozhuo Ge, Kai Cheng, and Robert Chun Hua Zhao. 2015. “Mesenchymal Stem Cells Inhibit Th17 Cells Differentiation via IFN-γ-Mediated SOCS3 Activation.” *Immunologic Research* 61 (3): 219–29. https://doi.org/10.1007/s12026-014-8612-2.

Llucià-Valldeperas, Aida, Carolina Soler-Botija, Carolina Gálvez-Montón, Santiago Roura, Cristina Prat-Vidal, Isaac Perea-Gil, Benjamin Sanchez, Ramon Bragos, Gordana Vunjak-Novakovic, and Antoni Bayes-Genis. 2017. “Electromechanical Conditioning of Adult Progenitor Cells Improves Recovery of Cardiac Function After Myocardial Infarction.” *Stem Cells Translational Medicine* 6 (3): 970–81. https://doi.org/10.5966/sctm.2016-0079.

Loke, P’ng, Iain Gallagher, Meera G Nair, Xingxing Zang, Frank Brombacher, Markus Mohrs, James P Allison, and Judith E Allen. 2007. “Alternative Activation Is an Innate Response to Injury That Requires CD4+ T Cells to Be Sustained during Chronic Infection.” *Journal of Immunology (Baltimore, Md. : 1950)* 179 (6): 3926–36. http://www.ncbi.nlm.nih.gov/pubmed/17785830.

Lötvall, Jan, Andrew F Hill, Fred Hochberg, Edit I Buzás, Dolores Di Vizio, Christopher Gardiner, Yong Song Gho, et al. 2014. “Minimal Experimental Requirements for Definition of Extracellular Vesicles and Their Functions: A Position Statement from the International Society for Extracellular Vesicles.” *Journal of Extracellular Vesicles* 3 (0). https://doi.org/10.3402/jev.v3.26913.

Lozano-Ramos, Inés, Ioana Bancu, Anna Oliveira-Tercero, María Pilar Armengol, Armando Menezes-Neto, Hernando A Del Portillo, Ricardo Lauzurica-Valdemoros, and Francesc E Borràs. 2015. “Size-Exclusion Chromatography-Based Enrichment of Extracellular Vesicles from Urine Samples.” *Journal of Extracellular Vesicles* 4 (January): 27369. https://doi.org/10.3402/jev.v4.27369.

Lozano-Ramos, S. Inés, Ioana Bancu, Laura Carreras-Planella, Marta Monguió-Tortajada, Laura Cañas, Javier Juega, Josep Bonet, M. Pilar Armengol, Ricardo Lauzurica, and Francesc E. Borràs. 2018. “Molecular Profile of Urine Extracellular Vesicles from Normo-Functional Kidneys Reveal Minimal Differences between Living and Deceased Donors.” *BMC Nephrology* 19 (1): 189. https://doi.org/10.1186/s12882-018-0985-3.

Lu, Wenbin, ZhuoYing Xie, Yong Tang, Ling Bai, Yuyu Yao, Cong Fu, and Genshan Ma. 2015. “Photoluminescent Mesoporous Silicon Nanoparticles with siCCR2 Improve the Effects of Mesenchymal Stromal Cell Transplantation after Acute Myocardial Infarction.” *Theranostics* 5 (10): 1068–82. https://doi.org/10.7150/thno.11517.

Luk, Franka, Laura Carreras-Planella, Sander S. Korevaar, Samantha F. H. de Witte, Francesc E. Borràs, Michiel G. H. Betjes, Carla C. Baan, Martin J. Hoogduijn, and Marcella Franquesa. 2017. “Inflammatory Conditions Dictate the Effect of Mesenchymal Stem or Stromal Cells on B Cell Function.” *Frontiers in Immunology* 8 (August): 1042. https://doi.org/10.3389/fimmu.2017.01042.

Luu, NT, HM Mcgettrick, CD Buckley, PN Newsome, GE Rainger, J Frampton, and GB Nash. 2013.

"Crosstalk Between Mesenchymal Stem Cells and Endothelial Cells Leads to Downregulation of Cytokine-Induced Leukocyte Recruitment." *STEM CELLS* 31 (12): 2690–2702. https://doi.org/10.1002/stem.1511.

Luz-Crawford, Patricia, Farida Djouad, Karine Toupet, Claire Bony, Marcella Franquesa, Martin J Hoogduijn, Christian Jorgensen, and Danièle Noël. 2016. "Mesenchymal Stem Cell-Derived Interleukin 1 Receptor Antagonist Promotes Macrophage Polarization and Inhibits B Cell Differentiation." *Stem Cells (Dayton, Ohio)* 34 (2): 483–92. https://doi.org/10.1002/stem.2254.

Luz-Crawford, Patricia, Monica Kurte, Javiera Bravo-Alegría, Rafael Contreras, Estefania Nova-Lamperti, Gautier Tejedor, Danièle Noël, et al. 2013. "Mesenchymal Stem Cells Generate a CD4+CD25+Foxp3+ Regulatory T Cell Population during the Differentiation Process of Th1 and Th17 Cells." *Stem Cell Research & Therapy* 4 (3): 65. https://doi.org/10.1186/scrt216.

Luz-Crawford, Patricia, Danièle Noël, Ximena Fernandez, Maroun Khoury, Fernando Figueroa, Flavio Carrión, Christian Jorgensen, and Farida Djouad. 2012. "Mesenchymal Stem Cells Repress Th17 Molecular Program through the PD-1 Pathway." *PloS One* 7 (9): e45272. https://doi.org/10.1371/journal.pone.0045272.

Ma, Haijun, Chang Liu, Bingyu Shi, Zhuoya Zhang, Ruihai Feng, Minghao Guo, Liwei Lu, et al. 2018. "Mesenchymal Stem Cells Control Complement C5 Activation by Factor H in Lupus Nephritis." *EBioMedicine* 32 (June): 21–30. https://doi.org/10.1016/j.ebiom.2018.05.034.

Madrigal, Marialaura, Kosagisharaf S Rao, and Neil H Riordan. 2014. "A Review of Therapeutic Effects of Mesenchymal Stem Cell Secretions and Induction of Secretory Modification by Different Culture Methods." *Journal of Translational Medicine* 12 (1): 260. https://doi.org/10.1186/s12967-014-0260-8.

Magaña-Guerrero, Fátima Sofía, Alfredo Domínguez-López, Pamela Martínez-Aboytes, Beatriz Buentello-Volante, and Yonathan Garfias. 2017. "Human Amniotic Membrane Mesenchymal Stem Cells Inhibit Neutrophil Extracellular Traps through TSG-6." *Scientific Reports* 7 (1): 12426. https://doi.org/10.1038/s41598-017-10962-2.

Majumdar, Ritankar, Aidin Tavakoli Tameh, and Carole A. Parent. 2016. "Exosomes Mediate LTB4 Release during Neutrophil Chemotaxis." Edited by Philippa Marrack. *PLOS Biology* 14 (1): e1002336. https://doi.org/10.1371/journal.pbio.1002336.

Maksimow, Mikael, Lea Kyhälä, Anne Nieminen, Leena Kylänpää, Kristiina Aalto, Kati Elima, Panu Mentula, et al. 2014. "Early Prediction of Persistent Organ Failure by Soluble CD73 in Patients with Acute Pancreatitis*." *Critical Care Medicine* 42 (12): 2556–64. https://doi.org/10.1097/CCM.0000000000000550.

Malliaras, Konstantinos, Yiqiang Zhang, Jeffrey Seinfeld, Giselle Galang, Eleni Tseliou, Ke Cheng, Baiming Sun, Mohammad Aminzadeh, and Eduardo Marbán. 2013. "Cardiomyocyte Proliferation and Progenitor Cell Recruitment Underlie Therapeutic Regeneration after Myocardial Infarction in the Adult Mouse Heart." *EMBO Molecular Medicine* 5 (2): 191–209. https://doi.org/10.1002/emmm.201201737.

Mancheño-Corvo, Pablo, Ramón Menta, Borja del Río, Marcella Franquesa, Cristina Ramírez, Martin J. Hoogduijn, Olga DelaRosa, Wilfried Dalemans, and Eleuterio Lombardo. 2015. "T Lymphocyte Prestimulation Impairs in a Time-Dependent Manner the Capacity of Adipose Mesenchymal Stem Cells to Inhibit Proliferation: Role of Interferon Γ, Poly I:C, and Tryptophan Metabolism in Restoring Adipose Mesenchymal Stem Cell Inhibitory Effect." *Stem Cells and Development* 24 (18): 2158–70. https://doi.org/10.1089/scd.2014.0508.

Mandapathil, Magis, Benedict Hilldorfer, Miroslaw J Szczepanski, Malgorzata Czystowska, Marta Szajnik, Jin Ren, Stephan Lang, Edwin K Jackson, Elieser Gorelik, and Theresa L Whiteside.

2010. “Generation and Accumulation of Immunosuppressive Adenosine by Human CD4+CD25highFOXP3+ Regulatory T Cells.” *The Journal of Biological Chemistry* 285 (10): 7176–86. https://doi.org/10.1074/jbc.M109.047423.

Mantovani, Alberto, Subhra K Biswas, Maria Rosaria Galdiero, Antonio Sica, and Massimo Locati. 2013. “Macrophage Plasticity and Polarization in Tissue Repair and Remodelling.” *The Journal of Pathology* 229 (2): 176–85. https://doi.org/10.1002/path.4133.

Mantovani, Alberto, Antonio Sica, Silvano Sozzani, Paola Allavena, Annunciata Vecchi, and Massimo Locati. 2004. “The Chemokine System in Diverse Forms of Macrophage Activation and Polarization.” *Trends in Immunology* 25 (12): 677–86. https://doi.org/10.1016/j.it.2004.09.015.

Martinez, F. O., L. Helming, R. Milde, A. Varin, B. N. Melgert, C. Draijer, B. Thomas, et al. 2013. “Genetic Programs Expressed in Resting and IL-4 Alternatively Activated Mouse and Human Macrophages: Similarities and Differences.” *Blood* 121 (9): e57–69. https://doi.org/10.1182/blood-2012-06-436212.

Martinez, Fernando O., Siamon Gordon, Massimo Locati, and Alberto Mantovani. 2006. “Transcriptional Profiling of the Human Monocyte-to-Macrophage Differentiation and Polarization: New Molecules and Patterns of Gene Expression.” *Journal of Immunology (Baltimore, Md. : 1950)* 177 (10): 7303–11. https://doi.org/10.4049/jimmunol.177.10.7303.

Martinez, Fernando O, and Siamon Gordon. 2014. “The M1 and M2 Paradigm of Macrophage Activation: Time for Reassessment.” *F1000prime Reports* 6 (January): 13. https://doi.org/10.12703/P6-13.

Maude, Shannon L, David Barrett, David T Teachey, and Stephan A Grupp. 2014. “Managing Cytokine Release Syndrome Associated with Novel T Cell-Engaging Therapies.” *Cancer Journal (Sudbury, Mass.)* 20 (2): 119–22. https://doi.org/10.1097/PPO.0000000000000035.

Meisel, Roland, Andree Zibert, Maurice Laryea, Ulrich Göbel, Walter Däubener, and Dagmar Dilloo. 2004. “Human Bone Marrow Stromal Cells Inhibit Allogeneic T-Cell Responses by Indoleamine 2,3-Dioxygenase-Mediated Tryptophan Degradation.” *Blood* 103 (12): 4619–21. https://doi.org/10.1182/blood-2003-11-3909.

Melief, Sara M, Sacha B Geutskens, Willem E Fibbe, and Helene Roelofs. 2013a. “Multipotent Stromal Cells Skew Monocytes towards an Anti-Inflammatory Function: The Link with Key Immunoregulatory Molecules.” *Haematologica* 98 (6): 888–95. https://doi.org/10.3324/haematol.2012.078055.

Melief, Sara M, Ellen Schrama, Martijn H Brugman, Machteld M Tiemessen, Martin J Hoogduijn, Willem E Fibbe, and Helene Roelofs. 2013. “Multipotent Stromal Cells Induce Human Regulatory T Cells through a Novel Pathway Involving Skewing of Monocytes toward Anti-Inflammatory Macrophages.” *Stem Cells (Dayton, Ohio)* 31 (9): 1980–91. https://doi.org/10.1002/stem.1432.

Menard, Cedric, Luciano Pacelli, Giulio Bassi, Joelle Dulong, Francesco Bifari, Isabelle Bezier, Jasmina Zanoncello, et al. 2013. “Clinical-Grade Mesenchymal Stromal Cells Produced Under Various Good Manufacturing Practice Processes Differ in Their Immunomodulatory Properties: Standardization of Immune Quality Controls.” *Stem Cells and Development* 22 (12): 1789–1801. https://doi.org/10.1089/scd.2012.0594.

Menezes-Neto, Armando de, María José Fidalgo Sáez, Inés Lozano-Ramos, Joan Segui-Barber, Lorena Martin-Jaular, Josep M Estanyol Ullate, Carmen Fernandez-Becerra, Francesc E Borrás, and Hernando A Del Portillo. 2015. “Size-Exclusion Chromatography as a Stand-

Alone Methodology Identifies Novel Markers in Mass Spectrometry Analyses of Plasma-Derived Vesicles from Healthy Individuals." *Journal of Extracellular Vesicles* 4 (January): 27378. http://www.pubmedcentral.nih.gov/articlerender.fcgi?artid=4495624&tool=pmcentrez&rendertype=abstract.

Mizumoto, Norikatsu, Tadashi Kumamoto, Simon C Robson, Jean Sévigny, Hiroyuki Matsue, Keiichi Enjyoji, and Akira Takashima. 2002. "CD39 Is the Dominant Langerhans Cell-Associated Ecto-NTPDase: Modulatory Roles in Inflammation and Immune Responsiveness." *Nature Medicine* 8 (4): 358–65. https://doi.org/10.1038/nm0402-358.

Moll, Guido, Regina Jitschin, Lena von Bahr, Ida Rasmusson-Duprez, Berit Sundberg, Lena Lönnies, Graciela Elgue, et al. 2011. "Mesenchymal Stromal Cells Engage Complement and Complement Receptor Bearing Innate Effector Cells to Modulate Immune Responses." Edited by Anna Carla Goldberg. *PLoS ONE* 6 (7): e21703. https://doi.org/10.1371/journal.pone.0021703.

Momen-Heravi, Fatemeh, Leonora Balaj, Sara Alian, Alexander J. Trachtenberg, Fred H. Hochberg, Johan Skog, and Winston Patrick Kuo. 2012. "Impact of Biofluid Viscosity on Size and Sedimentation Efficiency of the Isolated Microvesicles." *Frontiers in Physiology* 3 (May): 162. https://doi.org/10.3389/fphys.2012.00162.

Monguió-Tortajada, Marta, Marcella Franquesa, Maria-Rosa Sarrias, and Francesc E. Borràs. 2018. "Low Doses of LPS Exacerbate the Inflammatory Response and Trigger Death on TLR3-Primed Human Monocytes Article." *Cell Death and Disease* 9 (5): 499. https://doi.org/10.1038/s41419-018-0520-2.

Monguió-Tortajada, Marta, Ricardo Lauzurica, and Francesc E. Borràs. 2014. "Tolerance in Organ Transplantation: From Conventional Immunosuppression to Extracellular Vesicles." *Frontiers in Immunology* 5 (September): 1–12. https://doi.org/10.3389/fimmu.2014.00416.

Monguió-Tortajada, Marta, Santiago Roura, Carolina Gálvez-Montón, Marcella Franquesa, Antoni Bayes-Genis, and Francesc E Borràs. 2017. "Mesenchymal Stem Cells Induce Expression of CD73 in Human Monocytes In Vitro and in a Swine Model of Myocardial Infarction In Vivo." *Frontiers in Immunology* 8 (NOV): 1577. https://doi.org/10.3389/fimmu.2017.01577.

Monguió-Tortajada, Marta, Santiago Roura, Carolina Gálvez-Montón, Josep Maria Pujal, Gemma Aran, Lucía Sanjurjo, Marcel·la Franquesa, Maria-Rosa Sarrias, Antoni Bayes-Genis, and Francesc E Borràs. 2017. "Nanosized UCMSC-Derived Extracellular Vesicles but Not Conditioned Medium Exclusively Inhibit the Inflammatory Response of Stimulated T Cells: Implications for Nanomedicine." *Theranostics* 7 (2): 270–84. https://doi.org/10.7150/thno.16154.

Mosser, David M., and Justin P. Edwards. 2008. "Exploring the Full Spectrum of Macrophage Activation." *Nature Reviews Immunology* 8 (12): 958–69. https://doi.org/10.1038/nri2448.

Muller, Laurent, Chang-Sook Hong, Donna B Stolz, Simon C Watkins, and Theresa L Whiteside. 2014. "Isolation of Biologically-Active Exosomes from Human Plasma." *Journal of Immunological Methods*. https://doi.org/10.1016/j.jim.2014.06.007.

Muralidharan-Chari, Vandhana, James W Clancy, Alanna Sedgwick, and Crislyn D'Souza-Schorey. 2010. "Microvesicles: Mediators of Extracellular Communication during Cancer Progression." *Journal of Cell Science* 123 (Pt 10): 1603–11. https://doi.org/10.1242/jcs.064386.

Murphy, Patrick S, Jing Wang, Samir P Bhagwat, Joshua C Munger, William J Janssen, Terry W

Wright, and Michael R Elliott. 2017. “CD73 Regulates Anti-Inflammatory Signaling between Apoptotic Cells and Endotoxin-Conditioned Tissue Macrophages.” *Cell Death and Differentiation* 24 (3): 559–70. https://doi.org/10.1038/cdd.2016.159.

Murray, Peter J. J, Judith E. E Allen, Subhra K. K Biswas, Edward A. A Fisher, Derek W. W Gilroy, Sergij Goerdt, Siamon Gordon, et al. 2014. “Macrophage Activation and Polarization: Nomenclature and Experimental Guidelines.” *Immunity* 41 (1): 14–20. https://doi.org/10.1016/j.immuni.2014.06.008.

Nahrendorf, M., M. J. Pittet, and F. K. Swirski. 2010. “Monocytes: Protagonists of Infarct Inflammation and Repair After Myocardial Infarction.” *Circulation* 121 (22): 2437–45. https://doi.org/10.1161/CIRCULATIONAHA.109.916346.

Nahrendorf, Matthias, Filip K. Swirski, Elena Aikawa, Lars Stangenberg, Thomas Wurdinger, Jose-Luiz Figueiredo, Peter Libby, Ralph Weissleder, and Mikael J. Pittet. 2007. “The Healing Myocardium Sequentially Mobilizes Two Monocyte Subsets with Divergent and Complementary Functions.” *The Journal of Experimental Medicine* 204 (12): 3037–47. https://doi.org/10.1084/jem.20070885.

Nauta, Alma J., Alwine B. Kruisselbrink, Ellie Lurvink, Roel Willemze, and Willem E. Fibbe. 2006. “Mesenchymal Stem Cells Inhibit Generation and Function of Both CD34+-Derived and Monocyte-Derived Dendritic Cells.” *Journal of Immunology* 177 (4): 2080–87. https://doi.org/10.4049/jimmunol.177.4.2080.

Nauta, Alma J, Geert Westerhuis, Alwine B Kruisselbrink, Ellie G A Lurvink, Roel Willemze, and Willem E Fibbe. 2006. “Donor-Derived Mesenchymal Stem Cells Are Immunogenic in an Allogeneic Host and Stimulate Donor Graft Rejection in a Nonmyeloablative Setting.” *Blood* 108 (6): 2114–20. https://doi.org/10.1182/blood-2005-11-011650.

Németh, Krisztián, Asada Leelahavanichkul, Peter S T Yuen, Balázs Mayer, Alissa Parmelee, Kent Doi, Pamela G Robey, et al. 2009. “Bone Marrow Stromal Cells Attenuate Sepsis via Prostaglandin E(2)-Dependent Reprogramming of Host Macrophages to Increase Their Interleukin-10 Production.” *Nature Medicine* 15 (1): 42–49. https://doi.org/10.1038/nm.1905.

Nicola, Massimo Di, Carmelo Carlo-Stella, Michele Magni, Marco Milanesi, Paolo D Longoni, Paola Matteucci, Salvatore Grisanti, and Alessandro M Gianni. 2002. “Human Bone Marrow Stromal Cells Suppress T-Lymphocyte Proliferation Induced by Cellular or Nonspecific Mitogenic Stimuli.” *Blood* 99 (10): 3838–43. http://www.ncbi.nlm.nih.gov/pubmed/11986244.

Niel, Guillaume Van, Gisela D’Angelo, and Graça Raposo. 2018. “Shedding Light on the Cell Biology of Extracellular Vesicles.” *Nature Reviews Molecular Cell Biology*. https://doi.org/10.1038/nrm.2017.125.

Nikolova, Maria, Matthieu Carriere, Mohammad-Ali Jenabian, Sophie Limou, Mehwish Younas, Ayrin Kök, Sophie Huë, et al. 2011. “CD39/Adenosine Pathway Is Involved in AIDS Progression.” Edited by Ronald C. Desrosiers. *PLoS Pathogens* 7 (7): e1002110. https://doi.org/10.1371/journal.ppat.1002110.

Nolte-’t Hoen, Esther N M, Els J van der Vlist, Marian Aalberts, Hendrik C H Mertens, Berend Jan Bosch, Willem Bartelink, Enrico Mastrobattista, et al. 2012. “Quantitative and Qualitative Flow Cytometric Analysis of Nanosized Cell-Derived Membrane Vesicles.” *Nanomedicine : Nanotechnology, Biology, and Medicine* 8: 712–20. http://linkinghub.elsevier.com/retrieve/pii/S1549634110036?showall=true.

Obermajer, Nataša, Felix C Popp, Yorick Soeder, Jan Haarer, Edward K Geissler, Hans J Schlitt, and Marc H Dahlke. 2014. “Conversion of Th17 into IL-17A(neg) Regulatory T Cells: A Novel

Mechanism in Prolonged Allograft Survival Promoted by Mesenchymal Stem Cell-Supported Minimized Immunosuppressive Therapy." *Journal of Immunology (Baltimore, Md. : 1950)* 193 (10): 4988–99. https://doi.org/10.4049/jimmunol.1401776.

Ohta, Akio, and Michail Sitkovsky. 2014. "Extracellular Adenosine-Mediated Modulation of Regulatory T Cells." *Frontiers in Immunology* 5 (July): 304. https://doi.org/10.3389/fimmu.2014.00304.

Ohta, Masanori, Kazuyoshi Toyama, David D Gutterman, William B Campbell, Vincent Lemaître, Ryutaro Teraoka, and Hiroto Miura. 2013. "Ecto-5'-nucleotidase, CD73, Is an Endothelium-Derived Hyperpolarizing Factor Synthase." *Arteriosclerosis, Thrombosis, and Vascular Biology* 33 (3): 629–36. https://doi.org/10.1161/ATVBAHA.112.300600.

Olivetti, G, J M Capasso, L G Meggs, E H Sonnenblick, and P Anversa. 1991. "Cellular Basis of Chronic Ventricular Remodeling after Myocardial Infarction in Rats." *Circulation Research* 68 (3): 856–69. https://doi.org/10.1161/01.RES.68.3.856.

Padfield, Gareth J, Jehangir N Din, Elena Koushiappi, Nicholas L Mills, Simon D Robinson, Nicholas Le May Cruden, Andrew John Lucking, Stanley Chia, Scott A Harding, and David E Newby. 2013. "Cardiovascular Effects of Tumour Necrosis Factor α Antagonism in Patients with Acute Myocardial Infarction: A First in Human Study." *Heart* 99 (18): 1330–35. https://doi.org/10.1136/heartjnl-2013-303648.

Pan, B T, and R M Johnstone. 1983. "Fate of the Transferrin Receptor during Maturation of Sheep Reticulocytes in Vitro: Selective Externalization of the Receptor." *Cell* 33 (3): 967–78. http://www.ncbi.nlm.nih.gov/pubmed/6307529.

Pan, B T, K Teng, C Wu, M Adam, and R M Johnstone. 1985. "Electron Microscopic Evidence for Externalization of the Transferrin Receptor in Vesicular Form in Sheep Reticulocytes." *The Journal of Cell Biology* 101 (3): 942–48. http://www.ncbi.nlm.nih.gov/pubmed/2993317.

Panther, Elisabeth. 2001. "Expression and Function of Adenosine Receptors in Human Dendritic Cells." *The FASEB Journal* 15 (11): 1963–70. https://doi.org/10.1096/fj.01-0169com.

Patel, S A, J R Meyer, S J Greco, K E Corcoran, M Bryan, and P Rameshwar. 2010. "Mesenchymal Stem Cells Protect Breast Cancer Cells through Regulatory T Cells: Role of Mesenchymal Stem Cell-Derived TGF-." *The Journal of Immunology* 184 (10): 5885–94. https://doi.org/10.4049/jimmunol.0903143.

Peng, Y, X Chen, Q Liu, X Zhang, K Huang, L Liu, H Li, et al. 2015. "Mesenchymal Stromal Cells Infusions Improve Refractory Chronic Graft versus Host Disease through an Increase of CD5+ Regulatory B Cells Producing Interleukin 10." *Leukemia* 29 (3): 636–46. https://doi.org/10.1038/leu.2014.225.

Pennock, Nathan D, Jason T White, Eric W Cross, Elizabeth E Cheney, Beth A Tamburini, and Ross M Kedl. 2013. "T Cell Responses: Naive to Memory and Everything in Between." *Advances in Physiology Education* 37 (4): 273–83. https://doi.org/10.1152/advan.00066.2013.

Perea-Gil, Isaac, Carolina Gálvez-Montón, Cristina Prat-Vidal, Ignasi Jorba, Cristina Segú-Vergés, Santiago Roura, Carolina Soler-Botija, et al. 2018. "Head-to-Head Comparison of Two Engineered Cardiac Grafts for Myocardial Repair : From Scaffold Characterization to Pre-Clinical Testing." *Scientific Reports* (8)6708 (September 2017): 1–13. https://doi.org/10.1038/s41598-018-25115-2.

Perea-Gil, Isaac, Marta Monguió-Tortajada, Carolina Gálvez-Montón, Antoni Bayes-Genis, Francesc E Borràs, and Santiago Roura. 2015. "Preclinical Evaluation of the Immunomodulatory Properties of Cardiac Adipose Tissue Progenitor Cells Using Umbilical Cord Blood Mesenchymal Stem Cells: A Direct Comparative Study." *BioMed Research*

International 2015 (January): 439808. https://doi.org/10.1155/2015/439808.

Perea-Gil, Isaac, Cristina Prat-Vidal, and Antoni Bayes-Genis. 2015. "In Vivo Experience with Natural Scaffolds for Myocardial Infarction: The Times They Are a-Changin'." *Stem Cell Research & Therapy* 6 (1): 248. https://doi.org/10.1186/s13287-015-0237-4.

Perea-Gil, Isaac, Cristina Prat-Vidal, Carolina Gálvez-Montón, Santiago Roura, Aida Llucià-Valldeperas, Carolina Soler-Botija, Oriol Iborra-Egea, et al. 2016. "A Cell-Enriched Engineered Myocardial Graft Limits Infarct Size and Improves Cardiac Function: Pre-Clinical Study in the Porcine Myocardial Infarction Model." *JACC: Basic to Translational Science* 1 (5): 360–72. https://doi.org/10.1016/j.jacbts.2016.06.005.

Perea-Gil, Isaac, Juan J Uriarte, Cristina Prat-Vidal, Carolina Gálvez-Montón, Santiago Roura, Aida Llucià-Valldeperas, Carolina Soler-Botija, Ramon Farré, Daniel Navajas, and Antoni Bayes-Genis. 2015. "In Vitro Comparative Study of Two Decellularization Protocols in Search of an Optimal Myocardial Scaffold for Recellularization." *American Journal of Translational Research* 7 (3): 558–73. http://www.ncbi.nlm.nih.gov/pubmed/26045895.

Perea Gil, Isaac. 2017. "Cell-Enriched Engineered Cardiac Grafts Improve Heart Function and Promote Cardiac Regeneration: A Novel Therapy for Myocardial Infarction." Universitat de Barcelona. http://diposit.ub.edu/dspace/handle/2445/117202.

Perez-Hernandez, Daniel, Cristina Gutiérrez-Vázquez, Inmaculada Jorge, Soraya López-Martín, Angeles Ursa, Francisco Sánchez-Madrid, Jesús Vázquez, and María Yáñez-Mó. 2013. "The Intracellular Interactome of Tetraspanin-Enriched Microdomains Reveals Their Function as Sorting Machineries toward Exosomes." *The Journal of Biological Chemistry* 288 (17): 11649–61. https://doi.org/10.1074/jbc.M112.445304.

Petersen, C.B., A.-B. Nygård, B. Viuff, M. Fredholm, B. Aasted, and J. Salomonsen. 2007. "Porcine Ecto-Nucleotide Pyrophosphatase/phosphodiesterase 1 (NPP1/CD203a): Cloning, Transcription, Expression, Mapping, and Identification of an NPP1/CD203a Epitope for Swine Workshop Cluster 9 (SWC9) Monoclonal Antibodies." *Developmental & Comparative Immunology* 31 (6): 618–31. https://doi.org/10.1016/j.dci.2006.08.012.

Petersen, Kevin E., Eliana Manangon, Joshua L. Hood, Samuel A. Wickline, Diego P. Fernandez, William P. Johnson, and Bruce K. Gale. 2014. "A Review of Exosome Separation Techniques and Characterization of B16-F10 Mouse Melanoma Exosomes with AF4-UV-MALS-DLS-TEM." *Analytical and Bioanalytical Chemistry* 406 (30): 7855–66. https://doi.org/10.1007/s00216-014-8040-0.

Pinhal-Enfield, Grace, Madhuri Ramanathan, Gyorgy Hasko, Stefanie N. Vogel, Andrew L. Salzman, Geert-Jan Boons, and S. Joseph Leibovich. 2003. "An Angiogenic Switch in Macrophages Involving Synergy between Toll-Like Receptors 2, 4, 7, and 9 and Adenosine A2A Receptors." *The American Journal of Pathology* 163 (2): 711–21. https://doi.org/10.1016/S0002-9440(10)63698-X.

Pittenger, M F, A M Mackay, S C Beck, R K Jaiswal, R Douglas, J D Mosca, M A Moorman, D W Simonetti, S Craig, and D R Marshak. 1999. "Multilineage Potential of Adult Human Mesenchymal Stem Cells." *Science (New York, N.Y.)* 284 (5411): 143–47. https://doi.org/10.1126/SCIENCE.284.5411.143.

Plumas, J, L Chaperot, M-J Richard, J-P Molens, J-C Bensa, and M-C Favrot. 2005. "Mesenchymal Stem Cells Induce Apoptosis of Activated T Cells." *Leukemia* 19 (9): 1597–1604. https://doi.org/10.1038/sj.leu.2403871.

Pol, E. van der, A. Sturk, T. van Leeuwen, R. Nieuwland, F. Coumans, and ISTH-SSC-VB Working group. 2018. "Standardization of Extracellular Vesicle Measurements by Flow Cytometry through Vesicle Diameter Approximation." *Journal of Thrombosis and Haemostasis* 16 (6):

1236–45. https://doi.org/10.1111/jth.14009.

Pol, Edwin van der, Anita N Böing, Paul Harrison, Augueste Sturk, and Rienk Nieuwland. 2012. "Classification, Functions, and Clinical Relevance of Extracellular Vesicles." *Pharmacological Reviews* 64 (3): 676–705. https://doi.org/10.1124/pr.112.005983.

Polchert, David, Justin Sobinsky, Gw Douglas, Martha Kidd, Ada Moadsiri, Eduardo Reina, Kristyn Genrich, et al. 2008. "IFN-Gamma Activation of Mesenchymal Stem Cells for Treatment and Prevention of Graft versus Host Disease." *European Journal of Immunology* 38 (6): 1745–55. https://doi.org/10.1002/eji.200738129.

Prat-Vidal, C, S Roura, J Farré, C Gálvez, A Llach, C E Molina, L Hove-Madsen, J Garcia, J Cinca, and A Bayes-Genis. 2007. "Umbilical Cord Blood-Derived Stem Cells Spontaneously Express Cardiomyogenic Traits." *Transplantation Proceedings* 39 (7): 2434–37. https://doi.org/10.1016/j.transproceed.2007.06.016.

Prat-Vidal, Cristina, Carolina Gálvez-Montón, Verónica Puig-Sanvicens, Benjamin Sanchez, Idoia Díaz-Güemes, Paco Bogónez-Franco, Isaac Perea-Gil, et al. 2014. "Online Monitoring of Myocardial Bioprosthesis for Cardiac Repair." *International Journal of Cardiology* 174 (3): 654–61. https://doi.org/10.1016/j.ijcard.2014.04.181.

Pujol-Autonell, Irma, Rosa-Maria Ampudia, Raquel Planas, Silvia Marin-Gallen, Jorge Carrascal, Alex Sanchez, Ana Marin, et al. 2013. "Efferocytosis Promotes Suppressive Effects on Dendritic Cells through Prostaglandin E2 Production in the Context of Autoimmunity." Edited by Massimo Pietropaolo. *PLoS ONE* 8 (5): e63296. https://doi.org/10.1371/journal.pone.0063296.

Qi, Yu, Dongsheng Jiang, Anca Sindrilaru, Agatha Stegemann, Susanne Schatz, Nicolai Treiber, Markus Rojewski, et al. 2014. "TSG-6 Released from Intradermally Injected Mesenchymal Stem Cells Accelerates Wound Healing and Reduces Tissue Fibrosis in Murine Full-Thickness Skin Wounds." *Journal of Investigative Dermatology* 134 (2): 526–37. https://doi.org/10.1038/jid.2013.328.

Rafei, M., J. Hsieh, S. Fortier, M. Li, S. Yuan, E. Birman, K. Forner, et al. 2008. "Mesenchymal Stromal Cell-Derived CCL2 Suppresses Plasma Cell Immunoglobulin Production via STAT3 Inactivation and PAX5 Induction." *Blood* 112 (13): 4991–98. https://doi.org/10.1182/blood-2008-07-166892.

Raposo, G, H W Nijman, W Stoorvogel, R Liejendekker, C V Harding, C J Melief, and H J Geuze. 1996. "B Lymphocytes Secrete Antigen-Presenting Vesicles." *The Journal of Experimental Medicine* 183: 1161–72. https://doi.org/10.1084/jem.183.3.1161.

Rasmusson, I., K. Le Blanc, B. Sundberg, and O. Ringdén. 2007. "Mesenchymal Stem Cells Stimulate Antibody Secretion in Human B Cells." *Scandinavian Journal of Immunology* 65 (4): 336–43. https://doi.org/10.1111/j.1365-3083.2007.01905.x.

Regateiro, Frederico S, Stephen P Cobbold, and Herman Waldmann. 2013. "CD73 and Adenosine Generation in the Creation of Regulatory Microenvironments." *Clinical and Experimental Immunology* 171 (1): 1–7. https://doi.org/10.1111/j.1365-2249.2012.04623.x.

Regateiro, Frederico S, Duncan Howie, Kathleen F Nolan, Eleftherios I Agorogiannis, David R Greaves, Stephen P Cobbold, and Herman Waldmann. 2011. "Generation of Anti-Inflammatory Adenosine by Leukocytes Is Regulated by TGF-β." *European Journal of Immunology* 41 (10): 2955–65. https://doi.org/10.1002/eji.201141512.

Renner, P, E Eggenhofer, A Rosenauer, F C Popp, J F Steinmann, P Slowik, E K Geissler, P Piso, H J Schlitt, and M H Dahlke. 2009. "Mesenchymal Stem Cells Require a Sufficient, Ongoing Immune Response to Exert Their Immunosuppressive Function." *Transplantation*

Proceedings 41 (6): 2607–11. https://doi.org/10.1016/j.transproceed.2009.06.119.

Rossi, Jean-François, Zhao-Yang Lu, Michel Jourdan, and Bernard Klein. 2015. "Interleukin-6 as a Therapeutic Target." *Clinical Cancer Research : An Official Journal of the American Association for Cancer Research* 21 (6): 1248–57. https://doi.org/10.1158/1078-0432.CCR-14-2291.

Roura, Santiago, Juli R Bagó, Carolina Soler-Botija, Josep M Pujal, Carolina Gálvez-Montón, Cristina Prat-Vidal, Aida Llucià-Valldeperas, Jerónimo Blanco, and Antoni Bayes-Genis. 2012. "Human Umbilical Cord Blood-Derived Mesenchymal Stem Cells Promote Vascular Growth in Vivo." Edited by David S. Milstone. *PloS One* 7 (11): e49447. https://doi.org/10.1371/journal.pone.0049447.

Roura, Santiago, Carolina Gálvez-Montón, David de Gonzalo-Calvo, Ana Gámez Valero, Paloma Gastelurrutia, Elena Revuelta-López, Cristina Prat-Vidal, et al. 2017. "Extracellular Vesicles Do Not Contribute to Higher Circulating Levels of Soluble LRP1 in Idiopathic Dilated Cardiomyopathy." *Journal of Cellular and Molecular Medicine* 21 (11): 3000–3009. https://doi.org/10.1111/jcmm.13211.

Roura, Santiago, Carolina Gálvez-Montón, Josep Lupón, and Antoni Bayes-Genis. 2017. "Biotherapies and Biomarkers for Cardiovascular Diseases." *European Heart Journal* 38 (23): 1784–86. https://doi.org/10.1093/eurheartj/ehx265.

Roura, Santiago, Carolina Gálvez-Montón, Clémentine Mirabel, Joaquim Vives, and Antoni Bayes-Genis. 2017. "Mesenchymal Stem Cells for Cardiac Repair: Are the Actors Ready for the Clinical Scenario?" *Stem Cell Research & Therapy* 8 (1): 238. https://doi.org/10.1186/s13287-017-0695-y.

Roura, Santiago, Ana Gámez-Valero, Josep Lupón, Carolina Gálvez-Montón, Francesc E. Borràs, and Antoni Bayes-Genis. 2018. "Proteomic Signature of Circulating Extracellular Vesicles in Dilated Cardiomyopathy." *Laboratory Investigation*, March. https://doi.org/10.1038/s41374-018-0044-5.

Roura, Santiago, Carolina Soler-Botija, Juli R Bagó, Aida Llucià-Valldeperas, Marco A Férnandez, Carolina Gálvez-Montón, Cristina Prat-Vidal, Isaac Perea-Gil, Jerónimo Blanco, and Antoni Bayes-Genis. 2015. "Postinfarction Functional Recovery Driven by a Three-Dimensional Engineered Fibrin Patch Composed of Human Umbilical Cord Blood-Derived Mesenchymal Stem Cells." *Stem Cells Translational Medicine* 4 (8): 956–66. https://doi.org/10.5966/sctm.2014-0259.

Royo, Felix, Patricia Zuñiga-Garcia, Pilar Sanchez-Mosquera, Ainara Egia, Amparo Perez, Ana Loizaga, Raquel Arceo, et al. 2016. "Different EV Enrichment Methods Suitable for Clinical Settings Yield Different Subpopulations of Urinary Extracellular Vesicles from Human Samples." *Journal of Extracellular Vesicles* 5 (January): 29497. http://www.pubmedcentral.nih.gov/articlerender.fcgi?artid=4759834&tool=pmcentrez&rendertype=abstract.

Rutz, Sascha, and Wenjun Ouyang. 2011. "Regulation of Interleukin-10 and Interleukin-22 Expression in T Helper Cells." *Current Opinion in Immunology* 23 (5): 605–12. https://doi.org/10.1016/J.COI.2011.07.018.

Ryan, J M, F Barry, J M Murphy, and B P Mahon. 2007. "Interferon-Gamma Does Not Break, but Promotes the Immunosuppressive Capacity of Adult Human Mesenchymal Stem Cells." *Clinical and Experimental Immunology* 149 (2): 353–63. https://doi.org/10.1111/j.1365-2249.2007.03422.x.

Saeidi, Mohsen, Ahmad Masoud, Yadollah Shakiba, Jamshid Hadjati, Mandana Mohyeddin Bonab, Mohammad Hossein Nicknam, Mostafa Latifpour, and Behrooz Nikbin. 2013.

"Immunomodulatory Effects of Human Umbilical Cord Wharton's Jelly-Derived Mesenchymal Stem Cells on Differentiation, Maturation and Endocytosis of Monocyte-Derived Dendritic Cells." *Iranian Journal of Allergy, Asthma, and Immunology* 12 (1): 37–49. https://doi.org/012.01/ijaai.3749.

Sakaguchi, Katsuhisa, Tatsuya Shimizu, and Teruo Okano. 2015. "Construction of Three-Dimensional Vascularized Cardiac Tissue with Cell Sheet Engineering." *Journal of Controlled Release* 205 (May): 83–88. https://doi.org/10.1016/j.jconrel.2014.12.016.

Sala, Emanuela, Marco Genua, Luciana Petti, Achille Anselmo, Vincenzo Arena, Javier Cibella, Lucia Zanotti, et al. 2015. "Mesenchymal Stem Cells Reduce Colitis in Mice via Release of TSG6, Independently of Their Localization to the Intestine." *Gastroenterology* 149 (1): 163–176.e20. https://doi.org/10.1053/j.gastro.2015.03.013.

Saldanha-Araujo, Felipe, Flávia I S Ferreira, Patrícia V Palma, Amélia G Araujo, Regina H C Queiroz, Dimas T Covas, Marco A Zago, and Rodrigo A Panepucci. 2011. "Mesenchymal Stromal Cells up-Regulate CD39 and Increase Adenosine Production to Suppress Activated T-Lymphocytes." *Stem Cell Research* 7 (1): 66–74. https://doi.org/10.1016/j.scr.2011.04.001.

Sarig, Udi, and Marcelle Machluf. 2011. "Engineering Cell Platforms for Myocardial Regeneration." *Expert Opinion on Biological Therapy* 11 (8): 1055–77. https://doi.org/10.1517/14712598.2011.578574.

Sato, K., K. Ozaki, I. Oh, A. Meguro, K. Hatanaka, T. Nagai, K. Muroi, and K. Ozawa. 2007. "Nitric Oxide Plays a Critical Role in Suppression of T-Cell Proliferation by Mesenchymal Stem Cells." *Blood* 109 (1): 228–34. https://doi.org/10.1182/blood-2006-02-002246.

Saze, Zenichiro, Patrick J. Schuler, Chang-Sook Hong, Dongmei Cheng, Edwin K. Jackson, and Theresa L. Whiteside. 2013. "Adenosine Production by Human B Cells and B Cell-Mediated Suppression of Activated T Cells." *Blood* 122 (1): 9–18. https://doi.org/10.1182/blood-2013-02-482406.

Schena, Francesca, Claudio Gambini, Andrea Gregorio, Manuela Mosconi, Daniele Reverberi, Marco Gattorno, Simona Casazza, et al. 2010. "Interferon-γ-Dependent Inhibition of B Cell Activation by Bone Marrow-Derived Mesenchymal Stem Cells in a Murine Model of Systemic Lupus Erythematosus." *Arthritis & Rheumatism* 62 (9): 2776–86. https://doi.org/10.1002/art.27560.

Schenk, Ursula, Michela Frascoli, Michele Proietti, Robert Geffers, Elisabetta Traggiai, Jan Buer, Camillo Ricordi, et al. 2011. "ATP Inhibits the Generation and Function of Regulatory T Cells through the Activation of Purinergic P2X Receptors." *Science Signaling* 4 (162): ra12. https://doi.org/10.1126/scisignal.2001270.

Selmani, Zohair, Abderrahim Naji, Ines Zidi, Benoit Favier, Emilie Gaiffe, Laurent Obert, Christophe Borg, et al. 2008. "Human Leukocyte Antigen-G5 Secretion by Human Mesenchymal Stem Cells Is Required to Suppress T Lymphocyte and Natural Killer Function and to Induce CD4 $^{+}$ CD25 ^{high} FOXP3 $^{+}$ Regulatory T Cells." *Stem Cells* 26 (1): 212–22. https://doi.org/10.1634/stemcells.2007-0554.

Shi, Chao, and Eric G Pamer. 2011. "Monocyte Recruitment during Infection and Inflammation." *Nature Reviews. Immunology* 11 (11): 762–74. https://doi.org/10.1038/nri3070.

Shimizu, Tatsuya, Masayuki Yamato, Yuki Isoi, Takumitsu Akutsu, Takeshi Setomaru, Kazuhiko Abe, Akihiko Kikuchi, Mitsuo Umezu, and Teruo Okano. 2002. "Fabrication of Pulsatile Cardiac Tissue Grafts Using a Novel 3-Dimensional Cell Sheet Manipulation Technique and Temperature-Responsive Cell Culture Surfaces." *Circulation Research* 90 (3): e40. http://www.ncbi.nlm.nih.gov/pubmed/11861428.

Sica, Antonio, and Alberto Mantovani. 2012. “Macrophage Plasticity and Polarization: In Vivo Veritas.” *The Journal of Clinical Investigation* 122 (3): 787–95. https://doi.org/10.1172/JCI59643.

Sicco, Claudia Lo, Daniele Reverberi, Carolina Balbi, Valentina Ulivi, Elisa Principi, Luisa Pascucci, Pamela Becherini, et al. 2017. “Mesenchymal Stem Cell-Derived Extracellular Vesicles as Mediators of Anti-Inflammatory Effects: Endorsement of Macrophage Polarization.” *STEM CELLS Translational Medicine*, January. https://doi.org/10.1002/sctm.16-0363.

Singleton, Helen, Simon P. Graham, Katherine B. Bodman-Smith, Jean Pierre Frossard, and Falko Steinbach. 2016. “Establishing Porcine Monocyte-Derived Macrophage and Dendritic Cell Systems for Studying the Interaction with PRRSV-1.” *Frontiers in Microbiology* 7 (JUN): 1–15. https://doi.org/10.3389/fmicb.2016.00832.

Smail, E H, B N Cronstein, T Meshulam, A L Esposito, R W Ruggeri, and R D Diamond. 1992. “In Vitro, Candida Albicans Releases the Immune Modulator Adenosine and a Second, High-Molecular Weight Agent That Blocks Neutrophil Killing.” *Journal of Immunology (Baltimore, Md. : 1950)* 148 (11): 3588–95. http://www.ncbi.nlm.nih.gov/pubmed/1316920.

Soleymaninejadian, Ehsan, Krishna Pramanik, and Esmaeil Samadian. 2012. “Immunomodulatory Properties of Mesenchymal Stem Cells: Cytokines and Factors.” *American Journal of Reproductive Immunology* 67 (1): 1–8. https://doi.org/10.1111/j.1600-0897.2011.01069.x.

Soriano, Joan B., David Rojas-Rueda, Jordi Alonso, Josep M. Antó, Pere-Joan Cardona, Esteve Fernández, Alberto L. Garcia-Basteiro, et al. 2018. “La Carga de Enfermedad En España: Resultados Del Estudio de La Carga Global de Las Enfermedades 2016.” *Medicina Clínica*, July. https://doi.org/10.1016/j.medcli.2018.05.011.

Sotiropoulou, Panagiota A, Sonia A Perez, Angelos D Gritzapis, Constantin N Baxevanis, and Michael Papamichail. 2006. “Interactions between Human Mesenchymal Stem Cells and Natural Killer Cells.” *Stem Cells (Dayton, Ohio)* 24 (1): 74–85. https://doi.org/10.1634/stemcells.2004-0359.

Spaggiari, Grazia Maria, Heba Abdelrazik, Flavio Becchetti, and Lorenzo Moretta. 2009. “MSCs Inhibit Monocyte-Derived DC Maturation and Function by Selectively Interfering with the Generation of Immature DCs: Central Role of MSC-Derived Prostaglandin E2.” *Blood* 113 (26): 6576–83. https://doi.org/10.1182/blood-2009-02-203943.

Spaggiari, Grazia Maria, Andrea Capobianco, Heba Abdelrazik, Flavio Becchetti, Maria Cristina Mingari, and Lorenzo Moretta. 2008. “Mesenchymal Stem Cells Inhibit Natural Killer-Cell Proliferation, Cytotoxicity, and Cytokine Production: Role of Indoleamine 2,3-Dioxygenase and Prostaglandin E2.” *Blood* 111 (3): 1327–33. https://doi.org/10.1182/blood-2007-02-074997.

Stagg, John, Upulie Divisekera, Nicole McLaughlin, Janelle Sharkey, Sandra Pommey, Delphine Denoyer, Karen M Dwyer, and Mark J Smyth. 2010. “Anti-CD73 Antibody Therapy Inhibits Breast Tumor Growth and Metastasis.” *Proceedings of the National Academy of Sciences of the United States of America* 107 (4): 1547–52. https://doi.org/10.1073/pnas.0908801107.

Stewart, C. Andrew, Hannah Metheny, Noriho Iida, Loretta Smith, Miranda Hanson, Folkert Steinhagen, Robert M. Leighty, et al. 2013. “Interferon-Dependent IL-10 Production by Tregs Limits Tumor Th17 Inflammation.” *Journal of Clinical Investigation* 123 (11): 4859–74. https://doi.org/10.1172/JCI65180.

Strauer, Bodo-Eckehard, and Gustav Steinhoff. 2011. “10 Years of Intracoronary and Intramyocardial Bone Marrow Stem Cell Therapy of the Heart.” *Journal of the American*

College of Cardiology 58 (11): 1095–1104. https://doi.org/10.1016/j.jacc.2011.06.016.

Swirski, F. K., M. Nahrendorf, M. Etzrodt, M. Wildgruber, V. Cortez-Retamozo, P. Panizzi, J.-L. Figueiredo, et al. 2009. "Identification of Splenic Reservoir Monocytes and Their Deployment to Inflammatory Sites." *Science* 325 (5940): 612–16. https://doi.org/10.1126/science.1175202.

Szabo, C., and P. Pacher. 2012. "The Outsiders: Emerging Roles of Ectonucleotidases in Inflammation." *Science Translational Medicine* 4 (146): 146ps14-146ps14. https://doi.org/10.1126/scitranslmed.3004378.

Takahashi, Kazutoshi, and Shinya Yamanaka. 2006. "Induction of Pluripotent Stem Cells from Mouse Embryonic and Adult Fibroblast Cultures by Defined Factors." *Cell* 126 (4): 663–76. https://doi.org/10.1016/j.cell.2006.07.024.

Tanai, Edit, and Stefan Frantz. 2015. "Pathophysiology of Heart Failure." In *Comprehensive Physiology*, 187–214. Hoboken, NJ, USA: John Wiley & Sons, Inc. https://doi.org/10.1002/cphy.c140055.

Tang, Yue-Ting, Yi-Yao Huang, Lei Zheng, Si-Hua Qin, Xu-Ping Xu, Tai-Xue An, Yong Xu, et al. 2017. "Comparison of Isolation Methods of Exosomes and Exosomal RNA from Cell Culture Medium and Serum." *International Journal of Molecular Medicine* 40 (3): 834–44. https://doi.org/10.3892/ijmm.2017.3080.

Taylor, Doris A., Luiz C. Sampaio, Zannatul Ferdous, Andrea S. Gobin, and Lakeshia J. Taite. 2018. "Decellularized Matrices in Regenerative Medicine." *Acta Biomaterialia*, April. https://doi.org/10.1016/j.actbio.2018.04.044.

Taylor, Douglas D., and Sahil Shah. 2015. "Methods of Isolating Extracellular Vesicles Impact down-Stream Analyses of Their Cargoes." *Methods* 87 (October): 3–10. https://doi.org/10.1016/J.YMETH.2015.02.019.

Terness, Peter, Thomas M Bauer, Lars Röse, Christoph Dufter, Andrea Watzlik, Helmut Simon, and Gerhard Opelz. 2002. "Inhibition of Allogeneic T Cell Proliferation by Indoleamine 2,3-Dioxygenase-Expressing Dendritic Cells: Mediation of Suppression by Tryptophan Metabolites." *The Journal of Experimental Medicine* 196 (4): 447–57. http://www.ncbi.nlm.nih.gov/pubmed/12186837.

Thammavongsa, Vilasack, Justin W Kern, Dominique M Missiakas, and Olaf Schneewind. 2009. "Staphylococcus Aureus Synthesizes Adenosine to Escape Host Immune Responses." *The Journal of Experimental Medicine* 206 (11): 2417–27. https://doi.org/10.1084/jem.20090097.

Théry, Clotilde, Aled Clayton, Sebastian Amigorena, and Graca Raposo. 2006. "Isolation and Characterization of Exosomes from Cell Culture Supernatants." *Current Protocols in Cell Biology*, 3.22.1-3.22.29.

Thompson, Linda F., Holger K. Eltzschig, Juan C. Ibla, C. Justin Van De Wiele, Regina Resta, Julio C. Morote-Garcia, and Sean P. Colgan. 2004. "Crucial Role for Ecto-5'-Nucleotidase (CD73) in Vascular Leakage during Hypoxia." *The Journal of Experimental Medicine* 200 (11): 1395–1405. https://doi.org/10.1084/jem.20040915.

Timmers, Leo, Sai Kiang Lim, Fatih Arslan, Jeffrey S. Armstrong, Imo E. Hoefer, Pieter A. Doevendans, Jan J. Piek, et al. 2008. "Reduction of Myocardial Infarct Size by Human Mesenchymal Stem Cell Conditioned Medium." *Stem Cell Research* 1 (2): 129–37. https://doi.org/10.1016/J.SCR.2008.02.002.

Tipnis, Shabari, Chandra Viswanathan, and Anish S Majumdar. 2010. "Immunosuppressive Properties of Human Umbilical Cord-Derived Mesenchymal Stem Cells: Role of B7-H1 and

IDO." *Immunology and Cell Biology* 88 (8): 795–806. https://doi.org/10.1038/icb.2010.47.

Trajkovic, K., C. Hsu, S. Chiantia, L. Rajendran, D. Wenzel, F. Wieland, P. Schwille, B. Brugger, and M. Simons. 2008. "Ceramide Triggers Budding of Exosome Vesicles into Multivesicular Endosomes." *Science* 319 (5867): 1244–47. https://doi.org/10.1126/science.1153124.

Troyer, Deryl L, and Mark L Weiss. 2008. "Wharton's Jelly-Derived Cells Are a Primitive Stromal Cell Population." *Stem Cells (Dayton, Ohio)* 26 (3): 591–99. https://doi.org/10.1634/stemcells.2007-0439.

Tse, William T, John D Pendleton, Wendy M Beyer, Matthew C Egalka, and Eva C Guinan. 2003. "Suppression of Allogeneic T-Cell Proliferation by Human Marrow Stromal Cells: Implications in Transplantation." *Transplantation* 75 (3): 389–97. https://doi.org/10.1097/01.TP.0000045055.63901.A9.

Tsujioka, Hiroto, Toshio Imanishi, Hideyuki Ikejima, Akio Kuroi, Shigeho Takarada, Takashi Tanimoto, Hironori Kitabata, et al. 2009. "Impact of Heterogeneity of Human Peripheral Blood Monocyte Subsets on Myocardial Salvage in Patients With Primary Acute Myocardial Infarction." *Journal of the American College of Cardiology* 54 (2): 130–38. https://doi.org/10.1016/j.jacc.2009.04.021.

Tu, Zhidan, Qing Li, Hong Bu, and Feng Lin. 2010. "Mesenchymal Stem Cells Inhibit Complement Activation by Secreting Factor H." *Stem Cells and Development* 19 (11): 1803–9. https://doi.org/10.1089/scd.2009.0418.

Ullah, Mujib, Jan Eucker, Michael Sittinger, and Jochen Ringe. 2013. "Mesenchymal Stem Cells and Their Chondrogenic Differentiated and Dedifferentiated Progeny Express Chemokine Receptor CCR9 and Chemotactically Migrate toward CCL25 or Serum." *Stem Cell Research & Therapy* 4 (4): 99. https://doi.org/10.1186/scrt310.

van Niel, Guillaume, Stéphanie Charrin, Sabrina Simoes, Maryse Romao, Leila Rochin, Paul Saftig, Michael S. Marks, Eric Rubinstein, and Graça Raposo. 2011. "The Tetraspanin CD63 Regulates ESCRT-Independent and -Dependent Endosomal Sorting during Melanogenesis." *Developmental Cell* 21 (4): 708–21. https://doi.org/10.1016/J.DEVCEL.2011.08.019.

Varga, Tamas, Rémi Mounier, Andreas Patsalos, Péter Gogolák, Matthew Peloquin, Attila Horvath, Attila Pap, et al. 2016. "Macrophage PPARγ, a Lipid Activated Transcription Factor Controls the Growth Factor GDF3 and Skeletal Muscle Regeneration." *Immunity* 45 (5): 1038–51. https://doi.org/10.1016/j.immuni.2016.10.016.

Vilahur, Gemma, Manuel Gutiérrez, Laura Casani, Lourdes Varela, Antoni Capdevila, Guillem Pons-Lladó, Francesc Carreras, Leif Carlsson, Alberto Hidalgo, and Lina Badimon. 2016. "Protective Effects of Ticagrelor on Myocardial Injury After InfarctionClinical Perspective." *Circulation* 134 (22): 1708–19. https://doi.org/10.1161/CIRCULATIONAHA.116.024014.

Volpe, Elisabetta, Nicolas Servant, Raphaël Zollinger, Sofia I Bogiatzi, Philippe Hupé, Emmanuel Barillot, and Vassili Soumelis. 2008. "A Critical Function for Transforming Growth Factor-Beta, Interleukin 23 and Proinflammatory Cytokines in Driving and Modulating Human T(H)-17 Responses." *Nature Immunology* 9 (6): 650–57. https://doi.org/10.1038/ni.1613.

Wanderer, Alan A. 2008. "Ischemic-Reperfusion Syndromes: Biochemical and Immunologic Rationale for IL-1 Targeted Therapy." *Clinical Immunology* 128 (2): 127–32. https://doi.org/10.1016/J.CLIM.2008.03.514.

Wang, Nan, Qinggang Li, Li Zhang, Hongli Lin, Jie Hu, Diangeng Li, Suozhu Shi, et al. 2012. "Mesenchymal Stem Cells Attenuate Peritoneal Injury through Secretion of TSG-6." Edited by Niels Olsen Saraiva Câmara. *PLoS ONE* 7 (8): e43768. https://doi.org/10.1371/journal.pone.0043768.

Wang, T., D. M. Gilkes, N. Takano, L. Xiang, W. Luo, C. J. Bishop, P. Chaturvedi, J. J. Green, and G. L. Semenza. 2014. "Hypoxia-Inducible Factors and RAB22A Mediate Formation of Microvesicles That Stimulate Breast Cancer Invasion and Metastasis." *Proceedings of the National Academy of Sciences* 111 (31): E3234–42. https://doi.org/10.1073/pnas.1410041111.

Watt, Suzanne M, Francesca Gullo, Mark van der Garde, Daniel Markeson, Rosalba Camicia, Cheen P Khoo, and Jaap Jan Zwaginga. 2013. "The Angiogenic Properties of Mesenchymal Stem/stromal Cells and Their Therapeutic Potential." *British Medical Bulletin* 108 (January): 25–53. https://doi.org/10.1093/bmb/ldt031.

Welsh, Joshua A., Judith A. Holloway, James S. Wilkinson, and Nicola A. Englyst. 2017. "Extracellular Vesicle Flow Cytometry Analysis and Standardization." *Frontiers in Cell and Developmental Biology* 5 (August): 78. https://doi.org/10.3389/fcell.2017.00078.

Welton, Joanne Louise, Jason Paul Webber, Laur-Alexandru Botos, Michael Jones, and Aled Clayton. 2015. "Ready-Made Chromatography Columns for Extracellular Vesicle Isolation from Plasma." *Journal of Extracellular Vesicles* 4 (January): 27269. http://www.pubmedcentral.nih.gov/articlerender.fcgi?artid=4376847&tool=pmcentrez&rendertype=abstract.

Westman, Peter C, Michael J Lipinski, Dror Luger, Ron Waksman, Robert O Bonow, Edwin Wu, and Stephen E Epstein. 2016. "Inflammation as a Driver of Adverse Left Ventricular Remodeling After Acute Myocardial Infarction." *Journal of the American College of Cardiology* 67 (17): 2050–60. https://doi.org/10.1016/j.jacc.2016.01.073.

WHO Regional Office for Africa. 2014. "The African Regional Health Report 2014."

Wiklander, Oscar P. B., R. Beklem Bostancioglu, Joshua A. Welsh, Antje M. Zickler, Florian Murke, Giulia Corso, Ulrika Felldin, et al. 2018. "Systematic Methodological Evaluation of a Multiplex Bead-Based Flow Cytometry Assay for Detection of Extracellular Vesicle Surface Signatures." *Frontiers in Immunology* 9 (June): 1326. https://doi.org/10.3389/fimmu.2018.01326.

Willis, Gareth R., Stella Kourembanas, and S. Alex Mitsialis. 2017. "Toward Exosome-Based Therapeutics: Isolation, Heterogeneity, and Fit-for-Purpose Potency." *Frontiers in Cardiovascular Medicine* 4 (October): 63. https://doi.org/10.3389/fcvm.2017.00063.

Willms, Eduard, Carlos Cabañas, Imre Mäger, Matthew J. A. Wood, and Pieter Vader. 2018. "Extracellular Vesicle Heterogeneity: Subpopulations, Isolation Techniques, and Diverse Functions in Cancer Progression." *Frontiers in Immunology* 9 (April): 738. https://doi.org/10.3389/fimmu.2018.00738.

Willms, Eduard, Henrik J Johansson, Imre Mäger, Yi Lee, K Emelie M Blomberg, Mariam Sadik, Amr Alaarg, et al. 2016. "Cells Release Subpopulations of Exosomes with Distinct Molecular and Biological Properties." *Scientific Reports* 6 (1): 22519. https://doi.org/10.1038/srep22519.

Windecker, Stephan, Jeroen J Bax, Aung Myat, Gregg W Stone, and Michael S Marber. 2013. "Future Treatment Strategies in ST-Segment Elevation Myocardial Infarction." *The Lancet* 382 (9892): 644–57. https://doi.org/10.1016/S0140-6736(13)61452-X.

Witte, Samantha F.H. de, Franka Luk, Jesus M. Sierra Parraga, Madhu Gargesha, Ana Merino, Sander S. Korevaar, Anusha S. Shankar, et al. 2018. "Immunomodulation By Therapeutic Mesenchymal Stromal Cells (MSC) Is Triggered Through Phagocytosis of MSC By Monocytic Cells." *STEM CELLS* 36 (4): 602–15. https://doi.org/10.1002/stem.2779.

Witte, Samantha F H de, Marcella Franquesa, Carla C Baan, and Martin J Hoogduijn. 2015.

"Toward Development of iMesenchymal Stem Cells for Immunomodulatory Therapy." *Frontiers in Immunology* 6 (January): 648. https://doi.org/10.3389/fimmu.2015.00648.

Xu, Rong, David W. Greening, Alin Rai, Hong Ji, and Richard J. Simpson. 2015. "Highly-Purified Exosomes and Shed Microvesicles Isolated from the Human Colon Cancer Cell Line LIM1863 by Sequential Centrifugal Ultrafiltration Are Biochemically and Functionally Distinct." *Methods* 87 (October): 11–25. https://doi.org/10.1016/j.ymeth.2015.04.008.

Xu, Rong, Richard J. Simpson, and David W. Greening. 2017. "A Protocol for Isolation and Proteomic Characterization of Distinct Extracellular Vesicle Subtypes by Sequential Centrifugal Ultrafiltration." In *Methods in Molecular Biology (Clifton, N.J.)*, 1545:91–116. https://doi.org/10.1007/978-1-4939-6728-5_7.

Yan, Xiaoxiang, Atsushi Anzai, Yoshinori Katsumata, Tomohiro Matsuhashi, Kentaro Ito, Jin Endo, Tsunehisa Yamamoto, et al. 2013. "Temporal Dynamics of Cardiac Immune Cell Accumulation Following Acute Myocardial Infarction." *Journal of Molecular and Cellular Cardiology* 62 (September): 24–35. https://doi.org/10.1016/j.yjmcc.2013.04.023.

Yáñez-Mó, María, Pia R-M Siljander, Zoraida Andreu, Apolonija Bedina Zavec, Francesc E Borràs, Edit I Buzas, Krisztina Buzas, et al. 2015. "Biological Properties of Extracellular Vesicles and Their Physiological Functions." *Journal of Extracellular Vesicles* 4 (January): 27066. https://doi.org/10.3402/jev.v4.27066.

Yang, Jia, Xing-Xing Liu, Heng Fan, Qing Tang, Zhe-Xing Shou, Dong-Mei Zuo, Zhou Zou, et al. 2015. "Extracellular Vesicles Derived from Bone Marrow Mesenchymal Stem Cells Protect against Experimental Colitis via Attenuating Colon Inflammation, Oxidative Stress and Apoptosis." *PloS One* 10 (10): e0140551. https://doi.org/10.1371/journal.pone.0140551.

Yang, Mei, Jianchang Chen, Jing Zhao, and Mei Meng. 2014. "Etanercept Attenuates Myocardial Ischemia/Reperfusion Injury by Decreasing Inflammation and Oxidative Stress." Edited by John Calvert. *PLoS ONE* 9 (9): e108024. https://doi.org/10.1371/journal.pone.0108024.

Yang, Yuanyuan, Vesna Bucan, Heike Baehre, Juliane von der Ohe, Anna Otte, and Ralf Hass. 2015. "Acquisition of New Tumor Cell Properties by MSC-Derived Exosomes." *International Journal of Oncology* 47 (1): 244–52. https://doi.org/10.3892/ijo.2015.3001.

Yang, Zequan, Yuan-Ji Day, Marie-Claire Toufektsian, Yaqin Xu, Susan I Ramos, Melissa A Marshall, Brent A French, and Joel Linden. 2006. "Myocardial Infarct-Sparing Effect of Adenosine A2A Receptor Activation Is due to Its Action on CD4+ T Lymphocytes." *Circulation* 114 (19): 2056–64. https://doi.org/10.1161/CIRCULATIONAHA.106.649244.

Yegutkin, G. G., Sergei S Samburski, and Sirpa Jalkanen. 2003. "Soluble Purine-Converting Enzymes Circulate in Human Blood and Regulate Extracellular ATP Level via Counteracting Pyrophosphatase and Phosphotransfer Reactions." *The FASEB Journal* 17 (10): 1328–30. https://doi.org/10.1096/fj.02-1136fje.

Yu, Bo, Xiaomin Zhang, and Xiaorong Li. 2014. "Exosomes Derived from Mesenchymal Stem Cells." *International Journal of Molecular Sciences* 15 (3): 4142–57. https://doi.org/10.3390/ijms15034142.

Yue, Yuan, Xiao Yang, Kangni Feng, Lexun Wang, Jian Hou, Bo Mei, Han Qin, Mengya Liang, Guangxian Chen, and Zhongkai Wu. 2017. "M2b Macrophages Reduce Early Reperfusion Injury after Myocardial Ischemia in Mice: A Predominant Role of Inhibiting Apoptosis via A20." *International Journal of Cardiology* 245 (October): 228–35. https://doi.org/10.1016/j.ijcard.2017.07.085.

Zhang, Haiying, Haiying Zhang, and David Lyden. 2018. "A Protocol for Asymmetric-Flow Field-Flow Fractionation (AF4) of Small Extracellular Vesicles." *Protocol Exchange*, February.

https://doi.org/10.1038/protex.2018.002.

Zhang, Wei, Wei Ge, Changhong Li, Shengguo You, Lianming Liao, Qin Han, Weimin Deng, and Robert C H Zhao. 2004. “Effects of Mesenchymal Stem Cells on Differentiation, Maturation, and Function of Human Monocyte-Derived Dendritic Cells.” *Stem Cells and Development* 13 (3): 263–71. https://doi.org/10.1089/154732804323099190.

Zhao, Yuanyuan, Xiaoxian Sun, Wenming Cao, Jie Ma, Li Sun, Hui Qian, Wei Zhu, and Wenrong Xu. 2015. “Exosomes Derived from Human Umbilical Cord Mesenchymal Stem Cells Relieve Acute Myocardial Ischemic Injury.” *Stem Cells International* 2015 (January): 761643. https://doi.org/10.1155/2015/761643.

Zhou, Changhui, Bo Yang, Yi Tian, Hongliang Jiao, Wendi Zheng, Jian Wang, and Fangxia Guan. 2011. “Immunomodulatory Effect of Human Umbilical Cord Wharton’s Jelly-Derived Mesenchymal Stem Cells on Lymphocytes.” *Cellular Immunology* 272 (1): 33–38. https://doi.org/10.1016/j.cellimm.2011.09.010.

Zhou, Q, J Yan, P Putheti, Y Wu, X Sun, V Toxavidis, J Tigges, et al. 2009. “Isolated CD39 Expression on CD4+ T Cells Denotes Both Regulatory and Memory Populations.” *American Journal of Transplantation : Official Journal of the American Society of Transplantation and the American Society of Transplant Surgeons* 9 (10): 2303–11. https://doi.org/10.1111/j.1600-6143.2009.02777.x.

Zitvogel, Laurence, Armelle Regnault, Anne Lozier, Joseph Wolfers, Caroline Flament, Danielle Tenza, Paola Ricciardi-Castagnoli, Graca Raposo, and Sebastian Amigorena. 1998. “Eradication of Established Murine Tumors Using a Novel Cell-Free Vaccine: Dendritic Cell-Derived Exosomes.” *Nature Medicine* 4 (5): 594–600. https://doi.org/10.1038/nm0598-594.

FUNDING

Marta Monguió Tortajada performed her thesis thanks to public sponsoring: personal grant (2014FI B00649) from the "Agència de Gestió d'Ajuts Universitaris i de Recerca" (AGAUR) and by the "Pla Estratègic de Recerca i Innovació en Salut" (PERIS) 2016-2020 (SLT002/16/00234) from the Generalitat de Catalunya.

The work was supported in part by multiple agencies: Fundació La Marató TV3 (201502-30 and 201516-10), Societat Catalana de Cardiologia, SGR programme from the Generalitat de Catalunya (2017-SGR-301 REMAR Group, and 2017-SGR-483 ICREC Group), Instituto de Salud Carlos III: FIS grants (PI13/00050, PI14/01682, PI17/01487 and PI18/00014), the Redes temáticas de investigación cooperativa en salud (RETICS): Red de Investigación Renal – REDinREN (RD16/0009 Feder Funds) and Red de Terapia Celular – TerCel (RD12/0019/0029 and RD16/00111/0006); the Spanish Ministry of Economy and Competitiveness-MINECO (SAF2014-59892-R and SAF2017-84324-C2-1-R), CIBER Cardiovascular (CB16/11/00403), as part of the Plan Nacional de I+D+I, and co-funded by ISCIII-Subdirección General de Evaluación and the Fondo Europeo de Desarrollo Regional (FEDER), "La Caixa" Banking Foundation, Fundació Daniel Bravo Andreu and Sociedad Española de Cardiología. This work has been developed in the context of CERCA Programme (Generalitat de Catalunya) and AdvanceCat with the support of ACCIÓ (Catalonia Trade & Investment; Generalitat de Catalunya) under the Catalan ERDF operational program (European Regional Development Fund) 2014-2020.

APPENDICES

TABLE 7 | Summary of main points to be addressed while developing an advanced therapy medicinal product (ATMP) to cover the clinical and non-clinical data needed for scientific evaluation by EMA for clinical translation certification.

Issue	Requirements
Quality[1]	□ Nomenclature □ Structure: summary of the physical and biological characteristics of the substance (origin, phenotype, markers of cells, vector used, transgenes, etc.) including a description of any other materials such as bioactive molecules (growth factors, etc.) and structural components (scaffolds, medical devices, etc.), when these are an integral part of the substance. The purpose of adding these other materials should be explained. □ General properties: biological and where appropriate, the physicochemical and other relevant properties of the substance. Where available, a description of the biological activity (potency) should be included. *Manufacture:* □ Manufacturer(s) □ Description of manufacturing process and process controls □ Control of materials: including the presence of residual impurities including animal-derived raw materials, reagents or starting materials, that should be discussed in the risk analysis exercise. □ Control of critical steps and intermediates □ Process validation and/or evaluation *Characterization:* □ Structure and other characteristics: it should be sufficient to allow adequate description of the active substance. It should encompass all the components in the product (e.g. scaffolds, matrices, bio-materials, bio-molecules or other components), if applicable. For purity, tests should be applied to provide information on product and process related impurities including microbial (bacterial and fungal) and adventitious viral safety (see also section 3.2.A.2). These quality attributes constitute the first set of parameters on which reproducibility and specifications will be progressively elaborated during the development. □ Impurities: it is acknowledged that characterisation of product related impurities might not be available for products in initial development. The plans to identify and characterise these product related impurities and their impact should be addressed. *Control of substance:* □ Specifications: Formal specifications are not required for certification. However, a set of quality attributes established in *Characterisation* will generate the basis for setting specification at the time of MAA. Any preliminary specification should be provided, if available. □ Analytical procedures: the analytical methods used for the testing of the substance should be described. It is not necessary to provide a detailed description of all the analytical procedure, but the documentation should include principle of the method, reagents, assay controls and test procedures for each of the assay submitted for certification. □ Batch analyses: data on all the products manufactured with the current process should be provided in a tabular format. This should include, where applicable, the batch number, batch size, manufacturing site, manufacturing date, control

	□ Methods, acceptance criteria and the test results. At least the results from one batch manufactured using the equipment and methodology described, produced at any scale, should be provided. □ Reference standards or materials: when a reference standard has been used for any of the assays, characterisation data should be provided. The characterisation of a batch of substance should be initiated to establish a reference standard whenever applicable. International standards should be used, when available, for establishing the in-house reference standard. □ Finished-product manufacture and packaging. □ Stability: if the substance is not immediately processed into the medicinal product, at the minimum the storage conditions and storage period should be justified.
Safety	Safety analysis must be adapted to the therapeutic goal. For example, as treatment of chronic heart failure (CHF) is usually prolonged, long-term data on adverse effects should be provided. Special efforts should be made assess potential adverse effects that are characteristics of the class of drug being investigated. Particular attention should be paid to the following specific side effects: cardiovascular safety, hypotension/bradycardia, end-organ consequences, effect on cardiac rhythm, pro-ischaemic effects.[2]
Efficacy	Efficacy criteria must be adapted to the main therapeutic goal. In the case of CHF, criteria include[2]: mortality, worsening of HF, functional status (capacity and clinical symptoms), patient reported outcomes (quality of life), haemodynamic parameters, biomarkers, events from implantable devices and composite endpoints.
Pharmacovigilance[3]	Good manufacturing and laboratory practices (GMP and GLP) compliance Good clinical practice (GCP) inspections and compliance Good pharmacovigilance practices (GVP), including a Risk management plan (RMP)
Environmental Risk Assessment (ERA)[3]	The environmental risk assessment (ERA) concerns the risks to the environment arising from the use, storage, and disposal of the medicinal product. Risks arising from the synthesis or manufacture of the product are under the remits of the national competent authorities.

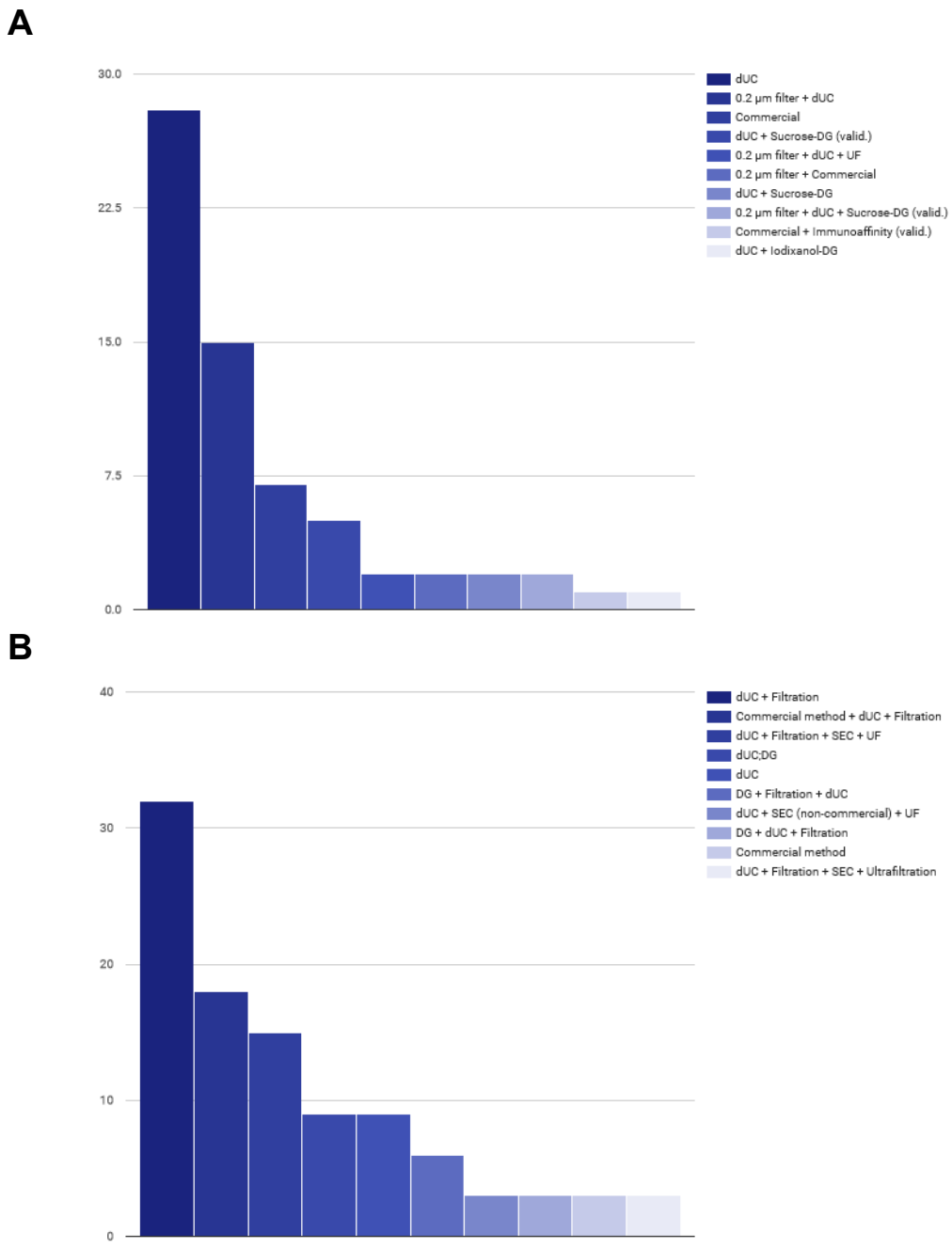

FIGURE 35 | Histogram representations of the most used isolation protocols in articles published with the *Study aim* on the *Function* of EVs for all articles published and registered in the EV-TRACK database (**A**, n=937) or for articles published only in 2017 (**B**, n=34). dUC is by far the most used EV isolation method, and used also in combination as starting steps to get rid of cell debris and large vesicles. Commercial methods mainly refer to proprietary methods based on precipitating agents, and appear overall as the second most used after dUC. DG is mostly used as a validation technique or in combination with dUC -to get rid of the gradient-forming solution- for downstream functional assays. While SEC is absent as one of the methods of choice when looking at all the literature (**A**), it appears as the 3rd (+10th, as both are the same; UF=Ultrafiltration) and 7th-positioned method of choice for EV isolation, always as a combination method as the one described in *Chapter 2*. DG: density gradient; dUC: differential ultrafiltration, SEC: size exclusion chromatography; UF: ultrafiltration.

List of publications

Publications are listed by chronological order, sorted by most recent. Of these, there are three complementary works performed during the PhD that are not included in the thesis but that are worth being highlighted for different reasons. They account for i) the study on TLR synergism and heterotolerance for endotoxin response in monocytes, ii) the participation in the EV-TRACK consortium for transparent reporting on EV research and iii) the seminal work on cATMSC immune properties:

1. Lozano-Ramos I, Bancu I, Carreras-Planella L, Monguió-Tortajada M, Cañas L, Juega J, Bonet J, Armengol MP, Lauzurica R, Borràs FE, '**Molecular profile of urine extracellular vesicles from normo-functional kidneys reveal minimal differences between living and deceased donors**', *BMC Nephrology*, 2018 Jul 31;19(1):189.

2. Carreras-Planella L*, Monguió-Tortajada M*, Palma E, Borràs FE, Franquesa M. "**Stem cells: immunotherapy in solid organ transplantation**". *Encyclopedia of Tissue Engineering and Regenerative Medicine*. 2018. *In press*. **shared first authorship*

3. Monguió-Tortajada M, Franquesa M, Sarrias MR, Borràs FE, '**Low doses of LPS exacerbate the inflammatory response and trigger death on TLR3-primed human monocytes**', *Cell Death and Disease*, 2018 May; 9:499.

   This publication is the result of a mind puzzling workout of unexpected results while studying the effect of a serum-derived protein on the activation of monocytes. At the end, we learnt the impressive effects of minimal endotoxin presence –within endotoxin-free ranges- on monocyte biology.

4. Monguió-Tortajada M*, Roura S*, Gálvez-Montón C, Franquesa M, Bayes-Genis A, and Borràs FE. '**Mesenchymal stem cells induce expression of CD73 in human monocytes *in vitro* and in a swine model of myocardial infarction *in vivo***', *Frontiers in Immunology*, 2017 Nov 20; 8:1577. **shared first authorship*

   Work included as **CHAPTER 1**.

5. Evans I, Mojoli A, Monguió-Tortajada M, Marcilla A, Aran V, Amorim M, Inal J, Borras FE, Ramirez MI, '**Microvesicles released from *Giardia intestinalis* disturb host-pathogen response *in vitro***', *European Journal of Cell Biology*, 2017 Mar; 96(2):131-142. Epub 2017 Jan 22.

6. EV-TRACK Consortium, Van Deun J, Mestdagh P, Agostinis P, Akay Ö, Anand S, Anckaert J, Martinez ZA, Baetens T, Beghein E, Bertier L, Berx G, Boere J, Boukouris S, Bremer M, Buschmann D, Byrd JB, Casert C, Cheng L, Cmoch A, Daveloose D, De Smedt E, Demirsoy S, Depoorter V, Dhondt B, Driedonks TA, Dudek A, Elsharawy A, Floris I, Foers AD, Gärtner K, Garg AD, Geeurickx E, Gettemans J, Ghazavi F, Giebel B, Kormelink TG, Hancock G, Helsmoortel H, Hill AF, Hyenne V, Kalra H, Kim D, Kowal J, Kraemer S, Leidinger P, Leonelli C, Liang Y, Lippens L, Liu S, Lo Cicero A, Martin S, Mathivanan S, Mathiyalagan P, Matusek T, Milani G, Monguió-Tortajada M, Mus LM, Muth DC, Németh A, Nolte-'t Hoen EN, O'Driscoll L, Palmulli R, Pfaffl MW, Primdal-Bengtson B, Romano E, Rousseau Q, Sahoo S, Sampaio N, Samuel M, Scicluna B, Soen B, Steels A, Swinnen JV,

Takatalo M, Thaminy S, Théry C, Tulkens J, Van Audenhove I, van der Grein S, Van Goethem A, van Herwijnen MJ, Van Niel G, Van Roy N, Van Vliet AR, Vandamme N, Vanhauwaert S, Vergauwen G, Verweij F, Wallaert A, Wauben M, Witwer KW, Zonneveld MI, De Wever O, Vandesompele J, Hendrix A. '**EV-TRACK: transparent reporting and centralizing knowledge in extracellular vesicle research**.' *Nature Methods*, 2017 Feb 28; 14(3):228-232.

During the first EV course at EMBL in 2014, the attendees agreed on a common problem found within the EV research field: the high heterogeneity and poor reporting on EV-related methodology and characterization. Then, the idea of creating a unified platform in an effort to improve transparency and good practice in the EV field took shape. This data mining translated into the EV-TRACK knowledgebase and the EV-METRIC value, based on a consensus checklist to assess the completeness of reporting of generic and method-specific information necessary to interpret and reproduce a given EV-related experiment. In order to start this knowledgebase, we created an international consortium to agree on the consensus minimal information required for reporting and gather data on EV-related articles published in scientific journals. Since then, the EV-TRACK platform has been growing in data and is encouraging more researchers to check their EV-METRIC value to know whether their controls and reporting of experimental parameters are sufficient or can be improved.

7. Monguió-Tortajada M*, Roura S*, Gálvez-Montón C, Pujal JM, Aran G, Sanjurjo L, Franquesa M, Sarrias MR, Bayes-Genis A, Borràs FE, '**Nanosized UCMSC-derived extracellular vesicles but not conditioned medium exclusively inhibit the inflammatory response of stimulated T cells: implications for nanomedicine**', *Theranostics*, 2017 Jan; 7(2):270-284. **shared first authorship*

   Work included as **CHAPTER 2**.

8. Martín-Jaular L, de Menezes-Neto A, Monguió-Tortajada M, Elizalde-Torrent A, Díaz-Varela M, Fernández-Becerra C, Borras FE, Montoya M, Del Portillo HA. '**Spleen-dependent immune protection elicited by CpG adjuvanted reticulocyte-derived exosomes from malaria infection is associated with changes in T cell subsets**' Distribution', *Frontiers in Cell and Developmental Biology*, 2016 Nov 16;4:131.

9. Gámez-Valero A, Monguió-Tortajada M, Carreras-Planella L, Franquesa M, Beyer K, Borràs FE, '**Size-exclusion chromatography-based isolation minimally alters extracellular vesicles' characteristics compared to precipitating agents**', *Scientific Reports*, 2016 Sep 19;6:33641.

10. Perea-Gil I*, Monguió-Tortajada M*, Gálvez-Montón C, Bayes-Genis A, Borràs FE & Roura S, '**Preclinical evaluation of the immunomodulatory properties of cardiac adipose tissue progenitor cells using umbilical cord blood mesenchymal stem cells: a direct comparative study**', *BioMed Research International*, 2015;2015:439808. **shared first authorship*

    In this work, we compared the immunomodulatory properties of cATMSC and UCBMSC towards allogeneic T cells, finding very similar properties for both MSC types. We described a dose-dependent abrogation of T cell alloproliferation and cytokine response induced by third-party mature MDDCs. These results set the groundwork to study cATMSCs' mechanisms for immune modulation.

11. Monguió-Tortajada M, Lauzurica-Valdemoros R & Borràs FE, '**Tolerance in organ transplantation: from conventional immunosuppression to extracellular vesicles**', *Frontiers in Immunology*, 2014 Sep 17;5:416.

Manuscript submitted or under review

1. Calle A, Gutiérrez-Reinoso MA, Re M, Blanco J, de la Fuente, J, Monguió-Tortajada M, Borràs FE, Yáñez-Mó M, Ramírez MA, '**Bovine peripheral blood MSC: tropism to an inflammation/embryo implantation niche for immunomodulation**'. *Submitted.*

2. Calle A, López-Martín S, Monguió-Tortajada M, Borràs FE, Yáñez-Mó M, Ramírez MA, '**Bovine endometrial MSC: mesenchymal to epithelial transition during luteolysis and tropism to inflammation niche for immunomodulation**'. *Submitted.*

3. Monguió-Tortajada M, Prat-Vidal C, Clos-Sansalvador M, Calle A, Morancho A, Gálvez-Montón C, Ramírez MA, Rosell A, Bayes-Genis A, Roura S*, Borràs FE*. '**Development of engineered three-dimensional extracellular vesicle-rich bioactive cardiac grafts**'. **co-corresponding authors*. *Submitted*

   Work included as **CHAPTER 3**.

Congress Communications

1. Marta Monguió-Tortajada, Marcel·la Franquesa, Maria-Rosa Sarrias, Francesc E. Borràs, '**Low doses of LPS exacerbate the inflammatory response and trigger death on TLR3-primed human monocytes**', Poster presented at the "X Jornada del Departament de Biologia Cel·lular, Fisiologia i Immunologia"; 5th June 2018; Cerdanyola del Vallès, Spain.
2. Marta Monguió-Tortajada, Marcel·la Franquesa, Maria-Rosa Sarrias, Francesc E. Borràs, '**Low doses of LPS exacerbate the inflammatory response and trigger death on TLR3-primed human monocytes**', Poster presented at the 52nd ESCI Annual Scientific Meeting; 30th May-1st June 2018; Barcelona, Spain.
3. Marta Monguió-Tortajada, Cristina Prat-Vidal, Carolina Gálvez-Montón, Antoni Bayes-Genis, Francesc E. Borràs, Santiago Roura, '**Validació de l'ús de matrius cardíaques per l'administració local de vesícules extracel·lulars multifuncionals per la regeneració del miocardi post-infart**' Poster presented at the 30 Congrés de la Societat Catalana de Cardiologia (SCC). 31st May – 1st June 2018, Barcelona, Spain.
4. Santiago Roura, Marta Monguió-Tortajada, Cristina Prat-Vidal, Carolina Gálvez-Montón, Francesc E. Borràs, Antoni Bayes-Genis, '**Validation of engineered cardiac grafts for the local delivery of multifunctional extracellular vesicles for myocardial repair**'. Poster presented at the 52nd ESCI Annual Scientific Meeting; 30th May-1st June 2018; Barcelona, Spain.
5. Marta Monguió-Tortajada, Cristina Prat-Vidal, Isaac Perea-Gil, Carolina Gálvez-Montón, Santiago Roura, Antoni Bayes-Genis, Francesc E. Borràs, '**Validation of engineered cardiac grafts for the local delivery of multifunctional extracellular vesicles for myocardial repair**'. Poster presented at the International Society for Extracellular Vesicles (ISEV) International meeting; 4-7th May 2018; Barcelona, Spain.
6. Laura Carreras-Planella, Marta Monguió-Tortajada, Jordi Soler-Majoral, Cristina Rubio-Esteve, Marcella Franquesa, Josep Bonet, Maria Isabel Troya-Saborido, Francesc E. Borràs, '**Characterization and proteomic profile of extracellular vesicles from peritoneal dialysis efflux**'. Poster presented at the International Society for Extracellular Vesicles (ISEV) International meeting; 4-7th May 2018; Barcelona, Spain.
7. Daniel Vivas Pradillo, Lluis Martorell, Raquel Cabrera-Pérez, Clémentine Mirabel, Clara Frago, Jordi Ayats, Marta Monguió-Tortajada, Ana Gámez-Valero, Joan Garcia, Sergi Querol, Antoni Bayès-Genís, Francesc E. Borràs, Santiago Roura, Joaquim Vives, '**Toward the use of Wharton's Jelly-derived multipotent mesenchymal stromal cells in bone tissue engineering strategies**'. Poster presented at the 24th Annual Meeting of the International Society for Cellular Therapy (ISCT); 2-5th May 2018; Montréal, Canada.
8. Marta Monguió-Tortajada, Santiago Roura, Carolina Gálvez-Montón, Marcella Franquesa, Antoni Bayés-Genís and Francesc E Borràs, '**Mesenchymal stem cells induce de novo expression of CD73 in human monocytes *in vitro* and in a swine model of myocardial infarction *in vivo***'. Oral communication at the XI

Congress of the Societat Catalana d'Immunologia (Catalan Society of Immunology); 16-17th November 2017; Barcelona, Spain.

9. Laura Carreras-Planella, Marta Monguió-Tortajada, Francesc E. Borràs, Marcella Franquesa, '**MSC induction of Breg is mediated by secreted soluble factors but not by extracellular vesicles**'. Oral communication at the XI Congress of the Societat Catalana d'Immunologia (Catalan Society of Immunology); 16-17th November 2017; Barcelona, Spain.
10. Santiago Roura, Marta Monguió-Tortajada, Carolina Gálvez-Montón, Marcel.la Franquesa, Francesc E. Borràs, Antoni Bayés-Genís, '**Efecto inmunomodulador de las células madre mesenquimales de grasa cardíaca: caracterización in vitro y preclínica en un modelo porcino de infarto de miocardio**', Poster presented at the Cardiovascular Diseases Congress of the Spanish Society of Cardiology, 26-28th October 2017; Madrid, Spain.
11. Ioana Bancu, Inés Lozano-Ramos, Laura Carreras-Planella, Marta Monguió-Tortajada, Laura Cañas-Solé, Javier Juega-Mariño, Pilar Armengol, Josep Bonet, Ricardo Lauzurica, Francesc E. Borràs, '**Las vesículas extracelulares de orina de los donantes vivos y de cadaver presentan diferencias significativas a nivel proteómico y de microRNA**'. Oral communication at the XLVII National congress of the Sociedad Española de Nefrología (Spanish Society of Nephrology); 6-9th October 2017; Burgos, Spain.
12. Daniel Vivas, Alba López Fernández, Daniel Chaverri, Marta Grau Vorster, Anna Del Mazo Barbara, Blanca Reyes, Marta Monguió Tortajada, Ana Gámez Valero, Francesc E. Borràs, Santiago Roura, Cristina Prat Vidal, Antoni Bayés Genís, Màrius Aguirre, Roberto Vélez, Irene Oliver Vila, Joaquim Vives, '**Mechanisms of bone remodelling induced by tissue engineering products composed of mesenchymal stromal cells and natural bone matrices**'. Poster presented at the European chapter meeting of the Tissue Engineering and Regenerative Medicine International Society (TERMIS); 26–30th June 2017; Davos, Switzerland.
13. Santiago Roura, Marta Monguió-Tortajada, Carolina Gálvez-Montón, Marcel·la Franquesa, Francesc E Borràs and Antoni Bayés-Genís, '**Caracterització de l'efecte immunomodulador de les cèl·lules mare mesenquimals de greix cardíac: estudi in vitro i preclínic en un model porcí d'infart de miocardi**'. Poster presented at the 29th congress of the Catalan Society of Cardiology (SCC); 25–26th May 2017; Barcelona, Spain.
14. Aran G, Sanjurjo L, Bárcena C, Monguió-Tortajada M, Borràs FE, Sala M, Armengol C, Sarrias MR. **Els factors secretats pels hepatòcits tumorals promouen un fenotip M2 en monòcits aïllats de sang perifèrica**. Poster presented at the XXVI Congress of the Societat Catalana de Digestologia, January 2017, Lleida, Spain.
15. Marta Monguió-Tortajada, Santiago Roura, Carolina Gálvez-Montón, Josep Maria Pujal, Marcel·la Franquesa, Antoni Bayés-Genís and Francesc E Borràs, '**UCMSC-derived extracellular vesicles but not conditioned medium exclusively inhibit the inflammatory response of stimulated T cells**'. Oral presentation at the 6th Expert meeting on therapeutic MSCs for immune modulation (MISOT); 27–28th October 2016; Regensburg, Germany.

16. Marta Monguió-Tortajada, Santiago Roura, Carolina Gálvez-Montón, Josep Maria Pujal, Marcel·la Franquesa, Antoni Bayés-Genís and Francesc E Borràs, '**UCMSC-derived extracellular vesicles but not conditioned medium exclusively inhibit the inflammatory response of stimulated T cells**'. Oral presentation at the III GEIVEX Symposium: Therapeutic applications of Extracellular Vesicles; 29-30th September 2016; Donostia-San Sebastián, Spain.

17. Ana Gámez-Valero, Marta Monguió-Tortajada, Laura Carreras-Planella, Marcel·la Franquesa, Katrin Beyer, Francesc E. Borràs, '**Impact of SEC, PEG and PROSPR isolation methods on extracellular vesicles: a comparative study**'. Poster presented at the III GEIVEX Symposium: Therapeutic applications of Extracellular Vesicles; 29-30th September 2016; Donostia-San Sebastián, Spain.

18. Marta Monguió-Tortajada, Santiago Roura, Anna Oliveira-Tercero, Marcel·la Franquesa, Antoni Bayes-Genis and Francesc E. Borràs, '**Polyclonal T cell proliferation is inhibited by Umbilical Cord MSC-derived EVs but not by MSC conditioned media**'. Oral presentation at the International Society for Extracellular Vesicles (ISEV) International meeting; 4-7th May 2016; Rotterdam, The Netherlands.

19. Lorena Martín-Jaular, Marta Monguió-Tortajada, Armando De Menezes-Neto, Aleix Elizalde, Carmen Fernandez-Becerra, Francesc E. Borras, Maria Montoya, Hernando A del Portillo. '**Spleen-dependent immune protection elicited by reticulocyte-derived exosomes from malaria infection revealed by T-cell population changes**'. Oral presentation at the International Society for Extracellular Vesicles (ISEV) International meeting; 4-7th May 2016; Rotterdam, The Netherlands.

20. Ana Gámez-Valero, Laura Carreras, Marta Monguió-Tortajada, Marcel·la Franquesa, Katrin Beyer and Francesc E. Borràs, '**Impact of SEC, PEG and PROSPR isolation methods on Extracellular Vesicles: A Comparative Study**'. Poster presented at the International Society for Extracellular Vesicles (ISEV) International meeting; 4-7th May 2016; Rotterdam, The Netherlands.

21. Santiago Roura, Isaac Perea-Gil, Marta Monguió-Tortajada, Carolina Gálvez-Montón, Francesc E Borràs and Antoni Bayés-Genís, '**Avaluació de les propietats immunomodulatòries de les cèl·lules progenitores derivades de teixit adipós epicardíac: un pas més vers el seu ús clínic en regeneració cardíaca**'. Poster presented at the 27th congress of the Catalan Society of Cardiology (SCC); 4–5th June 2015; Barcelona, Spain.

22. Isaac Perea-Gil, Marta Monguió-Tortajada, Carolina Gálvez-Montón, Antoni Bayes-Genis, Francesc E. Borràs, Santiago Roura, '**Evaluation of the immunomodulatory properties of cardiac adipose tissue progenitor cells: a step towards their use in cell-based cardiac regeneration**'. Poster presented at the Heart Failure – 2nd World congress on Acute Heart Failure by the European Society of Cardiology; 25th May 2015; Sevilla, Spain.

23. Marta Monguió-Tortajada, Ingrid Evans-Osses, Marcel I. Ramírez, Francesc E. Borràs, **'Capture of membrane-derived microvesicles from *Giardia intestinalis* induces activation of human monocyte-derived dendritic cells**'. Poster presented at the II GEIVEX Symposium – Extracellular vesicles: From the bench to the clinics; 9-10th October 2014; Tarragona, Spain. *Best poster communication award.*

24. Lorena Martín-Jaular, Marta Monguió-Tortajada, Aleix Elizalde, Carmen Fernandez-Becerra, Francesc E. Borràs, Maria Montoya, Hernando A del Portillo. '**Spleen-dependent immune protection elicited by reticulocyte-derived exosomes from malaria infection revealed by T cell population changes**'. Oral presentation at the II GEIVEX Symposium – Extracellular vesicles: From the bench to the clinics; 9-10th October 2014; Tarragona, Spain. *Best oral communication award.*
25. Marta Monguió-Tortajada, Ingrid Evans-Osses, Marcel I. Ramírez, Francesc E. Borràs, '**Capture of membrane-derived microvesicles from** *Giardia intestinalis* **induces activation of human monocyte-derived dendritic cells**'. Poster presented at the International Society for Extracellular Vesicles (ISEV) International meeting; 30th April – 3rd May 2014; Rotterdam, The Netherlands.
26. Lorena Martín-Jaular, Marta Monguió-Tortajada, Aleix Elizalde, Marco Fernández, Maria Montoya, Francesc E. Borràs, Hernando A del Portillo. '**Immunological analyses of the vaccine-induced protection elicited by reticulocyte-derived exosomes in malaria infections**'. Poster presented at the Molecular and Cell Biology of Malaria. Gordon Research Conferences; 4th – 9th August 2013; Tuscany, Italy.

Seminars and workshops

2018	Advance(Cat) – Accelerating Development of Advanced Therapies in Catalonia	H. Clínic, Barcelona
2018	X Jornada del Departament de Biologia Cel·lular, Fisiologia i Immunologia	UAB, Cerdanyola del Vallès
2018	II Cardionet workshop – Grup de Treball de Recerca Bàsica i Translació Clínica de la Societat Catalana de Cardiologia	H. Sant Pau, Barcelona
2017	REDiEx Workshop on Isolation and characterisation of extracellular vesicles obtained from different biological fluids	IGTP, Badalona
2017	Dendritic Cell MACS Day	L'Acadèmia, Barcelona
2016	6th Can Ruti Campus Symposium	HUGTiP, Badalona
2016	REDiEx Workshop in Imaging and exosomes	CNIO, Madrid
2015	Dendritic Cell MACS Day	L'Acadèmia, Barcelona
2014	4th Can Ruti Campus Symposium	IGTP, Badalona
2014	EMBL Advanced Course in Exosome Purification, Identification and Translation	EMBL, Heidelberg

National and International Scientific Congresses

2018	52nd European Society of Clinical Investigation (ESCI) Annual Scientific Meeting	Barcelona
2018	7th ISEV International meeting	Barcelona
2018	30th Congress of the Societat Catalana de Cardiologia (SCC)	Barcelona
2017	XI Congress of the Societat Catalana d'Immunologia (SCI)	Barcelona
2016	6th Expert meeting on therapeutic MSCs for immune modulation (MISOT)	Regensburg
2016	5th ISEV International meeting	Rotterdam
2015	TOLL meeting: Targeting Innate Immunity	Marbella
2015	III GEIVEX Symposium – Therapeutic applications of EVs	Donostia
2014	3rd ISEV International meeting	Rotterdam
2014	II GEIVEX Symposium – EVs: From the bench to the clinics	Tarragona

GEIVEX: Grupo Español de Innovación e Investigación en Vesículas Extracelulares
ISEV: International Society for Extracellular Vesicles

Awards

2014	FI-DGR scholarship for PhD studies	AGAUR
2014	Masters honours award, MSc in Advanced Immunology	Universitat de Barcelona
2014	Travel grant to the EMBL Advanced Course 'Exosome Purification, Identification and Translation'	Boehringer Ingelheim Fonds
2014	Best poster communication award	2nd GEIVEX Symposium

Teaching Activities

2014, 2015, 2016, 2017, 2018	Dendritic cell isolation strategies by FACS, module of the Flow Cytometry course	IGTP, Badalona
2013 – 2018	Supervising undergraduate and master students	IGTP, Badalona